Mathematical and Computational Methods in Photonics

Tutorial Notes

Habib Ammari, Brian Fitzpatrick, Erik Orvehed Hiltunen and Sanghyeon Yu

Contents

CHAPTER 1

Basic Mathematical Concepts and Numerical Methods

In this tutorial we give a short introduction to the concept of metamaterials and how the phenomenon of resonance can be exploited to create materials with remarkable properties, properties that are not found in naturally occurring materials. We also give an overview of the Nyström method for numerically solving 2-D boundary integral equations as this is the basis for many of the numerical illustrations that will be presented later in the module. Finally, we describe Muller's method which is a numerical method used to find complex roots of functions, in particular it can be used to find resonant frequencies that arise due to boundary value problems in photonics and phononics.

1.1. Introduction to subwavelength resonance

1.1.1. Problem setting. We are interested in the scattering of time-harmonic acoustic and electromagnetic waves. In this setting a wave $\hat{u}$ takes the form

$$\hat{u}(x,t) = u(x)e^{-\sqrt{-1}\omega t}, \qquad x \in \mathbb{R}^d.$$

Substituting this expression into the scalar wave equation leads to the Helmholtz equation

$$\Delta u(x) + \omega^2 u(x) = 0, \qquad x \in \mathbb{R}^d.$$

This equation represents the propagation of waves in free space.

Now, suppose we introduce an object, represented by a bounded domain D. Then we obtain a scattering problem, and depending on the choice of boundary conditions we impose, we can model different physical situations, e.g. waves transmitting into the domain, waves completely reflecting from the boundary of the domain, etc.

For convenience, we will consider acoustic waves. In acoustics, the relevant material parameters are bulk modulus and density. Denote by ρ and κ the density and bulk modulus of the background medium $\mathbb{R}^d \setminus \overline{D}$, and let ρ_b and κ_b represent the corresponding parameters for the domain D. Assume, for simplicity, that the material is homogeneous, so that these parameters are independent of position. In addition, we assume that they are independent of frequency. Let u^i represent an incident wave. The scattering problem for the domain D is then given by

$$\begin{cases} \Delta u + k^2 u = 0, \quad \text{in } \mathbb{R}^d \setminus D, \\ \Delta u + k_b^2 u = 0, \quad \text{in } D, \\ u_+ = u_-, \quad \text{on } \partial D, \\ \displaystyle \frac{1}{\rho}\frac{\partial u}{\partial \nu}\bigg|_+ = \frac{1}{\rho_b}\frac{\partial u}{\partial \nu}\bigg|_-, \quad \text{on } \partial D, \\ u^s := u - u^i \ \text{ satisfies the Sommerfeld radiation condition,} \end{cases} \tag{1.1}$$

where

$$k = \omega\sqrt{\frac{\rho}{\kappa}}, \quad k_b = \omega\sqrt{\frac{\rho_b}{\kappa_b}},$$

are the wavenumbers in the background medium, and in D, respectively. This problem is also known as a transmission problem, as the incident wave can transmit through the domain D. The boundary conditions represent continuity of the field and continuity of the flux at the boundary. The Sommerfeld radiation condition is needed to uniquely solve the transmission problem, and to ensure that we have a physically meaningful solution. It stipulates that we cannot have sources at infinity, or in other words, that we only allow as solutions waves that radiate outwards from the bounded domain D.

Various forms of this type of transmission BVP arise in phononics and photonics. In the simple case above the domain D represents a single object. However, in, say, a metasurface, D would represent an infinite periodic array of objects above some reflecting surface. In a phononic crystal on the other hand, D would represent an infinite number of periodically arranged objects that extends to infinity in all directions. The eigenvalues of these problems correspond to Minnaert resonances in phononics, and plasmon resonances in photonics.

1.1.2. Resonance in phononics. Our primary goals in photonics and phononics are:

- Determining resonances.
- Exploiting the effects on scattering that arise due to resonance.

In particular we are interested in low-frequency resonances. Low frequency implies a large wavelength. By exploiting low-frequency resonance we can exert control over waves that are orders of magnitude larger than the size of the resonating objects. Normally when a wave is much larger than an object, the waves that scatter from the object will have a negligible effect on overall wave propagation, i.e. the object is simply too small to have much of an influence on the overall wave propagation. However, at low-frequency resonances, a coupling occurs between the incident wave and the object, and the effect of scattering is greatly enhanced. For instance, an air bubble in water can be used to control waves that are over 300 times larger than the bubble!

Consider the transmission problem (1.1). Resonances here case correspond to eigenvalues of the transmission problem. They are the complex frequencies ω at which the problem has non-trivial solutions. We are not interested in just any resonance however, we specifically seek low-frequency resonances. Low-frequency resonance occurs when there is a high contrast between the density of the background medium and the object D. In the case of an air bubble in water, the density of water is around 1000 times greater than the density of air, and this gives rise to low-frequency resonance.

For resonance to arise in the first place, we must have some contrast between the material parameters of the background medium and the object D. Otherwise, if the density and bulk modulus of D were the same as the material parameters of the background medium, there would be nothing to differentiate D from the background medium, and the waves would propagate through it as if it were free-space.

So, if we have contrast, we will have resonance. For an intuitive idea of why high contrast, in particular, leads to low frequency resonance, consider the following artificial scenario. Suppose we let ρ_b in (1.1) become smaller and smaller until eventually it vanishes. Then we would have the following limiting problem

$$\begin{cases} \Delta u + k^2 u = 0, \quad \text{in } \mathbb{R}^d \setminus D, \\ \Delta u = 0, \quad \text{in } D, \\ u_+ = u_-, \quad \text{on } \partial D, \\ \left.\dfrac{\partial u}{\partial \nu}\right|_- = 0, \quad \text{on } \partial D, \\ u^s := u - u^i \;\text{ satisfies the Sommerfeld radiation condition,} \end{cases}$$

Waves no longer transmit into D as we have made the density of D infinitely small, i.e. zero. We can view this system as an exterior Helmholtz problem, and an interior Neumann problem. Now we ask, for what ω does this limiting problem have a non-trivial solution. Well, if we take $\omega = 0$ the problem becomes

$$\begin{cases} \Delta u = 0, \quad \text{in } \mathbb{R}^d \setminus D, \\ \Delta u = 0, \quad \text{in } D, \\ u_+ = u_-, \quad \text{on } \partial D, \\ \left.\dfrac{\partial u}{\partial \nu}\right|_- = 0, \quad \text{on } \partial D, \\ u^s := u - u^i \;\text{ satisfies the Sommerfeld radiation condition.} \end{cases}$$

We have an exterior Dirichlet problem, and an interior Neumann problem. Resonance is an inherent property of the object D and the background medium. It is not dependent on the incident wave. This is completely analogous to, says, a simple harmonic oscillator, which has an inherent natural resonance frequency. If the harmonic oscillator is driven by an external forcing close to its resonant frequency, the amplitude of oscillation will be enhanced. For acoustic waves, if the object is driven or *excited* by waves near the natural resonant frequency, scattering will be enhanced. In either case, resonant modes are inherent properties of the system, and correspond to non-trivial solutions in the case of no driving force or incident field. Hence, we don't need to concern ourselves with an incident wave to decide whether the system is resonant or not, so let us set the incident field to 0, which gives us

$$\begin{cases} \Delta u = 0, \quad \text{in } \mathbb{R}^d \setminus D, \\ \Delta u = 0, \quad \text{in } D, \\ u_+ = u_-, \quad \text{on } \partial D, \\ \left.\dfrac{\partial u}{\partial \nu}\right|_- = 0, \quad \text{on } \partial D, \\ u \;\text{ satisfies the Sommerfeld radiation condition.} \end{cases}$$

Now this system has a non-trivial solution, and therefore $\omega = 0$ is a resonant mode. To see this, let u be any constant function in D, and let it solve the Dirichlet problem in $\mathbb{R}^3 \setminus \overline{D}$. Then u will satisfy the Neumann problem inside D, and by construction it satisfies the Dirichlet problem outside D.

Now, if we increase ρ_b from 0 to some very small number, we return back to our original system, and as ω depends on the contrast continuously, the resonant frequency will shift slightly from 0, but it will still be a very low-frequency resonance. In essence, making the contrast higher can be viewed as forcing the resonant frequency towards zero. Gohberg-Sigal theory can be used to make rigorous this idea of perturbing a resonant frequency to a position slightly away from zero.

Now that we have an idea of resonance in a phononics problems, we need a method of determining resonance frequencies. Many problems in photonics and phononics can be dealt with using layer potential techniques. We are able to determine explicit formulas for the resonance frequencies in using low-frequency asymptotic expansions, and also to quantify the effects of scattering at resonance. Layer potentials are also useful when solving scattering problems numerically as they can serve as the foundation for numerical methods such as the boundary element method (BEM) or the Nystrom method. First we must transform the scattering problem (1.1) to the boundary of D.

1.2. Reformation of the scattering problem as a boundary integral problem

The Green's function $G(x,y)$ for the Helmholtz equation satisfies

$$(\Delta + k^2)G^k(x,y) = \delta_y(x),$$

where δ_y is the Dirac delta function for a source at $y \in \mathbb{R}^d$. The Green's function can be viewed as the impulse response of the system at a point x due to an input at a point y. The Green's function has the following representation:

$$G(x,y) = \begin{cases} -\dfrac{i}{4}H_0^{(1)}(k|x-y|)\ , & d = 2, \\ -\dfrac{e^{ik|x-y|}}{4\pi|x-y|}\ , & d = 3, \end{cases}$$

for $x \neq y$, where $H_0^{(1)}$ is the Hankel function of the first kind of order 0. We can construct the following boundary integral operators using the Green's function:

$$\begin{aligned} \mathcal{S}_D^k[\varphi](x) &= \int_{\partial D} G^k(x,y)\varphi(y)\, d\sigma(y), \\ \mathcal{D}_D^k[\varphi](x) &= \int_{\partial D} \frac{\partial G^k(x,y)}{\partial \nu(y)}\varphi(y)\, d\sigma(y), \\ \mathcal{K}_D^{k,*}[\varphi](x) &= \int_{\partial D} \frac{\partial G^k(x,y)}{\partial \nu(x)}\varphi(y)\, d\sigma(y), \end{aligned}$$

for some surface density $\varphi \in L^2(\partial\Omega)$. These operators are known as the single layer potential, the double layer potential, and the Neumann-Poincaré operator, respectively. The following *jump relations* hold for these operators, on the boundary of D:

$$\frac{\partial(\mathcal{S}_D^k[\varphi])}{\partial \nu}\bigg|_{\pm}(x) = \left(\pm\frac{1}{2}I + \mathcal{K}_D^{k,*}\right)[\varphi](x) \quad x \in \partial D, \tag{1.2}$$

$$(\mathcal{D}_D^k[\varphi])\bigg|_{\pm}(x) = \left(\mp\frac{1}{2}I + \mathcal{K}_D^{k}\right)[\varphi](x) \quad x \in \partial D. \tag{1.3}$$

Now, it can be shown that the solution u of the scattering problem (1.1) has the following boundary integral representation:

$$u(x) = \underbrace{\int_{\partial D} \frac{\partial G(x-y)}{\partial \nu(y)} u(y) d\sigma(y)}_{\mathcal{D}_D^k[u]} - \underbrace{\int_{\partial D} G(x-y) \frac{\partial u(y)}{\partial \nu(y)} d\sigma(y)}_{\mathcal{S}_D^k[\frac{\partial u}{\partial \nu}]}. \tag{1.4}$$

In this *direct approach*, the layer potentials are acting on the surface densities that are given by the field itself and its normal derivative, quantities which have physical meaning. However, by observing that the single and double layer potential both solve the Helmholtz equation by themselves, we could also take an *indirect approach* and choose to represent the solution as either a single layer potential $u(x) = \mathcal{S}_D^k[\varphi](x)$, or a double layer potential $\mathcal{D}_D^k[\varphi](x)$. In this case the surface density is unknown. In either case, we can find the required density function by evaluation on the boundary ∂D, and it can be shown that the . In fact, there are many options to choose from, which involve various combinations of layer potentials, when deciding upon a layer potential representation of our solution u. Different choices lead to integral equations with different properties, some of which can be advantageous or disadvantageous numerically.

Let us choose a single layer potential representation of the solution u both inside and outside D. We write

$$u(x) = \begin{cases} \underbrace{u^i(x)}_{\text{incident field}} + \underbrace{\mathcal{S}_D^k[\varphi](x)}_{\text{scattered field}}, & x \in \mathbb{R}^d \setminus \overline{D}, \\ \underbrace{\mathcal{S}_D^{k_b}[\varphi_b](x)}_{\text{interior field}}, & x \in D, \end{cases}$$

for some surface densities φ, φ_b in $L^2(\partial D)$. Recall that our original problem 1.1 required continuity of the solution and the flux at the boundary. For continuity of the solution u we must have

$$\mathcal{S}_D^{k_b}[\varphi_b](x) - \mathcal{S}_D^k[\varphi](x) = u^i, \qquad x \in \partial D. \tag{1.5}$$

For continuity of the flux we must we have

$$\frac{1}{\rho_b}\frac{\partial u}{\partial \nu}\bigg|_- = \frac{1}{\rho}\frac{\partial u}{\partial \nu}\bigg|_+ \iff \frac{\partial \mathcal{S}_D^{k_b}[\varphi_b]}{\partial \nu}\bigg|_- = \delta\left(\frac{\partial \mathcal{S}_D^k[\varphi]}{\partial \nu}\bigg|_+ + \frac{\partial u^i}{\partial \nu}\right),$$

where we the contrast parameter δ is defined by

$$\delta = \frac{\rho_b}{\rho}.$$

Using the jump relation for the single layer potential 1.2, we can write this condition as

$$\left(-\frac{1}{2}I + \mathcal{K}_D^{k,*}\right)[\varphi_b](x) + \delta\left(\frac{1}{2}I + \mathcal{K}_D^{k,*}\right)[\varphi](x) = \delta\frac{\partial u^i(x)}{\partial \nu}, \qquad x \in \partial D. \tag{1.6}$$

Finally, combining 1.5 and 1.6 we have the following system of boundary integral equations:

$$\mathcal{A}(\omega, \delta)[\Psi] = F,$$

where

$$\mathcal{A}(\omega,\delta) = \begin{pmatrix} \mathcal{S}_D^{k_b} & -\mathcal{S}_D^{k} \\ -\frac{1}{2}I + \mathcal{K}_D^{k_b,*} & -\delta(\frac{1}{2}I + \mathcal{K}_D^{k,*}) \end{pmatrix}, \Psi = \begin{pmatrix} \varphi_b \\ \varphi \end{pmatrix}, F = \begin{pmatrix} u^i \\ \delta\frac{\partial u^i(x)}{\partial \nu} \end{pmatrix}.$$

This problem is entirely equivalent to our original transmission scattering problem 1.1. Solving this system for the surface densities φ and φ_b gives us the solution, in terms of layer potentials, to the original problem everywhere in $\mathbb{R}^d$.

Likewise, determining the resonant frequencies, or *characteristic vales* to use Gohberg-Sigal terminology, of the operator-valued function $\mathcal{A}_\omega^d$ is equivalent to determining the eigenvalues of the original problem. The characteristic values are the ω such that the following equation has a non-trivial solution:

$$\mathcal{A}(\omega,\delta)[\Psi] = 0.$$

The smallest such characteristic value is low-frequency, or *quasi-static* resonance we want. Note that this equation does not make use of the incident wave. As we stated earlier, resonant frequencies are inherent properties of the system. They don't depend on the incident wave. However if an incident wave is used to excite an object near its resonant frequency, scattering will be greatly enhanced.

1.3. Operator approximation for Fredholm integral equations

The boundary integral equations that arise due to the layer potential framework are known as *Fredholm integral equations of the first kind* and *second kind*. For simplicity we will consider integral equations in which the *kernel* K of an integral operator A is continuous. For $x \in \partial D$ we have

- First kind:
$$A[\varphi](x) = f(x) \iff \int_{\partial D} K(x,y)\varphi(y)dy) = f(x).$$
- Second kind:
$$\varphi(x) - A[\varphi](x) = f(x) \iff \varphi(x) - \int_{\partial D} K(x,y)\varphi(y)dy = f(x).$$

When we discretize and solve this equation using the Nyström method, which is a numerical method for boundary integral equations, we want to quantify how accurately our numerical solution approximates the solution of the original integral equation. We can consider convergence in norm, or convergence pointwise. It turns out that Nyström method does not converge in norm, but it does converge pointwise. To give an idea of the Nyström convergence theory, we will prove that integral equations of the second kind with continuous kernels converge pointwise using the Nyström approach. First however, we discuss, in general, some notions of convergence.

1.3.1. Operator approximation. Let $A_n : X \to Y$ be an approximating sequence of bounded linear operators $A_n : X \to Y$ between Banach spaces X and Y, and let f_n be an approximating sequence with $f_n \to f$. We consider the replacement of an arbitrary operator equation

$$A\varphi = f,$$

by the equation

$$A_n\varphi_n = f_n.$$

Let's clarify some modes of convergence with a few definitions.

DEFINITION 1.1. (Pointwise convergence)
We say A_n converges pointwise to A if

$$\|A_n\varphi - A\varphi\| \to 0, \quad \text{as } n \to \infty, \text{ for every } \varphi \in X.$$

DEFINITION 1.2. (Norm convergence)
We say A_n converges in norm to A if

$$\|A_n - A\| \to 0, \quad \text{as } n \to \infty.$$

This may also be called uniform convergence.

REMARK 1.3. Another type of uniform convergence is uniform convergence with respect to sequences of functions, i.e. $\varphi_n(x) \to \varphi(x)$ uniformly as $n \to \infty$.

We will make use of the following theorem.

THEOREM 1.4. *(Neumann series)*
Let $A : X \to Y$ be a bounded linear operator on a Banach space X with $\|A\| < 1$ and let $I : X \to X$ denote the identity operator. Then $I - A$ has a bounded inverse on X that is given by the Neumann series

$$(I - A)^{-1} = \sum_{k=0}^{\infty} A^k,$$

and satisfies

$$\|(I - A)^{-1}\| \leq \frac{1}{1 - \|A\|}.$$

□

Error estimates for both norm convergence and pointwise converge involve finding a bound on an appropriate inverse operator.

THEOREM 1.5. *(Approximation through norm convergence)*
Let X and Y be Banach spaces and let $A : X \to Y$ be a bounded linear operator with a bounded inverse $A^{-1} : Y \to X$, i.e. an isomorphism. Assume the sequence $A_n : X \to Y$ of bounded linear operators to be norm convergent, i.e. $\|A_n - A\| \to 0$, as $n \to \infty$. Then for sufficiently large n, more precisely, for all n such that

$$\|A^{-1}(A_n - A)\| < 1,$$

the inverse operators $A_n^{-1} : Y \to X$ exist and are bounded by

$$\|A_n^{-1}\| \leq \frac{\|A^{-1}\|}{1 - \|A^{-1}(A_n - A)\|}.$$

For the solutions of the equations

$$A\varphi = f, \qquad A_n\varphi_n = f_n,$$

we have the estimate

$$\|\varphi_n - \varphi\| \leq C(\|(A_n - A)\varphi\| + \|f_n - f\|),$$

for n sufficiently large and some constant C.

PROOF. For an operator $T : X \to Y$ such that $\|T\| < 1$, by the Neuman series theorem 1.4, we have

$$\|(I-T)^{-1}\| = \frac{1}{1-\|T\|}.$$

Hence,

$$\|(I - A^{-1}(A - A_n))^{-1}\| \leq \frac{1}{1 - \|A^{-1}(A - A_n)\|}. \tag{1.7}$$

Then,

$$A^{-1}A_n = I - A^{-1}(A - A_n) \implies A_n = A(I - A^{-1}(A - A_n)),$$

and so the inverse of A_n is given by

$$A_n^{-1} = (I - A^{-1}(A - A_n))^{-1}A^{-1}.$$

Taking the norm of both sides and using (1.7) we obtain

$$\|A_n^{-1}\| \leq \frac{\|A^{-1}\|}{1 - \|A^{-1}(A_n - A)\|}.$$

Finally, to show the error estimate, subtracting the original integral equation from the approximate equation leads to

$$(\varphi_n - \varphi) = A_n^{-1}(f_n - f + (A - A_n)),$$

and hence

$$\|\varphi_n - \varphi\| \leq C(\|(A_n - A)\varphi\| + \|f_n - f\|),$$

where

$$C = \frac{\|A^{-1}\|}{1 - \|A^{-1}(A_n - A)\|}.$$

□

Before discussing approximation through pointwise convergence, which is needed for the Nyström method, we have to introduce the notion of collectively compact operators and some theorems.

DEFINITION 1.6. Collectively compact operators A set $\mathcal{A} = \{A : X \to Y\}$ of linear operators mapping a normed space X into a normed space Y is called collectively compact if for each bounded set $U \subset X$ the image set $\mathcal{A}(U) = \{A\varphi : \varphi \in U, A \in \mathcal{A}\}$ is relatively compact.

THEOREM 1.7. *(Convergence property of collectively compact operators)*
Let X be a Banach space and let $A_n : X \to X$ be collectively compact and pointwise convergent sequence with limit operator $A : X \to X$. Then

$$\|(A_n - A)A\| \to 0, \quad \textit{and} \quad \|(A_n - A)A_n\| \to 0, \quad n \to \infty.$$

□

The following theorem is a well-know result from functional analysis.

THEOREM 1.8. *(Fredholm alternative)*
Let $A : X \to X$ be a compact linear operator on a normed space X. Then $I - A$ is injective if and only if it is surjective. If $I - A$ is injective (and therefore also bijective), then the inverse operator $(I - A)^{-1} : X \to X$ is bounded, i.e. $I - A$ is an isomorpism.

□

We now give the describe approximation through pointwise convergence for second kind integral equations.

THEOREM 1.9. *(Approximation through pointwise convergence)*
Let $A : X \to X$ be a compact linear operator in a Banach space X and let $I - A$ be injective. Assume the sequence $A_n : X \to X$ is collectively compact and pointwise convergent, i.e. $A_n\varphi \to A\varphi$ as $n \to \infty$ for all $\varphi \in X$. Then for sufficiently large n, more precisely, for all n such that

$$\|(I-A)^{-1}(A_n - A)A_n\| < 1,$$

the inverse operators $(I - A_n)^{-1} : X \to X$ exist and are bounded by

$$\|(I - A_n)^{-1}\| \leq \frac{1 + \|(I-A)^{-1}A_n\|}{1 - \|(I-A)^{-1}(A_n - A)A_n\|}.$$

For the solutions of the equations

$$\varphi - A\varphi = f, \qquad \varphi_n - A_n\varphi_n = f_n,$$

we have the estimate

$$\|\varphi_n - \varphi\| \leq C(\|(A_n - A)\varphi\| + \|f_n + f\|).$$

PROOF. The estimate for pointwise convergence is clearly highly analogous to the estimate for convergence in norm.

As A is compact and $I - A$ is injective, by the Fredholm alternative 1.8, $(I - A)^{-1}$ exists and and is bounded. Then $(I - A)^{-1} = I + (I - A)^{-1}A$ suggests an approximate inverse B_n for $I - A_n$, i.e.

$$B_n(I - A_n) = I - S_n, \tag{1.8}$$

where

$$B_n := I + (I-A)^{-1}A_n, \qquad S_n := (I-A)^{-1}(A_n - A)A_n.$$

It can be shown from (1.8) that $I - A_n$ is injective, i.e. $(I - A_n)[\varphi] = 0$ if and only if $\varphi = 0$. As $I - A_n$ is injective, and A_n is compact, since it is an element of a collectively compact sequence, its inverse $(I - A_n)^{-1}$ exists by the Fredhom alternative 1.8.

From (1.8) we find

$$(I - A_n)^{-1} = (I - S_n)^{-1}B_n.$$

For n sufficiently large, by the convergence property of collectively compact operators 1.7 we have $\|S_n\| < 1$. Therefore we can use the Neumann series theorem 1.4 to estimate

$$\|(I - S_n)^{-1}\| \leq \frac{1}{1 - \|S_n\|}.$$

Using the expressions we have for B_n and S_n this gives

$$\|(I - A_n)^{-1}\| = \|(I - S_n)^{-1}B_n\| \leq \frac{1 + \|(I-A)^{-1}A_n\|}{1 - \|(I-A)^{-1}(A_n - A)A_n\|}.$$

Finally, subtracting the original integral equation from the approximate equation leads to

$$(\varphi_n - \varphi) = (I - A_n)^{-1}(f_n - f + (A - A_n)\varphi),$$

and hence

$$\|\varphi_n - \varphi\| \leq C(\|(A_n - A)\varphi\| + \|f_n - f\|),$$

where
$$C = \frac{1 + \|(I-A)^{-1}A_n\|}{1 - \|(I-A)^{-1}(A_n - A)A_n\|}.$$
□

1.4. The Nyström method

Using the results from the previous section, we will discuss the key points in the classical convergence theory for the Nyström method in the case of second kind integral equations with continuous kernels. Note that the layer potentials we defined previously do not have continuous kernels, i.e. they are singular when $x = y$. Many methods for handling singular kernels have been proposed in the literature, and the convergence theory for these methods is highly specific to the methods themselves. In any case, the aim of research into Nyström methods for weakly singular integral equations is to try and recover the efficiency of the method for continuous kernels. For further details see **[1, 2]**.

The Nyström method is based on two key ideas:

- using quadrature formulas to approximate the integrals in a boundary integral equation;
- requiring that the integral equation is satisfied at each of the discretization points.

1.4.1. Quadrature. Let $Q[g]$ be the integral defined by
$$Q[g] := \int_G w(x)g(x)dx,$$
where w is some weight function and $g \in C(G)$, with G some compact set. We define the quadrature rule $Q_n[g]$ by
$$Q_n[g] := \sum_{k=1}^{n} \alpha_k^{(n)} g(x_k^{(n)}) \approx \int_G w(x)g(x)dx = Q[g],$$
where $x_j^{(n)}$ are quadrature points in G and $\alpha_j^{(n)}$ are quadrature weights, for $j = 1, \ldots, n$. In the Nyström method we approximate integral operators using such quadrature rules. That is, we approximate the integral operator
$$A\varphi(x) := \int_G K(x,y)\varphi(y)dy, \quad x \in G,$$
where K is a continuous kernel, by a sequence of numerical integration operators
$$A_n\varphi(x) := \sum_{k=1}^{n} \alpha_k^{(n)} K(x, y_k^{(n)})\varphi(y_k^{(n)}), \quad x \in G,$$
Then we approximate the solution φ of the equation
$$\varphi(x) - A\varphi(x) = f(x), \qquad x \in G$$
by the solution φ_n of the equation
$$\varphi_n(x) - A_n\varphi_n(x) = f(x), \qquad x \in G.$$

In fact, it turns out that sovling the above approximate equation merely at the discretization points $x_1, \ldots, x_n$ is equivalent to solving it for all $x \in G$. This means that the Nyström method ultimately results in an $n \times n$ linear system that can be solved straightforward computationally.

THEOREM 1.10. *(Solution with Nyström method is equivalent to solution of linear system)*
Let φ_n be a solution of

$$\varphi_n(x) = \sum_{k=1}^{n} \alpha_k K(x, y_k^{(n)}) \varphi(y_k^{(n)}) = f(x), \qquad x \in G.$$

Then the values $\varphi_j^{(n)} = \varphi_n(x_j)$, at the quadrature points satisfy the linear system

$$\varphi_j^{(n)} = \sum_{k=1}^{n} \alpha_k K(x, y_k^{(n)}) \varphi(y_k^{(n)}) = f(x_j), \qquad j = 1, \dots, n.$$

Conversely, let $\varphi_j^{(n)}$, $j = 1, \dots, n$ be a solution of the previous equation. Then then function φ_n satisfies the problem

$$\varphi_n(x) = \sum_{k=1}^{n} \alpha_k K(x, y_k^{(n)}) \varphi(y_k^{(n)}) = f(x), \qquad x \in G.$$

□

We now prove that the sequence of integral operators A_n converge pointwise to the original operator A, but not in norm. It follows that the Nyström method not converge in norm.

THEOREM 1.11. *(Boundary integral operators converge pointwise, but not in norm)*

Assume that the quadrature formulas (Q_n) are convergent. Then the sequence (A_n) is collectively compact and pointwise convergent, i.e. $A_n\varphi \to A\varphi$, $n \to \infty$, for all $\varphi \in C(G)$, but not norm convergent.

PROOF. As the quadrature formulas (Q_n) that underline the approximation are convergent by assumption, it can be shown that there exists a constant C such that the weights $\alpha_j^{(n)}$ satisfy

$$C := \sup_{n \in \mathbb{N}} \sum_{j=1}^{n} |\alpha_j^{(n)}|,$$

for all $n \in \mathbb{N}$. Therefore we have the estimates

$$\|A_n \varphi\|_\infty \le C \max_{x,y \in G} |K(x,y)| \, \|\varphi\|_\infty, \tag{1.9}$$

and

$$|(A_n\varphi)(x_1) - (A_n\varphi)(x_2)| \le C \max_{y \in G} |K(x_1, y) - K(x_2, y)| \, \|\varphi\|_\infty, \tag{1.10}$$

for all $x_1, y_1 \in G$. Now let $U \subset C(G)$ be bounded, i.e. we only consider the bounded continuous functions. Equations (1.9) and (1.9) show that the set

$$\{A_n\varphi : \varphi \in U, n \in \mathbb{N}\}$$

is bounded and (uniformly) equicontinuous, because K is uniformly continuous on $G \times G$, i.e. because it is a continuous function on a compact set. By the Arzelá-Ascoli theorem this means that each operator A_n for $n \in \mathbb{N}$ is compact, and hence the sequence (A_n) is collectively compact.

Now, since the underlying quadrature is convergent by assumption, for fixed $\varphi \in G$, the sequence $(A_n\varphi)$ is pointwise convergent, i.e. $(A_n\varphi)(x) \to (A\varphi)(x)$ as $n \to \infty$. We already had that $(A_n\varphi)$ is equicontinuous. It holds that if a sequence is pointwise convergent and equicontinuous then it is uniformly convergent, and therefore we have

$$\|A_n\varphi - A\varphi\|_\infty \to 0, n \to \infty,$$

for any $\varphi \in C(G)$, i.e. we have pointwise convergence of A_n to A.

Finally, we show that the sequence (A_n) is not norm convergent. Let $\varepsilon > 0$ and choose a function $\psi_\varepsilon \in C(G)$ with $0 \leq \psi_\varepsilon(x) \leq 1$ for all $x \in G$ such that $\varphi_\varepsilon = 1$ for all $x \in G$ with $\min_{j=1,\dots,n} |x - x_j| \geq \varepsilon$ and $\psi_\varepsilon(x_j) = 0$, $j = 1, \dots, n$. Then

$$\|A\varphi\Psi_\varepsilon - A\varphi\|_\infty \leq \max_{x,y \in G} |K(x,y)| \int_G (1 - \Psi_\varepsilon) dy \to 0, \qquad \varepsilon \to 0,$$

for all $\varphi \in C(G)$ with $\|\varphi\|_\infty = 1$. Using this result, we can derive

$$\begin{aligned}
\|A - A_n\|_\infty &= \sup_{\|\varphi\|_\infty = 1} \|(A - A_n)\varphi\|_\infty \\
&\geq \sup_{\|\varphi\|_\infty = 1} \sup_{\varepsilon > 0} \|(A - A_n)\varphi\Psi_\varepsilon\|_\infty \\
&= \sup_{\|\varphi\|_\infty = 1} \sup_{\varepsilon > 0} \|A\varphi\Psi_\varepsilon\|_\infty \\
&= \sup_{\|\varphi\|_\infty = 1} \|A\varphi\|_\infty \\
&= \|A\|,
\end{aligned}$$

and hence the sequence (A_n) does not converge in norm. □

THEOREM 1.12. *(Nyström method converges uniformly)*
For a uniquely solveable integral equation of the second kind with a continuous kernel and a continuous right-hand side, the Nyström method with a convergent sequence of quadrature formulas is uniformly convergent.

PROOF. As the underlying quadrature is convergent by assumption, by Theorem 1.11 the sequence A_n is collectively compact and pointwise converges to A. Hence we can apply Theorem 1.9 to obtain

$$\|\varphi_n - \varphi\| \leq C(\|(A_n - A)\varphi\| + \|f_n - f\|),$$

where

$$C = \frac{1 + \|(I - A)^{-1}A_n\|}{1 - \|(I - A)^{-1}(A_n - A)A_n\|}.$$

This means that the solution of the Nyström method φ_n converges uniformly to φ. □

REMARK 1.13. It is worth mentioning that Nyström method inherits the converge order of the underlying quadrature rule used. When we deal with boundary integral equations we are dealing with periodic functions. It is well-known that for periodic analytic functions, exponential convergence of quadrature is achievable for the simple composite Trapezoidal rule. One recently proposed quadrature scheme worth highlighting that takes advantage of this fact, is Quadrature by Expansion (QBX) [**3**], which delivers high-order convergence for boundary integral operators with singular kernels.

1.5. Muller's Method

Muller's method is an efficient and reliable interpolation method for finding a zero of a function defined on the complex plane and, in particular, for determining a simple or multiple root of a polynomial. Compared to Newton's method, it has the advantage that the derivatives of the function need not be computed.

Muller's method can be viewed as a generalization of the secant method. The secant method is based on taking two points on the graph of a function f, and then finding an approximate root by determining the root of a linear function that passes through these two points. Muller's method, on the other hand, is based on taking three points on the graph of a function f, and then finding an approximate root by determining the root of a quadratic function that passes through these three points.

Denote by $Q_f(z)$ the quadratic interpolating polynomial for the function f that passes through the points $(z_0, f(z_0))$, $(z_1, f(z_1))$, and $(z_2, f(z_2))$, i.e.

$$Q_f(z) = a(z - z_2)^2 + b(z - z_2) + c,$$

with

$$\begin{aligned}
f(z_0) &= a(z_0 - z_2)^2 + b(z_0 - z_2) + c,\\
f(z_1) &= a(z_1 - z_2)^2 + b(z_1 - z_2) + c,\\
f(z_2) &= a(z_2 - z_2)^2 + b(z_2 - z_2) + c.
\end{aligned}$$

Solving for a, b, and c we obtain

$$\begin{aligned}
a &= \frac{(z_1 - z_2)(f(z_0) - f(z_2)) - (z_0 - z_2)(f(z_1) - f(z_2))}{(z_0 - z_1)(z_0 - z_2)(z_1 - z_2)},\\
b &= \frac{(z_0 - z_2)^2(f(z_1) - f(z_2)) - (z_1 - z_2)^2(f(z_0) - f(z_2))}{(z_0 - z_1)(z_0 - z_2)(z_1 - z_2)},\\
c &= f(z_2).
\end{aligned}$$

To determine the root $z = z_3$ of $Q(z)$, let $\tilde{z} = z_3 - z_2$, and then

$$Q_f(z_3) = a\tilde{z}^2 + b\tilde{z} + c = 0$$

can be solved using the quadratic formula. For numerical stability we use the following version of the quadratic formula:

$$\tilde{z} = \frac{-2c}{b \pm \sqrt{b^2 - 4ac}},$$

where the sign of the square root is chosen so as to maximize the absolute value of the denominator. This means that the root z_3 of $Q_f(z)$, which is the next approximation of an actual root of $f(z)$, is given by

$$z_3 = z_2 + \frac{2c}{b \pm \sqrt{b^2 - 4ac}}.$$

Once z_3 has been found we set $z_i = z_{1+1}$, for $i = 0, 1, 2$. We then repeat this procedure, which results in a sequence of approximate roots, until specific termination criteria are reached; we terminate the procedure when $f(z_3) < \tau_f$ and $|z_3 - z_2| < \tau_z$, where τ_f and τ_z are some given tolerances for the value of f at the root z_3, and the distance between the roots on successive iterations, respectively.

It can be shown that the errors $\delta_i = (z_i - \xi)$ of Muller's method in the proximity of a single zero ξ of $f(z) = 0$ satisfy

$$\delta_{i+1} = \delta_i \delta_{i-1} \delta_{i-2} \bigg(- \frac{f^{(3)}(\xi)}{6f'(\xi)} + O(\delta) \bigg),$$

where $\delta = \max(|\delta_i|, |\delta_{i-1}|, |\delta_{i-2}|)$. It can also be shown that Muller's method is at least of order the largest root q of the equation $\zeta^3 - \zeta^2 - \zeta - 1 = 0$, which is approximately 1.84.

The Matlab code is at Muller's Method. As an illustration, we consider the complex valued function

$$f(z) = \sin(z) + 5 + \sqrt{-1},$$

whose exact roots are given by $z_\alpha = 2\pi n - \sin^{-1}(5 + \sqrt{-1})$ or $z_\beta = 2\pi n + \pi + \sin^{-1}(5 + \sqrt{-1})$ for $n \in \mathbb{Z}$. We can obtain the roots of this function numerically using the code referenced above. For instance, if we take $n = 0$ then the exact root (to eight decimal places) is $z_\alpha = -1.36960125 - 2.31322094\sqrt{-1}$. Choosing appropriate initial guesses, say, $z_0 = 0.5$, $z_1 = 1 + 3\sqrt{-1}$, and $z_2 = -1 - 2\sqrt{-1}$, our numerical result for this root is also $-1.36960125 - 2.31322094\sqrt{-1}$.

1.6. Neumann-Poincaré operator

Resonance is a physical property that is of importance in many fields. In the case of photonics resonance is responsible for interesting phenomena such as enhanced scattering and absorption of light. A proper understanding of the resonance characteristics of a system paves the way for super-resolution and superfocusing using plasmonic nanoparticles; the fabrication of metamaterials that can manipulate propagating waves in ways not possible in naturally occurring materials; and the design of photonic crystals that can prevent the propagation of waves in certain frequency ranges.

In order to mathematically formulate these concepts we must first characterize the spectral properties of the Neumann-Poincaré operator. We will see that in the case of simple domains, such as a disk in $\mathbb{R}^2$ or a ball in $\mathbb{R}^3$, an explicit representation can be found for the Neumann-Poincaré operator, which we can then use to obtain explicit representations for its eigenvalues and eigenfunctions.

Let us define the operator $\mathcal{K}_\Omega^0 : L^2(\partial\Omega) \to L^2(\partial\Omega)$ by

$$\mathcal{K}_\Omega^0[\varphi](x) := \frac{1}{\omega_d} \text{p.v.} \int_{\partial\Omega} \frac{\langle y - x, \nu(y) \rangle}{|x - y|^d} \varphi(y)\, d\sigma(y),$$

where p.v. stands for the Cauchy principal value. We then define the Neumann-Poincaré operator $(\mathcal{K}_\Omega^0)^*$ to be the L^2-adjoint of $\mathcal{K}_\Omega^0$ which is given by

$$(\mathcal{K}_\Omega^0)^*[\varphi](x) = \frac{1}{\omega_d} \text{p.v.} \int_{\partial\Omega} \frac{\langle x - y, \nu(x) \rangle}{|x - y|^d} \varphi(y)\, d\sigma(y), \quad \varphi \in L^2(\partial\Omega).$$

If $\partial\Omega$ is of class $\mathcal{C}^{1,\eta}$ for some $\eta > 0$, then the operators $\mathcal{K}_\Omega^0$ and $(\mathcal{K}_\Omega^0)^*$ are compact in $L^2(\partial\Omega)$.

Now suppose that Ω is a two-dimensional disk with radius r_0. Then for $x \in \partial\Omega$ we have $\nu_x = x/|x| = x/r_0$ and therefore $\forall\, x, y \in \partial\Omega, x \neq y$ we have

$$\frac{< x - y, \nu_x >}{|x-y|^2} = \frac{(x-y)\cdot x}{|x-y|^2 r_0} = \frac{|x|^2 - x\cdot y}{(|x|^2 - 2x\cdot y + |y|^2) r_0}.$$

Noting that $|x| = |y|$ on $\partial\Omega$ we obtain

$$\frac{|x|^2 - x\cdot y}{(|x|^2 - 2x\cdot y + |y|^2) r_0} = \frac{|x|^2 - x\cdot y}{2(|x|^2 - x\cdot y) r_0} = \frac{1}{2r_0}. \tag{1.11}$$

Therefore, for any $\phi \in L^2(\partial\Omega)$,

$$(\mathcal{K}_\Omega^0)^*[\phi](x) = \mathcal{K}_\Omega[\phi](x) = \frac{1}{4\pi r_0}\int_{\partial\Omega}\phi(y)\, d\sigma(y)\ , \tag{1.12}$$

for all $x \in \partial\Omega$. Similarly for $d \geq 3$, if Ω is a ball with radius r_0, then we have

$$\frac{< x-y, \nu_x >}{|x-y|^d} = \frac{1}{2r_0}\frac{1}{|x-y|^{d-2}} \quad \forall\, x, y \in \partial\Omega, x \neq y\ ,$$

and for any $\phi \in L^2(\partial\Omega)$ and $x \in \partial\Omega$,

$$(\mathcal{K}_\Omega^0)^*[\phi](x) = \mathcal{K}_\Omega[\phi](x) = \frac{(2-d)}{2r_0}\mathcal{S}_\Omega^0[\phi](x).$$

In the case of an ellipse we can also a find simplified representation of the Neumann-Poincaré operator. Let Ω be an ellipse whose semi-axes are on the x_1- and x_2-axes and of length a and b, respectively. Using the parametric representation $X(t) = (a\cos t, b\sin t), 0 \leq t \leq 2\pi$, for the boundary $\partial\Omega$, we have that

$$\mathcal{K}_\Omega[\phi](x) = \frac{ab}{2\pi(a^2+b^2)}\int_0^{2\pi}\frac{\phi(X(t))}{1 - Q\cos(t+\theta)}\, dt, \tag{1.13}$$

where $x = X(\theta)$ and $Q = (a^2 - b^2)/(a^2 + b^2)$.

1.6.1. Symmetrization of the Neumann-Poincaré operator. Although $(\mathcal{K}_\Omega^0)^*$ is compact in $L^2(\partial\Omega)$ it is not self-adjoint which prevents us from obtaining a spectral decomposition of the operator. This can be remedied through symmetrization. For $\Omega \in \mathbb{R}^3$ the single layer potential is a unitary operator from $H^{-1/2}(\partial\Omega)$ onto $H^{1/2}(\partial\Omega)$ and by symmetrizing $(\mathcal{K}_\Omega^0)^*$ using the Calderon's identity

$$\mathcal{S}_\Omega^0(\mathcal{K}_\Omega^0)^* = \mathcal{K}_\Omega^0\mathcal{S}_\Omega^0 \quad \text{on } H^{-1/2}(\partial\Omega),$$

we can make $(\mathcal{K}_\Omega^0)^*$ self-adjoint. Let $\mathcal{H}^*(\partial\Omega)$ be the space $H^{-1/2}(\partial\Omega)$ with the inner product

$$< u, v >_{\mathcal{H}^*} = - < \mathcal{S}_\Omega^0[v], u >_{\frac{1}{2},-\frac{1}{2}}\ ,$$

which is equivalent to the original one (on $H^{-1/2}(\partial\Omega)$). In two dimensions complications arise as the single layer potential may not be invertible nor injective. In order to make $(\mathcal{K}_\Omega^0)^*$ self-adjoint we can still use the symmetrization approach but first we must define a substitute for the single layer potential. We define $\widetilde{\mathcal{S}}_\Omega[\psi]$ by

$$\widetilde{\mathcal{S}}_\Omega[\psi] = \begin{cases} \mathcal{S}_\Omega^0[\psi] & \text{if } < \chi(\partial\Omega), \psi >_{\frac{1}{2},-\frac{1}{2}} = 0\,, \\ -\chi(\partial\Omega) & \text{if } \psi = \varphi_0\,, \end{cases}$$

where φ_0 is the unique eigenfunction of $(\mathcal{K}^0_\Omega)^*$ associated with eigenvalue $1/2$ such that $< \chi(\partial\Omega), \varphi_0 >_{\frac{1}{2},-\frac{1}{2}} = 1$. Note that, from the jump relations of the layer potentials, $\mathcal{S}^0_\Omega[\varphi_0]$ is constant.

The operator $\widetilde{\mathcal{S}}_\Omega : H^{-1/2}(\partial\Omega) \to H^{1/2}(\partial\Omega)$ is invertible. Moreover, a similar Calderón identity to the one for the three dimensional case holds: $\mathcal{K}^0_\Omega \widetilde{\mathcal{S}}_\Omega = \widetilde{\mathcal{S}}_\Omega (\mathcal{K}^0_\Omega)^*$. With this, define

$$< u, v >_{\mathcal{H}^*} = - < \widetilde{\mathcal{S}}_\Omega[v], u >_{\frac{1}{2},-\frac{1}{2}} .$$

Thanks to the invertibility and positivity of $-\widetilde{\mathcal{S}}_\Omega$, this defines an inner product for which $(\mathcal{K}^0_\Omega)^*$ is self-adjoint and $\mathcal{H}^*$ is equivalent to $H^{-1/2}(\partial\Omega)$. Then, if Ω is $\mathcal{C}^{1,\eta}$, $\eta > 0$, we have the following results:

Let $d = 2$. Let Ω be a $\mathcal{C}^{1,\eta}, \eta > 0$, bounded simply connected domain of $\mathbb{R}^2$ and let $\widetilde{\mathcal{S}}_\Omega$ be the operator defined in (1.6.1). Then,

(i) The operator $(\mathcal{K}^0_\Omega)^*$ is compact self-adjoint in the Hilbert space $\mathcal{H}^*(\partial\Omega)$ equipped with the inner product defined by

$$< u, v >_{\mathcal{H}^*} = - < \widetilde{\mathcal{S}}_D[v], u >_{\frac{1}{2},-\frac{1}{2}} ;$$

(ii) Let (λ_j, φ_j), $j = 0, 1, 2, \ldots$, be the eigenvalue and normalized eigenfunction pair of $(\mathcal{K}^0_\Omega)^*$ with $\lambda_0 = \frac{1}{2}$. Then, $\lambda_j \in (-\frac{1}{2}, \frac{1}{2}]$ and $\lambda_j \to 0$ as $j \to \infty$;

(iii) $\mathcal{H}^*(\partial\Omega) = \mathcal{H}^*_0(\partial\Omega) \oplus \{\mu\varphi_0,\ \mu \in \mathbb{C}\}$, where $\mathcal{H}^*_0(\partial\Omega)$ is the zero mean subspace of $\mathcal{H}^*(\partial\Omega)$;

(iv) The following representation formula holds: for any $\psi \in H^{-1/2}(\partial\Omega)$,

$$(\mathcal{K}^0_\Omega)^*[\psi] = \sum_{j=0}^{\infty} \lambda_j < \varphi_j, \psi >_{\mathcal{H}^*} \ \varphi_j . \tag{1.14}$$

When Ω is a disk, using (1.11) and (1.12), it is clear that if we take ψ to be constant, then the spectrum of $(\mathcal{K}^0_\Omega)^*$ is $\{0, 1/2\}$. If Ω is an ellipse of semi-axes a and b, then

$$\lambda_j = \begin{cases} \dfrac{1}{2} & j = 0, \\ \pm\dfrac{1}{2}\left(\dfrac{a-b}{a+b}\right)^j & j \geq 1, \end{cases} \tag{1.15}$$

are the eigenvalues of $(\mathcal{K}^0_\Omega)^*$, which can be expressed by (1.13).

Next we consider the case when Ω represents two separated disks. Let $\Omega = B_1 \cup B_2$ where B_j is a circular disk of radius r. Let $\epsilon > 0$ be the distance between the two disks, that is, $\epsilon := \mathrm{dist}(B_1, B_2)$. Set

$$\alpha = \sqrt{\epsilon(r + \frac{\epsilon}{4})} \quad \text{and} \quad \xi_0 = \sinh^{-1}\left(\frac{\alpha}{r}\right), \quad \text{for } j = 1, 2, \tag{1.16}$$

where r is the radii of the two disks and ϵ is their separation distance. For the two disks Ω, the associated NP-operator is defined as follows:

$$\mathbb{K}^* := \begin{bmatrix} (\mathcal{K}^0_{B_1})^* & \dfrac{\partial}{\partial\nu^{(1)}}\mathcal{S}^0_{B_2} \\ \dfrac{\partial}{\partial\nu^{(2)}}\mathcal{S}^0_{B_1} & (\mathcal{K}^0_{B_2})^* \end{bmatrix} .$$

Here, $\nu^{(i)}$ is the outward normal on ∂B_i, $i = 1,2$. Again, this is not self-adjoint in $L^2(\partial B_1) \times L^2(\partial B_2)$. However we can symmetrize it by introducing the new inner product defined by

$$\langle \varphi, \psi \rangle_{\mathcal{H}^*} := -\langle \varphi, \mathbb{S}[\psi] \rangle,$$

where the operator $\mathbb{S}$ is given as

$$\mathbb{S} = \begin{bmatrix} \mathcal{S}_{B_1} & \mathcal{S}_{B_2} \\ \mathcal{S}_{B_1} & \mathcal{S}_{B_2} \end{bmatrix}.$$

It can be shown that the eigenvalues of $\mathbb{K}^*$ on $\mathcal{H}_0^*$ are given by

$$\lambda^{\pm}_{\epsilon,j} = \pm \frac{1}{2} e^{-2|j|\xi_0}, \quad j \in \mathbb{Z}. \tag{1.17}$$

We will demonstrate these formulas along with some applications of the Neumann-Poincaré through numerical simulation in MatLab. First though we must discuss the discretization of $(\mathcal{K}^0_\Omega)^*$.

1.7. Numerical representation

In order to utilize the Neumann-Poincaré operator in applications we must define an appropriate numerical representation for it. We first partition $\partial\Omega \in \mathbb{R}^2$ into N sections

$$[x^{(1)}, x^{(2)}], [x^{(2)}, x^{(3)}], \dots, [x^{(N-1)}, x^{(N)}], [x^{(N)}, x^{(1)}],$$

where the section $[x^{(i)}, x^{(j)}]$ is represented by the point $x^{(i)} = (x_1^{(i)}, x_2^{(i)}) \in \partial\Omega \subset \mathbb{R}^2$.

We approximate ψ on each section $[x^{(i)}, x^{(j)}]$ with its projection $\overline{\psi}_i := \langle \psi, \delta_{x^{(i)}} \rangle = \psi(x^{(i)})$ onto a dirac delta basis at $x^{(i)}$. So we are representing $\psi \in L^2(\partial\Omega)$ with the piecewise constant function $\overline{\psi} \in L^2(\partial\Omega)$.

We represent the infinite dimensional operator $(\mathcal{K}^0_\Omega)^*$ acting on the function ψ by a finite dimensional matrix K acting on the coefficient vector $c = (\overline{\psi}_1, \overline{\psi}_2, \dots, \overline{\psi}_N)$. That is

$$(\mathcal{K}^0_\Omega)^*[\psi](x) = \frac{1}{2\pi} \text{p.v.} \int_{\partial\Omega} \Gamma_0(x,y)\psi(y)\, d\sigma(y), \quad \psi \in L^2(\partial\Omega),$$

has the numeric representation

$$Kc = \begin{pmatrix} \alpha_{11} & a_{12} & \cdots & \alpha_{1N} \\ \alpha_{21} & \alpha_{22} & \cdots & \alpha_{2N} \\ \vdots & & \ddots & \vdots \\ \alpha_{N1} & \cdots & \cdots & \alpha_{NN} \end{pmatrix} \begin{pmatrix} \overline{\psi}_1 \\ \overline{\psi}_2 \\ \vdots \\ \overline{\psi}_N \end{pmatrix},$$

where

$$\alpha_{ij} = \Gamma_0(x^{(i)}, x^{(j)}) = \frac{1}{2\pi} \frac{\langle x^{(i)} - x^{(j)}, \nu(x^{(i)}) \rangle}{|x^{(i)} - x^{(j)}|^2} \sigma(x^{(j)}) \quad i \neq j,$$

and $\sigma(x^{(i)})$ represents the magnitude of the section $[x^{(i)}, x^{(i+1)}]$. If we parametrize $\partial\Omega$ as $x(t), t \in [0, 2\pi]$ with a uniform discretization in t, we have

$$\sigma(x^{(i)}) = \frac{2\pi |T(x^{(i)})|}{\text{N}},$$

with $T(x_i)$ being the tangent vector at $x^{(i)}$ in this parametrization.

1.7.1. Handling singularities on the diagonal. Complications arise in the diagonal terms of K as we have a singularity whenever $i = j$. Handling singularities in the diagonal terms of a matrix is an issue that we encounter frequently when working with discretized operators in photonics. The problematic variable is

$$\frac{\langle x^{(i)} - x^{(j)}, \nu(x^{(i)})\rangle}{|x^{(i)} - x^{(j)}|^2},$$

when $i = j$. In order to derive an expression for this term consider an arc in our partition of $\partial\Omega$ with end-points $x^{(i)}$ and $x^{(i+1)}$. These points can expressed as a parameterization of the boundary by $x^{(i)} := r(t)$ and $x^{(i+1)} := r(t+h)$. Let us denote by

$$\begin{aligned}
T^{(i)} &= T(t) = r'(t), \\
\nu^{(i)} &= \nu(t), \\
a^{(i)} &= a(t) = r''(t) = a_T(t)T(t) + a_\nu(t)\nu(t),
\end{aligned}$$

the tangent vector, the unit normal vector, and the acceleration vector respectively. Taylor expanding $r(t+h)$ gives

$$r(t+h) = r(t) + T(t)h + \frac{h^2}{2}a(t) + \mathcal{O}(h^3).$$

By taking the projection of both sides of the equation with the normal vector the tangential terms vanish and we have

$$\begin{aligned}
\langle r(t+h) - r(t), \nu(t)\rangle &= \frac{h^2}{2}\langle a_\nu(t)\nu(t), \nu(t)\rangle + \mathcal{O}(h^3) \\
&= \frac{h^2}{2}a_\nu(t) + o(h^3)
\end{aligned}$$

Finally, upon observing that

$$\begin{aligned}
|x^{(i)} - x^{(i+1)}|^2 &= |r(t+h) - r(t)|^2 \\
&= |hT(t)|^2 + \mathcal{O}(h^3)
\end{aligned}$$

we obtain that as $h \to 0$

$$\begin{aligned}
\frac{\langle x^{(i)} - x^{(i+1)}, \nu(x^{(i)})\rangle}{|x^{(i)} - x^{(i+1)}|^2} &= \frac{\langle r(t) - r(t+h), \nu(t)\rangle}{(h|T(t)|)^2} \\
&= -\frac{\langle a^{(i)}, \nu^{(i)}\rangle}{2|T^{(i)}|^2},
\end{aligned}$$

which means we have found an appropriate expression for the diagonal terms of K. When we encounter periodic and quasi-periodic operators later in the course we will also need to account for the periodicity when deriving the diagonal terms.

1.8. Numerical illustrations of the spectrum

We now present some examples that demonstrate the spectrum of the Neumann-Poincaré operator in various situations.

1.8.1. Spectrum of the Neumann-Poincaré operator for an ellipse.

Code:	1.2 Neumann Poincare Operator	DemoSpectrumEllipse.m

We first compute the spectrum of $(\mathcal{K}_\Omega^0)^*$ for an ellipse with semi-axes $a = 10$, and $b = 1$. Table1.1 compares the first few eigenvalues obtained numerically with the eigenvalues obtained via the formula given in (1.15).

Theoretical	Numerical
0.5000	0.5000
0.4091	0.4091
-0.4091	-0.4091
0.3347	0.3347
-0.3347	-0.3347
0.2739	0.2739
-0.2739	-0.2739
0.2241	0.2241

TABLE 1.1. Spectrum of the Neumann-Poincaré operator for an ellipse.

1.8.2. Spectrum of the Neumann-Poincaré operator for two disks.

Code:	1.2 Neumann Poincare Operator	DemoSpectrumTwoCircles.m

We now compute the spectrum of $(\mathcal{K}_\Omega^0)^*$ for two disks with $r = 2$, and $\epsilon = 0.3$. Table1.2 compares the first few eigenvalues obtained numerically with the eigenvalues obtained via the formula given in (1.17).

Theoretical	Numerical
0.5000	0.5000
0.5000	0.5000
-0.2315	-0.2315
-0.2315	-0.2315
0.2315	0.2315
0.2315	0.2315
-0.1072	-0.1072
-0.1072	-0.1072

TABLE 1.2. Spectrum of the Neumann-Poincaré operator for two disks.

1.8.3. Conductivity Problem.

Code:	1.2 Neumann Poincare Operator	DemoConductivitySolver.m

Let B be a Lipschitz bounded domain in $\mathbb{R}^d$ and suppose that the origin $O \in B$. Let $0 < k \neq 1 < +\infty$ and denote $\lambda(k) := (k+1)/(2(k-1))$. Let h be a harmonic function in $\mathbb{R}^d$, and let u be the solution to the following transmission problem in free space:

$$\begin{cases} \nabla \cdot ((1 + (k-1)\chi(B))\nabla u_k) = 0 \quad \text{in } \mathbb{R}^d, \\ u_k(x) - h(x) = O(|x|^{1-d}) \quad \text{as } |x| \to +\infty. \end{cases} \tag{1.18}$$

It can be shown that the solution $u_k(x)$ of this problem is given by

$$u_k(x) = h(x) + \mathcal{S}_B^0[\phi](x) \quad \text{for } x \in \mathbb{R}^d, \tag{1.19}$$

where $\phi \in L_0^2(\partial D)$ satisfies

$$(\lambda I - (\mathcal{K}_B^0)^*)[\phi] = \frac{\partial h}{\partial \nu}|_{\partial B}.$$

Therefore,

$$\phi = (\lambda I - (\mathcal{K}_B^0)^*)^{-1}[\frac{\partial h}{\partial \nu}|_{\partial, B}].$$

and the problem essentially reduces to inverting the operator $\lambda I - (\mathcal{K}_B^0)^*$. Note that the spectrum of λ lies in the interval $]-1/2, 1/2]$. We also have that $\lambda I - (\mathcal{K}_B^0)^*$ is one to one on $L_0^2(\partial D)$ if $|\lambda| \geq 1/2$, and for $\lambda \in]-\infty, -1/2] \cup]1/2, +\infty[$, $\lambda I - (\mathcal{K}_B^0)^*$ is one to one on $L^2(\partial D)$.

With a particular choice of parameters we can obtain an explicit solution to this problem. Let B be a disk of radius $R = 5$ located at the origin in $\mathbb{R}^2$. Let us take the conductivity in B to be $k = 3$ which means $\lambda = 1$. We also assume that $h(x) = x_1$. It can be shown that the explicit solution is given by

$$u(r,\theta) = \begin{cases} r\cos(\theta) - \dfrac{k-1}{k+1} R^2 r^{-1} \cos(\theta), & |r| > R, \\ \dfrac{2}{k+1} r\cos(\theta), & |r| \leq R, \end{cases} \tag{1.20}$$

where (r, θ) are the polar coordinates.

Likewise, we can obtain a numerical solution by using Equation (4.2). This involves inverting the operator $\lambda I - (\mathcal{K}_B^0)^*$ which is possible in this case as $\lambda = 1$. A comparison between the exact solution and the numerical solution is shown in Figure 1.1. We evaluate the solution $u(x)$ on the circle $|x| = 10$.

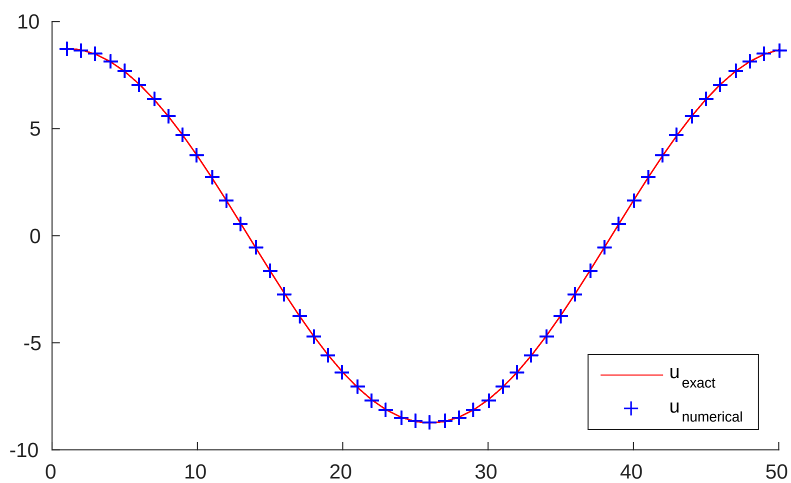

FIGURE 1.1. The exact solution u_e and the numerical solution u_n of the conductivity problem (4.1) evaluated on the circle $|x| = 10$.

CHAPTER 2

Eigenvalues of the Laplacian and Their Perturbations

In this section we transform eigenvalue problems of $-\Delta$ on an open bounded connected domain Ω, with either Neumann, Dirichlet, Robin or mixed boundary conditions, into the determination of the characteristic values of certain integral operator-valued functions in the complex plane. This results in a considerable advantage as it allows us to reduce the dimension of the eigenvalue problem. After discretization of the kernels of the integral operators, the problem can be turned into a complex root finding process for a scalar function. Many tools are available for finding complex roots of scalar functions. Muller's method described in Section 1.5 is both efficient and robust.

Moreover, with the help of the generalized argument principle, the integral formulations can also be used to study perturbations of the eigenvalues with respect to changes in Ω as we will see in Subsection 2.4. Furthermore, the splitting problem in the evolution of multiple eigenvalues can be easily handled. In Subsection 2.4.2 we present a method for performing sensitivity analysis of multiple eigenvalues with respect to changes in Ω which relies upon finding a polynomial of degree equal to the geometric multiplicity of the eigenvalue such that its zeros are precisely the perturbations.

2.1. Layer potentials for the Helmholtz equation

In this section we review a number of basic facts and results regarding the layer potentials associated with the Helmholtz equation. The integral equations that correspond to the eigenvalue problem will be obtained from a study of these layer potentials.

2.1.1. Fundamental Solution. For $\omega > 0$, a fundamental solution $\Gamma_\omega(x)$ to the Helmholtz operator $\Delta + \omega^2$ in $\mathbb{R}^d$, $d = 2, 3$, is given by

$$\Gamma_\omega(x) = \begin{cases} -\dfrac{i}{4} H_0^{(1)}(\omega|x|)\,, & d = 2, \\ -\dfrac{e^{i\omega|x|}}{4\pi|x|}\,, & d = 3, \end{cases} \tag{2.1}$$

for $x \neq 0$, where $H_0^{(1)}$ is the Hankel function of the first kind of order 0. The only relevant fact we shall recall here is the following behavior of the Hankel function near 0:

$$-\frac{i}{4} H_0^{(1)}(\omega|x|) = \frac{1}{2\pi}\ln|x| + \tau + \sum_{n=1}^{+\infty}(b_n \ln(\omega|x|) + c_n)(\omega|x|)^{2n}, \tag{2.2}$$

where

$$b_n = \frac{(-1)^n}{2\pi} \frac{1}{2^{2n}(n!)^2}, \quad c_n = -b_n\left(\gamma - \ln 2 - \frac{\pi i}{2} - \sum_{j=1}^{n} \frac{1}{j}\right),$$

with the constant $\tau = (1/2\pi)(\ln\omega + \gamma - \ln 2) - i/4$, γ being the Euler constant.

2.1.2. Single- and Double-Layer Potentials. For a bounded Lipschitz domain Ω in $\mathbb{R}^d$ and $\omega > 0$, let $\mathcal{S}_\Omega^\omega$ and $\mathcal{D}_\Omega^\omega$ be the single- and double-layer potentials defined by Γ_ω; that is,

$$\mathcal{S}_\Omega^\omega[\varphi](x) = \int_{\partial\Omega} \Gamma_\omega(x-y)\varphi(y)\,d\sigma(y), \quad x \in \mathbb{R}^d, \tag{2.3}$$

$$\mathcal{D}_\Omega^\omega[\varphi](x) = \int_{\partial\Omega} \frac{\partial\Gamma_\omega(x-y)}{\partial\nu(y)}\varphi(y)\,d\sigma(y)\;, \quad x \in \mathbb{R}^d \setminus \partial\Omega, \tag{2.4}$$

for $\varphi \in L^2(\partial\Omega)$. Then $\mathcal{S}_\Omega^\omega[\varphi]$ and $\mathcal{D}_\Omega^\omega[\varphi]$ satisfy the Helmholtz equation

$$(\Delta + \omega^2)u = 0 \quad \text{in } \Omega \text{ and in } \mathbb{R}^d \setminus \overline{\Omega}.$$

Moreover, both of them satisfy the Sommerfeld radiation condition, namely,

$$\left|\frac{\partial u}{\partial r} - i\omega u\right| = O\left(r^{-(d+1)/2}\right) \quad \text{as } r = |x| \to +\infty \quad \text{uniformly in } \frac{x}{|x|}. \tag{2.5}$$

Let us make note of a Green's formula to be used later. If $(\Delta + \omega^2)u = 0$ in Ω and $\partial u/\partial\nu \in L^2(\partial\Omega)$, then

$$-\mathcal{S}_\Omega^\omega\left[\frac{\partial u}{\partial\nu}\Big|_-\right](x) + \mathcal{D}_\Omega^\omega[u](x) = \begin{cases} u(x), & x \in \Omega, \\ 0, & x \in \mathbb{R}^d \setminus \overline{\Omega}. \end{cases} \tag{2.6}$$

The following formulas give the jump relations obeyed by the double-layer potential and by the normal derivative of the single-layer potential on general Lipschitz domains:

$$\frac{\partial(\mathcal{S}_\Omega^\omega[\varphi])}{\partial\nu}\bigg|_\pm(x) = \left(\pm\frac{1}{2}I + (\mathcal{K}_\Omega^\omega)^*\right)[\varphi](x) \quad \text{a.e. } x \in \partial\Omega, \tag{2.7}$$

$$(\mathcal{D}_\Omega^\omega[\varphi])\bigg|_\pm(x) = \left(\mp\frac{1}{2}I + \mathcal{K}_\Omega^\omega\right)[\varphi](x) \quad \text{a.e. } x \in \partial\Omega, \tag{2.8}$$

for $\varphi \in L^2(\partial\Omega)$, where $\mathcal{K}_\Omega^\omega$ is the singular integral operator defined by

$$\mathcal{K}_\Omega^\omega[\varphi](x) = \text{p.v.}\int_{\partial\Omega} \frac{\partial\Gamma_\omega(x-y)}{\partial\nu(y)}\varphi(y)\,d\sigma(y)$$

and $(\mathcal{K}_\Omega^\omega)^*$ is the L^2-adjoint of $\mathcal{K}_\Omega^{-\omega}$, that is,

$$(\mathcal{K}_\Omega^\omega)^*[\varphi](x) = \text{p.v.}\int_{\partial\Omega} \frac{\partial\Gamma_\omega(x-y)}{\partial\nu(x)}\varphi(y)d\sigma(y).$$

Moreover, for $\varphi \in H^{\frac{1}{2}}(\partial\Omega)$,

$$\frac{\partial}{\partial\nu}\mathcal{D}_\Omega^\omega[\varphi]\bigg|_-(x) = \frac{\partial}{\partial\nu}\mathcal{D}_\Omega^\omega[\varphi]\bigg|_+(x) \quad \text{in } H^{-\frac{1}{2}}(\partial\Omega). \tag{2.9}$$

The singular integral operators $\mathcal{K}_\Omega^\omega$ and $(\mathcal{K}_\Omega^\omega)^*$ are bounded on $L^2(\partial\Omega)$. Since $\Gamma_\omega(x) - \Gamma_0(x) = C + O(|x|)$ as $|x| \to 0$ where C is constant, we deduce that

$\mathcal{K}_\Omega^\omega - \mathcal{K}_\Omega^0$ is bounded from $L^2(\partial\Omega)$ into $H^1(\partial\Omega)$ and hence is compact on $L^2(\partial\Omega)$. If Ω is $\mathcal{C}^{1,\eta}$, $\eta > 0$, then $\mathcal{K}_\Omega^0$ itself is compact on $L^2(\partial\Omega)$ and so is $\mathcal{K}_\Omega^\omega$.

2.2. Laplace eigenvalues

2.2.1. Eigenvalue Characterization. We first restrict our attention to the three-dimensional case. We note that because of the holomorphic dependence of Γ_ω as given in (2.1), $\mathcal{K}_\Omega^\omega$ is an operator-valued holomorphic function in $\mathbb{C}$. Indeed, the following result holds.

PROPOSITION 2.1 (Neumann Eigenvalue characterization). *Suppose that Ω is of class $\mathcal{C}^{1,\eta}$ for some $\eta > 0$. Let $\omega > 0$. Then ω^2 is an eigenvalue of $-\Delta$ on Ω with Neumann boundary condition if and only if ω is a positive real characteristic value of the operator $-(1/2)\, I + \mathcal{K}_\Omega^\omega$.*

PROOF. Suppose that ω^2 is an eigenvalue of

$$\begin{cases} \Delta u + \omega^2 u = 0 & \text{in } \Omega, \\ \dfrac{\partial u}{\partial \nu} = 0 & \text{on } \partial\Omega. \end{cases} \tag{2.10}$$

By Green's formula, we have

$$u(x) = \mathcal{D}_\Omega^\omega[u|_{\partial\Omega}](x), \quad x \in \Omega.$$

It then follows from the jump relations that $(-I/2 + \mathcal{K}_\Omega^\omega)[u|_{\partial\Omega}] = 0$ and $u|_{\partial\Omega} \neq 0$ since otherwise the unique continuation property for $\Delta + \omega^2$ would imply that $u \equiv 0$ in Ω. Thus ω is a characteristic value of $\mathcal{A}(\omega) := -(1/2)\, I + \mathcal{K}_\Omega^\omega$.

Suppose now that ω is a characteristic value of $-(1/2)\, I + \mathcal{K}_\Omega^\omega$; *i.e.*, there is a nonzero $\psi \in L^2(\partial\Omega)$ such that

$$\left(-\frac{1}{2} I + \mathcal{K}_\Omega^\omega\right)[\psi] = 0.$$

Then $u = \mathcal{D}_\Omega^\omega[\psi]$ on $\mathbb{R}^d \setminus \overline{\Omega}$ is a solution to the Helmholtz equation with the boundary condition $u|_+ = 0$ on $\partial\Omega$ and satisfies the radiation condition (2.5). The uniqueness of the Helmholtz equation implies that $\mathcal{D}_\Omega^\omega[\psi] = 0$ in $\mathbb{R}^d \setminus \overline{\Omega}$. Since $\partial\mathcal{D}_\Omega^\omega[\psi]/\partial\nu$ exists and has no jump across $\partial\Omega$, we get

$$\frac{\partial \mathcal{D}_\Omega^\omega[\psi]}{\partial \nu}\Big|_+ = \frac{\partial \mathcal{D}_\Omega^\omega[\psi]}{\partial \nu}\Big|_- \quad \text{on } \partial\Omega.$$

Hence, we deduce that $\mathcal{D}_\Omega^\omega[\psi]$ is a solution of (2.10). Note that $\mathcal{D}_\Omega^\omega[\psi] \neq 0$ in Ω, since otherwise

$$\psi = \mathcal{D}_\Omega^\omega[\psi]\big|_- - \mathcal{D}_\Omega^\omega[\psi]\big|_+ = 0.$$

Thus ω^2 is an eigenvalue of $-\Delta$ on Ω with Neumann condition, and so the proposition is proved. $\square$

Proposition 2.1 asserts that $-(1/2)\, I + \mathcal{K}_\Omega^\omega$ is invertible on $L^2(\partial\Omega)$ for all positive ω except for a discrete set. The following result shows that $(-(1/2)\, I + \mathcal{K}_\Omega^\omega)^{-1}$ has a continuation to an operator-valued meromorphic function on $\mathbb{C}$.

PROPOSITION 2.2. *$-(1/2)\, I + \mathcal{K}_\Omega^\omega$ is invertible on $L^2(\partial\Omega)$ for all $\omega \in \mathbb{C}$ except for a discrete set, and $(-(1/2)\, I + \mathcal{K}_\Omega^\omega)^{-1}$ is an operator-valued meromorphic function on $\mathbb{C}$.*

In the two-dimensional case, Proposition 2.1 holds true. Moreover, due to the logarithmic behavior of the Hankel function, $(-(1/2)\, I + \mathcal{K}_\Omega^\omega)^{-1}$ has a continuation to an operator-valued meromorphic function on only $\mathbb{C} \setminus i\mathbb{R}^-$.

2.2.2. Eigenvalues in Circular Domains. Let κ_{nm} be the positive zeros of $J_n(z)$ (Dirichlet), $J_n'(z)$ (Neumann), and $J_n'(z) + \lambda J_n(z)$ (Robin). The index $n = 0, 1, 2, \ldots$ counts the order of Bessel functions of the first kind J_n while $m = 1, 2, \ldots$ counts their positive zeros. The rotational symmetry of a disk $\Omega = \{x : |x| < R\}$ of radius R leads to an explicit representation of the eigenfunctions in polar coordinates:

$$u_{nml}(r, \theta) = J_n(\frac{\kappa_{nm} r}{R}) \times \begin{cases} \cos(n\theta), & l = 1, \\ \sin(n\theta), & l = 2 \ (n \neq 0). \end{cases} \tag{2.11}$$

The eigenvalues of $-\Delta$ on Ω are given by κ_{nm}^2 / R^2. They are independent of the index l. They are simple for $n = 0$ and twice degenerate for $n > 0$. In the latter case, the eigenfunction is any nontrivial linear combination of u_{nm1} and u_{nm2}.

2.3. Numerical implementation

2.3.1. Discretization of the operator $\mathcal{K}_\Omega^\omega$. Similarly to the case of the Neumann-Poincaré operator $(\mathcal{K}_\Omega^0)^*$ in Section 1.7 we must now define an appropriate numerical representation for the operator $\mathcal{K}_\Omega^\omega$.

Suppose that the boundary $\partial\Omega$ is parametrized by $x(t)$ for $t \in [0, 2\pi)$. We first partition the interval $[0, 2\pi)$ into N pieces

$$[t_1, t_2), [t_2, t_3), \ldots, [t_N, t_{N+1}),$$

with $t_1 = 0$ and $t_{N+1} = 2\pi$. We then approximate the boundary $\partial\Omega = \{x(t) : t \in [0, 2\pi)\}$ by $x^{(i)} = x(t_i)$ for $1 \le i \le N$.

We approximate the density function φ with $\overline{\varphi}_i := \varphi(x^{(i)})$. We represent the infinite dimensional operator $\mathcal{K}_\Omega^\omega$ by a finite dimensional matrix K. That is

$$\begin{aligned} \mathcal{K}_\Omega^\omega[\varphi](x) &= \int_{\partial\Omega} \frac{\partial \Gamma_\omega}{\partial \nu_y}(x, y) \varphi(y)\, d\sigma(y) \\ &= \int_{\partial\Omega} \frac{i}{4} H_1^{(1)}(\omega |x - y|) \omega \frac{\langle y - x, \nu_y \rangle}{|y - x|} \varphi(y) d\sigma(y) \end{aligned}$$

for $\psi \in L^2(\partial\Omega)$. It has the numeric representation

$$K\tilde{\psi} = \begin{pmatrix} K_{11} & K_{12} & \cdots & K_{1N} \\ K_{21} & K_{22} & \cdots & K_{2N} \\ \vdots & & \ddots & \vdots \\ K_{N1} & \cdots & \cdots & K_{NN} \end{pmatrix} \begin{pmatrix} \overline{\varphi}_1 \\ \overline{\varphi}_2 \\ \vdots \\ \overline{\varphi}_N \end{pmatrix},$$

where

$$K_{ij} = \frac{i}{4} H_1^{(1)}(\omega |x^{(i)} - x^{(j)}|) \omega \frac{\langle x^{(j)} - x^{(i)}, \nu_y \rangle}{|x^{(j)} - x^{(i)}|} |T(x^{(j)})| (t_{j+1} - t_j) \quad i \neq j,$$

with $T(x^{(i)})$ being the tangent vector at $x^{(i)}$.

Note that in the above representation, the case when $i = j$ is not covered. Recall that $\Gamma_0(x) = \frac{1}{2\pi} \ln |x|$ and in Subsection 1.7.1 we showed how to compute the diagonal elements in the case of the Neumann-Poincaré operator $(\mathcal{K}_\Omega^0)^*$. In view of (2.2), the kernel $\partial\Gamma_\omega/\partial\nu_y(x,y)$ has the same singularity as that of the Neumann-Poincaré operator. Therefore using the following formula allows us to compute the diagonal elements of K:

$$\lim_{y\to x}\frac{\partial\Gamma_\omega}{\partial\nu_y}(x,y)=\frac{1}{4\pi}\frac{\langle a(x),\nu(x)\rangle}{|T(x)|^2}.$$

2.3.2. Finding the eigenvalue by Muller's method.

Code:	2.1 Eigenvalues of the Laplacian	DemoCharDisk.m

We will now now describe how to compute the Laplace eigenvalues (or the characteristic values of $\mathcal{A}(\omega)$) using Muller's method and then present an example. Let us define a function $f:\mathbb{C}\to\mathbb{C}$ such that $f(z)$ is the smallest eigenvalue of $\mathcal{A}(z)$. This means that $f(\omega)=0$ whenever ω is a characteristic value of $\mathcal{A}$. By applying Muller's method to the equation $f(z)=0$ we can compute the characteristic value ω of $\mathcal{A}$.

Now we present a numerical example. Assume that Ω is a unit disk. We discretize the boundary $\partial\Omega$ with $N=500$ points. As discussed previously, characteristic values are zeros of $J_n'(z)=0$. The first zero is approximately 1.8412. Upon computing a characteristic value near 1.8 using Muller's method we find that there is a good agreement with the exact value, as can be seen in Table 2.1.

Theoretical	Numerical
$1.8412+0.0000i$	$1.8421-0.0026i$

TABLE 2.1. Characteristic value of $\mathcal{A}$ near 1.8.

2.4. Perturbation of Laplace eigenvalues

2.4.1. Shape derivative of the Laplace eigenvalues. In this subsection, we compute shape derivatives of Laplace eigenvalues by using the generalized argument principle. Let Ω be a bounded domain of class $\mathcal{C}^2$. We consider Neumann eigenvalues in the two-dimensional case and let Ω_ϵ be given by

$$\partial\Omega_\epsilon=\left\{\tilde{x}:\tilde{x}=x+\epsilon h(x)\nu(x),\ x\in\partial\Omega\right\},$$

where $h\in\mathcal{C}^2(\partial\Omega)$ and $0<\epsilon\ll 1$.

To fix ideas, we set μ_j for $j>1$ to be a Neumann eigenvalue of $-\Delta$ on Ω and consider the integral operator-valued function

$$\omega\mapsto\mathcal{A}_\epsilon(\omega):=-\frac{1}{2}I+\mathcal{K}^\omega_{\Omega_\epsilon},\tag{2.12}$$

when ω is in a small complex neighborhood of $\sqrt{\mu_j}$.

By using the compactness of $\mathcal{K}^\omega_{\Omega_\epsilon}$ and the analyticity of $H_0^{(1)}$ in $\mathbb{C}\setminus i\mathbb{R}^-$, the following results hold.

LEMMA 2.3. *The operator-valued function $\mathcal{A}_\epsilon(\omega)$ is Fredholm analytic with index* 0 *in $\mathbb{C}\setminus i\mathbb{R}^-$ and $(\mathcal{A}_\epsilon)^{-1}(\omega)$ is a meromorphic function. If ω is a real characteristic value of the operator-valued function $\mathcal{A}_\epsilon$ (or equivalently, a real pole of $(\mathcal{A}_\epsilon)^{-1}(\omega)$), then there exists j such that $\omega=\sqrt{\mu_j^\epsilon}$.*

LEMMA 2.4. *Any $\sqrt{\mu_j}$ is a simple pole of the operator-valued function $(\mathcal{A}_0)^{-1}(\omega)$.*

PROOF. We define $\phi(\omega)$ as the root function corresponding to $\sqrt{\mu_j}$ as a characteristic value of $\mathcal{A}_0(\omega)$. Recall that the multiplicity of $\phi(\omega)$ is the order of $\sqrt{\mu_j}$ as a zero of $\mathcal{A}_0(\omega)\phi(\omega)$. Since the order of $\sqrt{\mu_j}$ as a pole of $(\mathcal{A}_0)^{-1}(\omega)$ is precisely the maximum of the ranks of eigenvectors in $\mathrm{Ker}\mathcal{A}_0(\sqrt{\mu_j})$, it suffices to show that the rank of an arbitrary eigenvector is equal to one. Let us write

$$\mathcal{A}_0(\omega)\phi(\omega) = (\omega^2 - \mu_j)\psi(\omega),$$

where $\psi(\omega)$ is a holomorphic function in $L^2(\partial\Omega)$. For ω in a small neighborhood V_{δ_0} of $\sqrt{\mu_j}$, we denote by $u(\omega)$ the unique solution to

$$\begin{cases} (\Delta + \omega^2)u(\omega) = 0 \quad \text{in } \Omega, \\ \frac{\partial u}{\partial \nu} = (\omega^2 - \mu_j)\psi(\omega) \quad \text{on } \partial\Omega, \end{cases}$$

Integrating by parts over Ω, we find that

$$\int_\Omega u(\omega)\overline{u(\sqrt{\mu_j})}dx = \int_{\partial\Omega} \psi(\omega)\overline{u(\sqrt{\mu_j})}d\sigma,$$

which implies that

$$\int_{\partial\Omega} \psi(\sqrt{\mu_j})\overline{u(\sqrt{\mu_j})}d\sigma = 1,$$

since $\omega \mapsto \int_\Omega u(\omega)\overline{u(\sqrt{\mu_j})}dx$ is holomorphic in V_{δ_0}. Therefore, $\int_{\partial\Omega} |\psi(\sqrt{\mu_j})|^2 \neq 0$ and thus, the function $\psi(\sqrt{\mu_j})$ is not trivial. $\square$

LEMMA 2.5. *Let $\omega_0 = \sqrt{\mu_j}$ and suppose that μ_j is simple. Then there exists a positive constant δ_0 such that for $|\delta| < \delta_0$, the operator-valued function $\omega \mapsto \mathcal{A}_\epsilon(\omega)$ has exactly one characteristic value in $\overline{V_{\delta_0}}(\omega_0)$, where $V_{\delta_0}(\omega_0)$ is a disk of center ω_0 and radius $\delta_0 > 0$. This characteristic value is analytic with respect to ϵ in $]-\epsilon_0, \epsilon_0[$. Moreover, the following assertions hold:*

(i) $\mathcal{M}(\mathcal{A}_\epsilon(\omega); \partial V_{\delta_0}) = 1$,
(ii) $(\mathcal{A}_\epsilon)^{-1}(\omega) = (\omega - \omega_\epsilon)^{-1}\mathcal{L}_\epsilon + \mathcal{R}_\epsilon(\omega)$,
(iii) $\mathcal{L}_\epsilon : Ker((\mathcal{A}_\epsilon(\omega_\epsilon))^*) \to Ker(\mathcal{A}_\epsilon(\omega_\epsilon))$,

where $\mathcal{R}_\epsilon(\omega)$ is a holomorphic function with respect to $(\epsilon, \omega) \in]-\epsilon_0, \epsilon_0[\times V_{\delta_0}(\omega_0)$ and $\mathcal{L}_\epsilon$ is a finite-dimensional operator.

PROOF. Note that the kernel of $\mathcal{K}_{\Omega_\epsilon}^{\omega}$ is jointly analytic with respect to ϵ in $]-\epsilon_0, \epsilon_0[$ and $\omega \in V_{\delta_0}$ for ϵ_0 and δ_0 small enough. Since μ_j is simple, it is clear that $\mathcal{M}(\mathcal{A}_\epsilon(\omega); \partial V_{\delta_0}) = 1$. Furthermore, from Lemmas 2.3 and 2.4, it follows that

$$(\mathcal{A}_\epsilon)^{-1}(\omega) = (\omega - \omega_\epsilon)^{-1}\mathcal{L}_\epsilon + \mathcal{R}_\epsilon(\omega),$$

where

$$\mathcal{L}_\epsilon : Ker((\mathcal{A}_\epsilon(\omega_\epsilon))^*) \to Ker(\mathcal{A}_\epsilon(\omega_\epsilon))$$

is a finite-dimensional operator and $\mathcal{R}_\epsilon(\omega)$ is a holomorphic function with respect to (ϵ, ω). $\square$

Let $\omega_0 = \sqrt{\mu_j}$ and suppose that μ_j is simple. Then, from the generalized argument principle it follows that $\omega_\epsilon = \sqrt{\mu_j^\epsilon}$ is given by

$$\omega_\epsilon - \omega_0 = \frac{1}{2i\pi} \operatorname{tr} \int_{\partial V_{\delta_0}} (\omega - \omega_0) \mathcal{A}_\epsilon(\omega)^{-1} \frac{d}{d\omega} \mathcal{A}_\epsilon(\omega) d\omega. \tag{2.13}$$

We will need an asymptotic expansion of the operator $\mathcal{K}_{\Omega_\epsilon}^\omega$ as follows:

$$\mathcal{K}_{\Omega_\epsilon}^\omega[\tilde{\phi}] \circ \Psi_\epsilon = \mathcal{K}_\Omega^\omega[\phi] + \epsilon \mathcal{K}_\Omega^{(1)}[\phi] + O(\epsilon^2), \tag{2.14}$$

where Ψ_ϵ is a diffeomorphism which is given by $\Psi_\epsilon(x) = x + \epsilon h(x)\nu(x)$ and the explicit expression of the operator $\mathcal{K}_\Omega^{(1)}$ is given in subsection 2.4.3. We then obtain the following shape derivative of the Neumann eigenvalues.

THEOREM 2.6 (Shape derivative of Neumann eigenvalues). *The following asymptotic expansion holds:*

$$\sqrt{\mu_j^\epsilon} - \sqrt{\mu_j} = -\epsilon \frac{1}{2i\pi} \operatorname{tr} \int_{\partial V_{\delta_0}} \mathcal{A}_0(\omega)^{-1} \mathcal{K}_\Omega^{(1)}(\omega) d\omega + O(\epsilon^2), \tag{2.15}$$

where V_{δ_0} is a disk of center $\sqrt{\mu_j}$ and radius δ_0 small enough, $\mathcal{A}_0(\omega) = -(1/2)I + \mathcal{K}_\Omega^\omega$ and $\mathcal{K}_\Omega^{(1)}(\omega)$ is given by (2.21).

PROOF. If ϵ is small enough, then the following expansion is uniform with respect to ω in ∂V_{δ_0}:

$$\mathcal{A}_\epsilon(\omega)^{-1} = \mathcal{A}_0(\omega)^{-1} - \epsilon \mathcal{A}_0(\omega)^{-1} \mathcal{K}_\Omega^{(1)}(\omega) \mathcal{A}_0(\omega)^{-1} + O(\epsilon^2),$$

and therefore,

$$\begin{aligned} \omega_\epsilon - \omega_0 \quad = \quad & \frac{1}{2i\pi} \operatorname{tr} \int_{\partial V_{\delta_0}} (\omega - \omega_0) \Big[\mathcal{A}_0(\omega)^{-1} \frac{d}{d\omega} \mathcal{A}_0(\omega) \\ & - \epsilon \mathcal{A}_0(\omega)^{-1} \mathcal{K}_\Omega^{(1)}(\omega) \mathcal{A}_0(\omega)^{-1} \frac{d}{d\omega} \mathcal{A}_0(\omega) + \epsilon \mathcal{A}_0(\omega)^{-1} \frac{d}{d\omega} \mathcal{K}_\Omega^{(1)}(\omega) \Big] d\omega + O(\epsilon^2). \end{aligned}$$

Because of Lemma 2.4, ω_0 is a simple pole of $\mathcal{A}_0(\omega)^{-1}$ and $\mathcal{A}_0(\omega)$ is analytic, and hence we get

$$\int_{\partial V_{\delta_0}} (\omega - \omega_0) \mathcal{A}_0(\omega)^{-1} \frac{d}{d\omega} \mathcal{A}_0(\omega) d\omega = 0. \tag{2.16}$$

Moreover, by using the property $\operatorname{tr} \int AB = \operatorname{tr} \int BA$ of the trace together with the identity

$$\frac{d}{d\omega} \mathcal{A}_0(\omega)^{-1} = -\mathcal{A}_0(\omega)^{-1} \frac{d\mathcal{A}_0}{d\omega}(\omega) \mathcal{A}_0(\omega)^{-1}, \tag{2.17}$$

we arrive at

$$\omega_\epsilon - \omega_0 = \epsilon \frac{1}{2i\pi} \operatorname{tr} \int_{\partial V_{\delta_0}} (\omega - \omega_0) \frac{d}{d\omega} \left[\mathcal{A}_0^{-1}(\omega) \mathcal{K}_\Omega^{(1)}(\omega) \right] d\omega.$$

Now, a simple integration by parts yields the desired result. □

2.4.2. Splitting of Multiple Eigenvalues. The main difficulty in deriving asymptotic expansions of perturbations in multiple eigenvalues of the unperturbed configuration relates to their continuation. Multiple eigenvalues may evolve, under perturbations, as separated, distinct eigenvalues, and the splitting may only become apparent at high orders in their Taylor expansions with respect to the perturbation parameter.

In this subsection, as an example, we address the splitting problem in the evaluation of perturbations of the Neumann eigenvalues due to shape deformations. Our approach applies to the other eigenvalue perturbation problems as well.

Let ω_0^2 denote an eigenvalue of the Neumann problem for $-\Delta$ on Ω with geometric multiplicity m. We call the ω_0-group the totality of the perturbed eigenvalues ω_ϵ^2 of $-\Delta$ on Ω_ϵ for $\epsilon > 0$ that are generated due to the splitting of ω_0^2.

In exactly the same way as Lemma 2.5 we can show that the eigenvalues are precisely the characteristic values of $\mathcal{A}_\epsilon$ defined by (2.12). We then proceed from the generalized argument principle to investigate the splitting problem.

LEMMA 2.7. *Let $\omega_0 = \sqrt{\mu_j}$ and suppose that μ_j is a multiple Neumann eigenvalue of $-\Delta$ on Ω with geometric multiplicity m. Then there exists a positive constant δ_0 such that for $|\delta| < \delta_0$, the operator-valued function $\omega \mapsto \mathcal{A}_\epsilon(\omega)$ defined by (2.12) has exactly m characteristic values (counted according to their multiplicity) in $\overline{V_{\delta_0}}(\omega_0)$, where $V_{\delta_0}(\omega_0)$ is a disk of center ω_0 and radius $\delta_0 > 0$. These characteristic values form the ω_0-group associated to the perturbed eigenvalue problem and are analytic with respect to ϵ in $]-\epsilon_0, \epsilon_0[$. They satisfy $\omega_\epsilon^i|_{\epsilon=0} = \omega_0$ for $i = 1, \ldots, m$. Moreover, if $(\omega_\epsilon^i)_{i=1}^n$ denotes the set of distinct values of $(\omega_\epsilon^i)_{i=1}^m$, then the following assertions hold:*

(i) $\mathcal{M}(\mathcal{A}_\epsilon(\omega); \partial V_{\delta_0}) = \displaystyle\sum_{i=1}^n \mathcal{M}(\mathcal{A}_\epsilon(\omega_\epsilon^i); \partial V_{\delta_0}) = m$,

(ii) $(\mathcal{A}_\epsilon)^{-1}(\omega) = \displaystyle\sum_{i=1}^n (\omega - \omega_\epsilon^i)^{-1} \mathcal{L}_\epsilon^i + \mathcal{R}_\epsilon(\omega)$,

(iii) $\mathcal{L}_\epsilon^i : Ker((\mathcal{A}_\epsilon(\omega_\epsilon^i))^*) \to Ker(\mathcal{A}_\epsilon(\omega_\epsilon^i))$,

where $\mathcal{R}_\epsilon(\omega)$ is a holomorphic function with respect to $\omega \in V_{\delta_0}(\omega_0)$ and $\mathcal{L}_\epsilon^i$ for $i = 1, \ldots, n$ is a finite-dimensional operator. Here $\mathcal{M}(\mathcal{A}_\epsilon(\omega_\epsilon^i); \partial V_{\delta_0})$ is defined by

$$\mathcal{M}(A(z); \partial V) = \sum_{i=1}^{\sigma} M(A(z_i)). \tag{2.18}$$

Let, for $l \in \mathbb{N}$, $a_l(\epsilon)$ denote

$$a_l(\epsilon) = \frac{1}{2\pi i} \operatorname{tr} \int_{\partial V_{\delta_0}} (\omega - \omega_0)^l \mathcal{A}_\epsilon(\omega)^{-1} \frac{d}{d\omega} \mathcal{A}_\epsilon(\omega) d\omega.$$

By the generalized argument principle, we find

$$a_l(\epsilon) = \sum_{i=1}^m (\omega_\epsilon^i - \omega_0)^l \quad \text{for } l \in \mathbb{N}.$$

We can prove the following asymptotic expansion of $a_l(\epsilon)$ in the same manner as Theorem 2.6, THEOREM 2.8. *The following asymptotic expansion holds:*

$$a_l(\epsilon) = \epsilon \frac{1}{2i\pi} \operatorname{tr} \int_{\partial V_{\delta_0}} l(\omega - \omega_0)^{l-1} \mathcal{A}_0(\omega)^{-1} \mathcal{K}_\Omega^{(1)}(\omega) d\omega + O(\epsilon^2), \tag{2.19}$$

where V_{δ_0} is a disk of center $\sqrt{\mu_j}$ and radius δ_0 small enough, $\mathcal{A}_0(\omega) = -(1/2)I + \mathcal{K}_\Omega^\omega$ and $\mathcal{K}_\Omega^{(1)}(\omega)$ is given by (2.21).

The following theorem holds.

THEOREM 2.9 (Splitting of a multiple eigenvalue). *There exists a polynomial-valued function $\omega \mapsto Q_\epsilon(\omega)$ of degree m and of the form*

$$Q_\epsilon(\omega) = \omega^m + c_1(\epsilon)\omega^{m-1} + \ldots + c_i(\epsilon)\omega^{m-i} + \ldots + c_m(\epsilon)$$

such that the perturbations $\omega_\epsilon^i - \omega_0$ are precisely its zeros. The polynomial coefficients $(c_i)_{i=1}^m$ are given by the recurrence relation

$$a_{l+m} + c_1 a_{l+m-1} + \ldots + c_m a_l = 0 \quad \textit{for } l = 0, 1, \ldots, m-1.$$

Based on Theorem 2.9, our strategy for deriving asymptotic expansions of the perturbations $\omega_\epsilon^i - \omega_0$ relies on finding a polynomial of degree m such that its zeros are precisely the perturbations $\omega_\epsilon^i - \omega_0$. We then obtain complete asymptotic expansions of the perturbations in the eigenvalues by computing the Taylor series of the polynomial coefficients.

Notice that in the cases where the multiplicity $m \in \{2, 3, 4\}$, there is no need to use Theorem 2.9, because we can explicitly obtain expressions for the perturbed eigenvalues as functions of $(a_l)_{l=1}^m$. For example, if $m = 2$ which is the case when Ω is a disk, we can easily see when the splitting occurs. It suffices that one of the terms in the expansion of $2a_2(\epsilon) - a_1^2(\epsilon)$ in terms of ϵ does not vanish. Necessarily the order of splitting is even (because of the analyticity of the eigenvalues). Let $a_j(\epsilon) = \sum_n a_{j,n}\epsilon^n$ and write

$$2a_2(\epsilon) - a_1^2(\epsilon) = \sum_{n \geq 2} \alpha_n \epsilon^n, \quad \alpha_n = 2a_{2,n} - \sum_{p=1}^{n} a_{1,p} a_{1,n-p}.$$

Suppose that the splitting order is $2s$, we obtain

$$\omega_\epsilon^j = \omega_0 + \sum_{i \geq 1} \lambda_i^{(j)} \epsilon^i, \quad j = 1, 2$$

with

$$\begin{aligned} &\lambda_i^{(1)} = \lambda_i^{(2)} \quad \text{for } i \leq 2s-1, \\ &\lambda_{2s}^{(1)} = \tfrac{a_{1,2s}}{2} - \sqrt{\alpha_{2s}}, \quad \lambda_{2s}^{(2)} = \tfrac{a_{1,2s}}{2} + \sqrt{\alpha_{2s}}. \end{aligned}$$

Explicit formulas for $\lambda_i^{(j)}$ for $j = 1, 2$, and $i \geq 2s+1$ can be obtained.

If we assume $m = 2$, then we can derive the following explicit expressions for ω_ϵ^1 and ω_ϵ^2:

$$\omega_\epsilon^i - \omega_0 = \frac{1}{2}\left(a_1(\epsilon) + (-1)^i \sqrt{2a_2(\epsilon) - a_1(\epsilon)^2} \right), \quad i \in \{1, 2\}. \tag{2.20}$$

2.4.3. Explicit expression of $\mathcal{K}_\Omega^{(1)}$. Here we present a precise expression of the operator $\mathcal{K}_\Omega^{(1)}$ which is given as follows:

$$\mathcal{K}_\Omega^{(1)}[\varphi] = \int_{\partial\Omega} k_1(x,y)\varphi(y)d\sigma(y), \tag{2.21}$$

where

$$k_1(x,y) = \frac{i\omega}{4}(L_0 M_0 N_1 + (L_0 M_1 + L_1 M_0)N_0)(x,y).$$

In the above, the functions L_0, L_1, M_0, M_1, N_0 and N_1 are given by

$$\begin{aligned}
L_0(x,y) &= H_1^{(1)}(\omega|x-y|), \quad M_0(x,y) = |x-y|, \quad N_0(x,y) = \tfrac{\langle y-x,\nu_y\rangle}{|x-y|^2},\\
L_1(x,y) &= (H_1^{(1)})'(\omega|x-y|)\frac{\langle x-y, h(x)\nu(x)-h(y)\nu(y)\rangle}{|x-y|},\\
M_1(x,y) &= \frac{\langle x-y, h(x)\nu(x)-h(y)\nu(y)\rangle}{|x-y|},\\
N_1(x,y) &= N_0(x,y)\widetilde{F}(x,y) + K_1(x,y)\\
K_1(x,y) &= \frac{\langle h(y)\nu(y)-h(x)\nu(x), \nu(y)\rangle}{|x-y|^2} - \frac{\langle y-x, \tau(y)h(y)\nu(y)+h'(y)T(y)\rangle}{|x-y|^2},\\
\widetilde{F}(x,y) &= -2M_1(x,y) + \tau(x)h(x) - \tau(y)h(y).
\end{aligned}$$

Here, $\tau(x)$ represents the curvature at the point x.

2.4.4. Numerical implementation.

Code:	2.1 Eigenvalues of the Laplacian	DemoCharPerturbed.m

We now present a numerical example for computing perturbed eigenvalues using the shape derivative. We assume Ω is a unit disk. We use the polar coordinates (r,θ) to parametrize the boundary $\partial\Omega$. For perturbation of the boundary, we set $\epsilon = 0.01$ and $h(\theta) = \cos(2\theta)$. We discretize the boundary $\partial\Omega_\epsilon$ with $N = 100$ points. By applying Muller's method, we compute the perturbed characteristic values near $\omega_0 = 0.8412....$ Then we compute their approximation by using the shape derivative. A comparison between the perturbed eigenvalues obtained via Muller's Method and approximation by the shape derivative is provided in Table 2.2.

Muller's method	Shape derivative
$1.8623 - 0.0126i$	$1.8619 + 0.0008i$
$1.8288 - 0.0126i$	$1.8204 - 0.0007i$

TABLE 2.2. Perturbed characteristic values of the operator $\mathcal{A}_\epsilon$.

CHAPTER 3

Periodic and Quasi-Periodic Green's Functions and Layer Potentials

In order to analyze structures which exhibit periodicity such as photonic crystals and metasurfaces we require periodic and quasi-periodic Green's functions. In this chapter we discuss periodic and quasi-periodic Green's function for both the Laplace equation and the Helmholtz equation in two dimensions. The periodicity can be one dimensional or two-dimensional (biperiodic).

We focus in particular on the numerical implementation of these Green's functions. Closed-form expressions of these functions are usually not attainable, instead we have representations in terms of very slowly converging infinite series which can pose a significant computational challenge. A technique for accelerating the convergence of these series is necessary in order to make their calculation feasible. The technique we use is known as Ewald's method and results in a drastic improvement in convergence speed.

We will also discuss periodic layer potentials that utilize these Green's functions and derive appropriate representations for the singular terms in their discretized form.

3.1. Periodic Green's function and layer potentials for the Laplace equation

Code:	3.1 Periodic Green's Function Laplace	DemoPerLaplaceG.m

To begin with, we consider the Green's function for the Laplace equation for a one-dimensional lattice (grating) in $\mathbb{R}^2$. Consider a function $G_\sharp : \mathbb{R}^2 \to \mathbb{C}$ satisfying

$$\Delta G_\sharp(x) = \sum_{m\in\mathbb{Z}} \delta_0(x + (m,0)). \tag{3.1}$$

We call $G_\sharp$ a periodic Green's function for the one-dimensional grating in $\mathbb{R}^2$.

LEMMA 3.1. *Let* $x = (x_1, x_2)$. *Then*

$$G_\sharp(x) = \frac{1}{4\pi} \ln\big(\sinh^2(\pi x_2) + \sin^2(\pi x_1)\big), \tag{3.2}$$

satisfies (3.1).

PROOF. We have

$$\begin{aligned} \Delta G_\sharp(x) &= \sum_{m\in\mathbb{Z}} \delta_0(x + (m,0)) \\ &= \sum_{m\in\mathbb{Z}} \delta_0(x_2)\delta_0(x_1 + m) \\ &= \sum_{m\in\mathbb{Z}} \delta_0(x_2) e^{i2\pi m x_1}, \end{aligned} \tag{3.3}$$

where we have used the Poisson summation formula $\sum_{m\in\mathbb{Z}} \delta_0(x_1+m) = \sum_{m\in\mathbb{Z}} e^{i2\pi m x_1}$.

On the other hand, as $G_\sharp$ is periodic in x_1 of period 1, we have

$$G_\sharp(x) = \sum_{m\in\mathbb{Z}} \beta_m(x_2) e^{i2\pi m x_1}, \tag{3.4}$$

therefore

$$\Delta G_\sharp(x) = \sum_{m\in\mathbb{Z}} (\beta_m''(x_2) + (i2\pi m)^2 \beta_m) e^{i2\pi m x_1}. \tag{3.5}$$

Comparing (3.3) and (3.5) yields

$$\beta_m''(x_2) + (i2\pi m)^2 \beta_m = \delta_0(x_2). \tag{3.6}$$

A solution to the previous equation can be found by using standard techniques for ordinary differential equations. We have

$$\begin{aligned}
\beta_0 &= \frac{1}{2}|x_2| + c,\\
\beta_m &= \frac{-1}{4\pi|m|} e^{-2\pi|m||x_2|}, \quad n \neq 0,
\end{aligned}$$

where c is a constant. Subsequently,

$$\begin{aligned}
G_\sharp(x) &= \frac{1}{2}|x_2| + c - \sum_{m\in\mathbb{Z}\setminus\{0\}} \frac{1}{4\pi|m|} e^{-2\pi|m||x_2|} e^{i2\pi m x_1}\\
&= \frac{1}{2}|x_2| + c - \sum_{m\in\mathbb{N}\setminus\{0\}} \frac{1}{2\pi m} e^{-2\pi m|x_2|} \cos(2\pi m x_1)\\
&= \frac{1}{4\pi} \ln\big(\sinh^2(\pi x_2) + \sin^2(\pi x_1)\big),
\end{aligned}$$

where we have used the summation identity (see, for instance, [**?**, pp. 813-814])

$$\begin{aligned}
\sum_{m\in\mathbb{N}\setminus\{0\}} \frac{1}{2\pi m} e^{-2\pi m|x_2|} \cos(2\pi m x_1) = \frac{1}{2}|x_2| - \frac{\ln(2)}{2\pi}\\
-\frac{1}{4\pi} \ln\big(\sinh^2(\pi x_2) + \sin^2(\pi x_1)\big),
\end{aligned}$$

and defined $c = -\dfrac{\ln(2)}{2\pi}$. □

Let us denote by $G_\sharp(x,y) := G_\sharp(x-y)$. In the following we define the one-dimensional periodic single layer potential and the one-dimensional periodic Neumann-Poincaré operator, respectively, for a bounded domain $\Omega \Subset \big(-\frac{1}{2}, \frac{1}{2}\big) \times \mathbb{R}$ which we assume to be of class $\mathcal{C}^{1,\eta}$ for some $\eta > 0$. Let

$$\begin{aligned}
\mathcal{S}_{\Omega,\sharp} : H^{-\frac{1}{2}}(\partial\Omega) &\longrightarrow H^1_{\mathrm{loc}}(\mathbb{R}^2), H^{\frac{1}{2}}(\partial\Omega)\\
\varphi &\longmapsto \mathcal{S}_{\Omega,\sharp}[\varphi](x) = \int_{\partial\Omega} G_\sharp(x,y)\varphi(y)d\sigma(y)
\end{aligned}$$

for $x \in \mathbb{R}^2, x \in \partial\Omega$ and let

$$\begin{aligned} \mathcal{K}^*_{\Omega,\sharp} : H^{-\frac{1}{2}}(\partial\Omega) &\longrightarrow H^{-\frac{1}{2}}(\partial\Omega) \\ \varphi &\longmapsto \mathcal{K}^*_{\Omega,\sharp}[\varphi](x) = \int_{\partial\Omega} \frac{\partial G_\sharp(x,y)}{\partial\nu(x)}\varphi(y)d\sigma(y) \end{aligned}$$

for $x \in \partial\Omega$. As in the previous subsections, the periodic Neumann-Poincaré operator $\mathcal{K}^*_{\Omega,\sharp}$ can be symmetrized. The following lemma holds.

LEMMA 3.2. (i) *For any $\varphi \in H^{-\frac{1}{2}}(\partial\Omega)$, $\mathcal{S}_{\Omega,\sharp}[\varphi]$ is harmonic in Ω and in $\left(-\frac{1}{2},\frac{1}{2}\right) \times \mathbb{R} \setminus \overline{\Omega}$;*

(ii) *The following trace formula holds: for any $\varphi \in H^{-\frac{1}{2}}(\partial\Omega)$,*

$$\left(-\frac{1}{2}I + \mathcal{K}^*_{\Omega,\sharp}\right)[\varphi] = \frac{\partial \mathcal{S}_{\Omega,\sharp}[\varphi]}{\partial\nu}\Big|_- ;$$

(iii) *The following Calderón identity holds: $\mathcal{K}_{\Omega,\sharp}\mathcal{S}_{\Omega,\sharp} = \mathcal{S}_{\Omega,\sharp}\mathcal{K}^*_{\Omega,\sharp}$, where $\mathcal{K}_{\Omega,\sharp}$ is the L^2-adjoint of $\mathcal{K}^*_{\Omega,\sharp}$;*

(iv) *The operator $\mathcal{K}^*_{\Omega,\sharp} : H_0^{-\frac{1}{2}}(\partial\Omega) \to H_0^{-\frac{1}{2}}(\partial\Omega)$ is compact self-adjoint equipped with the following inner product:*

$$< u, v >_{\mathcal{H}_0^*} = - < \mathcal{S}_{\Omega,\sharp}[v], u >_{\frac{1}{2},-\frac{1}{2}} \tag{3.7}$$

which makes $\mathcal{H}_0^*$ equivalent to $H_0^{-\frac{1}{2}}(\partial\Omega)$. Here, by E_0 we denote the zero-mean subspace of E.

(v) *Let (λ_j, φ_j), $j = 1, 2, \ldots$ be the eigenvalue and normalized eigenfunction pair of $\mathcal{K}^*_{\Omega,\sharp}$ in $\mathcal{H}_0^*(\partial\Omega)$, then $\lambda_j \in (-\frac{1}{2}, \frac{1}{2})$ and $\lambda_j \to 0$ as $j \to \infty$.*

PROOF. First, note that a Taylor expansion of $\sinh^2(\pi x_2) + \sin^2(\pi x_1)$ yields

$$G_\sharp(x) = \frac{\ln|x|}{2\pi} + R(x), \tag{3.8}$$

where R is a smooth function such that

$$R(x) = \frac{1}{4\pi}\ln(1 + O(x_2^2 - x_1^2)).$$

We can decompose the operators $\mathcal{S}_{\Omega,\sharp}$ and $\mathcal{K}^*_{\Omega,\sharp}$ on $\mathcal{H}_0^*(\partial\Omega)$ accordingly. Since $\mathcal{S}_{\Omega,\sharp} - \mathcal{S}^0_\Omega$ and $\mathcal{K}^*_{\Omega,\sharp} - (\mathcal{K}^0_\Omega)^*$ are smoothing operators, the proof of Lemma 3.2 follows the same arguments as those given in the previous subsections. ☐

3.1.1. Numerical implementation of the operators $\mathcal{S}_{\Omega,\sharp}$ and $\mathcal{K}^*_{\Omega,\sharp}$.

Code:	3.1 Periodic Green's Function Laplace	DemoPerLaplaceS.m DemoPerLaplaceK.m

The periodic single layer potential $\mathcal{S}_{\Omega,\sharp}$ can be represented numerically in the same fashion as described previously for the Neumann–Poincaré operator $(\mathcal{K}^0_\Omega)^*$ in Subsection 1.7. Recall that the boundary $\partial\Omega$ is parametrized by $x(t)$ for $t \in [0, 2\pi)$. After partitioning the interval $[0, 2\pi)$ into N pieces

$$[t_1, t_2), [t_2, t_3), \ldots, [t_N, t_{N+1}),$$

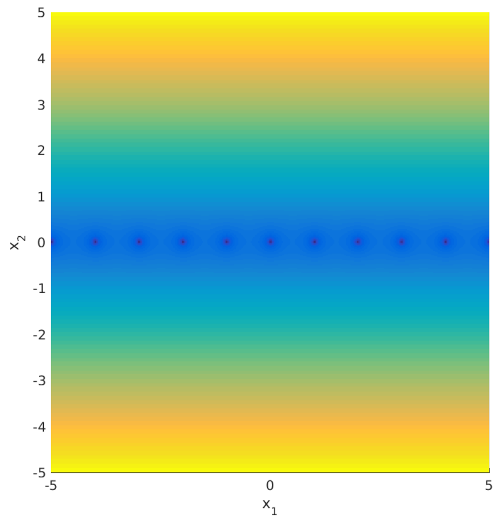

FIGURE 3.1. The periodic Greens function $G_\sharp$ with periodicity 1 for the Laplace equation.

with $t_1 = 0$ and $t_{N+1} = 2\pi$, we approximate the boundary $\partial\Omega = \{x(t) \in \mathbb{R}^2 : t \in [0, 2\pi)\}$ by $x^{(i)} = x(t_i)$ for $1 \le i \le N$. We then represent the infinite dimensional operator $\mathcal{S}_{\Omega,\sharp}$ acting on the density φ by a finite dimensional matrix S acting on the coefficient vector $\overline{\varphi}_i := \varphi(x^{(i)})$ for $1 \le i \le N$. We have

$$\mathcal{S}_{\Omega,\sharp}[\varphi](x) \quad = \int_{\partial\Omega} G_\sharp(x,y)\varphi(y)\, d\sigma(y),$$

for $\psi \in L^2(\partial\Omega)$ and we represent it numerically by

$$S\tilde{\psi} = \begin{pmatrix} S_{11} & S_{12} & \dots & S_{1N} \\ S_{21} & S_{22} & \dots & S_{2N} \\ \vdots & & \ddots & \vdots \\ S_{N1} & \dots & \dots & S_{NN} \end{pmatrix} \begin{pmatrix} \overline{\varphi}_1 \\ \overline{\varphi}_2 \\ \vdots \\ \overline{\varphi}_N \end{pmatrix},$$

where

$$S_{ij} = \frac{1}{4\pi} \ln\left(\sinh^2(\pi(x_2^{(i)} - x_2^{(j)})) + \sin^2(\pi(x_1^{(i)} - x_1^{(j)}))\right) |T(x^{(j)})|(t_{j+1} - t_j), \quad i \neq j,$$

with $T(x^{(i)})$ being the tangent vector at $x^{(i)}$. When $i = j$ we have a logarithmic singularity and therefore we must handle the diagonal terms carefully. Let us explicitly calculate the integrals for the diagonal terms. Let the portion of the boundary starting at $x^{(i)}$ and ending at $x^{(i+1)}$ be parameterized by $s \in [0, \varepsilon = \frac{2\pi}{N})$ and note that $\varepsilon \to 0$ as the number of discretization points $N \to \infty$. Therefore, using the Taylor expansion (3.8) given in the proof of Lemma 3.2 the expression we need to calculate for the diagonal terms is:

$$S_{ii} = \frac{1}{2\pi} \int_0^\varepsilon \ln(|x^{(i)} - x(s)|)|T(s)|ds.$$

Taylor expanding for small s this expression becomes

$$S_{ii} = \frac{1}{2\pi}\int_0^{\varepsilon} \ln(|x^{(i)} - (x(0) + x'(0)s + O(s^2))|)|T(0) + T'(0)s + O(s^2)|ds.$$

Noting that $x^{(i)} = x(0)$ and $T(0) = x'(0)$ we have

$$S_{ii} \approx \frac{|T(0)|}{2\pi}\int_0^{\varepsilon} \ln(|T(0)|s)ds,$$

as $\varepsilon \to 0$. As $\int_0^{\varepsilon} \ln(as)ds = \varepsilon(\ln(a\varepsilon) - 1)$ this means that

$$\begin{aligned} S_{ii} &\approx \frac{|T(0)|\varepsilon}{2\pi}\Big(\ln(|T(0)|\varepsilon) - 1\Big) \\ &= \frac{|T(0)|}{N}\left(\ln\left(\frac{2\pi}{N}|T(0)|\right) - 1\right), \end{aligned}$$

and we have found an explicit representation for the diagonal terms of the matrix S. Note that this expression also corresponds to the diagonal terms of the non-periodic single layer potential.

For the periodic Neumann–Poincaré operator $\mathcal{K}^*_{\Omega,\sharp}$, the terms of the corresponding discretization matrix K are given by

$$\begin{aligned} K_{ij} =& \frac{1}{2}\Bigg[\frac{\nu_1^{(i)}\sin(\pi\tilde{x}_1)\cos(\pi\tilde{x}_1)}{\sinh^2(\pi\tilde{x}_2) + \sin^2(\pi\tilde{x}_1)} \\ &+ \frac{\nu_2^{(i)}\sinh(\pi\tilde{x}_2)\cosh(\pi\tilde{x}_2)}{\sinh^2(\pi\tilde{x}_2) + \sin^2(\pi\tilde{x}_1)}\Bigg]|T^{(j)}|(t_{j+1} - t_j), \quad i \neq j, \end{aligned}$$

where $\tilde{x} = x^{(i)} - x^{(i+1)}$. With regard to the diagonal terms, observe that in light of (3.8) we have precisely the same singularity as for the non-periodic case and therefore we can use the same expression for the diagonal terms of the periodic version of the discretization matrix, that is:

$$K_{ii} \approx -\frac{1}{2N}\frac{\langle a^{(i)}), \nu^{(i)}\rangle}{|T^{(i)}|}. \tag{3.9}$$

The periodic Green's function $G_\sharp$, which can be seen in Figure 3.2, and the associated layer potentials $\mathcal{S}_{\Omega,\sharp}$ and $\mathcal{K}^*_{\Omega,\sharp}$ are implemented in Code Periodic Green's Function Laplace.

3.2. Quasi-periodic Green's function and layer potentials for the Helmholtz equation

We now discuss the quasi-periodic and quasi-biperiodic Green's functions for the Helmholtz equation along with their corresponding layer potentials. Both of these functions contain infinite series that suffer from extremely slow convergence and thus require acceleration prior to numerical implementation. We use Ewald's method to achieve this acceleration.

There are numerous variants of Ewald's method as it can be applied to many permutations of spatial and array dimensions. For example, we may be dealing with a two dimensional lattice of line sources in three dimensions. Or we could have a three dimensional array of points sources in three dimensions. In this section we are going to focus on the Ewald representation for two specific situations:

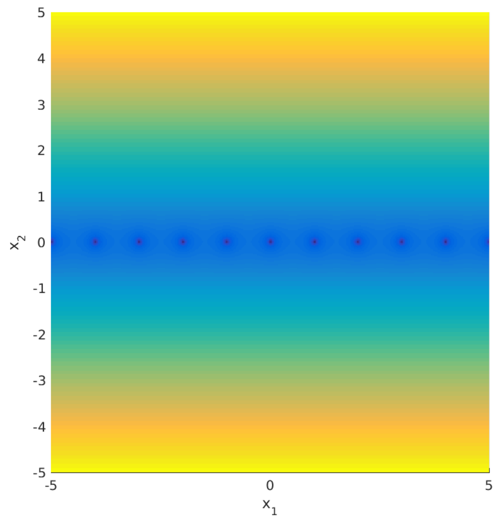

FIGURE 3.2. The periodic Green's function $G_\sharp$ for the Laplace equation.

i). A two dimensional (biperiodic) lattice of point sources in two dimensions.
ii). A one dimensional (periodic) array of point sources in two dimensions.

First let us define the quasi-biperiodic Green's function.

3.2.1. Quasi-biperiodic Green's function for the Helmholtz equation. We denote by α the quasi-momentum variable in the Brillouin zone $B = [0, 2\pi)^2$. We introduce the two-dimensional quasi-periodic Green's function (or fundamental solution) $G^{\alpha,\omega}$, which satisfies

$$(\Delta + \omega^2) G^{\alpha,\omega}(x, y) = \sum_{n \in \mathbb{Z}^2} \delta_0(x - y - n) e^{\sqrt{-1} n \cdot \alpha}. \tag{3.10}$$

If $\omega \neq |2\pi n + \alpha|, \forall\, n \in \mathbb{Z}^2$, then by using Poisson's summation formula

$$\sum_{n \in \mathbb{Z}^2} e^{\sqrt{-1}(2\pi n + \alpha) \cdot x} = \sum_{n \in \mathbb{Z}^2} \delta_0(x - n) e^{\sqrt{-1} n \cdot \alpha}, \tag{3.11}$$

the quasi-periodic fundamental solution $G^{\alpha,\omega}$ can be represented as a sum of augmented plane waves over the reciprocal lattice:

$$G^{\alpha,\omega}(x, y) = \sum_{n \in \mathbb{Z}^2} \frac{e^{\sqrt{-1}(2\pi n + \alpha) \cdot (x - y)}}{\omega^2 - |2\pi n + \alpha|^2}. \tag{3.12}$$

Moreover, it can also be shown that $G^{\alpha,\omega}$ can be alternatively represented as a sum of images:

$$G^{\alpha,\omega}(x, y) = -\frac{\sqrt{-1}}{4} \sum_{n \in \mathbb{Z}^2} H_0^{(1)}(\omega |x - n - y|) e^{\sqrt{-1} n \cdot \alpha}, \tag{3.13}$$

where $H_0^{(1)}$ is the Hankel function of the first kind of order 0. The series in the spatial representation (3.13) of the Green's function converges uniformly for x, y in compact sets of $\mathbb{R}^2$ and $\omega \neq |2\pi n + \alpha|$ for all $n \in \mathbb{Z}^2$. From (3.13) and the well-known fact that $H_0^{(1)}(z) = (2\sqrt{-1}/\pi)\ln z + O(1)$ as $z \to 0$ (see (2.2)), it follows that $G^{\alpha,\omega}(x,y) - (1/2\pi)\ln|x-y|$ is smooth for all $x, y \in Y$. A disadvantage of the form (8.15), which is often referred to as the spectral representation of the Green's function, is that the singularity as $|x-y| \to 0$ is not explicit.

In all the sequel, we assume that $\omega \neq |2\pi n + \alpha|$ for all $n \in \mathbb{Z}^2$. Let D be a bounded domain in $\mathbb{R}^2$, with a connected Lipschitz boundary ∂D. Let ν denote the unit outward normal to ∂D. For $\omega > 0$ let $\mathcal{S}^{\alpha,\omega}$ and $\mathcal{D}^{\alpha,\omega}$ be the quasi-periodic single- and double-layer potentials[1] associated with $G^{\alpha,\omega}$ on D; that is, for a given density $\varphi \in L^2(\partial D)$,

$$\mathcal{S}^{\alpha,\omega}[\varphi](x) = \int_{\partial D} G_\omega^\alpha(x,y)\varphi(y)\, d\sigma(y), \quad x \in \mathbb{R}^2,$$

$$\mathcal{D}^{\alpha,\omega}[\varphi](x) = \int_{\partial D} \frac{\partial G_\omega^\alpha(x,y)}{\partial \nu(y)}\varphi(y)\, d\sigma(y), \quad x \in \mathbb{R}^2 \setminus \partial D.$$

Then, $\mathcal{S}^{\alpha,\omega}[\varphi]$ and $\mathcal{D}^{\alpha,\omega}[\varphi]$ satisfy $(\Delta + \omega^2)\mathcal{S}^{\alpha,\omega}[\varphi] = (\Delta + \omega^2)\mathcal{D}^{\alpha,\omega}[\varphi] = 0$ in D and $Y \setminus \overline{D}$ where Y is the periodic cell $[0,1)^2$, and they are α-quasi-periodic. Here we assume $\overline{D} \subset Y$.

The next formulas give the jump relations obeyed by the double-layer potential and by the normal derivative of the single-layer potential on general Lipschitz domains:

$$\frac{\partial(\mathcal{S}^{\alpha,\omega}[\varphi])}{\partial \nu}\bigg|_{\pm}(x) = \left(\pm \frac{1}{2}I + (\mathcal{K}^{-\alpha,\omega})^*\right)[\varphi](x) \quad \text{a.e. } x \in \partial D, \tag{3.14}$$

$$(\mathcal{D}^{\alpha,\omega}[\varphi])\bigg|_{\pm}(x) = \left(\mp \frac{1}{2}I + \mathcal{K}^{\alpha,\omega}\right)[\varphi](x) \quad \text{a.e. } x \in \partial D, \tag{3.15}$$

for $\varphi \in L^2(\partial D)$, where $\mathcal{K}^{\alpha,\omega}$ is the operator on $L^2(\partial D)$ defined by

$$\mathcal{K}^{\alpha,\omega}[\varphi](x) = \text{p.v.}\int_{\partial D} \frac{\partial G^{\alpha,\omega}(x,y)}{\partial \nu(y)}\varphi(y)\, d\sigma(y) \tag{3.16}$$

and $(\mathcal{K}^{-\alpha,\omega})^*$ is the L^2-adjoint operator of $\mathcal{K}^{-\alpha,\omega}$, which is given by

$$(\mathcal{K}^{-\alpha,\omega})^*[\varphi](x) = \text{p.v.}\int_{\partial D} \frac{\partial G^{\alpha,\omega}(x,y)}{\partial \nu(x)}\varphi(y)\, d\sigma(y). \tag{3.17}$$

The singular integral operators $\mathcal{K}^{\alpha,\omega}$ and $(\mathcal{K}^{-\alpha,\omega})^*$ are bounded on $L^2(\partial D)$ as an immediate consequence of the fact that $G^{\alpha,\omega}(x,y) - (1/2\pi)\ln|x-y|$ is smooth for all x, y.

3.2.2. Quasi-periodic Green's function for the Helmholtz equation. We now move on to the one-dimensional quasi-periodic Green's function. This time letting

[1] From now on we use $\mathcal{S}^{\alpha,\omega}$ and $\mathcal{D}^{\alpha,\omega}$ instead of $\mathcal{S}_D^{\alpha,\omega}$ and $\mathcal{D}_D^{\alpha,\omega}$ for layer potentials on D. This is to keep the notation simple.

α denote the quasi-momentum variable in the Brillouin zone $B = [0, 2\pi)$ we introduce the Green's function $G^{\alpha,\omega}$, which satisfies

$$(\Delta + k^2)G^{\alpha,\omega}(x,y) = \sum_{m\in\mathbb{Z}} \delta_0(x - y - (m,0))e^{im\alpha},$$

whose solution can be represented as

$$G^{\alpha,\omega}(x,y) = -\frac{i}{4}\sum_{m\in\mathbb{Z}} H_0^{(1)}(k|x - y - (m,0)|)e^{im\alpha},$$

where $H_0^{(1)}$ is the Hankel function of the first kind of order 0. Both the quasi-periodic and quasi-biperiodic Green's functions feature conditionally convergent infinite series that are not satisfactory in terms of numerical computation. For instance, for large values of t we have

$$H_0^{(1)}(t) = \sqrt{\frac{2}{\pi t}}e^{\sqrt{-1}(t-\frac{\pi}{4})}\left[1 + O\left(\frac{1}{t}\right)\right],$$

and therefore the terms of the summation in Equation (3.2.2) are of order $1/\sqrt{m}$ when m becomes large which makes the series extremely slow to converge.

Let us now discuss Ewald's method for the case of the quasi-periodic Green's function in order to remedy this problem. This technique will provide us with a representation of the quasi-periodic Green's function that is both absolutely convergent and rapidly convergent. A similar procedure can used to accelerate the quasi-biperiodic Green's function.

3.3. Ewald representation of the quasi-periodic Green's function for the Helmholtz equation

Code:	3.2 Quasi-Periodic Green's Function Helmholtz	DemoQPerHelmholtzG.m

Ewald's method was originally developed to treat long range electrostatic interactions in periodic structures. The key idea behind Ewald's method is to split the periodic Green's function into spectral and spatial parts that, after some careful manipulation, both converge rapidly. So our goal in this section is to determine representations for $G^{\alpha,\omega}_{\text{spec}}$ and $G^{\alpha,\omega}_{\text{spat}}$ such that the periodic Green's function

$$G^{\alpha,\omega}(x,y) = G^{\alpha,\omega}_{\text{spec}}(x,y) + G^{\alpha,\omega}_{\text{spat}}(x,y)$$

is exponentially convergent. We begin by determining an integral representation for the Hankel function of the first kind of order zero that is often used in the literature as the starting point for a derivation of the Ewald method applied to a specific spatial and array configuration.

LEMMA 3.3. *The Hankel function of the first kind of order zero can be represented as*

$$H_0^{(1)}(\omega r) = \frac{2}{\sqrt{-1}\pi}\int_\gamma t^{-1}\exp\left(-r^2t^2 + \frac{\omega^2}{4t^2}\right)dt, \tag{3.18}$$

where γ is an integration path in the complex plane, shown in Figure 3.3, that begins at the origin with direction $e^{-\sqrt{-1}\pi/4}$, and goes to infinity in some direction $e^{\sqrt{-1}\phi}$, with $\phi \in (-\pi/4, \pi/4)$.

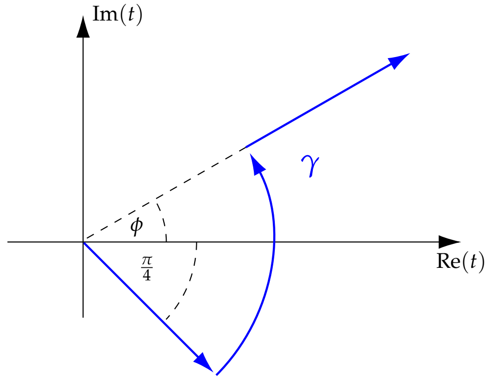

FIGURE 3.3. The integration path γ, in (3.18), that begins at the origin with direction $e^{-\sqrt{-1}\pi/4}$, and goes to infinity in some direction $e^{\sqrt{-1}\phi}$, with $\phi \in (-\pi/4, \pi/4)$.

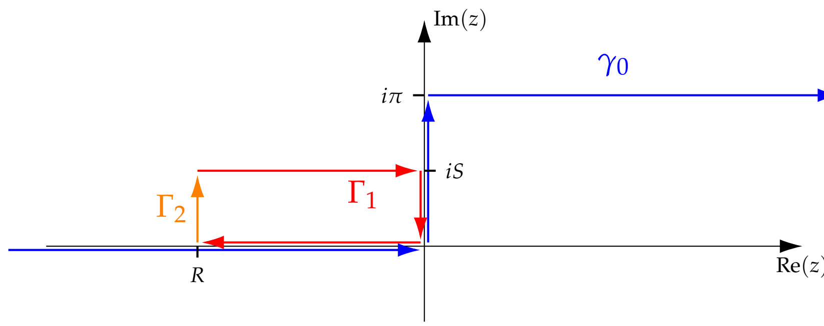

FIGURE 3.4. γ_0 is the path of integration taken in (3.19). Γ_1 and Γ_2 are specific paths of integration for which the integrals in (3.20) go towards zero as $R \to \infty$, and which cancel against γ_0.

PROOF. We have the following representation for the Hankel function of the first kind of order zero:

$$H_0^{(1)}(x) = \frac{1}{\sqrt{-1}\pi} \int_{\gamma_0} e^{x \sinh z} dz, \qquad |\arg(x)| < \frac{\pi}{2}, \tag{3.19}$$

where the path of integration γ_0, which is shown in Figure 3.4, is given by

$$\gamma_0 = \{t : -\infty < t \leq 0\} \cup \{\sqrt{-1}t : 0 < t \leq \pi\} \cup \{t + \sqrt{-1}\pi : 0 < t < \infty\}.$$

We now define a separate path of integration for the same integrand. Let $R, S > 0$ and denote by

$$\Gamma_1 := \{-t : 0 \leq t \leq R\} \cup \{\sqrt{-1}t : 0 < t < S\} \cup \{-t + \sqrt{-1}S : 0 \leq t \leq R\},$$
$$\Gamma_2 := \{-R + \sqrt{-1}t : 0 < t < S\},$$

These paths share the same starting point and end point, and as the integrand is holomorphic in z, by Cauchy's integral theorem, the integral over the contour is

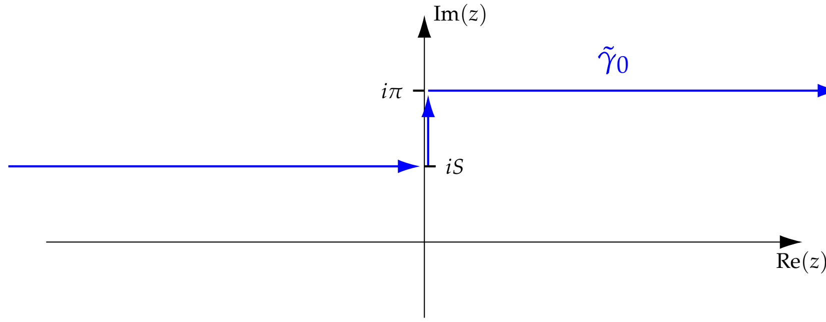

FIGURE 3.5. The integration path $\tilde{\gamma}_0$ in (3.21).

path independent. Therefore

$$\begin{aligned}\int_{\Gamma_1} e^{x\sinh z} dz &= \int_{\Gamma_2} e^{x\sinh z} dz \\ &= \int_0^S e^{x\sinh(-R+it)} dt.\end{aligned}$$

Suppose that $0 < \arg(x) < \pi/2$, $0 < S < \pi/2$, $t \in (0, S)$. Then the integral goes to 0 as R gets large because

$$\Re(x\sinh(-R+\sqrt{-1}t)) = -\Re(x)\cos(t)\sinh(R) - \Im(x)\sin(t)\cosh(R) < 0.$$

We have

$$\lim_{R\to\infty} \int_{\Gamma_1} e^{x\sinh z} dz = \lim_{R\to\infty} \int_{\Gamma_2} e^{x\sinh z} dz = 0. \tag{3.20}$$

We can combine the integrals on the paths Γ_1 and Γ_2 with the integral in (3.19) without changing its value, i.e.

$$H_0^{(1)}(x) = \frac{1}{\sqrt{-1}\pi} \int_{\gamma_0} e^{x\sinh z} dz + \int_{\Gamma_1} e^{x\sinh z} dz + \int_{\Gamma_2} e^{x\sinh z} dz, \quad \text{as } R \to \infty.$$

Choosing $S = \pi/2 - \arg(x)$ for $0 < \arg(x) < \pi/2$, noting that cancellation occurs due to the way the contours have been defined, and letting $R \to \infty$, we obtain the representation:

$$H_0^{(1)}(x) = \frac{1}{\sqrt{-1}\pi} \int_{\tilde{\gamma}_0} e^{x\sinh z} dz, \qquad \arg(x) < \frac{\pi}{2}, \tag{3.21}$$

where the integration path

$\tilde{\gamma}_0 = \{t + \sqrt{-1}S : -\infty < t < 0\} \cup \{\sqrt{-1}t : S \le t \le \pi\} \cup \{t + \sqrt{-1}\pi : 0 < t < \infty\}$,

is shown in Figure 3.5. Rewriting this as

$$H_0^{(1)}(x) = \frac{1}{\sqrt{-1}\pi} \int_{\tilde{\gamma}_0} \exp\left(\frac{x}{2}(e^z - e^{-z})\right) dz,$$

and making the substitution $s = e^z$ gives

$$H_0^{(1)}(x) = \frac{1}{\sqrt{-1}\pi} \int_{\gamma_1} s^{-1} \exp\left(\frac{x}{2}\left(s - \frac{1}{s}\right)\right) ds,$$

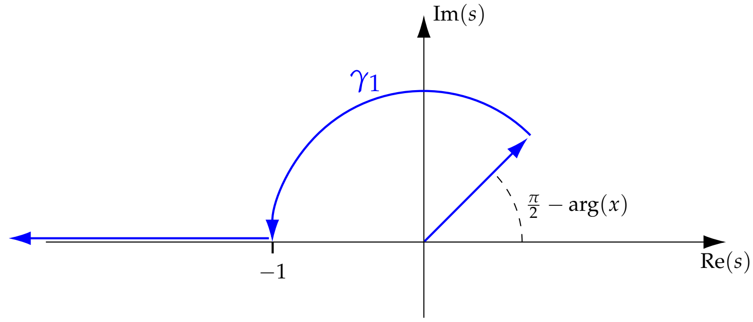

FIGURE 3.6. The integration path γ_1 in (3.21).

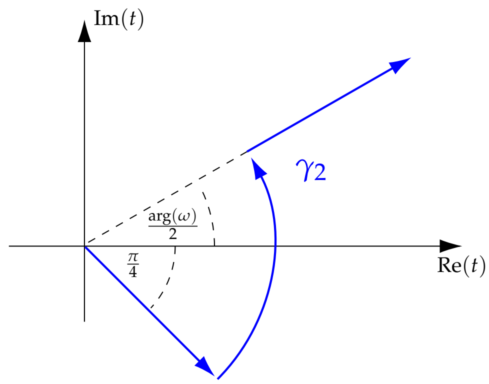

FIGURE 3.7. The integration path γ_2 in (3.22).

where γ_1, shown in Figure 3.6, is a contour that begins at the origin with direction $e^{\sqrt{-1}(\pi/2-\arg(x))}$, and sweeps around the origin to the point $s=-1$ before tending to minus infinity on the negative real axis.

Setting $x=\omega r$ with $r>0$, we obtain

$$H_0^{(1)}(\omega r) = \frac{1}{\sqrt{-1}\pi}\int_{\gamma_1} s^{-1}\exp\left(\frac{\omega r}{2}\left(s-\frac{1}{s}\right)\right)ds.$$

Making another substitution, this time with $s=-2rt^2/\omega$, we arrive at

$$H_0^{(1)}(\omega r) = \frac{2}{\sqrt{-1}\pi}\int_{\gamma_2} t^{-1}\exp\left(-r^2t^2+\frac{\omega^2}{4t^2}\right)dt, \tag{3.22}$$

where γ_2, shown in Figure 3.7, is an integration path in the complex plane that begins at the origin with direction $e^{-\sqrt{-1}\pi/4}$, follows the arc $|t|=\sqrt{|\omega|/(2r)}$ until the point $\sqrt{\omega/(2r)}e^{\sqrt{-1}(\arg(\omega))/2}$, and finally goes to infinity in the direction $e^{\sqrt{-1}(\arg(\omega))/2}$. The path of integration can be altered as long as (i) it begins at the origin with direction $e^{-\sqrt{-1}\pi/4}$, which ensures convergence as $|t|\to 0$, and (ii) it goes to infinity in the direction $e^{\sqrt{-1}\phi}$, with $\phi\in(-\pi/4,\pi/4)$, which ensures convergence as $|t|\to\infty$. So we have(3.18) with $\gamma=\gamma_2$.

$\square$

By Lemma 3.3 we have

$$-\frac{\sqrt{-1}}{4}H_0^{(1)}(\omega r) = -\frac{1}{2\pi}\int_\gamma \frac{e^{-r^2t^2+\frac{\omega^2}{4t^2}}}{t}dt,$$

and then recalling the definition of the quasi-periodic Green's function

$$G^{\alpha,\omega}(x,y) = -\frac{\sqrt{-1}}{4}\sum_{m\in\mathbb{Z}} H_0^{(1)}(\omega|x-y-(m,0)|)e^{\sqrt{-1}m\alpha},$$

we obtain

$$G^{\alpha,\omega}(x,y) = -\frac{1}{2\pi}\sum_{m\in\mathbb{Z}} e^{\sqrt{-1}m\alpha}\int_\gamma \frac{e^{-R_m^2t^2+\frac{\omega^2}{4t^2}}}{t}dt, \tag{3.23}$$

where $R_m = \sqrt{(x_2-y_2)+(x_1-y_1-m)^2}$.

Let $\mathcal{E}$ be a point on the positive real axis, and let γ_1 be a contour starting from 0 following the ray $e^{-\sqrt{-1}\frac{\pi}{4}}$, then following the arc $\gamma = \mathcal{E}$ until the point $\mathcal{E}$. Let γ_2 be the contour starting at $\mathcal{E}$ following the arc $r = \mathcal{E}$ until $\mathcal{E}e^{\sqrt{-1}\phi}$, with $\phi \in (-\frac{\pi}{4}, \frac{\pi}{4})$, and then following the ray $e^{\sqrt{-1}\phi}$ to infinity. Then the integral $\int_\gamma$ in (3.23) is equivalent to $\int_{\gamma_1} + \int_{\gamma_2}$.

LEMMA 3.4. *Consider a lossy medium such that $\Im(\omega) > 0$. Then the quasi-periodic Green's function $G^{\alpha,\omega}$ can be split into two parts such that*

$$G^{\alpha,\omega}(x,y) = G^{\alpha,\omega}_{spec}(x,y) + G^{\alpha,\omega}_{spat}(x,y),$$

with

$$\begin{aligned} G^{\alpha,\omega}_{spec}(x,y) = &-\frac{1}{4}\sum_{p\in\mathbb{Z}} \frac{e^{-\sqrt{-1}\omega_{xp}(x_1-y_1)}}{\sqrt{-1}\omega_{yp}} \\ &\times\left[e^{\sqrt{-1}\omega_{yp}|x_2-y_2|}erfc\left(\frac{\sqrt{-1}\omega_{yp}}{2\mathcal{E}} + |x_2-y_2|\mathcal{E}\right)\right. \\ &\left.+ e^{-\sqrt{-1}\omega_{yp}|x_2-y_2|}erfc\left(\frac{\sqrt{-1}\omega_{yp}}{2\mathcal{E}} - |x_2-y_2|\mathcal{E}\right)\right], \end{aligned}$$

$$G^{\alpha,\omega}_{spat}(x,y) = -\frac{1}{4\pi}\sum_{m\in\mathbb{Z}} e^{\sqrt{-1}\alpha m}\sum_{q=0}^{\infty}\left(\frac{\omega}{2\mathcal{E}}\right)^{2q}\frac{1}{q!}E_{q+1}(R_m^2\mathcal{E}^2),$$

where $\omega_{xp} = -\alpha + \frac{2\pi p}{d}$, $\omega_{yp} = -\sqrt{\omega^2 - \omega_{xp}^2}$, $erfc(z)$ is the complementary error function

$$erfc(z) = \frac{2}{\sqrt{\pi}}\int_z^\infty e^{-t^2}dt,$$

and E_q is the qth order exponential integral which is defined as

$$E_q(z) = \int_1^\infty \frac{e^{-zt}}{t^q}dt.$$

PROOF. We first split (3.23) into two parts and define

$$G^{\alpha,\omega}_{\text{spec}}(x,y) = -\frac{1}{2\pi}\sum_{m\in\mathbb{Z}} e^{\sqrt{-1}m\alpha}\int_{\gamma_1}\frac{e^{-R_m^2 s^2+\frac{\omega^2}{4s^2}}}{s}ds, \tag{3.24}$$

and

$$G^{\alpha,\omega}_{\text{spat}}(x,y) = -\frac{1}{2\pi}\sum_{m\in\mathbb{Z}} e^{\sqrt{-1}m\alpha}\int_{\gamma_2}\frac{e^{-R_m^2 s^2+\frac{\omega^2}{4s^2}}}{s}ds, \tag{3.25}$$

where γ_1 and γ_2 are the complex paths of integration defined previously. Note that the convergence of $G^{\alpha,\omega}_{\text{spat}}$ is already exponential as for large m it can be shown that the terms in the series behave like $e^{-n^2\mathcal{E}^2}/(n^2\mathcal{E}^2)$. The terms in $G^{\alpha,\omega}_{\text{spec}}$ on the other hand decay like $1/\sqrt{m}$ due to the asymptotic behavior of $H_0^{(1)}(z)$ for large z. This term is the one we would like to accelerate.

We use the Poisson summation formula

$$\sum_{m\in\mathbb{Z}} f(m) = \frac{1}{d}\sum_{p\in\mathbb{Z}}\hat{f}(2\pi p), \tag{3.26}$$

where $\hat{f}(2\pi p)$ is the Fourier coefficient, namely,

$$\hat{f}(\beta) = \int_{-\infty}^{\infty} f(\xi)e^{-\sqrt{-1}\beta\xi}d\xi.$$

Let $f(m)$ be

$$f(m) = -\frac{e^{\sqrt{-1}\alpha m}}{2\pi}\int_{\gamma_1}\frac{e^{-[(x_2-y_2)^2+(x_1-y_1-m)^2]s^2+\frac{k^2}{4s^2}}}{s}ds,$$

so that

$$\hat{f}(2\pi p) = -\frac{1}{2\pi}\int_{-\infty}^{\infty}d\xi\int_{\gamma_1}ds\frac{e^{-[(x_2-y_2)^2+(x_1-y_1-\xi)^2]s^2+\frac{k^2}{4s^2}}}{s}e^{-\sqrt{-1}\omega_{xp}\xi},$$

where $\omega_{xp} = -\alpha + 2\pi p$. Noting that the s integral is convergent on the path γ_1 for $\mathcal{E} \in]-\infty,\infty[$ as $\Re(s^2) > 0$, we can switch the order of integration. Then applying the formula $\int_{-\infty}^{\infty} e^{-a\xi^2+b\xi}d\xi = \sqrt{\pi/a}e^{b^2/4a}$ results in

$$\hat{f}(2\pi p) = -\frac{e^{-\sqrt{-1}\omega_{xp}(x_1-y_1)}}{2\sqrt{\pi}}\int_{\gamma_1}\frac{e^{-(x_2-y_2)^2s^2}e^{\omega_{yp}^2/4s^2}}{s^2}ds,$$

where $\omega_{yp} = -\sqrt{\omega^2-\omega_{xp}^2}$ and we have taken the negative of the square root in order to ensure convergence. Making the change of variables $\tilde{s} = 1/s$ we have

$$\hat{f}(2\pi p) = -\frac{e^{-\sqrt{-1}\omega_{xp}(x_1-y_1)}}{2\sqrt{\pi}}\int_{\tilde{\gamma}_1} e^{-(x_2-y_2)^2/\tilde{s}^2}e^{(\omega_{yp}^2\tilde{s}^2)/4}d\tilde{s},$$

and the path of integration is mapped from γ_1 onto $\tilde{\gamma}_1$. Note that since γ_1 is of the form $te^{-\sqrt{-1}\frac{\pi}{4}}$, $\tilde{\gamma}_1$ is of the form $t^{-1}e^{\sqrt{-1}\frac{\pi}{4}}$ near ∞. That is, $\Re(\omega_{zp}^2\tilde{s}^2) < 0$ for every $p \in \mathbb{Z}$, ensuring convergence. Finally, using the identity

$$\int e^{a^2x^2-\frac{b^2}{x^2}}dx = -\frac{\sqrt{\pi}}{4a}\left[e^{2ab}\text{erfc}(ax+\frac{b}{x}) + e^{-2ab}\text{erfc}(ax-\frac{b}{x})\right] + \text{const},$$

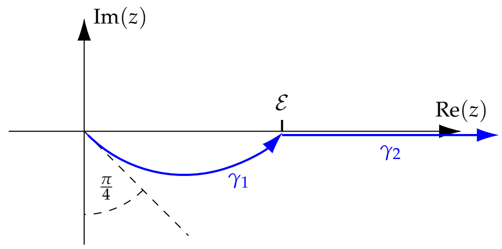

FIGURE 3.8. The complex paths of integration γ_1 and γ_2 when $\phi = 0$.

we obtain

$$\hat{f}(2\pi p) = -\frac{e^{-\sqrt{-1}\omega_{xp}(x_1-y_1)}}{4\sqrt{-1}\omega_{yp}} \tag{3.27}$$

$$\times \left[e^{\sqrt{-1}\omega_{yp}|x_2-y_2|}\mathrm{erfc}\left(\frac{\sqrt{-1}\omega_{yp}}{2\mathcal{E}} + |x_2-y_2|\mathcal{E}\right)\right. \tag{3.28}$$

$$\left. + e^{-\sqrt{-1}\omega_{yp}|x_2-y_2|}\mathrm{erfc}\left(\frac{\sqrt{-1}\omega_{yp}}{2\mathcal{E}} - |x_2-y_2|\mathcal{E}\right)\right]. \tag{3.29}$$

Inserting this into (3.26) gives us $G^{\alpha,\omega}_{\text{spec}}$.

Now we turn to $G^{\alpha,\omega}_{\text{spat}}$. Although this function is already exponentially convergent we will transform it into a form more suitable for computation. Consider the integral I in (3.25) ,with ϕ set to 0:

$$I = \int_{\mathcal{E}}^{\infty} \frac{e^{-R_m^2 t^2 + \frac{\omega^2}{4t^2}}}{s} ds.$$

The contours γ_1 and γ_2 when $\phi = 0$ are shown in Figure 3.8. It can be shown that after changing variables with $u = s^2$, applying the Taylor expansion $e^{\frac{\omega^2}{4u}} = \sum_{q=0}^{\infty}(\frac{\omega}{2})^{2q}/(q!u^q)$, and then changing variables again with $t = u/\mathcal{E}^2$ we have

$$I = \frac{1}{2}\sum_{q=0}^{\infty}\left(\frac{\omega}{2\mathcal{E}}\right)^{2q}\frac{1}{q!}E_{q+1}(R_m^2\mathcal{E}^2).$$

Using this representation of I in (3.25) gives us the desired form of $G^{\alpha,\omega}_{\text{spat}}$. □

The complementary error function converges very quickly, and this is the key to the acceleration of the convergence speed of $G^{\alpha,\omega}_{\text{spec}}$. This representation of $G^{\alpha,\omega}_{\text{spec}}$ is also efficient in terms of numerical computation as only $E_1(z)$ needs to be evaluated explicitly. The higher order exponential integral terms can be computed with the recurrence relation $E_{q+1}(z) = \frac{1}{q}(e^{-z} - zE_q(z))$ for $q = 1, 2, \ldots$.

Note that the optimal value of the splitting parameter $\mathcal{E}$ for wavelengths somewhat larger or smaller than the periodicity is given by $\mathcal{E} = \sqrt{\pi}/d$. It is also worth mentioning that very few terms are required in the summations in $G^{\alpha,\omega}_{\text{spec}}$ and $G^{\alpha,\omega}_{\text{spat}}$ to obtain a relative error of less than $1e-03$. Furthermore, although we assumed that $\Im(\omega) > 0$ in order to obtain these expressions, due to analytic continuation the expressions actually hold for all $\omega \in \mathbb{C}$.

For the quasi-periodic Neumann–Poincairé operator we need the gradient of the quasi-periodic Green's function. We note that

$$\nabla G^{\alpha,\omega}(x,y) = \nabla G^{\alpha,\omega}_{\text{spec}}(x,y) + \nabla G^{\alpha,\omega}_{\text{spat}}(x,y),$$

with

$$\begin{aligned}
\nabla G^{\alpha,\omega}_{\text{spec}}(x,y) = -\frac{1}{4}\sum_{p\in\mathbb{Z}} \frac{e^{-\sqrt{-1}\omega_{xp}(x_1-y_1)}}{\sqrt{-1}\omega_{yp}} & \\
\Big\{ & [-\sqrt{-1}\hat{x}\omega_{xp} - \sqrt{-1}\hat{y}\omega_{yp}\text{sgn}(x_2-y_2)] \\
& \times e^{-\sqrt{-1}\omega_{yp}|x_2-y_2|}\text{erfc}\left(\frac{\sqrt{-1}\omega_{yp}}{2\mathcal{E}} - |x_2-y_2|\mathcal{E}\right) \\
& \times [-\sqrt{-1}\hat{x}\omega_{xp} + \sqrt{-1}\hat{y}\omega_{yp}\text{sgn}(x_2-y_2)] \\
& \times e^{\sqrt{-1}\omega_{yp}|x_2-y_2|}\text{erfc}\left(\frac{\sqrt{-1}\omega_{yp}}{2\mathcal{E}} + |x_2-y_2|\mathcal{E}\right) \\
& - \hat{z}\text{sgn}(x_2-y_2)\mathcal{E}e^{-\sqrt{-1}\omega_{yp}|x_2-y_2|} \\
& \times \text{erfc}'\left(\frac{\sqrt{-1}\omega_{yp}}{2\mathcal{E}} - |x_2-y_2|\mathcal{E}\right) \\
& + \hat{z}\text{sgn}(x_2-y_2)\mathcal{E}e^{\sqrt{-1}\omega_{yp}|x_2-y_2|} \\
& \times \text{erfc}'\left(\frac{\sqrt{-1}\omega_{yp}}{2\mathcal{E}} + |x_2-y_2|\mathcal{E}\right)\Big\}, \\
\nabla G^{\alpha,\omega}_{\text{spat}}(x,y) = \frac{\mathcal{E}^2}{2\pi}\sum_{m\in\mathbb{Z}} & \Big[\hat{x}(x_1-y_1-m) + \hat{z}(x_2-y_2)\Big]e^{\sqrt{-1}\alpha m} \\
& \times \sum_{q=0}^{\infty}\left(\frac{\omega}{2\mathcal{E}}\right)^{2q}\frac{1}{q!}E_q(R_m^2\mathcal{E}^2),
\end{aligned}$$

where $\hat{x}$ and $\hat{y}$ are unit vectors along the x and y axes, respectively, and $\text{erfc}(z)' = -\frac{2}{\sqrt{\pi}}e^{-z^2}$.

Figure 3.9 shows the quasi-periodic Green's function obtained by using Ewald's method in Code Quasi-Periodic Green's Function Helmholtz.

3.3.1. Numerical Implementation of the Operators $\mathcal{S}^{\alpha,\omega}$ and $(\mathcal{K}^{-\alpha,\omega})^*$.

Code:	3.2 Quasi-Periodic Green's Function Helmholtz	DemoQPerHelmholtzSK.m

In this section we discuss the numerical implementation of $\mathcal{S}^{\alpha,\omega}$ and $(\mathcal{K}^{-\alpha,\omega})^*$ assuming we are in a low frequency regime. After performing the usual boundary discretization procedure, as described in Subsection 1.7, we represent the infinite dimensional operator $\mathcal{S}^{\alpha,\omega}$ acting on the density φ by a finite dimensional matrix S acting on the coefficient vector $\overline{\varphi}_i := \varphi(x^{(i)})$ for $1 \le i \le N$. That is

$$\mathcal{S}^{\alpha,\omega}[\varphi](x) \quad = \int_{\partial\Omega} G^{\alpha,\omega}(x,y)\varphi(y)\,d\sigma(y),$$

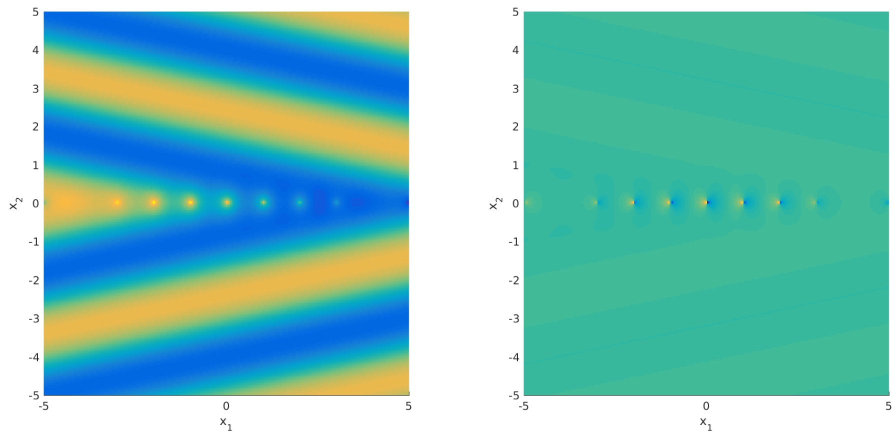

$\mathrm{Re}(G_{\sharp}^{\alpha,k})$ $\qquad$ $\mathrm{Re}(\frac{\partial}{\partial x_2} G_{\sharp}^{\alpha,k})$

FIGURE 3.9. The quasi-periodic Green's function, and the x_2 component of its gradient, for the Helmholtz equation for a one-dimensional lattice of dirac mass source points with periodicity 1. The quasi-momentum paramater α is set to $\pi/8$.

for $\psi \in L^2(\partial\Omega)$, is represented numerically as

$$S\tilde{\psi} = \begin{pmatrix} S_{11} & S_{12} & \dots & S_{1N} \\ S_{21} & S_{22} & \dots & S_{2N} \\ \vdots & & \ddots & \vdots \\ S_{N1} & \dots & \dots & S_{NN} \end{pmatrix} \begin{pmatrix} \overline{\varphi}_1 \\ \overline{\varphi}_2 \\ \vdots \\ \overline{\varphi}_N \end{pmatrix},$$

where

$$S_{ij} = G^{\alpha,\omega}(x^{(i)} - x^{(j)})|T(x^{(j)})|(t_{j+1} - t_j), \quad i \neq j,$$

and $G^{\alpha,\omega}(x^{(i)} - x^{(j)})$ refers to the Ewald representation of the Green's function. This discrerization matrix S features singularities in the diagonal terms and therefore we must approximate these terms by explicit calculation. Let the portion of the boundary starting at $x^{(i)}$ and ending at $x^{(i+1)}$ be parameterized by $s \in [0, \varepsilon = \frac{2\pi}{N})$ and note that $\varepsilon \to 0$ as the number of discretization points $N \to \infty$. Observe that for $G^{\alpha,\omega} = G^{\alpha,\omega}_{\text{spec}} + G^{\alpha,\omega}_{\text{spat}}$ the singularity appears in the $G^{\alpha,\omega}_{\text{spat}}$ term precisely when $x = y$ and $m = 0$. Therefore

$$S_{ii} = \int_0^\varepsilon G^{\alpha,\omega}(x^{(i)} - x(s))|T(s)|ds \approx \int_0^\varepsilon G^{\alpha,\omega}_{\text{spat}}(x^{(i)} - x(s))|T(s)|ds,$$

as $\varepsilon \to 0$. Now retaining only the $m = 0$ term in $G^{\alpha,\omega}_{\text{spat}}$ we have

$$G^{\alpha,\omega}_{\text{spat}} \approx -\frac{1}{4\pi} \sum_{q=0}^{\infty} \left(\frac{\omega}{2\mathcal{E}}\right)^{2q} \frac{1}{q!} E_{q+1}(R_0^2 \mathcal{E}^2),$$

where $R_0 = \sqrt{(x_1^{(i)} - x_1(s))^2 + (x_2^{(i)} - x_2(s))^2}$. Noting that the behavior of the exponential integrals E_{q+1} for small argument is $E_{q+1}(z) = -(-z)^q(\ln z)/q!$ gives

$$\begin{aligned} G^{\alpha,\omega}_{\mathrm{spat}} &\approx -\frac{1}{4\pi}\sum_{q=0}^{\infty}\left(\frac{\omega}{2\mathcal{E}}\right)^{2q}\frac{1}{q!}\left(-\frac{(-R_0^2\mathcal{E}^2)^q}{q!}\ln(R_0^2\mathcal{E}^2)\right) \\ &\approx \frac{1}{2\pi}\ln(R_0\mathcal{E}), \\ &\approx \frac{1}{2\pi}\ln(R_0), \end{aligned}$$

where only the $q = 0$ term has been retained as $R_0 \ll 1$. Therefore,

$$\begin{aligned} S_{ii} &\approx \frac{1}{2\pi}\int_0^{\varepsilon}\ln(|x^{(i)} - x(s)|)|T(s)|ds \\ &= \frac{|T(0)|\varepsilon}{2\pi}\Big(\ln(|T(0)|\varepsilon) - 1\Big) \\ &= \frac{|T(0)|}{N}\left(\ln\left(\frac{2\pi}{N}|T(0)|\right) - 1\right). \end{aligned}$$

The discretization matrix K for the quasi-periodic Neumann–Poincaré operator $(\mathcal{K}^{-\alpha,\omega})^*$ requires no special treatment since, similarly to Subsection 3.1.1 it is clear that it features the same singularity as the non-periodic Neumann–Poincaré operator and thus the usual expression (3.9) holds for the diagonal terms of its corresponding discretized matrix. We remark that the approximations used for the diagonal terms of S and K are appropriate for low frequencies but are not stable when the frequency is high. For instance, the $q \neq 0$ terms provide a non-negligble contribution to $G^{\alpha,\omega}_{\mathrm{spat}}$ when ω is high and cannot be ignored. Ewald's method for computing $\mathcal{S}^{\alpha,\omega}$ and $(\mathcal{K}^{-\alpha,\omega})^*$ in low frequency regimes is implemented in Code Quasi-Periodic Green's Function Helmholtz.

3.3.2. Ewald representation of the quasi-biperiodic Green's function for the Helmholtz equation.

Code:	3.3 Quasi-Biperiodic Green's Function Helmholtz	DemoQBiPerHelmholtzG.m

The quasi-biperiodic Green's function satisfies

$$(\Delta + k^2)G^{\alpha,\omega}(x,y) = \sum_{m\in\mathbb{Z}^2}\delta_0(x - y - m)e^{\sqrt{-1}m\cdot\alpha}. \tag{3.30}$$

This Green's function has the representation

$$G^{\alpha,\omega}(x,y) = -\frac{\sqrt{-1}}{4}\sum_{m\in\mathbb{Z}^2}H_0^{(1)}(\omega R_m)e^{\sqrt{-1}m\cdot\alpha}, \tag{3.31}$$

where $R_m = \sqrt{(x_1 - y_1 - m_1)^2 + (x_2 - y_2 - m_2)^2}$. Through an analogous procedure to the one used in Section 3.3 for the quasi-periodic Green's function, it can be shown that there exists a rapidly converging Ewald representation of the quasi-biperiodic Green's function such that

$$G^{\alpha,\omega}(x,y) = G^{\alpha,\omega}_{\mathrm{spec}}(x,y) + G^{\alpha,\omega}_{\mathrm{spat}}(x,y),$$

with

$$G_{\text{spec}}^{\alpha,\omega}(x,y) = -\sum_{p,q\in\mathbb{Z}} \frac{1}{\gamma_{pq}^2} e^{-\gamma_{pq}^2/4\mathcal{E}} e^{-\sqrt{-1}\omega_{pq}\cdot(x-y)},$$

and

$$G_{\text{spat}}^{\alpha,\omega}(x,y) = -\frac{1}{4\pi}\sum_{m\in\mathbb{Z}^2} e^{\sqrt{-1}\alpha\cdot m} \sum_{q=0}^{\infty} \left(\frac{\omega}{2\sqrt{\mathcal{E}}}\right)^{2q} \frac{1}{q!} E_{q+1}(R_m^2\mathcal{E}),$$

where

$$\gamma_{pq} = \sqrt{|\omega_{pq}^2 - \omega^2|}, \omega_{pq} = \omega_{xp}\hat{x} + \omega_{yq}\hat{y}, \omega_{xp} = -\alpha_1 + 2\pi p, \omega_{yq} = -\alpha_2 + 2\pi q.$$

Taking the gradient of $G^{\alpha,\omega}(x,y)$ gives us the representation required for the quasi-biperiodic Neumann–Poincaré operator. We have

$$\nabla G^{\alpha,\omega}(x,y) = \nabla G_{\text{spec}}^{\alpha,\omega}(x,y) + \nabla G_{\text{spat}}^{\alpha,\omega}(x,y),$$

with

$$\nabla G_{\text{spec}}^{\alpha,\omega}(x,y) = \sqrt{-1}\sum_{p,q\in\mathbb{Z}} \frac{\omega_{pq}}{\gamma_{pq}^2} e^{-\gamma_{pq}^2/4\mathcal{E}} e^{-\sqrt{-1}\omega_{pq}\cdot(x-y)}$$

$$\begin{aligned}\nabla G_{\text{spat}}^{\alpha,\omega}(x,y) &= \frac{\mathcal{E}}{2\pi}\sum_{m\in\mathbb{Z}^2}^{\infty} (x-y-\hat{m}) e^{\sqrt{-1}\alpha\cdot\hat{m}} \\ &\quad \times \sum_{q=0}^{\infty} \left(\frac{\omega}{2\sqrt{\mathcal{E}}}\right)^{2q} \frac{1}{q!} E_q(R_m^2\mathcal{E}).\end{aligned}$$

The numerical results shown in Figure 3.10 are obtained by using Code Quasi-Biperiodic Green's Function Helmholtz.

3.4. Biperiodic and quasi-biperiodic and Green's function for the Laplace equation

Code:	3.4 Biperiodic and Quasi-Biperiodic Green's Function Laplace	DemoBiPerLaplaceG.m DemoQBiPerLaplaceG.m

The quasi-biperiodic Green's function $G^{\alpha,0}$ for the Laplace equation is given by

$$G^{\alpha,0}(x,y) = -\sum_{m\in\mathbb{Z}^2} \frac{e^{\sqrt{-1}(2\pi m+\alpha)\cdot(x-y)}}{|2\pi m+\alpha|^2} \quad \text{for } \alpha \neq 0,$$

Yet again, these functions feature infinite series that are very slow to converge. In order to utilize Ewald's method and accelerate the convergence we will need the following lemma.

LEMMA 3.5. *As $k \to 0$, $G^{\alpha,k}$ can be decomposed as*

$$G^{\alpha,k}(x,y) = G^{\alpha,0}(x,y) - \sum_{l=1}^{+\infty} k^{2l} \underbrace{\sum_{n\in\mathbb{Z}^2} \frac{e^{\sqrt{-1}(2\pi n+\alpha)\cdot(x-y)}}{|2\pi n+\alpha|^{2(l+1)}}}_{:=-G_l^{\alpha,k}(x,y)},$$

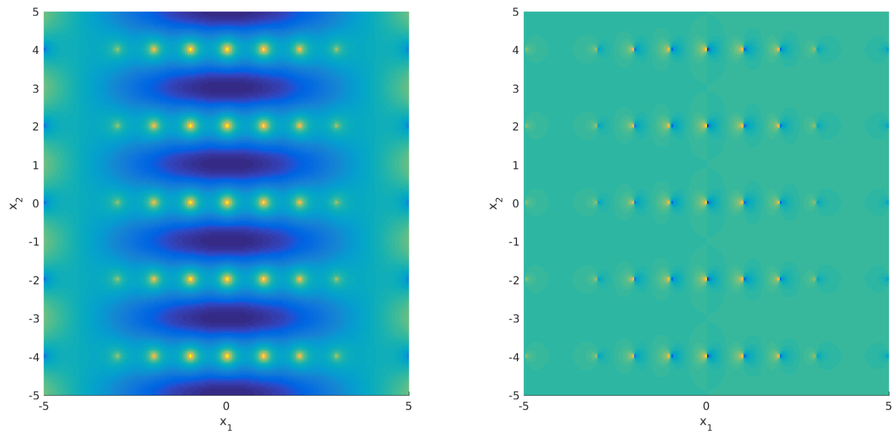

$\mathrm{Re}(G^{\alpha,k}_{\sharp})$ $\qquad$ $\mathrm{Re}(\frac{\partial}{\partial x_1} G^{\alpha,k}_{\sharp})$

FIGURE 3.10. The quasi-biperiodic Green's function, and the x_1 component of its gradient, for the Helmholtz equation for a two-dimensional lattice of dirac mass source points with periodicity 1 in the x_1 direction and 2 in the x_2 direction. The quasi-momentum paramater α is set to $(\pi/8, 0)$.

for $\alpha \neq 0$, while for $\alpha = 0$, the following decomposition holds:

$$G^{0,k}(x,y) = \frac{1}{k^2} + G^{0,0}(x,y) - \sum_{l=1}^{+\infty} \underbrace{k^{2l} \sum_{n \in \mathbb{Z}^2 \setminus \{0\}} \frac{e^{\sqrt{-1}2\pi n \cdot (x-y)}}{(4\pi^2)^{l+1} |n|^{2(l+1)}}}_{:= -G_l^{0,k}(x,y)}.$$

Therefore the quasi-biperiodic Green's function for the Laplace equation is given by

$$G^{\alpha,0}(x,y) = G^{\alpha,k}(x,y) - \sum_{l=1}^{\infty} G_l^{\alpha,k}(x,y), \tag{3.32}$$

while the periodic Green's function is given by

$$G^{0,0}(x,y) = G^{0,k}(x,y) - \frac{1}{k^2} - \sum_{l=1}^{\infty} G_l^{\alpha,k}(x,y). \tag{3.33}$$

We already have a Ewald representation corresponding to $G^{\alpha,0}$ for any α in the Brillouin zone $[0, 2\pi)^2$ and the infinite series in Equations (3.32) and (3.33) are relatively quick to converge. Therefore this representaton of these Green's functions is appropriate for efficient numerical implementation.

CHAPTER 4

Polarization Tensors and Scattering Coefficients

In this section we introduce the concepts of Generalized Polarization Tensors (GPTs) and Scattering Coefficients (SCs). GPTs and SCs naturally arise when we derive a far field expansion of the solution to the conductivity problem and the Helmholtz equation, respectively. They are key mathematical concepts for effectively reconstructing small conductivity or electromagnetic inclusions from boundary measurements, as well as in calculating accurate, effective electrical or elastic properties of composite materials. Moreover, they can be used to develop a highly efficient invisibility cloaking device.

4.1. Conductivity problem in free space

Code:	4.1 Polariazation Tensors	DemoPT.m DemoEquivEllipse.m

4.1.1. Far-Field Expansion. Let B be a Lipschitz bounded domain in $\mathbb{R}^d$ and suppose that the origin $O \in B$. Let $0 < k \neq 1 < +\infty$ and denote $\lambda(k) := (k+1)/(2(k-1))$. Let h be a harmonic function in $\mathbb{R}^d$, and let u be the solution to the following transmission problem in free space:

$$\begin{cases} \nabla \cdot ((1+(k-1)\chi(B))\nabla u_k) = 0 \quad \text{in } \mathbb{R}^d, \\ u_k(x) - h(x) = O(|x|^{1-d}) \quad \text{as } |x| \to +\infty. \end{cases} \tag{4.1}$$

For a multi-index $\alpha = (\alpha_1, \ldots, \alpha_d) \in \mathbb{N}^d$, let $\partial^\alpha f = \partial_1^{\alpha_1} \cdots \partial_d^{\alpha_d} f$ and $x^\alpha := x_1^{\alpha_1} \cdots x_d^{\alpha_d}$, we can easily prove that

$$u_k(x) = h(x) + \mathcal{S}_B^0 (\lambda(k) I - (\mathcal{K}_B^0)^*)^{-1} [\frac{\partial h}{\partial \nu}|_{\partial B}](x) \quad \text{for } x \in \mathbb{R}^d, \tag{4.2}$$

which together with the Taylor expansion

$$\Gamma_0(x-y) = \sum_{\beta, |\beta|=0}^{+\infty} \frac{(-1)^{|\beta|}}{\beta!} \partial_x^\beta \Gamma_0(x) y^\beta, \quad y \text{ in a compact set}, \quad |x| \to +\infty,$$

yields the far-field expansion

$$(u_k - h)(x) = \sum_{|\alpha|, |\beta|=1}^{+\infty} \frac{(-1)^{|\beta|}}{\alpha! \beta!} \partial_x^\beta \Gamma_0(x) \partial^\alpha h(0) \int_{\partial B} (\lambda(k) I - (\mathcal{K}_B^0)^*)^{-1} \left[\nu(x) \cdot \nabla x^\alpha\right](y) y^\beta \, d\sigma(y), \tag{4.3}$$

as $|x| \to +\infty$.

DEFINITION 4.1. For $\alpha, \beta \in \mathbb{N}^d$, we define the generalized polarization tensor $M_{\alpha\beta}$ by

$$M_{\alpha\beta}(\lambda(k), B) := \int_{\partial B} y^\beta \phi_\alpha(y)\, d\sigma(y), \tag{4.4}$$

where ϕ_α is given by

$$\phi_\alpha(y) := (\lambda(k)I - (\mathcal{K}_B^0)^*)^{-1}\big[\nu(x) \cdot \nabla x^\alpha\big](y), \quad y \in \partial B. \tag{4.5}$$

If $|\alpha| = |\beta| = 1$, we denote $M_{\alpha\beta}$ by $(m_{pq})_{p,q=1}^d$ with

$$m_{pq} := \int_{\partial B} y_q (\lambda(k)I - (\mathcal{K}_B^0)^*)^{-1}\big[\nu_p\big](y)\, d\sigma(y), \tag{4.6}$$

and $\nu = (\nu_1, \ldots, \nu_d)$. In this case we call $M = (m_{pq})_{p,q=1}^d$ simply the polarization tensor.

It can be seen from Formula (4.3) that generalized polarization tensors provide us with complete information about the far-field expansion of u:

$$(u_k - h)(x) = \sum_{|\alpha|,|\beta|=1}^{+\infty} \frac{(-1)^{|\beta|}}{\alpha!\beta!} \partial_x^\beta \Gamma_0(x) M_{\alpha\beta}(\lambda(k), B) \partial^\alpha h(0)$$

as $|x| \to +\infty$.

4.1.2. Spectral Representation of the Polarization Tensor. In this subsection, we derive some important properties satisfied by the polarization tensor. It is worth mentioning that the concept of a polarization tensor has been widely used in various areas such as the imaging of small particles and effective medium theory.

For a $\mathcal{C}^{1,\eta}$, $\eta > 0$, domain B in $\mathbb{R}^d$, using (1.14) we can write

$$(\lambda(k)I - (\mathcal{K}_B^0)^*)^{-1}[\psi] = \sum_{j=0}^{\infty} \frac{< \psi, \varphi_j >_{\mathcal{H}^*} \otimes \varphi_j}{\lambda(k) - \lambda_j},$$

with (λ_j, φ_j) being the eigenvalues and eigenvectors of $(\mathcal{K}_B^0)^*$ in $\mathcal{H}^*$. Hence, the entries of the polarization tensor M can be decomposed as

$$m_{pq}(\lambda(k), B) = \sum_{j=1}^{\infty} \frac{< \nu_p, \varphi_j >_{\mathcal{H}^*} < \varphi_j, x_q >_{-\frac{1}{2},\frac{1}{2}}}{\lambda(k) - \lambda_j}. \tag{4.7}$$

Note that $< \nu_p, \chi(\partial B) >_{-\frac{1}{2},\frac{1}{2}} = 0$. So, considering the fact that $\lambda_0 = 1/2$, we have $< \nu_p, \varphi_0 >_{\mathcal{H}^*} = 0$. Moreover, in three dimensions, since

$$\begin{aligned}
< \varphi_j, x_q >_{-\frac{1}{2},\frac{1}{2}} &= \Big\langle \big(\frac{1}{2} - \lambda_j\big)^{-1} \big(\frac{1}{2}I - (\mathcal{K}_B^0)^*\big)[\varphi_j], x_q \Big\rangle_{-\frac{1}{2},\frac{1}{2}} \\
&= \frac{-1}{1/2 - \lambda_j} \Big\langle \frac{\partial \mathcal{S}_B^0[\varphi_j]}{\partial \nu}\Big|_-, x_q \Big\rangle_{-\frac{1}{2},\frac{1}{2}} \\
&= \int_{\partial B} \frac{\partial x_q}{\partial \nu} \mathcal{S}_B^0[\varphi_j] d\sigma - \int_B \Big(\Delta x_q \mathcal{S}_B^0[\varphi_j] - x_q \Delta \mathcal{S}_B^0[\varphi_j]\Big) dx \\
&= \frac{< \nu_q, \varphi_j >_{\mathcal{H}^*}}{1/2 - \lambda_j},
\end{aligned}$$

it follows that

$$(4.8)\quad m_{pq}(\lambda(k),B) = \sum_{j=1}^{\infty} \frac{< \nu_p, \varphi_j >_{\mathcal{H}^*} < \nu_q, \varphi_j >_{\mathcal{H}^*}}{(1/2-\lambda_j)(\lambda(k)-\lambda_j)} = \sum_{j=1}^{\infty} \frac{\alpha_{pq}^{(j)}}{(1/2-\lambda_j)(\lambda(k)-\lambda_j)} .$$

Here, we have used the fact that $\mathcal{S}_B^0[\varphi_j]$ is harmonic in B and introduced

$$\alpha_{pq}^{(j)} := < \nu_p, \varphi_j >_{\mathcal{H}^*} < \nu_q, \varphi_j >_{\mathcal{H}^*} .$$

It can be shown that $\alpha_{pq}^{(j)} \geq 0$, for all $p, q = 1, \ldots, d$, and $j \geq 1$.

From (4.8), one can see that the following properties of the polarization tensor hold.

PROPOSITION 4.2. *The polarization tensor $M(\lambda(k), B)$ is symmetric and if $k > 1$, then $M(\lambda(k), B)$ is positive definite, and it is negative definite if $0 < k < 1$.*

4.1.3. Example 1 (ellipse). If B is an ellipse of the form $R(B')$ where R is a rotation by θ and B' is an ellipse of the form

$$\frac{x^2}{a^2} + \frac{y^2}{b^2} \leq 1,$$

then it is known that its polarization tensor is given by
(4.9)

$$M(\lambda(k),B) = (k-1)|B| R \begin{pmatrix} \dfrac{a+b}{a+kb} & 0 \\ 0 & \dfrac{a+b}{ak+b} \end{pmatrix} R^t = R \begin{pmatrix} \dfrac{|B|}{\lambda(k) - \frac{1}{2}\frac{a-b}{a+b}} & 0 \\ 0 & \dfrac{|B|}{\lambda(k) + \frac{1}{2}\frac{a-b}{a+b}} \end{pmatrix} R^t.$$

Recall that, in $\mathcal{H}^*(\partial B)$,

$$\sigma((\mathcal{K}_B^0)^*) \backslash \{1/2\} = \left\{ \pm \frac{1}{2} \left(\frac{a-b}{a+b} \right)^j, \quad j = 1, 2, \ldots \right\} .$$

Hence we see that the polarization tensor is represented in a spectral form.

As a numerical example, we compute the PT for an ellipse with $a = 5$, $b = 3$ and $\theta = 0$. We also assume $k = 3$ (or equivalently, $\lambda(k) = 1$). We give a comparison between the numerical values and the exact values in Table 4.1.

	Theoretical	Numerical
$M(\lambda(k), B)$	$\begin{pmatrix} 53.8559 & 0.0000 \\ -0.0000 & 41.8879 \end{pmatrix}$	$\begin{pmatrix} 53.8559 & 0.0000 \\ -0.0000 & 41.8879 \end{pmatrix}$

TABLE 4.1. Polarization Tensor $M(\lambda(k), B)$ when B is an ellipse unit circular disk. The parameters are given as $a = 5$, $b = 3$, $\theta = 0$ and $k = 3$.

4.1.4. Example 2 (two circular disks). Next we consider the case when B represents two separated disks. Let $B = B_1 \cup B_2$ where B_j is a circular disk of radius r centered at $(-1)^j(r + \frac{\epsilon}{2}, 0)$ for $j = 1, 2$. Let $\epsilon > 0$ be the distance between the two disks, that is, $\epsilon := \operatorname{dist}(B_1, B_2)$. Set

$$\alpha = \sqrt{\epsilon(r + \frac{\epsilon}{4})} \quad \text{and} \quad s = \sinh^{-1}\left(\frac{\alpha}{r}\right), \quad \text{for } j = 1, 2, \tag{4.10}$$

where r is the radii of the two disks and ϵ is their separation distance.

The PT can be defined when the domain D is multiply connected. In the case of two inclusions (that is, $D = B_1 \cup B_2$), it is defined as follows:

$$M_{ij}(\lambda(k), D) = \int_{\partial B_1} y_j \phi_i^{(1)}\, d\sigma(y) + \int_{\partial B_2} y_j \phi_i^{(2)}\, d\sigma(y), \quad \text{for } i, j = 1, 2,$$

where

$$\begin{bmatrix} \phi_i^{(1)} \\ \phi_i^{(2)} \end{bmatrix} = (\lambda \mathbb{I} - \mathbb{K}^*)^{-1} \begin{bmatrix} \nu_i|_{\partial B_1} \\ \nu_i|_{\partial B_2} \end{bmatrix}.$$

Recall that the associated NP-operator for two inclusions is defined as follows:

$$\mathbb{K}^* := \begin{bmatrix} (\mathcal{K}_{B_1}^0)^* & \dfrac{\partial}{\partial \nu^{(1)}} \mathcal{S}_{B_2}^0 \\ \dfrac{\partial}{\partial \nu^{(2)}} \mathcal{S}_{B_1}^0 & (\mathcal{K}_{B_2}^0)^* \end{bmatrix}.$$

Here, $\nu^{(i)}$ is the outward normal on ∂B_i, $i = 1, 2$. Recall also that the eigenvalues of $\mathbb{K}^*$ on $\mathcal{H}_0^*$ are given by

$$\lambda_{\epsilon,j}^{\pm} = \pm \frac{1}{2} e^{-2|j|s}, \quad j \in \mathbb{Z}. \tag{4.11}$$

The polarization tensor for the two circular disks $B_1 \cup B_2$ is given by the following formula:

$$M(\lambda(k), D) = 8\pi\alpha^2 \begin{pmatrix} \displaystyle\sum_{j=1}^{\infty} \frac{j e^{-2js}}{\lambda(k) - \frac{1}{2} e^{-2js}} & 0 \\ 0 & \displaystyle\sum_{j=1}^{\infty} \frac{j e^{-2js}}{\lambda(k) + \frac{1}{2} e^{-2js}} \end{pmatrix}. \tag{4.12}$$

Again, it is represented in a spectral form.

As a numerical example, we compute the PT for two disks with $r = 1$, $\epsilon = 0.3$ and $\theta = 0$. We also assume $k = 3$ (or equivalently, $\lambda(k) = 1$). We give a comparison between the numerical values and the exact values in Table 4.2.

	Theoretical	Numerical
$M(\lambda(k), B)$	$\begin{pmatrix} 6.9789 & 0.0000 \\ 0.0000 & 5.7629 \end{pmatrix}$	$\begin{pmatrix} 6.9789 & 0.0000 \\ 0.0000 & 5.7629 \end{pmatrix}$

TABLE 4.2. Polarization Tensor $M(\lambda(k), B)$ when B is two circular disks of radius $r = 1$ separated by a distance $\epsilon = 0.3$. We also assume $k = 3$.

4.1.5. Equivalent ellipse. Consider the polarization tensor for some object(s). It can be shown that there exists a corresponding unique ellipse $\mathcal{E}$ that has precisely the same polarization tensor. We will call $\mathcal{E}$ the equivalent ellipse. The equivalent ellipse represents the essential nature of the inclusion. From a given polarization tensor M, we can reconstruct the paramters for the equivalent ellipse using the following formula:

$$a = eb, \quad b = \sqrt{\frac{E}{\pi e}}, \quad E = \frac{\lambda_1(e+k)}{(e+1)(k-1)}, \quad e = \frac{\lambda_2 - k\lambda_1}{\lambda_1 - k\lambda_2}, \tag{4.13}$$

where λ_1, λ_2 are the eigenvalues of M and $[e_{11}, e_{12}]^T$, $[e_{21}, e_{22}]^T$ are the associated normalized eigenvectors.

Next we present a numerical example. Let B represent two circular disks. We set $r = 1$, $\epsilon = 0.3$ and $k = 1.4$. We also rotate the two disks abount an angle of $\theta_B = \pi/6$ with respect to the point which is midway between the centers of each of the two disks. From (4.13), the reconstructed paramaters for the equivalent ellipse $\mathcal{E}$ turn out to be $a = 1.713224, b = 1.167994$, and $\theta = 0.523599$. The two disks B and the equivalent ellipse $\mathcal{E}$ are shown in Figure 4.1.

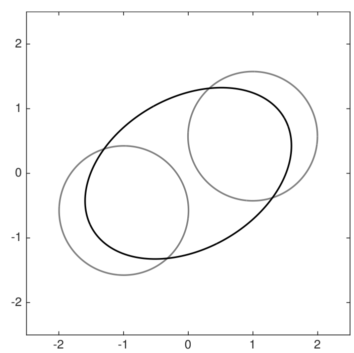

FIGURE 4.1. Two circular disks (gray) and their equivalent ellipse (black). The parameters are given as $r = 1, \epsilon = 0.3, \theta_B = \pi/6$ and $k = 1.4$.

4.2. Helmholtz Equation and scattering coefficients

Code:	4.2 Helmholtz Equation and Scattering Coefficients	DemoHelmholtzSolver.m DemoScatteringCoeff.m

4.2.1. Transmission Problem. Let D be a bounded smooth domain in $\mathbb{R}^d$. Let μ and ε be two piecewise constant functions such that $\mu(x) = \mu_m$ and $\varepsilon(x) = \varepsilon_m$ for $x \in \mathbb{R}^d \setminus \overline{D}$ and $\mu(x) = \mu_c$ and $\varepsilon(x) = \varepsilon_c$ for $x \in D$. Suppose that $\mu_m, \varepsilon_m, \mu_c$, and ε_c are positive and let $k_m = \omega\sqrt{\varepsilon_m \mu_m}$ and $k_c = \omega\sqrt{\varepsilon_c \mu_c}$.

We consider the following transmission problem for the Helmholtz equation:

$$\begin{cases} \nabla \cdot \dfrac{1}{\mu} \nabla u + \omega^2 \varepsilon u = 0 \quad \text{in } \mathbb{R}^d, \\ u^s := u - u^i \text{ satisfies the Sommerfeld radiation condition,} \end{cases} \tag{4.14}$$

where u^i is an incident wave. Here, the Sommerfeld radiation condition reads:

$$\left|\frac{\partial u^s}{\partial r} - \sqrt{-1}k_m u^s\right| = O\left(r^{-(d+1)/2}\right) \quad \text{as } r = |x| \to +\infty \quad \text{uniformly in } \frac{x}{|x|}. \tag{4.15}$$

In fact, the above problem is equivalent to the following equation:

$$\begin{cases} \Delta u + k_c^2 u = 0 \quad \text{in } D, \\ \Delta u + k_m^2 u = 0 \quad \text{in } \mathbb{R}^d \setminus \overline{D}, \\ u|_+ = u|_- \quad \text{on } \partial D, \\ \dfrac{1}{\mu_m} \dfrac{\partial u}{\partial \nu}\Big|_+ = \dfrac{1}{\mu_c} \dfrac{\partial u}{\partial \nu}\Big|_- \quad \text{on } \partial D, \\ u^s := u - u^i \text{ satisfies the Sommerfeld radiation condition.} \end{cases} \tag{4.16}$$

4.2.2. Uniqueness Results. We will need the following important result from the theory of the Helmholtz equation. It will help us prove uniqueness for exterior Helmholtz problems.

LEMMA 4.3 (Rellich's lemma). *Let $R_0 > 0$ and $B_R = \{|x| < R\}$. Let u satisfy the Helmholtz equation $\Delta u + \omega^2 u = 0$ for $|x| > R_0$. Assume, furthermore, that*

$$\lim_{R \to +\infty} \int_{\partial B_R} |u(x)|^2 \, d\sigma(x) = 0.$$

Then, $u \equiv 0$ for $|x| > R_0$.

Note that the assertion of this lemma does not hold if ω is imaginary or $\omega = 0$.

Now, using Lemma 4.3, we can establish the following uniqueness result for the exterior Helmholtz problem.

LEMMA 4.4. *Suppose $d = 2$ or 3. Let Ω be a bounded Lipschitz domain in $\mathbb{R}^d$. Let $u \in H^1_{\mathrm{loc}}(\mathbb{R}^d \setminus \overline{\Omega})$ satisfy*

$$\begin{cases} \Delta u + \omega^2 u = 0 \quad \textit{in } \mathbb{R}^d \setminus \overline{\Omega}, \\ \left|\dfrac{\partial u}{\partial r} - \sqrt{-1}\omega u\right| = O\left(r^{-(d+1)/2}\right) \quad \textit{as } r = |x| \to +\infty \quad \textit{uniformly in } \dfrac{x}{|x|}, \\ u = 0 \textit{ or } \dfrac{\partial u}{\partial \nu} = 0 \quad \textit{on } \partial\Omega. \end{cases}$$

Then, $u \equiv 0$ in $\mathbb{R}^d \setminus \overline{\Omega}$.

PROOF. Let $B_R = \{|x| < R\}$. For R large enough, $\Omega \subset B_R$. Notice first that by multiplying $\Delta u + \omega^2 u = 0$ by $\overline{u}$ and integrating by parts over $B_R \setminus \overline{\Omega}$, we arrive at

$$\Im \int_{\partial B_R} \overline{u} \frac{\partial u}{\partial \nu} \, d\sigma = 0.$$

But

$$\Im \int_{\partial B_R} \overline{u} \left(\frac{\partial u}{\partial \nu} - \sqrt{-1}\omega u\right) d\sigma = -\omega \int_{\partial B_R} |u|^2.$$

Applying the Cauchy–Schwarz inequality,

$$\left| \Im \int_{\partial B_R} \overline{u} \left(\frac{\partial u}{\partial \nu} - \sqrt{-1}\omega u \right) d\sigma \right| \\ \leq \left(\int_{\partial B_R} |u|^2 \right)^{1/2} \left(\int_{\partial B_R} \left| \frac{\partial u}{\partial \nu} - \sqrt{-1}\omega u \right|^2 d\sigma \right)^{1/2},$$

and using the radiation condition (2.5), we get

$$\left| \Im \int_{\partial B_R} \overline{u} \left(\frac{\partial u}{\partial \nu} - \sqrt{-1}\omega u \right) d\sigma \right| \leq \frac{C}{R} \left(\int_{\partial B_R} |u|^2 \right)^{1/2},$$

for some positive constant C independent of R. Consequently, we obtain that

$$\left(\int_{\partial B_R} |u|^2 \right)^{1/2} \leq \frac{C}{R},$$

which indicates by Rellich's lemma that $u \equiv 0$ in $\mathbb{R}^d \setminus \overline{B_R}$. Hence, by the unique continuation property for $\Delta + \omega^2$, we can conclude that $u \equiv 0$ up to the boundary $\partial\Omega$. This finishes the proof. □

By using Rellich's lemma, we can prove that the following uniqueness result holds.

LEMMA 4.5. *If u satisfies (4.14) with $u^i = 0$, then $u \equiv 0$ in $\mathbb{R}^d$.*

PROOF. Using the fact that

$$\int_{\partial D} \frac{\partial u}{\partial \nu}\bigg|_+ \bar{u}\, d\sigma = \frac{\mu_m}{\mu_c} \int_{\partial D} \frac{\partial u}{\partial \nu}\bigg|_- \bar{u}\, d\sigma = \frac{\mu_m}{\mu_c} \int_D (|\nabla u|^2 - k_c^2 |u|^2)\, dx\,,$$

we find that

$$\Im \int_{\partial D} \frac{\partial u}{\partial \nu}\bigg|_+ \bar{u}\, d\sigma = 0\,,$$

which gives, by applying Lemma 4.4, that $u \equiv 0$ in $\mathbb{R}^d \setminus D$. Now u satisfies $(\Delta + k_c^2)u = 0$ in D and $u = \partial u / \partial \nu = 0$ on ∂D. By the unique continuation property of $\Delta + k_c^2$, we readily get $u \equiv 0$ in D, and hence in $\mathbb{R}^d$. □

4.2.3. Representation formula. Here we represent the solution u using the single layer potential. The following result is of importance to us for establishing a representation formula for the solution u to (4.14).

PROPOSITION 4.6. *Suppose that k_m^2 is not a Dirichlet eigenvalue for $-\Delta$ on D. For each $(F, G) \in H^1(\partial D) \times L^2(\partial D)$, there exists a unique solution $(f, g) \in L^2(\partial D) \times L^2(\partial D)$ to the system of integral equations*

$$\begin{cases} \mathcal{S}_D^{k_c}[f] - \mathcal{S}_D^{k_m}[g] = F \\ \dfrac{1}{\mu_c} \dfrac{\partial (\mathcal{S}_D^{k_c}[f])}{\partial \nu}\bigg|_- - \dfrac{1}{\mu_m} \dfrac{\partial (\mathcal{S}_D^{k_m}[g])}{\partial \nu}\bigg|_+ = G \end{cases} \quad \text{on } \partial D. \tag{4.17}$$

Furthermore, there exists a constant C independent of F and G such that

$$\|f\|_{L^2(\partial D)} + \|g\|_{L^2(\partial D)} \leq C \Big(\|F\|_{H^1(\partial D)} + \|G\|_{L^2(\partial D)} \Big), \tag{4.18}$$

where in the three-dimensional case the constant C can be chosen independently of k_m and k_c if k_m and k_c go to zero.

By using Proposition 4.6, the following representation formula holds.

THEOREM 4.7. *Suppose that k_0^2 is not a Dirichlet eigenvalue for $-\Delta$ on D. Let u be the solution of (4.14). Then u can be represented using the single-layer potentials $\mathcal{S}_D^{k_m}$ and $\mathcal{S}_D^{k_c}$ as follows:*

$$u(x) = \begin{cases} u^i(x) + \mathcal{S}_D^{k_m}[\psi](x), & x \in \mathbb{R}^2 \setminus \overline{D}\,, \\ \mathcal{S}_D^{k_c}[\varphi](x), & x \in D\,, \end{cases} \tag{4.19}$$

where the pair $(\varphi, \psi) \in L^2(\partial D) \times L^2(\partial D)$ is the unique solution to

$$\begin{cases} \mathcal{S}_D^{k_c}[\varphi] - \mathcal{S}_D^{k_m}[\psi] = u^i \\ \displaystyle \frac{1}{\mu_c} \frac{\partial(\mathcal{S}_D^{k_c}[\varphi])}{\partial \nu}\bigg|_- - \frac{1}{\mu_m} \frac{\partial(\mathcal{S}_D^{k_m}[\psi])}{\partial \nu}\bigg|_+ = \frac{1}{\mu_m}\frac{\partial u^i}{\partial \nu} \end{cases} \quad \text{on } \partial D. \tag{4.20}$$

4.2.4. Scattering Coefficients. We first define the scattering coefficients of a particle D in two dimensions. Assume that k_m^2 is not a Dirichlet eigenvalue for $-\Delta$ on D. Then, the solution u to (4.14) (for $d = 2$) can be represented using the single-layer potentials $\mathcal{S}_D^{k_m}$ and $\mathcal{S}_D^{k_c}$ by (4.19) where the pair $(\varphi, \psi) \in L^2(\partial D) \times L^2(\partial D)$ is the unique solution to (4.20). Moreover, by using Proposition 4.6 it follows that there exists a constant $C = C(k_c, k_m, D)$ such that

$$\|\varphi\|_{L^2(\partial D)} + \|\psi\|_{L^2(\partial D)} \le C(\|u^i\|_{L^2(\partial D)} + \|\nabla u^i\|_{L^2(\partial D)})\,. \tag{4.21}$$

Furthermore, the constant C can be chosen to be scale independent. There exists δ_0 such that if one denotes by $(\varphi_\delta, \psi_\delta)$ the solution of (4.20) with k_c and k_m respectively replaced by δk_c and δk_m, then

$$\|\varphi_\delta\|_{L^2(\partial D)} + \|\psi_\delta\|_{L^2(\partial D)} \le C(\|u^i\|_{L^2(\partial D)} + \|\nabla u^i\|_{L^2(\partial D)})\,. \tag{4.22}$$

Recall Graf's addition formula:

$$H_0^{(1)}(k|x-y|) = \sum_{l \in \mathbb{Z}} H_l^{(1)}(k|x|) e^{\sqrt{-1} l \theta_x} J_l(k|y|) e^{-\sqrt{-1} l \theta_y} \quad \text{for } |x| > |y|, \tag{4.23}$$

where $x = (|x|, \theta_x)$ and $y = (|y|, \theta_y)$ in polar coordinates and $H_l^{(1)}$ is the Hankel function of the first kind of order l and J_l is the Bessel function of order l.

From (4.19) and (4.23), the following asymptotic formula holds as $|x| \to \infty$:

$$u(x) - u^i(x) = -\frac{\sqrt{-1}}{4} \sum_{l \in \mathbb{Z}} H_l^{(1)}(k_m|x|) e^{\sqrt{-1} l \theta_x} \int_{\partial D} J_l(k_m|y|) e^{-\sqrt{-1} l \theta_y} \psi(y) d\sigma(y)\,. \tag{4.24}$$

Let $(\varphi_{l'}, \psi_{l'})$ be the solution to (4.20) with $J_{l'}(k_m|x|)e^{\sqrt{-1} l' \theta_x}$ in place of $u^i(x)$. We define the *scattering coefficient* as follows.

DEFINITION 4.8. The scattering coefficients $W_{ll'}$, $l, l' \in \mathbb{Z}$, associated with the permittivity and permeability distributions ε, μ and the frequency ω (or k_c, k_m, D) are defined by

$$W_{ll'} = W_{ll'}[\varepsilon, \mu, \omega] := \int_{\partial D} J_l(k_m|y|) e^{-\sqrt{-1} l \theta_y} \psi_{l'}(y) d\sigma(y)\,. \tag{4.25}$$

4.3. Numerical illustration

In this section we explain how to solve the transmission problem (4.16) for the Helmholtz equation.

4.3.1. Numerical implementation. To obtain the solution u numerically, we have to solve the boundary integral equation (4.20). Let us briefly discuss how to disretize the integral equation.

We perform the usual boundary discretization procedure as in the previous chapters. Suppose that the boundary $\partial\Omega$ is parametrized by $x(t)$ for $t \in [0, 2\pi)$. We partition the interval $[0, 2\pi)$ into N pieces

$$[t_1, t_2), [t_2, t_3), \ldots, [t_N, t_{N+1}),$$

with $t_1 = 0$ and $t_{N+1} = 2\pi$. We then approximate the boundary $\partial\Omega = \{x(t) : t \in [0, 2\pi)\}$ by $x^{(i)} = x(t_i)$ for $1 \le i \le N$. We approximate the density functions φ and ψ with $\overline{\varphi}_i := \varphi(x^{(i)})$ and $\overline{\psi}_i := \psi(x^{(i)})$. We also discretize the Dirichlet data $u^i|_{\partial D}$ and Neumann data $\partial u^i/\partial\nu|_{\partial D}$ of the incident wave u_i as follows: $u_d = u^i(x^{(j)})$ and $u_n = \partial u^i/\partial\nu(x^{(j)})$. Then the integral equation (4.20) is represented numerically as

$$\begin{pmatrix} S_- & -S_+ \\ \frac{1}{\mu_c}S'_- & -\frac{1}{\mu_m}S'_+ \end{pmatrix} \begin{pmatrix} \overline{\varphi} \\ \overline{\psi} \end{pmatrix} = \begin{pmatrix} u_d \\ u_n \end{pmatrix},$$

where $S_\pm$ and $S'_\pm$ are $N \times N$ matrices given by

$$(S_-)_{ij} = \Gamma^{k_m}(x^{(i)} - x^{(j)})|T(x^{(j)})|(t_{j+1} - t_j), \tag{4.26}$$

$$(S_+)_{ij} = \Gamma^{k_c}(x^{(i)} - x^{(j)})|T(x^{(j)})|(t_{j+1} - t_j) \tag{4.27}$$

$$(S'_-)_{ij} = -\frac{1}{2}\delta_{ij} + \frac{\partial\Gamma^{k_c}}{\partial\nu_x}(x^{(i)} - x^{(j)})|T(x^{(j)})|(t_{j+1} - t_j), \tag{4.28}$$

$$(S'_+)_{ij} = \frac{1}{2}\delta_{ij} + \frac{\partial\Gamma^{k_m}}{\partial\nu_x}(x^{(i)} - x^{(j)})|T(x^{(j)})|(t_{j+1} - t_j), \tag{4.29}$$

for $i \ne j$ and $i, j = 1, 2, ..., N$. Here, the singularity for $i = j$ can be treated as explained in the previous chapters. By solving the above linear system of equations, we can obtain approximations for the density functions φ and ψ. Then we can get the numerical solution for u from the formula (4.19). We can also obtain the scattering coefficients $W_{ll'}$ numerically from the definition in (4.25).

4.3.2. Explicit solution for a disk. For the special case when the domain B is a disk, we can obtain an explicit solution to the transmission problem. Let B be a disk of radius R located at the origin in $\mathbb{R}^2$. We also assume that the incident wave is given by $u^i(x) = J_n(k_m r)e^{in\theta}$. Then it can be shown that the explicit solution is given by

$$u(r, \theta) = \begin{cases} J_n(k_m r)e^{in\theta} + a_n H_n^{(1)}(k_m r)e^{in\theta}, & |r| > R, \\ b_n J_n(k_c r)e^{in\theta}, & |r| <= R, \end{cases} \tag{4.30}$$

where (r, θ) are the polar coordinates and the constants a_n and b_n are given by

$$a_n = \frac{\frac{k_m}{\mu_m} J_n(k_c R) J_n'(k_m R) - \frac{k_c}{\mu_c} J_n(k_m R) J_n'(k_c R)}{\frac{k_c}{\mu_c} H_n^{(1)}(k_m R) J_n'(k_c R) - \frac{k_m}{\mu_m} J_n(k_c R) H_n'(k_m R)},$$

$$b_n = \frac{J_n(k_m R) + a_n H_n^{(1)}(k_m R)}{J_n(k_c R)}.$$

In fact, the above result provides an explicit expression for the scattering coefficients. By comparing it with the expansion, we have

$$W_{nn'} = 0, \quad n \neq n',$$
$$W_{nn} = 4ia_n, \quad n \in \mathbb{Z}.$$

4.3.3. Numerical Example. Let B be a disk of radius $R = 1$ located at the origin in $\mathbb{R}^2$. Let us take the parameters as $\omega = 2, \varepsilon_m = 1, \varepsilon_c = 1, \mu_m = 1$ and $\mu_c = 5$. We also assume that $u^i(x) = J_3(k_m r)e^{i3\theta}$. We obtain a numerical solution to (4.20) and then compare it with the exact solution. We evaluate the solution $u(x)$ on the circle $|x| = 2$. See figure 4.2.

We also compute the scattering coefficients W_{nn} numerically for $n = 1, 2, ..., 7$ and then compare it with theoretical results (See Table 4.3). The decaying property of the scattering coefficients is clearly shown.

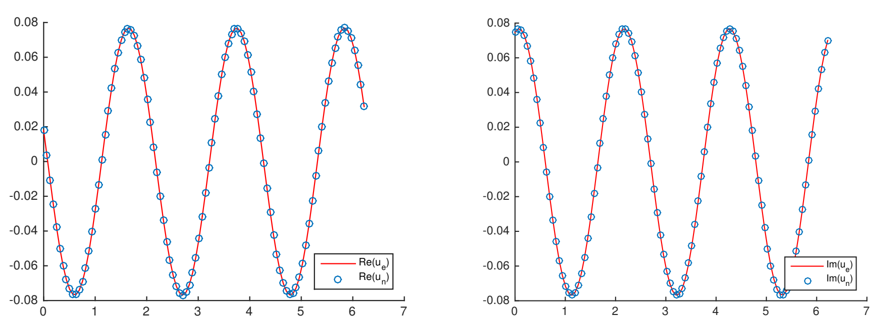

FIGURE 4.2. The exact solution u_e and the numerical solution u_n of the Helmholtz equation problem (4.16). The inclusion D is a circular disk with radius 1. The parameters are given as $\omega = 2, \varepsilon_m = 1, \varepsilon_c = 1, \mu_m = 1$ and $\mu_c = 5$. We assume that $u^i(x) = J_3(k_m r)e^{i3\theta}$. The solutions are evaluated on the circle $|x| = 2$.

n	Theoretical	Numerical
1	$1.7866 - 1.1036i$	$1.7866 - 1.1011i$
2	$-0.9673 - 3.7540i$	$-0.9601 - 3.7545i$
3	$-0.6487 - 0.1081i$	$-0.6487 - 0.1081i$
4	$-0.0462 - 0.0005i$	$-0.0462 - 0.0005i$
5	$-0.0023 - 0.0000i$	$-0.0023 - 0.0000i$
6	$-0.0001 - 0.0000i$	$-0.0001 - 0.0000i$
7	$-0.0000 - 0.0000i$	$-0.0000 - 0.0000i$

TABLE 4.3. Scattering coefficients W_{nn} for $n = 1, 2, ..., 7$ when D is a unit circular disk. The parameters are given as $\omega = 2, \varepsilon_m = 1, \varepsilon_c = 1, \mu_m = 1$ and $\mu_c = 5$.

CHAPTER 5

Direct Imaging and Super-resolution in High Contrast Media

In this chapter we discuss direct imaging using a MUSIC-type algorithm for inclusion detection, and how super-resolution imaging can be achieved in high contrast media.

Before discussing the MUSIC-type algorithm for inclusion detection we first take a look at Pisarenko's method for frequency estimation which is essentially a special case of the classical MUSIC frequency detection algorithm. Both MUSIC and Pisarenko's method are subspace methods that decompose an autocovariance matrix which characterizes a signal into *signal subspace* and a *noise subspace*. In Pisarenko's method the noise subspace is spanned by a single vector whereas in the MUSIC algorithm d minus p vectors are used to span the noise subspace where d is the number of measurements and p is the number of complex exponentials in the signal. Both methods proceed along the same lines which as follows:

i) A set of measurements of the data is taken.
ii) These measurements are used to construct a matrix that characterizes the data.
iii) The matrix is decomposed into a signal subspace and a noise subspace.
iv) A set of test data is generated.
v) Elements of the test data set are projected against the noise subspace.
vi) We plot the results and observe large peaks when the parameters used for the test data are close to the parameters present in the original data.

5.1. Pisarenko harmonic decomposition

Code:	5.1 Pisarenko Harmonic Decomposition	PisarenkoHarmonicDecomposition.m

Let $f = \{f_1, f_2, \ldots, f_p\}$ be a set of p frequencies and let s_j be a complex exponential given by

$$s_j(f_j, t) = e^{i2\pi f_j t}, \quad j = 1, \ldots, p.$$

Let $s(f, t)$ be a wide sense stationary signal given by summing the p complex exponentials s_j. Then the autocovariance function (the inverse Fourier Transform of the Power Spectral Density) of the signal s is given by

$$\sigma_{ss}(\tau) = \sum_{j=1}^{p} e^{i2\pi f_j \tau},$$

where τ is the lag time. Assume we have measurements for d lag times where $d = p + 1$. Calculating the autocovariance for $\tau = 0, \ldots, d-1$ lets us construct the autocovariance matrix C_{ss}. For example, in the case where $d = 3$, C_{ss} is given by

$$C_{ss} = \begin{pmatrix} \sigma_{ss}(0) & \overline{\sigma_{ss}}(1) & \overline{\sigma_{ss}}(2) \\ \sigma_{ss}(1) & \sigma_{ss}(0) & \overline{\sigma_{ss}}(1) \\ \sigma_{ss}(2) & \sigma_{ss}(1) & \sigma_{ss}(0) \end{pmatrix}.$$

The covariance matrix can also be written as

$$C_{ss} = \sum_{j=1}^{p} \hat{s}_j \, \hat{s}_j^H,$$

where $\hat{s}_j = (1, e^{i2\pi f_j}, e^{i4\pi f_j}, \ldots, e^{i2\pi(d-1)f_j})$ represents the jth component of the signal evaluated at the d lag times.

Now suppose the signal also contains noise by defining $r(f,t) = s(f,t) + w$ where the noise w has variance σ^2. Then the autocovariance matrix is given by

$$C_{rr} = C_{ss} + \sigma^2 I_d,$$

where I_d is the identity matrix of dimension d. C_{rr} is a Hermitian matrix with p linearly independent columns so taking an eigendecomposition of C_{rr} gives

$$C_{rr} = QDQ^H,$$

where D is a diagonal matrix containing the eigenvalues of C_{rr}, ordered as $\lambda_1 \geq \lambda_2 \geq \cdots \geq \lambda_d$ and Q contains orthogonal eigenvectors ψ_j, $j = 1, \ldots, d$. We have p degrees of freedom in the data and hence the first p eigenvectors form a basis for what is known as the signal subspace. The remaining eigenvector forms a basis for the noise subspace. Hence the covariance matrix can be written in terms of these subspaces as

$$C_{rr} = \sum_{j=1}^{p} (\lambda_j + \sigma^2) \psi_j \psi_j^H + \sigma^2 \psi_d \psi_d^H.$$

The fact that the signal subpspace and the noise subspace are othogonal to each other means that

$$\hat{s}_j \cdot \psi_d = 0,$$

and this allows us to determine whether a particular frequency is a component of the signal. That is, we consider $I_{pisa}[\hat{s}(f)] = \frac{1}{\hat{s}(f)\cdot\psi_d}$ over a range of frequencies f. If f is close to a frequency in the signal then I_{pisa} will show a large peak at this location.

5.2. Overview of the MUSIC-type algorithm

Code: 5.2 Direct Imaging With MUSIC DemoHelmholtzAnomalyImaging.m

We now focus on imaging small inclusions using a version of the MUSIC algorithm geared towards inclusion localization. The procedure used in this section can be viewed as a generalization of the much simpler Pisarenko's method for frequency estimation.

We probe a medium D using time-harmonic waves emitted from and recorded with a sensor array. Due to the presence of small inclusions boundary measurements of the field will be perturbed slightly from the boundary measurements given by a field in the absence of inclusions. We can use these boundary measurement perturbations to define an imaging functional for each combination of emitted and received wave. By considering all combinations of emitted and received waves for a finite set of sources and receivers we can define a set of imaging functionals. These imaging functionals are used to construct a multi-static response marix (MSR) A which is analogous to the covariance matrix C_{ss} in Pisarkeno's method.

Once we have calculated the MSR matrix which characterizes the data we must generate a set of test data over a range of inclusion locations. We project this test data against the noise subspace of the MSR matrix and this leads to large peaks at position which correspond to the locations of the inclusions.

It is should be noted that the distance from the inclusions to the boundary, and the distance from the inclusions to each other should be much greater than the wavelength. If this is not the case the effective rank of the singular value decomposition of the MSR matrix will be reduced and we will not be able to differentiate the inclusions.

5.2.1. Multistatic Response Matrix: Statistical Structure. In multistatic wave imaging, waves are emitted by a set of sources and they are recorded by a set of sensors in order to probe an unknown medium. The responses between each pair of source and receiver are collected and assembled in the form of the multi-static response (MSR) matrix. The indices of the MSR matrix are the index of the source and the index of the receiver. When the data are corrupted by additive noise, we study the structure of the MSR matrix using random matrix theory.

In the standard acquisition scheme, the response matrix is measured during a sequence of N_s experiments. In the mth experiment, $m = 1, \dots, N_s$, the mth source generates the incident field and the N_r receivers record the scattered wave which means that they measure

$$A^{\text{meas}}_{nm} = A^0_{nm} + W_{nm}, \quad n = 1, \dots, N_r, \quad m = 1, \dots, N_s \ ,$$

which gives the matrix

$$A^{\text{meas}} = A^0 + W \ , \tag{5.1}$$

where A^0 is the unperturbed response matrix and W_{nm} are independent complex Gaussian random variables with mean zero and variance σ^2_{noise} (which means that the real and imaginary parts are independent real Gaussian random variables with mean zero and variance $\sigma^2_{\text{noise}}/2$).

Throughout this section, we only consider the two-dimensional full-view case, where the sensor arrays englobe the reflectors or the inclusions to be imaged.

5.2.2. Point Reflectors and SVD of Multistatic Response Matrices. Suppose that $\varepsilon_0 = \mu_0 = 1$. Consider the Helmholtz equation:

$$\Delta_z \Phi_\omega(z, x) + \omega^2 \Big(1 + \sum_{j=1}^{r} V_j(z)\Big) \Phi_\omega(z, x) = \delta_x(z) \quad \text{in } \mathbb{R}^2 \tag{5.2}$$

for $x \in \mathbb{R}^2$, with the Sommerfeld radiation condition imposed on Φ_ω. Here r is the number of localized reflectors, x is the location of the source, and

$$V_j(z) := \eta_j \chi(\tilde{D}_j)(z - z_j) \ , \tag{5.3}$$

where, for $j = 1, \dots, r$, $\tilde{D}_j$ is a compactly supported domain with volume $|\tilde{D}_j|$, $\chi(\tilde{D}_j)$ is the characteristic function of $\tilde{D}_j$, z_j is the center of the jth inclusion, and

$\eta_j := \varepsilon_j - 1$ is the dielectric contrast (also called the strength of the point reflector at z_j).

Suppose that we have a transmitter array of N_s sources located at $\{x_1, \dots, x_{N_s}\}$ and a receiver array of N_r elements located at $\{y_1, \dots, y_{N_r}\}$. The $N_r \times N_s$ response matrix A describes the transmit-receive process performed at these arrays. The field received by the nth receiving element y_n when the wave is emitted from x_m is $\Phi_\omega(y_n, x_m)$. If we remove the incident field then we obtain the (n, m)-th entry of the unperturbed response matrix A^0:

$$A^0_{nm} = -\Phi_\omega(y_n, x_m) + \Gamma_\omega(y_n, x_m) \ . \tag{5.4}$$

The incident field is $\Gamma_\omega(y, x_m)$.

Finally, taking into account measurement noise, the measured response matrix A^{meas} is

$$A^{\text{meas}} = A^0 + \frac{1}{\sqrt{N_s}} W \ , \tag{5.5}$$

where the matrix W represents the additive measurement noise, which is a random matrix with independent and identically distributed complex entries with Gaussian statistics, mean zero and variance σ^2_{noise}. This particular scaling for the noise level is the right one to get non-trivial asymptotic regimes in the limit $N_s \to \infty$. Furthermore, it is the regime that emerges from the use of the Hadamard acquisition scheme for the response matrix.

In the Born approximation, where the volume $|\tilde{D}_j|$ of $\tilde{D}_j, j = 1, \dots, r$, goes to zero, the measured field has approximately the following form. We include a proof for the readers' sake.

THEOREM 5.1. *We have*

$$\Phi_\omega(y_n, x_m) \approx \Gamma_\omega(y_n, x_m) - \sum_{j=1}^{r} \rho_j \Gamma_\omega(y_n, z_j) \Gamma_\omega(z_j, x_m) \tag{5.6}$$

for $n = 1, \dots, N_r$, $m = 1, \dots, N_s$, *where* ρ_j *is the coefficient of reflection defined by*

$$\rho_j = \omega^2 \eta_j |\tilde{D}_j| \ . \tag{5.7}$$

PROOF. Suppose for simplicity that the number of reflectors is 1 ($r = 1$). Let us consider the full fundamental solution $\Phi_\omega(z, x)$ and the background fundamental solution $\Gamma_\omega(z, y)$, namely,

$$\begin{aligned} \Delta_z \Phi_\omega(z, x) + \omega^2 \Phi_\omega(z, x) &= -\omega^2 V(z) \Phi_\omega(z, x) + \delta_x(z) \\ \Delta_z \Gamma_\omega(z, y) + \omega^2 \Gamma_\omega(z, y) &= \delta_y(z) \ , \end{aligned}$$

with the radiation condition. We multiply the first equation by $\Gamma_\omega(x, y)$ and subtract the second equation multiplied by $\Phi_\omega(x, z)$:

$$\begin{aligned} &\nabla_z \cdot \Big[\Gamma_\omega(z, y) \nabla_z \Phi_\omega(z, x) - \Phi_\omega(z, y) \nabla_z \Gamma_\omega(z, x) \Big] \\ &= -\omega^2 V(z) \Phi_\omega(z, x) \Gamma_\omega(z, y) + \Gamma_\omega(z, y) \delta_x(z) - \Phi_\omega(z, x) \delta_y(z) \\ &= -\omega^2 V(z) \Phi_\omega(z, x) \Gamma_\omega(z, y) + \Gamma_\omega(x, y) \delta_x(z) - \Phi_\omega(y, x) \delta_y(z) \\ &\overset{\text{reciprocity}}{=} -\omega^2 V(z) \Phi_\omega(x, z) \Gamma_\omega(z, y) + \Gamma_\omega(x, y) \delta_x(z) - \Phi_\omega(x, y) \delta_y(z) \ . \end{aligned}$$

We integrate over B_R (with R large enough so that it encloses the support of V) and send R to infinity to obtain thanks to the Sommerfeld radiation condition that

$$0 = -\omega^2 \int_{\mathbb{R}^2} \Phi_\omega(x,z) V(z) \Gamma_\omega(z,y) dz + \Gamma_\omega(x,y) - \Phi_\omega(x,y) .$$

We therefore obtain the Lippmann-Schwinger equation, which is exact:

$$\Phi_\omega(x,y) = \Gamma_\omega(x,y) - \omega^2 \int_{\mathbb{R}^2} \Phi_\omega(x,z) V(z) \Gamma_\omega(z,y) dz .$$

This equation is used as a basis for expanding the fundamental solution Φ_ω when the reflectivity V is small. If Φ_ω in the right-hand side is replaced by the background fundamental solution Γ_ω, then we obtain:

$$\Phi_\omega(x,y) \approx \Gamma_\omega(x,y) - \omega^2 \int \Gamma_\omega(x,z) V(z) \Gamma_\omega(z,y) dz , \tag{5.8}$$

which is the (first-order) Born approximation. When the volume $|\tilde{D}_1|$ is small, the integral in (5.8) can be replaced by $-\omega^2 \eta_1 |\tilde{D}_1| \Gamma_\omega(x,z_1) \Gamma_\omega(z_1,y)$, which gives the desired result. □

We introduce the normalized vector of fundamental solutions from the receiver array to the point z:

$$w(z) := \frac{1}{\left(\sum_{l=1}^{N_r} |\Gamma_\omega(z,y_l)|^2 \right)^{\frac{1}{2}}} \left(\Gamma_\omega(z,y_n) \right)_{n=1,\ldots,N_r} , \tag{5.9}$$

and the normalized vector of fundamental solutions from the transmitter array to the point z, known as the illumination vector,

$$v(z) := \frac{1}{\left(\sum_{l=1}^{N_s} |\Gamma_\omega(z,x_l)|^2 \right)^{\frac{1}{2}}} \left(\overline{\Gamma_\omega(z,x_m)} \right)_{m=1,\ldots,N_s} . \tag{5.10}$$

Using (5.6) we can then write the unperturbed response matrix approximately in the form

$$A^0 = \sum_{j=1}^{r} \sigma_j w(z_j) v(z_j)^* , \tag{5.11}$$

with

$$\sigma_j := \rho_j \Big(\sum_{n=1}^{N_r} |\Gamma_\omega(z_j,y_n)|^2 \Big)^{\frac{1}{2}} \Big(\sum_{m=1}^{N_s} |\Gamma_\omega(z_j,x_m)|^2 \Big)^{\frac{1}{2}} . \tag{5.12}$$

Here * denotes the conjugate transpose.

We assume that the arrays of transmitters and receivers are equi-distributed on a disk englobing the point reflectors. Moreover, the point reflectors are at a distance from the arrays of transmitter and receivers much larger than the wavelength $2\pi/\omega$. Provided that the positions z_j of the reflectors are far from one another or well-separated (*i.e.*, farther than the wavelength $2\pi/\omega$), the vectors $w(z_j)$, $j = 1,\ldots,r$, are approximately orthogonal to one another, as well as are the vectors $v(z_j)$, $j = 1,\ldots,r$. In fact, from the Helmholtz-Kirchhoff identity, we have

$$\frac{1}{N_r} \sum_n \Gamma_\omega(z_j,y_n) \overline{\Gamma_\omega(z_i,y_n)} \approx \frac{1}{\omega} J_0(\omega |z_i - z_j|) \tag{5.13}$$

as $N_r \to +\infty$, where J_0 is the Bessel function of the first kind and of order zero. Moreover, $J_0(\omega|z_i - z_j|) \approx 0$ when $|z_j - z_i|$ is much larger than the wavelength. The matrix A^0 then has rank r and its nonzero singular values are σ_j, $j = 1, \ldots, r$, with the associated left and right singular vectors $w(z_j)$ and $v(z_j)$.

5.2.3. Helmholtz Equation. Suppose that an electromagnetic medium occupies a bounded domain Ω in $\mathbb{R}^d$, with a connected $\mathcal{C}^2$-boundary $\partial\Omega$. Suppose that Ω contains a small inclusion of the form $D = \delta B + z$, where $z \in \Omega$ and B is a $\mathcal{C}^2$-bounded domain in $\mathbb{R}^d$ containing the origin.

Let μ_0 and ε_0 denote the permeability and the permittivity of the background medium Ω, and assume that μ_0 and ε_0 are positive constants. Let $\mu_\star$ and $\varepsilon_\star$ denote the permeability and the permittivity of the inclusion D, which are also assumed to be positive constants. Introduce the piecewise constant magnetic permeability

$$\mu_\delta(x) = \begin{cases} \mu_0\,, & x \in \Omega \setminus \overline{D}\,, \\ \mu_\star\,, & x \in D\,. \end{cases}$$

The piecewise constant electric permittivity, $\varepsilon_\delta(x)$, is defined analogously.

Let the electric field u denote the solution to the Helmholtz equation

$$\nabla \cdot (\frac{1}{\mu_\delta} \nabla u) + \omega^2 \varepsilon_\delta u = 0 \ \text{ in } \Omega\,, \tag{5.14}$$

with the boundary condition $u = f \in W^2_{\frac{1}{2}}(\partial\Omega)$, where $\omega > 0$ is a given frequency.

Problem (5.14) can be written as

$$\begin{cases} (\Delta + \omega^2 \varepsilon_0 \mu_0) u = 0 & \text{in } \Omega \setminus \overline{D}\,, \\ (\Delta + \omega^2 \varepsilon_\star \mu_\star) u = 0 & \text{in } D\,, \\ \dfrac{1}{\mu_\star} \dfrac{\partial u}{\partial \nu}\Big|_- - \dfrac{1}{\mu_0} \dfrac{\partial u}{\partial \nu}\Big|_+ = 0 & \text{on } \partial D\,, \\ u\big|_- - u\big|_+ = 0 & \text{on } \partial D\,, \\ u = f & \text{on } \partial\Omega\,. \end{cases}$$

Assuming that

$$\begin{aligned} &\omega^2 \varepsilon_0 \mu_0 \text{ is not an eigenvalue for the operator } -\Delta \text{ in } L^2(\Omega) \\ &\qquad\qquad \text{with homogeneous Dirichlet boundary conditions,} \end{aligned} \tag{5.15}$$

we can prove existence and uniqueness of a solution to (5.14) at least for δ small enough.

THEOREM 5.2 (Boundary Perturbations). *Suppose that (5.15) holds. Let u be the solution of (5.14) and let the function U be the background solution as before. For any $x \in \partial\Omega$,*

$$\begin{aligned} \frac{\partial u}{\partial \nu}(x) = \frac{\partial U}{\partial \nu}(x) + \delta^d \Bigg(&\nabla U(z) \cdot M(\lambda, B) \frac{\partial \nabla_z G_{k_0}(x,z)}{\partial \nu_x} \\ &+ k_0^2 (\frac{\varepsilon_\star}{\varepsilon_0} - 1) |B| U(z) \frac{\partial G_{k_0}(x,z)}{\partial \nu_x} \Bigg) + O(\delta^{d+1})\,, \end{aligned} \tag{5.16}$$

where $M(\lambda, B)$ is the polarization tensor defined in (4.4) with λ given by

$$\lambda := \frac{(\mu_0/\mu_\star)+1}{2((\mu_0/\mu_\star)-1)} \; . \tag{5.17}$$

Here G_{k_0} is the Dirichlet Green.

5.2.4. Formal Derivations. From the Lippman-Schwinger integral representation formula

$$\begin{aligned} u(x) &= U(x) + (\frac{\mu_0}{\mu_\star} - 1)\int_D \nabla u(y)\cdot \nabla_y G_{k_0}(x,y)\,dy \\ &+ k_0^2(\frac{\varepsilon_\star}{\varepsilon_0} - 1)\int_D u(y) G_{k_0}(x,y)\,dy, \quad x \in \Omega\,, \end{aligned}$$

it follows that for any $x \in \partial\Omega$,

$$\begin{aligned} \frac{\partial u}{\partial \nu}(x) &= \frac{\partial U}{\partial \nu}(x) + (\frac{\mu_0}{\mu_\star} - 1)\int_D \nabla u(y)\cdot \frac{\partial \nabla_y G_{k_0}(x,y)}{\partial \nu_x}\,dy \\ &+ k_0^2(\frac{\varepsilon_\star}{\varepsilon_0} - 1)\int_D u(y) \frac{\partial G_{k_0}(x,y)}{\partial \nu_x}\,dy\,. \end{aligned}$$

Using a Taylor expansion of $G_{k_0}(x,y)$ for $y \in D$, we readily see that for any $x \in \partial\Omega$,

$$\begin{aligned} \frac{\partial u}{\partial \nu}(x) &\approx \frac{\partial U}{\partial \nu}(x) + (\frac{\mu_0}{\mu_\star} - 1)\frac{\partial \nabla_z G_{k_0}(x,z)}{\partial \nu_x}\cdot (\int_D \nabla u(y)\,dy) \\ &+ k_0^2(\frac{\varepsilon_\star}{\varepsilon_0} - 1)\frac{\partial G_{k_0}(x,z)}{\partial \nu_x}(\int_D u(y)\,dy)\,. \end{aligned} \tag{5.18}$$

By taking an asymptotic expansion one can easily check that $u(y) \approx U(z)$, for $y \in D$, and

$$\int_D \nabla u(y)\,dy \approx \delta^d \left(\int_B \nabla \hat{v}(\xi)\,d\xi \right) \cdot \nabla U(z)\,,$$

where $\hat{v}$ is the solution to:

$$\begin{cases} \Delta \hat{v} = 0 \quad \text{in } \mathbb{R}^d \setminus \overline{B}\,, \\ \Delta \hat{v} = 0 \quad \text{in } B\,, \\ \hat{v}|_- - \hat{v}|_+ = 0 \quad \text{on } \partial B\,, \\ k\dfrac{\partial \hat{v}}{\partial \nu}\Big|_- - \dfrac{\partial \hat{v}}{\partial \nu}\Big|_+ = 0 \quad \text{on } \partial B\,, \\ \hat{v}(\xi) - \xi \to 0 \quad \text{as } |\xi| \to +\infty\,. \end{cases} \tag{5.19}$$

with $k = \mu_0/\mu_\star$. Next, we compute

$$\begin{aligned} \int_B \nabla \hat{v}(\xi)\,d\xi &= \int_B (I + \nabla \mathcal{S}_B(\lambda I - \mathcal{K}_B^*)^{-1}[\nu](\xi))\,d\xi \\ &= |B| I + \int_{\partial B} (-\frac{1}{2}I + \mathcal{K}_B^*)(\lambda I - \mathcal{K}_B^*)^{-1}[\nu](\xi)\xi^T\,d\sigma(\xi) \\ &= \frac{1}{k-1}\int_{\partial B} (\lambda I - \mathcal{K}_B^*)^{-1}[\nu](\xi)\,\xi^T\,d\sigma(\xi)\,, \end{aligned}$$

where $|B|$ is the volume of B. Inserting these two approximations into (5.18) leads to (5.16).

Before concluding this section, we make a remark. Consider the Helmholtz equation with the Neumann data g in the presence of the inclusion D:

$$\begin{cases} \nabla \cdot \dfrac{1}{\mu_\delta} \nabla u + \omega^2 \varepsilon_\delta u = 0 \ \text{ in } \Omega \, , \\ \dfrac{\partial u}{\partial \nu} = g \ \text{ on } \partial \Omega \, . \end{cases} \tag{5.20}$$

Let the background solution U satisfy

$$\begin{cases} \Delta U + k_0^2 U = 0 \ \text{ in } \Omega \, , \\ \dfrac{\partial U}{\partial \nu} = g \ \text{ on } \partial \Omega \, . \end{cases} \tag{5.21}$$

The following asymptotic expansion of the solution of the Neumann problem holds. For any $x \in \partial\Omega$, we have

$$\begin{aligned} u(x) = U(x) + \delta^d \Big(& \nabla U(z) M(\lambda, B) \nabla_z N_{k_0}(x,z) \\ & + k_0^2 (\frac{\varepsilon_\star}{\varepsilon_0} - 1) |B| U(z) N_{k_0}(x,z) \Big) + O(\delta^{d+1}) \, , \end{aligned} \tag{5.22}$$

where N_{k_0} is the Neumann function defined by

$$\begin{cases} \Delta_x N_{k_0}(x,z) + {k_0}^2 N_{k_0}(x,z) = -\delta_z \quad \text{in } \Omega \, , \\ \dfrac{\partial N_{k_0}}{\partial \nu_x} \Big|_{\partial \Omega} = 0 \quad \text{for } z \in \Omega \, . \end{cases} \tag{5.23}$$

The following useful relation between the Neumann function and the fundamental solution Γ_{k_0} holds:

$$(-\frac{1}{2} I + \mathcal{K}_\Omega^{k_0})[N_{k_0}(\cdot, z)](x) = \Gamma_{k_0}(x,z), \quad x \in \partial\Omega, \ z \in \Omega \, . \tag{5.24}$$

5.2.5. Direct imaging algorithms for the Helmholtz equation at a fixed frequency. In this section, we design direct imaging functionals for small inclusions at a fixed frequency ω. Consider the Helmholtz equation (5.20) with the Neumann data g in the presence of the inclusion D and let the background solution U be defined by (5.21).

Let w be a smooth function such that $(\Delta + k_0^2) w = 0$ in Ω. The weighted boundary measurements $I_w[U, \omega]$ defined by

$$I_w[U, \omega] := \int_{\partial \Omega} (u - U)(x) \frac{\partial w}{\partial \nu}(x) \, d\sigma(x) \tag{5.25}$$

satisfies

$$\begin{aligned} I_w[U, \omega] &= -\delta^d \Big(\nabla U(z) \cdot M(\lambda, B) \nabla w(z) + k_0^2 (\frac{\varepsilon_\star}{\varepsilon_0} - 1) |B| U(z) w(z) \Big) \\ &+ o(\delta^d) \, , \end{aligned} \tag{5.26}$$

with λ given by (5.17).

We apply the asymptotic formulas (5.16) and (5.26) for the purpose of identifying the location and certain properties of the inclusions.

Consider P well-separated inclusions $D_p = z_p + \delta B_p$, $p = 1, \dots, P$. The magnetic permeability and electric permittivity of D_p are denoted by μ_p and ε_p, respectively. Suppose that all the domains B_p are disks. In this case, we have

$$I_w[U,\omega] \approx -\sum_{p=1}^{P} |D_p| \Big(2\frac{\mu_p - \mu_0}{\mu_0 + \mu_p} \nabla U(z) \cdot \nabla w(z) + k_0^2 (\frac{\varepsilon_p}{\varepsilon_0} - 1) U(z) w(z) \Big) .$$

5.2.6. MUSIC-type algorithm. Let $(\boldsymbol{\theta}_1, \dots, \boldsymbol{\theta}_n)$ be n unit vectors in $\mathbb{R}^d$. For $\boldsymbol{\theta} \in \{\boldsymbol{\theta}_1, \dots, \boldsymbol{\theta}_n\}$, we assume that we are in possession of the boundary data u when the domain Ω is illuminated with the plane wave $U(x) = e^{ik_0 \boldsymbol{\theta} \cdot x}$. Taking the harmonic function $w(x) = e^{-ik_0 \boldsymbol{\theta}' \cdot x}$ for $\boldsymbol{\theta}' \in \{\boldsymbol{\theta}_1, \dots, \boldsymbol{\theta}_n\}$ and using (4.9) shows that the weighted boundary measurement is approximately equal to

$$I_w[U,\omega] \approx -\sum_{p=1}^{P} |D_p| k_0^2 \Big(2\frac{\mu_0 - \mu_p}{\mu_0 + \mu_p} \boldsymbol{\theta} \cdot \boldsymbol{\theta}' + \frac{\varepsilon_p}{\varepsilon_0} - 1 \Big) e^{ik_0 (\boldsymbol{\theta} - \boldsymbol{\theta}') \cdot z_p} .$$

Define the response matrix $A = (A_{ll'})_{l,l'=1}^n \in \mathbb{C}^{n \times n}$ by

$$A_{ll'} := I_{w_{l'}}[U_l, \omega] , \tag{5.27}$$

where $U_l(x) = e^{ik_0 \boldsymbol{\theta}_l \cdot x}, w_l(x) = e^{-ik_0 \boldsymbol{\theta}_l \cdot x}, l = 1, \dots, n$. It is approximately given by

$$A_{ll'} \approx -\sum_{p=1}^{P} |D_p| k_0^2 \Big(2\frac{\mu_0 - \mu_p}{\mu_0 + \mu_p} \boldsymbol{\theta}_l \cdot \boldsymbol{\theta}_{l'} + \frac{\varepsilon_p}{\varepsilon_0} - 1 \Big) e^{ik_0 (\boldsymbol{\theta}_l - \boldsymbol{\theta}_{l'}) \cdot z_p} , \tag{5.28}$$

for $l, l' = 1, \dots, n$. Introduce the n-dimensional vector fields $g^{(j)}(z^S)$, for $z^S \in \Omega$ and $j = 1, \dots, d+1$, by

$$g^{(j)}(z^S) = \frac{1}{\sqrt{n}} \big(e_j \cdot \boldsymbol{\theta}_1 e^{ik_0 \boldsymbol{\theta}_1 \cdot z^S}, \dots, e_j \cdot \boldsymbol{\theta}_n e^{ik_0 \boldsymbol{\theta}_n \cdot z^S} \big)^T, \quad j = 1, \dots, d , \tag{5.29}$$

and

$$g^{(d+1)}(z^S) = \frac{1}{\sqrt{n}} \left(e^{ik_0 \boldsymbol{\theta}_1 \cdot z^S}, \dots, e^{ik_0 \boldsymbol{\theta}_n \cdot z^S} \right)^T , \tag{5.30}$$

where $\{e_1, \dots, e_d\}$ is an orthonormal basis of $\mathbb{R}^d$. Let $g(z^S)$ be the $n \times d$ matrix whose columns are $g^{(1)}(z^S), \dots, g^{(d)}(z^S)$. Then (5.28) can be written as

$$A \approx -n \sum_{p=1}^{P} |D_p| k_0^2 \Big(2\frac{\mu_0 - \mu_p}{\mu_0 + \mu_p} g(z_p) \overline{g(z_p)}^T + (\frac{\varepsilon_p}{\varepsilon_0} - 1) g^{(d+1)}(z_p) \overline{g^{(d+1)}(z_p)}^T \Big) .$$

Let $\mathbb{P}_{\text{noise}} = I - \mathbb{P}$, where $\mathbb{P}$ is the orthogonal projection onto the range of A as before. The MUSIC-type imaging functional is defined by

$$\mathcal{I}_{\text{MU}}(z^S, \omega) := \Big(\sum_{j=1}^{d+1} \| \mathbb{P}_{\text{noise}} [g^{(j)}](z^S) \|^2 \Big)^{-1/2} . \tag{5.31}$$

This functional has large peaks only at the locations of the inclusions.

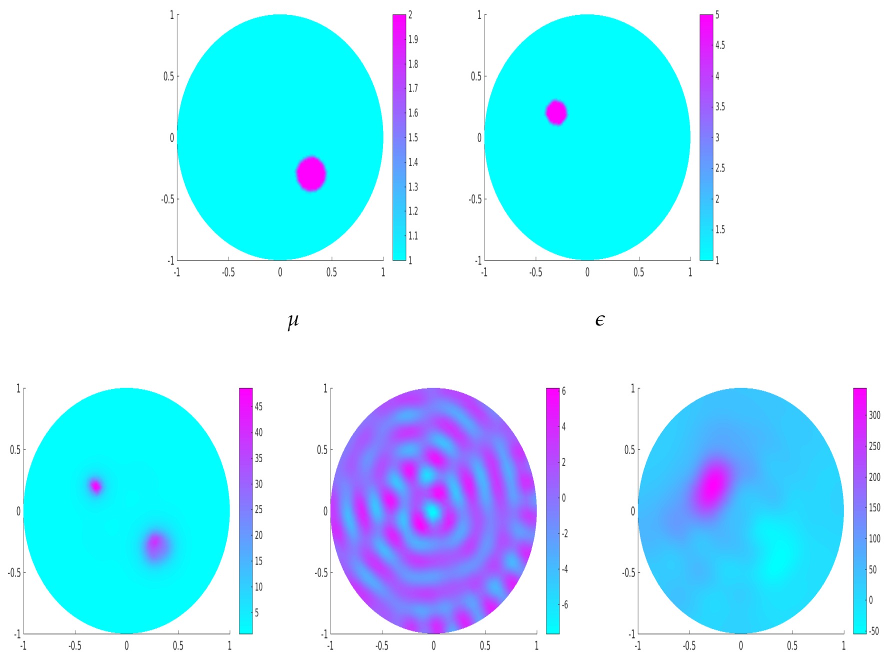

μ ϵ

MUSIC reconstruction Backprojection Kirchhoff migration

FIGURE 5.1. Top: The magnetic inclusion with coefficient μ and the electrical inclusion with coefficient ε in the domain Ω. Bottom: Reconstructed fields using MUSIC, backprojection, and Kirchhoff migration.

5.2.7. Backpropagation-type algorithms. Let $(\boldsymbol{\theta}_1, \ldots, \boldsymbol{\theta}_n)$ be n unit vectors in $\mathbb{R}^d$. A backpropagation-type imaging functional at a single frequency ω is given by

$$\mathcal{I}_{\mathrm{BP}}(z^S, \omega) := \frac{1}{n} \sum_{l=1}^{n} e^{-2ik_0 \boldsymbol{\theta}_l \cdot z^S} I_{w_l}[U_l, \omega] \, , \tag{5.32}$$

where $U_l(x) = w_l(x) = e^{ik_0 \boldsymbol{\theta}_l \cdot x}, l = 1, \ldots, n$. Suppose that $(\boldsymbol{\theta}_1, \ldots, \boldsymbol{\theta}_n)$ are equidistant points on the unit sphere S^{d-1}. For sufficiently large n, we have

$$\frac{1}{n} \sum_{l=1}^{n} e^{ik_0 \boldsymbol{\theta}_l \cdot x} \approx 4(\frac{\pi}{k_0})^{d-2} \Im m \left\{ \Gamma_{k_0}(x, 0) \right\} = \begin{cases} \operatorname{sinc}(k_0|x|) & \text{for } d = 3 \, , \\ J_0(k_0|x|) & \text{for } d = 2 \, , \end{cases} \tag{5.33}$$

where $\operatorname{sinc}(s) = \sin(s)/s$ is the sinc function and J_0 is the Bessel function of the first kind and of order zero.

Therefore, it follows that

$$\mathcal{I}_{\mathrm{BP}}(z^S, \omega) \approx -\sum_{p=1}^{P} |D_p| k_0^2 \Big(2 \frac{\mu_p - \mu_0}{\mu_0 + \mu_p} + (\frac{\varepsilon_p}{\varepsilon_0} - 1) \Big) \times \begin{cases} \operatorname{sinc}(2k_0|z^S - z_p|) & \text{for } d = 3, \\ J_0(2k_0|z^S - z_p|) & \text{for } d = 2 \, . \end{cases}$$

These formulas show that the resolution of the imaging functional is the standard diffraction limit. It is of the order of half the wavelength $\lambda = 2\pi/k_0$.

Note that $\mathcal{I}_{\mathrm{BP}}$ uses only the diagonal terms of the response matrix A, defined by (5.27). Using the whole matrix, we arrive at the Kirchhoff migration functional:

$$\mathcal{I}_{\mathrm{KM}}(z^S, \omega) = \sum_{j=1}^{d+1} \overline{g^{(j)}(z^S)} \cdot A g^{(j)}(z^S) \ , \tag{5.34}$$

where $g^{(j)}$ are defined by (5.29) and (5.30).

5.3. Super-resolution in high contrast media

It is well-known that the resolution in the homogeneous space for far-field imaging system is limited by half the operating wave-length, which is a direct consequence of Abbe's diffraction limit. In order to differentiate point sources which are located less than half the wavelength apart, super-resolution techniques have to be used. While many techniques exist in practice, here we are only interested in one using resonant media.

The basic idea is the following: suppose that we have sources that are densely located in a homogeneous space of size the wavelength of the wave the sources can emit, and we want to differentiate them by making measurements in the far-field. While this is impossible in the homogeneous space, it is possible if the medium around these sources is changed so that the point spread function, which is the imaginary part of the Green function in the new medium, displays a much sharper peak than the homogeneous one and thus can resolve sub-wavelength details. The key issue in such an approach is to design the surrounding medium so that the corresponding Green function has the tailored property. In this section, we develop the mathematical theory for realizing this approach by using high contrast media. We show that in high contrast media the super-resolution is due to the propagating sub-wavelength resonant modes excited in the media and is limited by the finest structure in these modes.

We also explain how to compute Green's function numerically and present an example to show a sharp peak of imaginary part of Green's function can be achieved using high contrast media.

5.3.1. Green's Function for a high-contrast resonator. Throughout this section, we put the wavenumber ω to be the unit and suppress its presence in what follows. We assume that the wave speed in the free space is one. The free-space wavelength is given by 2π. We consider the following Helmholtz equation with a delta source term:

$$\Delta_x G(x, x_0) + G(x, x_0) + \tau n(x) \chi(D)(x) G(x, x_0) = \delta(x - x_0) \quad \text{in } \mathbb{R}^d, \tag{5.35}$$

where $\chi(D)$ is the characteristic function of D, which has size of order of the free space wavelength, $n(x)$ is a positive function of order one in the space of $\mathcal{C}^1(\overline{D})$ and $\tau \gg 1$ is the contrast. We denote by $G_0(x, x_0)$ the free-space Green's function $\Gamma_1(x - x_0)$.

Write $G = v + G_0$, we can show that

$$\Delta v + v = -\tau n(x) \chi(D)(v + G_0). \tag{5.36}$$

Thus,

$$v(x, x_0) = -\tau \int_D n(y) G_0(x, y) \Big(v(y, x_0) + G_0(y, x_0) \Big)\, dy.$$

Define

$$\mathrm{K}_D[f](x) = -\int_D n(x) G_0(x, y) f(y)\, dy. \tag{5.37}$$

Then, $v = v(x) = v(x, x_0)$ satisfies the following integral equation:

$$(I - \tau \mathrm{K}_D)[v] = \tau \mathrm{K}_D[G(\cdot, x_0)], \tag{5.38}$$

and hence,

$$v(x) = (\frac{1}{\tau} - \mathrm{K}_D)^{-1} \mathrm{K}_D[G(\cdot, x_0)].$$

In what follows, we present properties of the integral operator K_D.

LEMMA 5.3. *The operator K_D is compact from $L^2(D)$ to $L^2(D)$. In fact, K_D is bounded from $L^2(D)$ to $H^2(D)$. Moreover, K_D is a Hilbert-Schmidt operator.*

LEMMA 5.4. *Let $\sigma(K_D)$ be the spectrum of K_D defined by (5.37). We have*

(i) *$\sigma(K_D) = \{0, \lambda_1, \lambda_2, ..., \lambda_n, ...\}$, where $|\lambda_1| \geq |\lambda_2| \geq |\lambda_3| \geq ...$ and $\lambda_n \to 0$;*
(ii) *$\{0\} = \sigma(K_D) \backslash \sigma_p(K_D)$ with $\sigma_p(K_D)$ being the point spectrum of K_D.*

PROOF. We need only to prove the second assertion. Assume that $\mathrm{K}_D[u] = \int_D G_0(x, y) n(y) u(y)\, dy = 0$. We have $0 = (\triangle + 1)\mathrm{K}_D[u] = nu$, which shows that $u = 0$. The assertion is then proved. □

LEMMA 5.5. *Let K_D be defined by (5.37). Then, $\lambda \in \sigma(K_D)$ if and only if there is a nontrivial solution in $H^2_{\mathrm{loc}}(\mathbb{R}^d)$ to the following problem:*

$$(\Delta + 1) u(x) = \tfrac{1}{\lambda} n(x) u(x) \quad \text{in } D, \tag{5.39}$$

$$(\Delta + 1) u = 0 \quad \text{in } \mathbb{R}^d \backslash D, \tag{5.40}$$

(5.41) *u satisfies the Sommerfeld radiation condition.*

PROOF. Assume that $\mathrm{K}_D[u] = \lambda u$. We define $\tilde{u}(x) = \int_D G_0(x, y) n(y) u(y)\, dy$, where $x \in \mathbb{R}^d$. Then $\tilde{u}$ satisfies the required equations. □

Notice that the resonant modes have sub-wavelength structures in D for $|\lambda| < 1$.

LEMMA 5.6. *Let $\mathcal{H}_j$ denote the generalized eigenspace of the operator K_D for the eigenvalue λ_j. The following decomposition holds:*

$$L^2(D) = \overline{\bigcup_{j=1}^{\infty} \mathcal{H}_j}.$$

PROOF. By the same argument as the one in the proof of Lemma 5.4, we can show that $\operatorname{Ker} \mathrm{K}_D^* = \{0\}$. As a result, we have

$$\overline{\mathrm{K}_D\big(L^2(D)\big)} = \big(\operatorname{Ker} \mathrm{K}_D^*\big)^{\perp} = L^2(D).$$

The lemma is proved. □

LEMMA 5.7. *There exists a basis $\{u_{j,l,k}\}$, $1 \le l \le m_j, 1 \le k \le n_{j,l}$ for $\mathcal{H}_j$ such that*

$$\kappa_D(u_{j,1,1}, ..., u_{j,m_j,n_{j,m_j}}) = (u_{j,1,1}, ..., u_{j,m_j,n_{j,m_j}}) \begin{pmatrix} J_{j,1} & & \\ & \ddots & \\ & & J_{j,m_j} \end{pmatrix},$$

where $J_{j,l}$ is the canonical Jordan matrix of size $n_{j,l}$ in the form

$$J_{j,l} = \begin{pmatrix} \lambda_j & 1 & & \\ & \ddots & \ddots & \\ & & \lambda_j & 1 \\ & & & \lambda_j \end{pmatrix}.$$

PROOF. This follows from the Jordan theory applied to the linear operator $\kappa_D|_{\mathcal{H}_j} : \mathcal{H}_j \to \mathcal{H}_j$ on the finite dimensional space $\mathcal{H}_j$. $\square$

We denote $\Gamma = \{(j,l,k) \in \mathbb{N} \times \mathbb{N} \times \mathbb{N}; 1 \le l \le m_j, 1 \le k \le n_{j,l}\}$ the set of indices for the basis functions. We introduce a partial order on $\mathbb{N} \times \mathbb{N} \times \mathbb{N}$. Let $\gamma = (j,k,l) \in \Gamma, \gamma' = (j',l',k') \in \Gamma$, we say that $\gamma' \preceq \gamma$ if one of the following conditions are satisfied:

(i) $j > j'$;
(ii) $j = j', l > l'$;
(iii) $j = j', l = l', k \ge k'$.

By Gram-Schmidt orthonormalization process, the following result is obvious.

LEMMA 5.8. *There exists orthonormal basis $\{e_\gamma : \gamma \in \Gamma\}$ for $L^2(D)$ such that*

$$e_\gamma = \sum_{\gamma' \preceq \gamma} a_{\gamma,\gamma'} u_{\gamma'},$$

where $a_{\gamma,\gamma'}$ are constants and $a_{\gamma,\gamma} \neq 0$.

We can regard $A = \{a_{\gamma,\gamma'}\}_{\gamma,\gamma' \in \Gamma}$ as a matrix. It is clear that A is upper-triangular and has non-zero diagonal elements. Its inverse is denoted by $B = \{b_{\gamma,\gamma'}\}_{\gamma,\gamma' \in \Gamma}$ which is also upper-triangular and has non-zero diagonal elements. We have

$$u_\gamma = \sum_{\gamma' \preceq \gamma} b_{\gamma,\gamma'} e_{\gamma'}.$$

LEMMA 5.9. *The functions $\{e_\gamma(x)\overline{e_{\gamma'}(y)}\}$ form a normal basis for the Hilbert space $L^2(D \times D)$. Moreover, the following completeness relation holds:*

$$\delta(x-y) = \sum_\gamma e_\gamma(x)\overline{e_\gamma(y)}.$$

By standard elliptic theory, we have $G(x, x_0) \in L^2(D \times D)$ for fixed τ. Thus we have

$$G(x, x_0) = \sum_{\gamma,\gamma'} \alpha_{\gamma,\gamma'} e_\gamma(x)\overline{e_{\gamma'}}(x_0), \tag{5.42}$$

for some constants $\alpha_{\gamma,\gamma'}$ satisfying

$$\sum_{\gamma,\gamma'} |\alpha_{\gamma,\gamma'}|^2 = \|G(x, x_0)\|^2_{L^2(D\times D)} < \infty.$$

To analyze the Green function G, we need to find the constants $\alpha_{\gamma,\gamma'}$. For doing so, we first note that

$$G_0(x,x_0) = \frac{1}{n(x_0)} \mathrm{K}_D[\delta(\cdot - x_0)].$$

Thus,

$$\begin{aligned} G(x,x_0) &= G_0(x,x_0) + (\frac{1}{\tau} - \mathrm{K}_D)^{-1}\mathrm{K}_D^2[\delta(\cdot - x_0)] \\ &= G_0(x,x_0) + \frac{1}{n(x_0)} \sum_{\gamma} \overline{e_\gamma}(x_0)(\frac{1}{\tau} - \mathrm{K}_D)^{-1}\mathrm{K}_D^2[e_\gamma]. \end{aligned}$$

We next compute $(\frac{1}{\tau} - \mathrm{K}_D)^{-1}\mathrm{K}_D^2[e_\gamma]$. For ease of notation, we define $u_{j,l,k} = 0$ for $k \leq 0$. We have

$$\begin{aligned} \mathrm{K}_D[u_{j,l,k}] &= \lambda_j u_{j,l,k} + u_{j,l,k-1} \quad \text{for all } j,l,k, \\ \mathrm{K}_D^2[u_{j,l,k}] &= \lambda_j^2 u_{j,l,k} + 2\lambda_j u_{j,l,k-1} + u_{j,l,k-2} \quad \text{for all } j,l,k. \end{aligned}$$

On the other hand, for $z \notin \sigma(\mathrm{K}_D)$, we have

$$(z - \mathrm{K}_D)^{-1}[u_{j,l,k}] = \frac{1}{z-\lambda_j} u_{j,l,k} + \frac{1}{(z-\lambda_j)^2} u_{j,l,k-1} + ... + \frac{1}{(z-\lambda_j)^k} u_{j,l,1},$$

and therefore, it follows that

$$\begin{aligned} (z - \mathrm{K}_D)^{-1}\mathrm{K}_D^2[u_{j,l,k}] &= \frac{\lambda_j^2}{z-\lambda_j} u_{j,l,k} + \frac{\lambda_j^2}{(z-\lambda_j)^2} u_{j,l,k-1} \cdots + \frac{\lambda_j^2}{(z-\lambda_j)^k} u_{j,l,1} \\ &\quad + \frac{2\lambda_j}{z-\lambda_j} u_{j,l,k-1} + \frac{2\lambda_j}{(z-\lambda_j)^2} u_{j,l,k-2} \cdots + \frac{2\lambda_j}{(z-\lambda_j)^{k-1}} u_{j,l,1} \\ &\quad + \frac{1}{z-\lambda_j} u_{j,l,k-2} + \frac{1}{(z-\lambda_j)^2} u_{j,l,k-3} \cdots + \frac{1}{(z-\lambda_j)^{k-2}} u_{j,l,1} \\ &= \frac{\lambda_j^2}{z-\lambda_j} u_{j,l,k} + \Big(\frac{\lambda_j^2}{(z-\lambda_j)^2} + \frac{2\lambda_j}{z-\lambda_j} \Big) u_{j,l,k-1} \\ &\quad + \Big(\frac{\lambda_j^2}{(z-\lambda_j)^3} + \frac{2\lambda_j}{z-\lambda_j} + \frac{1}{z-\lambda_j} \Big) u_{j,l,k-2} \\ &\quad + ... + \Big(\frac{\lambda_j^2}{(z-\lambda_j)^k} + \frac{2\lambda_j}{(z-\lambda_j)^{k-1}} + \frac{1}{(z-\lambda_j)^{k-2}} \Big) u_{j,l,1} \\ &= \sum_{\gamma'} d_{\gamma,\gamma'} u_{\gamma'}, \end{aligned}$$

where we have introduced the matrix $D = \{d_{\gamma,\gamma'}\}_{\gamma,\gamma' \in \Gamma}$, which is upper-triangular and has block-structure.

With these calculations, by taking $z = 1/\tau$, we arrive at the following result.

THEOREM 5.10. *The following expansion holds for the Green function*

$$G(x,x_0) = G_0(x,x_0) + \sum_{\gamma \in \Gamma} \sum_{\gamma''' \in \Gamma} \alpha_{\gamma,\gamma'''} \overline{e_\gamma}(x_0) e_{\gamma'''}(x), \tag{5.43}$$

where

$$\alpha_{\gamma,\gamma'''} = \frac{1}{n(x_0)} \sum_{\gamma' \preceq \gamma} \sum_{\gamma'' \preceq \gamma'} a_{\gamma,\gamma'} d_{\gamma',\gamma''} b_{\gamma'',\gamma'''}.$$

Moreover, for τ^{-1} belonging to a compact subset of $\mathbb{R} \setminus \big(\mathbb{R} \cap \sigma(\mathcal{K}_D)\big)$, we have the following uniform bound:

$$\sum_{\gamma,\gamma'} |\alpha_{\gamma,\gamma'}|^2 < \infty.$$

Alternatively, if we start from the identity,

$$\begin{aligned} \delta(x - x_0) &= \sum_{\gamma''} e_{\gamma''}(x) \overline{e_{\gamma''}(x_0)} \\ &= \sum_{\gamma''} \sum_{\gamma' \preceq \gamma''} \sum_{\gamma''' \preceq \gamma''} a_{\gamma'',\gamma'} \overline{a}_{\gamma'',\gamma'''} u_{\gamma'}(x) \overline{u_{\gamma'''}}(x_0), \end{aligned}$$

then we can obtain an equivalent expansion for the Green function in terms of the basis of resonant modes.

THEOREM 5.11. *The following expansion holds for the Green function:*

$$G(x, x_0) = G_0(x, x_0) + \sum_{\gamma'' \in \Gamma} \sum_{\gamma''' \preceq \gamma''} \sum_{\gamma \preceq \gamma''} \beta_{\gamma'',\gamma,\gamma'''} u_{\gamma}(x) \overline{u_{\gamma'''}}(x_0), \tag{5.44}$$

where

$$\beta_{\gamma'',\gamma,\gamma'''} = \frac{1}{n(x_0)} \sum_{\gamma' \preceq \gamma''} \overline{a}_{\gamma'',\gamma'''} a_{\gamma'',\gamma'} d_{\gamma',\gamma}. \tag{5.45}$$

Here, the infinite summation can be interpreted as follows:

$$\lim_{\gamma_0 \to \infty} \sum_{\gamma'' \leq \gamma_0} \sum_{\gamma' \preceq \gamma''} \sum_{\gamma''' \preceq \gamma''} \beta_{\gamma'',\gamma,\gamma'''} u_{\gamma}(x) \overline{u_{\gamma'''}}(x_0) = G(x, x_0) - G_0(x, x_0) \quad in \quad L^2(D \times D). \tag{5.46}$$

In order to have some idea of the expansions of the Green function $G(x, y)$, we compare them to the expansion of the Green function in the homogeneous space, *i.e.*, $G_0(x, y)$. For this purpose, we introduce the matrix $H = \{h_{\gamma,\gamma'}\}_{\gamma,\gamma' \in \Gamma}$, which is defined by

$$\mathcal{K}_D[u_\gamma] = \sum_{\gamma'} h_{\gamma,\gamma'} u_{\gamma'}.$$

In fact, we have

$$h_{j,l,k,j',l',k'} = \lambda_j \delta_{j,j'} \delta_{l,l'} \delta_{k,k'} + \delta_{j,j'} \delta_{l,l'} \delta_{k-1,k'},$$

where δ denotes the Kronecker symbol.

LEMMA 5.12. (i) *In the normal basis $\{e_\gamma\}_{\gamma \in \Gamma}$, the following expansion holds for the Green function $G_0(x, x_0)$:*

$$G_0(x, x_0) = \sum_{\gamma \in \Gamma} \sum_{\gamma''' \in \Gamma} \tilde{\alpha}_{\gamma,\gamma'''} \overline{e_\gamma}(x_0) e_{\gamma'''}(x), \tag{5.47}$$

where

$$\tilde{\alpha}_{\gamma,\gamma'''} = \frac{1}{n(x_0)} \sum_{\gamma' \preceq \gamma} \sum_{\gamma'' \preceq \gamma'} a_{\gamma,\gamma'} h_{\gamma',\gamma''} b_{\gamma'',\gamma'''}.$$

Moreover, we have the following uniform bound:

$$\sum_{\gamma,\gamma'} |\tilde{\alpha}_{\gamma,\gamma'}|^2 < C < \infty.$$

(ii) *In the basis of resonant modes $\{u_\gamma\}_{\gamma\in\Gamma}$, the following expansion holds for the Green function $G_0(x, x_0)$:*

$$G_0(x,x_0) = \sum_{\gamma''\in\Gamma} \sum_{\gamma'''\preceq\gamma''} \sum_{\gamma\preceq\gamma''} \tilde{\beta}_{\gamma'',\gamma,\gamma'''} u_\gamma(x)\overline{u_{\gamma'''}}(x_0), \tag{5.48}$$

where

$$\tilde{\beta}_{\gamma'',\gamma,\gamma'''} = \frac{1}{n(x_0)} \sum_{\gamma'\preceq\gamma''} \overline{a}_{\gamma'',\gamma'''} a_{\gamma'',\gamma'} h_{\gamma',\gamma}. \tag{5.49}$$

Here, the infinite summation can be interpreted as follows:

$$\lim_{\gamma_0\to\infty} \sum_{\gamma''\leq\gamma_0} \sum_{\gamma'''\preceq\gamma''} \sum_{\gamma\preceq\gamma''} \tilde{\beta}_{\gamma'',\gamma,\gamma'''} u_\gamma(x)\overline{u_{\gamma'''}}(x_0) = G_0(x,x_0) \quad \text{in } L^2(D\times D).$$

By comparing the coefficients $\alpha_{\gamma,\gamma'}$ (or $\beta_{\gamma,\gamma'}$) and $\tilde{\alpha}_{\gamma,\gamma'}$ (or $\tilde{\beta}_{\gamma,\gamma'}$), we can see that the imaginary part of $G(x,y)$ may have a sharper peak than $G_0(x,y)$ due to the excited high frequency resonant modes.

5.4. Numerical illustration

Code:	5.3 Super-resolution in High Contrast Media	DemoGreenHighContrast.m

In this section we explain how to compute the Green's function numerically. We also present a numerical example in which a high contrast medium is represented as a disk.

5.4.1. Solving an integral equation for the Green's function. The Green's function G is the solution to the following problem:

$$\begin{cases} \nabla\cdot\dfrac{1}{\mu}\nabla G(\cdot,x_0) + \omega^2\varepsilon G(\cdot,x_0) = \dfrac{1}{\mu_c}\delta_{x_0} \quad \text{in } \mathbb{R}^d, \\ G(\cdot,x_0) \text{ satisfies the Sommerfeld radiation condition.} \end{cases} \tag{5.50}$$

It can be shown that the above problem is equivalent to the following system of equations:

$$\begin{cases} (\Delta + k_c^2)G(\cdot,x_0) = \delta_{x_0} \quad \text{in } D, \\ (\Delta + k_m^2)G(\cdot,x_0) = 0 \quad \text{in } \mathbb{R}^d\setminus\overline{D}, \\ G(\cdot,x_0)|_+ = G(\cdot,x_0)|_- \quad \text{on } \partial D, \\ \dfrac{1}{\mu_m}\dfrac{\partial G(\cdot,x_0)}{\partial\nu}\Big|_+ = \dfrac{1}{\mu_c}\dfrac{\partial G(\cdot,x_0)}{\partial\nu}\Big|_- \quad \text{on } \partial D, \\ G(\cdot,x_0) \text{ satisfies the Sommerfeld radiation condition.} \end{cases} \tag{5.51}$$

Note that here the wave number k_c plays the role of the high contrast parameter analogously to τ in the previous theoretical analysis.

Let $G_0^{k_c}$ be the free space Green's function with a wave number k_c. Since $G_0^{k_c}$ satisfies

$$(\Delta + k_c^2)G_0^{k_c}(\cdot,x_0) = \delta_{x_0}, \quad \text{in } \mathbb{R}^d, \tag{5.52}$$

we see that $v := G - G_0^{k_c}$ satisfies $\Delta v + k_c^2 v = 0$ in D. So we can represent the Green's function G using the single layer potential as follows:

$$G(x, x_0) = \begin{cases} G_0^{k_c}(x, x_0) + \mathcal{S}_D^{k_c}[\varphi](x), & x \in D, \\ \mathcal{S}_D^{k_m}[\psi](x), & x \in \mathbb{R}^d \setminus D, \end{cases} \tag{5.53}$$

Next we determine the density functions φ and ψ. From the transmission conditions on ∂D and the jump relations for the single layer potentials, we get (5.54)

$$\begin{cases} \mathcal{S}_D^{k_c}[\varphi] - \mathcal{S}_D^{k_m}[\psi] = -G_0^{k_c}(\cdot, x_0) \\ \dfrac{1}{\mu_c}(-\dfrac{1}{2}I + (\mathcal{K}_D^{k_c})^*)[\varphi]\Big|_- - \dfrac{1}{\mu_m}(\dfrac{1}{2}I + (\mathcal{K}_D^{k_m})^*)[\psi]\Big|_+ = -\dfrac{1}{\mu_c}\dfrac{\partial G_0^{k_c}(\cdot, x_0)}{\partial \nu} \end{cases} \quad \text{on } \partial D.$$

The above integral equation has the same form as that of (4.20). We have already discussed how to solve that equation numerically in the previous chapter.

5.4.2. Explicit expression of Green's function for a disk. For the special case of the domain B, we can obtain an explicit solution to the transmission problem. Let B be a disk of radius R located at the origin in $\mathbb{R}^2$. Then it can be shown that the explicit solution is given by

$$G(r, \theta) = \begin{cases} -\dfrac{i}{4}H_0^{(1)}(k_c r) + aJ_0(k_c r), & |r| \le R, \\ bH_0^{(1)}(k_m r), & |r| > R, \end{cases} \tag{5.55}$$

where (r, θ) are the polar coordinates and the constants a and b are given by

$$a = -\frac{i}{4}\frac{\frac{k_m}{\mu_m}H_0^{(1)}(k_c R)(H_0^{(1)})'(k_m R) - \frac{k_c}{\mu_c}H_0^{(1)}(k_m R)(H_0^{(1)})'(k_c R)}{\frac{k_c}{\mu_c}H_0^{(1)}(k_m R)J_0'(k_c R) - \frac{k_m}{\mu_m}J_0(k_c R)(H_0^{(1)})'(k_m R)},$$

$$b = -\frac{i}{4}\frac{\frac{k_c}{\mu_c}H_0^{(1)}(k_c R)J_0'(k_c R) - \frac{k_c}{\mu_c}(H_0^{(1)})'(k_c R)J_0(k_c R)}{\frac{k_c}{\mu_c}H_0^{(1)}(k_m R)J_0'(k_c R) - \frac{k_m}{\mu_m}J_0(k_c R)(H_0^{(1)})'(k_m R)}.$$

5.4.3. Resonant wave number k_c for a disk. It is also worth emphasizing that we can derive resonant values for k_c. From the expressions for a and b, we can immediately see that the n-th resonant value $k_{c,n}$ is n-th zero of

$$\frac{k_c}{\mu_c}H_0^{(1)}(k_m R)J_0'(k_c R) - \frac{k_m}{\mu_m}J_0(k_c R)(H_0^{(1)})'(k_m R) = 0. \tag{5.56}$$

So the resonant values for k_c can be computed using Muller's method. When we solve the above equation, we need to be careful because μ_c depends on k_c via $\mu_c = k_c^2/(\omega^2\epsilon_c)$.

5.4.4. Numerical example. Let D be a disk of radius $R = 2$ centered at the origin O in $\mathbb{R}^2$. We fix $\omega = 1$, $\epsilon_c = \epsilon_m = 1$ and $\mu_m = 1$. Then μ_c is determined by $\mu_c = k_c^2$.

First, let us compute how the resonant values for k_c are distributed. In order to do this, we plot the LHS of (5.56) as a function of k_c. The plot is shown in Figure 5.2 and it shows that there are many local maximum points which converge to zero as their corresponding wave number k_c increases. It reflects the fact that the resonant values $k_{c,n}$ (or the corresponding eigenvalues of the operator K_D) are complex numbers and $1/k_{c,n}$ converges to zero as $n \to \infty$. This is in accordance with our previous theoretical analysis of the super-resolution phenomenon because a large wave number k_c plays the role of the high contrast parameter τ.

n	$k_c(A_n)$	$k_c(B_n)$
1	1.86	2.74
2	3.48	4.32
3	5.08	5.9

TABLE 5.1. The value of k_c corresponding to the points A_n and B_n.

Next we determine how the shape of $\mathrm{Im}\{G\}$ changes as a function of k_c. We choose three local maximum (or minimum) points A_1, A_2 and A_3 (or B_1, B_2 and B_3) as shown in Figure 5.2. At the point A_1, A_2 or A_3, we expect that the corresponding Green's function $\mathrm{Im}\{G\}$ doesn't have a sharp peak because the LHS of (5.56) is not small, which means k_c is not close to a resonant value. On the other hand, we expect that $\mathrm{Im}\{G\}$ has a sharper peak than that of the free space Green function $\mathrm{Im}\{G_0^{k_m}\}$ at the points B_1, B_2 and B_3. The (approximate) numerical values of k_c corresponding to the points A_n and B_n are shown in Table 5.1.

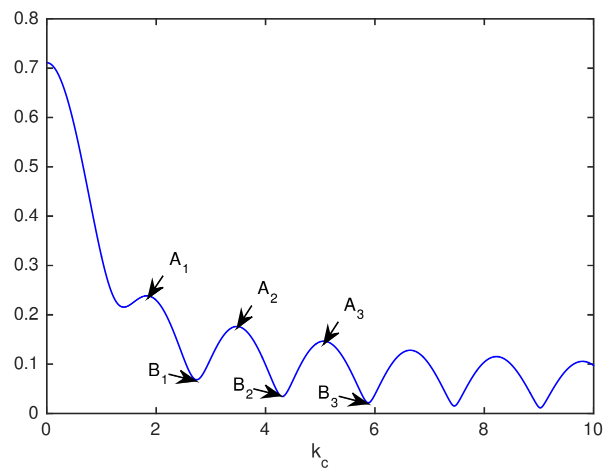

FIGURE 5.2. A plot for the LHS of (5.56) as a function of k_c. The inclusion D is a circular disk with radius $R = 2$. The parameters are given as $\omega = 1, \varepsilon_m = 1, \varepsilon_c = 1, \mu_m = 1$ and μ_c is determined by $\mu_c = k_c^2/(\varepsilon_c \omega^2)$. Three local maximums (or minimums) are marked as A_n (or B_n), respectively.

First we consider non-resonant case. In Figure 5.3, we plot $\mathrm{Im}\{G\}$ when $k_c = k_c(A_n)$, $n = 1, 2, 3$ over the line segment from $(-R, 0)$ to $(R, 0)$. The dotted line represents the imaginary part of the free space green function $G_0^{k_m}$. The blue circles and the red lines represent the exact values and the numerically computed values, respectively. We note that in this case the peak is not sharper than that of the free space Green's function.

Next, we consider the resonant case. In Figure 5.4, we plot $\mathrm{Im}\{G\}$ when $k_c = k_c(B_n),\ n = 1, 2, 3$ over the line segment from $(-R, 0)$ to $(R, 0)$. In contrast to the previous case, in the case of a resonant k_c the peak is sharper than that of the free space Green's function. Also the subwavelength structure of the resonant mode is clearly shown.

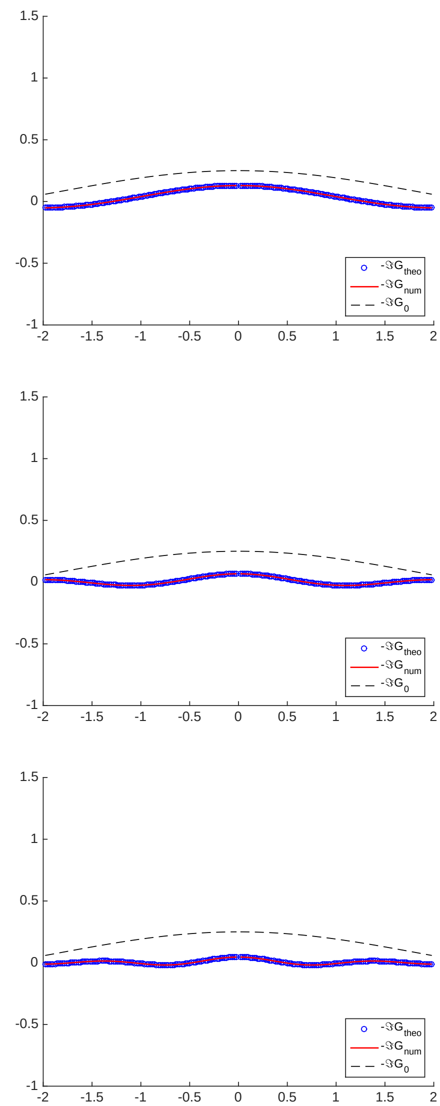

FIGURE 5.3. The plot for $\text{Im}\{G\}$ when $k_c = k_c(A_n), n = 1, 2, 3$ over the line segment from $(-R, 0)$ to $(R, 0)$. The dotted line represents the imaginary part of the free space green function $G_0^{k_m}$. The blue circles and the red lines represent the exact values and the numerically computed values, respectively. In this case the peak is not sharper than that of the free space Green's function.

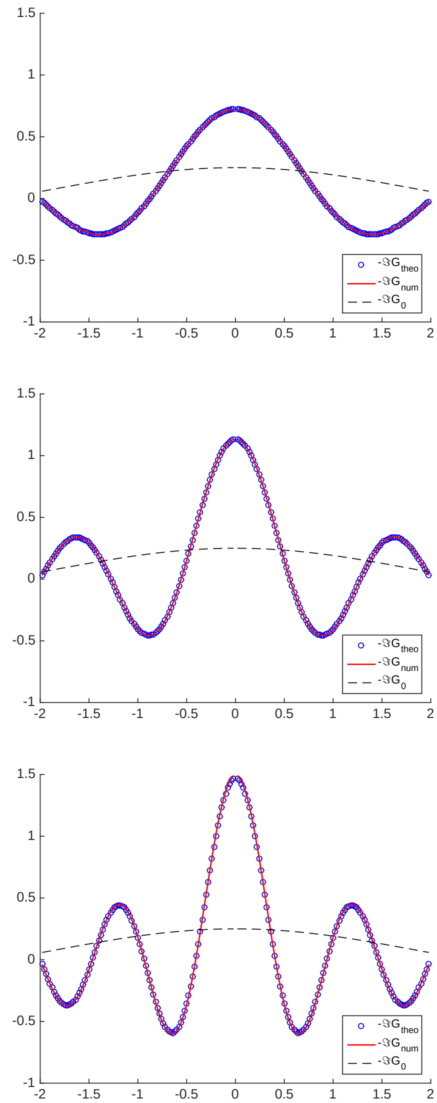

FIGURE 5.4. The plot for $\mathrm{Im}\{G\}$ when $k_c = k_c(B_n), n = 1, 2, 3$ over the line segment from $(-R, 0)$ to $(R, 0)$. The dotted line represents the imaginary part of the free space green function $G_0^{k_m}$. The blue circles and the red lines represent the exact values and the numerically computed values, respectively. In this case the peak is sharper than that of the free space Green's function. Also the subwavelength structure of the resonant mode is clearly shown.

CHAPTER 6

Maxwell's Equations and Scattering Coefficients

In this chapter, we consider the full Maxwell's equations along with the integral representation of their solution. We also introduce the concept of scattering coefficients in the context of Maxwell's equations. We demonstrate how the scattering coefficients for a multi-layer spherical shell can be computed. A numerical example is also provided.

6.1. Maxwell's equations

6.1.1. Time harmonic Maxwell's equations. Here we introduce Maxwell's equations which describe general electromagnetic fields. Consider the time-dependent Maxwell's equations

$$\begin{cases} \nabla \times \mathcal{E} = -\mu \frac{\partial}{\partial t}\mathcal{H}, \\ \nabla \times \mathcal{H} = \epsilon \frac{\partial}{\partial t}\mathcal{E}, \end{cases}$$

where μ is the magnetic permeability and ϵ is the electric permittivity.

In the time-harmonic regime, one looks for electromagnetic fields of the form

$$\begin{cases} \mathcal{H}(x,t) = H(x)e^{-i\omega t}, \\ \mathcal{E}(x,t) = E(x)e^{-i\omega t}, \end{cases}$$

where ω is the frequency. The pair (E, H) is a solution to the harmonic Maxwell equations

$$\begin{cases} \nabla \times E = i\omega\mu H, \\ \nabla \times H = -i\omega\epsilon E. \end{cases} \tag{6.1}$$

One says that (E, H) is radiating if it satisfies the Silver-Müller radiation condition:

$$\lim_{|x|\to\infty} |x|(\sqrt{\mu}H \times \hat{x} - \sqrt{\epsilon}E) = 0,$$

where $\hat{x} = x/|x|$. In the sequel, one sets the wave number $k = \omega\sqrt{\epsilon\mu}$.

6.1.2. Layer potentials. Assume that D is bounded, simply connected, and of class $\mathcal{C}^{1,\eta}$ for $\eta > 0$ and let

$$H^s_T(\partial D) = \left\{ \varphi \in \left(H^s(\partial D)\right)^3, \nu \cdot \varphi = 0 \right\}.$$

We introduce the surface gradient, surface divergence and Laplace-Beltrami operator and denote them by $\nabla_{\partial D}$, $\nabla_{\partial D}\cdot$ and $\Delta_{\partial D}$, respectively. We define the vectorial and scalar surface curl by $\vec{\mathrm{curl}}_{\partial D}\varphi = -\nu \times \nabla_{\partial D}\varphi$ for $\varphi \in H^{\frac{1}{2}}(\partial D)$ and

$\mathrm{curl}_{\partial D}\varphi = -\nabla_{\partial D}\cdot(\nu\times\varphi)$ for $\varphi \in H_T^{-\frac{1}{2}}(\partial D)$, respectively. We recall that

$$\begin{array}{rcl} \nabla_{\partial D}\cdot\nabla_{\partial D} & = & \Delta_{\partial D}, \\ \mathrm{curl}_{\partial D}\vec{\mathrm{curl}}_{\partial D} & = & -\Delta_{\partial D}, \\ \nabla_{\partial D}\cdot\vec{\mathrm{curl}}_{\partial D} & = & 0, \\ \mathrm{curl}_{\partial D}\nabla_{\partial D} & = & 0. \end{array}$$

We introduce the following functional space:

$$H_T^{-\frac{1}{2}}(\mathrm{div},\partial D) \quad = \quad \left\{\varphi\in H_T^{-\frac{1}{2}}(\partial D), \nabla_{\partial D}\cdot\varphi\in H^{-\frac{1}{2}}(\partial D)\right\}.$$

Define the following boundary integral operators:

$$\begin{array}{rcl} \vec{\mathcal{S}}_D^k[\varphi]: H_T^{-\frac{1}{2}}(\partial D) & \longrightarrow & H_T^{\frac{1}{2}}(\partial D) \text{ or } H^1_{\mathrm{loc}}(\mathbb{R}^3)^3 \\ \varphi & \longmapsto & \vec{\mathcal{S}}_D^k[\varphi](x) = \displaystyle\int_{\partial D}\Gamma_k(x-y)\varphi(y)d\sigma(y); \end{array}$$

$$\begin{array}{rcl} \mathcal{M}_D^k[\varphi]: H_T^{-\frac{1}{2}}(\mathrm{div},\partial D) & \longrightarrow & H_T^{-\frac{1}{2}}(\mathrm{div},\partial D) \\ \varphi & \longmapsto & \mathcal{M}_D^k[\varphi](x) = \displaystyle\int_{\partial D}\nu(x)\times\nabla_x\times\Gamma_k(x-y)\varphi(y)d\sigma(y); \end{array}$$

$$\begin{array}{rcl} \mathcal{L}_D^k[\varphi]: H_T^{-\frac{1}{2}}(\mathrm{div},\partial D) & \longrightarrow & H_T^{-\frac{1}{2}}(\mathrm{div},\partial D) \\ \varphi & \longmapsto & \mathcal{L}_D^k[\varphi](x) = \nu(x)\times\left(k^2\vec{\mathcal{S}}_D^k[\varphi](x)+\nabla\mathcal{S}_D^k[\nabla_{\partial D}\cdot\varphi](x)\right). \end{array}$$

The operator $\vec{\mathcal{S}}_D^k$ satisfies the following jump formmula.

$$\left(\nu\times\nabla\times\vec{\mathcal{S}}_D^k[\varphi]\right)\Big|_{\partial D}^{\pm} = (\mp\frac{1}{2}I+\mathcal{M}_D^k)[\varphi].$$

Furthermore it holds that

$$\left(\nu\times\nabla\times\nabla\times\vec{\mathcal{S}}_D^k[\varphi]\right)\Big|_{\partial D} = \mathcal{L}_D^k[\varphi].$$

6.1.3. Layer potential formulation for electromagnetic scattering. We consider the scattering problem of a time-harmonic electromagnetic wave incident on D. The homogeneous medium is characterized by electric permittivity ε_m and magnetic permeability μ_m, while D is characterized by electric permittivity ε_c and magnetic permeability μ_c, both of which depend on the frequency. Define

$$k_m = \omega\sqrt{\varepsilon_m\mu_m}, \quad k_c = \omega\sqrt{\varepsilon_c\mu_c},$$

and

$$\varepsilon_D = \varepsilon_m\chi(\mathbb{R}^3\setminus\overline{D})+\varepsilon_c\chi(D), \quad \mu_D = \varepsilon_m\chi(\mathbb{R}^3\setminus\overline{D})+\varepsilon_c\chi(D).$$

For a given incident plane wave (E^i, H^i) that is a solution to the Maxwell equations in free space, that is,

$$\left\{\begin{array}{rcll} \nabla\times E^i & = & \sqrt{-1}\omega\mu_m H^i & \text{in } \mathbb{R}^3, \\ \nabla\times H^i & = & -\sqrt{-1}\omega\varepsilon_m E^i & \text{in } \mathbb{R}^3, \end{array}\right. \tag{6.2}$$

the scattering problem can be modeled by the following system of equations:

$$
\left\{
\begin{array}{lcl}
\nabla \times E & = & \sqrt{-1}\omega\mu_D H \quad \text{in } \mathbb{R}^3 \setminus \partial D, \\
\nabla \times H & = & -\sqrt{-1}\omega\varepsilon_D E \quad \text{in } \mathbb{R}^3 \setminus \partial D, \\
\nu \times E\big|_+ - \nu \times E\big|_- & = & \nu \times H\big|_+ - \nu \times H\big|_- = 0 \quad \text{on } \partial D,
\end{array}
\right. \tag{6.3}
$$

subject to the Silver-Müller radiation condition:

$$
\lim_{|x|\to\infty} |x| \Big(\sqrt{\mu_m}(H - H^i)(x) \times \frac{x}{|x|} - \sqrt{\varepsilon_m}(E - E^i)(x) \Big) = 0 \tag{6.4}
$$

uniformly in $x/|x|$.

Using the boundary integral operators $\vec{\mathcal{S}}_D^k, \mathcal{M}_D^k$ and $\mathcal{L}_D^k$, the solution to (6.3) can be represented as

(6.5)

$$
E(x) = \left\{
\begin{array}{ll}
E^i(x) + \mu_m \nabla \times \vec{\mathcal{S}}_D^{k_m}[\psi](x) + \nabla \times \nabla \times \vec{\mathcal{S}}_D^{k_m}[\phi](x), & x \in \mathbb{R}^3 \setminus \overline{D}, \\
\mu_c \nabla \times \vec{\mathcal{S}}_D^{k_c}[\psi](x) + \nabla \times \nabla \times \vec{\mathcal{S}}_D^{k_c}[\phi](x), & x \in D,
\end{array}
\right.
$$

and

$$
H(x) = -\frac{\sqrt{-1}}{\omega\mu_D}(\nabla \times E)(x) \quad x \in \mathbb{R}^3 \setminus \partial D, \tag{6.6}
$$

where the pair $(\varphi, \psi) \in \big(H_T^{-\frac{1}{2}}(\mathrm{div}, \partial D)\big)^2$ satisfies

(6.7)

$$
\begin{pmatrix}
\frac{\mu_c + \mu_m}{2} I + \mu_c \mathcal{M}_D^{k_c} - \mu_m \mathcal{M}_D^{k_m} & \mathcal{L}_D^{k_c} - \mathcal{L}_D^{k_m} \\
\mathcal{L}_D^{k_c} - \mathcal{L}_D^{k_m} & \left(\frac{k_c^2}{2\mu_c} + \frac{k_m^2}{2\mu_m} \right) I + \frac{k_c^2}{\mu_c}\mathcal{M}_D^{k_c} - \frac{k_m^2}{\mu_m}\mathcal{M}_D^{k_m}
\end{pmatrix}
\begin{bmatrix} \psi \\ \phi \end{bmatrix}
= \begin{bmatrix} \nu \times E^i \\ \sqrt{-1}\omega\nu \times H^i \end{bmatrix} \Bigg|_{\partial D}.
$$

It can be shown that that the system of equations (6.7) on $TH(\mathrm{div}, \partial D) \times TH(\mathrm{div}, \partial D)$ has a unique solution and there exists there a positive constant $C = C(\varepsilon, \mu, \omega)$ such that

(6.8)

$$
\|\psi\|_{TH(\mathrm{div},\partial D)} + \|\phi\|_{TH(\mathrm{div},\partial D)} \leq C\big(\|E^i \times \nu\|_{TH(\mathrm{div},\partial D)} + \|H^i \times \nu\|_{TH(\mathrm{div},\partial D)}\big).
$$

6.2. Scattering coefficients

6.2.1. Multipole solutions to the Maxwell equations. For a wave number $k > 0$, $l' = -l, \ldots, l$ and $l = 1, 2, \ldots$, the function

$$
v_{ll'}(k; x) = h_l^{(1)}(k|x|) Y_l^{l'}(\hat{x}) \tag{6.9}
$$

satisfies the Helmholtz equation $\Delta v + k^2 v = 0$ in $\mathbb{R}^3 \setminus \{0\}$ and the Sommerfeld radiation condition:

$$
\lim_{|x|\to\infty} |x| \big(\frac{\partial v_{ll'}}{\partial |x|}(k; x) - \sqrt{-1} k v_{ll'}(k; x) \big) = 0.
$$

Here, $Y_l^{l'}$ is the spherical harmonic defined on the unit sphere S, $\hat{x} = x/|x|$, and $h_l^{(1)}$ is the spherical Hankel function of the first kind and order l which satisfies the

Sommerfeld radiation condition in three dimensions. Similarly, we define $\tilde{v}_{ll'}(x)$ by

$$\tilde{v}_{ll'}(k;x) = j_l(k|x|)Y_l^{l'}(\hat{x}), \tag{6.10}$$

where j_l is the spherical Bessel function of the first kind. The function $\tilde{v}_{ll'}$ satisfies the Helmholtz equation in all $\mathbb{R}^3$.

In a similar manner, one can form solutions to the Maxwell system with the vector version of spherical harmonics. Define the vector spherical harmonics as

$$U_{ll'} = \frac{1}{\sqrt{l(l+1)}} \nabla_S Y_l^{l'}(\hat{x}) \quad \text{and} \quad V_{ll'} = \hat{x} \times U_{ll'}, \tag{6.11}$$

for $l' = -l, \dots, l$ and $l = 1, 2, \dots$. Here, $\hat{x} \in S$ and ∇_S denotes the surface gradient on the unit sphere S. The vector spherical harmonics defined in (6.11) form a complete orthogonal basis for $L^2_T(S)$, where $L^2_T(S) = \{\mathbf{u} \in (L^2(S))^3 \mid \nu \cdot u = 0\}$ and ν is the outward unit normal to S.

By multiplying the vector spherical harmonics with the Hankel function, one can construct so-called multipole solutions to the Maxwell system. To keep the analysis simple, one separates the solutions into transverse electric, $(E \cdot x) = 0$, and transverse magnetic, $(H \cdot x) = 0$. Define the exterior transverse electric multipoles to the Maxwell equations in free space as

$$\begin{cases} E_{ll'}^{TE}(k;x) = -\sqrt{l(l+1)} h_l^{(1)}(k|x|) V_{ll'}(\hat{x}), \\ H_{ll'}^{TE}(k;x) = -\dfrac{\sqrt{-1}}{\omega\mu} \nabla \times \Big(-\sqrt{l(l+1)} h_l^{(1)}(k|x|) V_{ll'}(\hat{x}) \Big), \end{cases} \tag{6.12}$$

and the exterior transverse magnetic multipoles as

$$\begin{cases} E_{ll'}^{TM}(k;x) = \dfrac{\sqrt{-1}}{\omega\varepsilon} \nabla \times \Big(-\sqrt{l(l+1)} h_l^{(1)}(k|x|) V_{ll'}(\hat{x}) \Big), \\ H_{ll'}^{TM}(k;x) = -\sqrt{l(l+1)} h_l^{(1)}(k|x|) V_{ll'}(\hat{x}). \end{cases} \tag{6.13}$$

The exterior electric and magnetic multipole satisfy the radiation condition. In the same manner, one defines the interior multipoles $(\widetilde{E}_{ll'}^{TE}, \widetilde{H}_{ll'}^{TE})$ and $(\widetilde{E}_{ll'}^{TM}, \widetilde{H}_{ll'}^{TM})$ with $h_l^{(1)}$ replaced by j_l, *i.e.*,

$$\begin{cases} \widetilde{E}_{ll'}^{TE}(k;x) = -\sqrt{l(l+1)} j_l^{(1)}(k|x|) V_{ll'}(\hat{x}), \\ \widetilde{H}_{ll'}^{TE}(k;x) = -\dfrac{\sqrt{-1}}{\omega\mu} \nabla \times \widetilde{E}_{ll'}^{TE}(k;x), \end{cases} \tag{6.14}$$

and

$$\begin{cases} \widetilde{H}_{ll'}^{TM}(k;x) = -\sqrt{l(l+1)} j_l^{(1)}(k|x|) V_{ll'}(\hat{x}), \\ \widetilde{E}_{ll'}^{TM}(k;x) = \dfrac{\sqrt{-1}}{\omega\varepsilon} \nabla \times \widetilde{H}_{ll'}^{TM}(k;x). \end{cases} \tag{6.15}$$

Note that one has

$$(6.16)\qquad \nabla\times E^{TE}_{ll'}(k;x)=\frac{\sqrt{l(l+1)}}{|x|}\mathcal{H}_l(k|x|)U_{ll'}(\hat{x})+\frac{l(l+1)}{|x|}h^{(1)}_l(k|x|)Y^{l'}_l(\hat{x})\hat{x},$$

$$(6.17)\qquad \nabla\times \widetilde{E}^{TE}_{ll'}(k;x)=\frac{\sqrt{l(l+1)}}{|x|}\mathcal{J}_l(k|x|)U_{ll'}(\hat{x})+\frac{l(l+1)}{|x|}j^{(1)}_l(k|x|)Y^{l'}_l(\hat{x})\hat{x},$$

where $\mathcal{H}_l(t)=h^{(1)}_l(t)+t\left(h^{(1)}_l\right)'(t)$ and $\mathcal{J}_l(t)=j_l(t)+tj_l'(t)$.

The solutions to the Maxwell system can be represented as separated variable sums of the multipole solutions. Using multipole solutions together with the Helmholtz solutions in (6.9) and (6.10), it is also possible to expand the fundamental solution Γ_k to the Helmholtz operator.

Let p be a fixed vector in $\mathbb{R}^3$. For $|x|>|y|$, the following addition formula holds:

$$\begin{aligned}\Gamma_k(x-y)p=&-\sum_{l=1}^{\infty}\frac{\sqrt{-1}k}{l(l+1)}\frac{\varepsilon}{\mu}\sum_{l'=-l}^{l}E^{TM}_{ll'}(k;x)\overline{\widetilde{E}^{TM}_{ll'}(k;y)}\cdot p\\&+\sum_{l=1}^{\infty}\frac{\sqrt{-1}k}{l(l+1)}\sum_{l'=-l}^{l}E^{TE}_{ll'}(k;x)\overline{\widetilde{E}^{TE}_{ll'}(k;y)}\cdot p\\&-\frac{\sqrt{-1}}{k}\sum_{l=1}^{\infty}\sum_{l'=-l}^{l}\nabla v_{ll'}(k;x)\overline{\nabla\tilde{v}_{ll'}(k;y)}\cdot p,\end{aligned}\qquad(6.18)$$

with $v_{ll'}$ and $\tilde{v}_{ll'}$ being defined by (6.9) and (6.10).

Plane wave solutions to the Maxwell equations have expansions using multipole solutions as well. The incoming wave

$$E^i(x)=\sqrt{-1}k(q\times p)\times qe^{\sqrt{-1}kq\cdot x},$$

where $q\in S$ is the direction of propagation and the vector $p\in\mathbb{R}^3$ is the direction of polarization, is expressed as

(6.19)

$$E^i(x)=\sqrt{-1}k\sum_{l=1}^{\infty}\frac{4\pi(\sqrt{-1})^l}{\sqrt{l(l+1)}}\sum_{l'=-l}^{l}\left[\big(V_{ll'}(q)\cdot c\big)\widetilde{E}^{TE}_{ll'}(x)-\frac{1}{\sqrt{-1}\omega\mu}\big(U_{ll'}(q)\cdot c\big)\widetilde{E}^{TM}_{ll'}(x)\right],$$

where $c=(q\times p)\times q$.

6.2.2. Scattering coefficients. This subsection introduces the notion of scattering coefficients associated with the Maxwell equations. It extends the notions and results established in the previous section for the Helmholtz equation.

From (6.18) (with k_m in the place of k) and (6.5) it follows that, for sufficiently large $|x|$,

$$(6.20)\qquad (E-E^i)(x)=\sum_{l=1}^{\infty}\frac{\sqrt{-1}k_m}{l(l+1)}\sum_{l'=-l}^{l}\Big(\alpha_{ll'}E^{TE}_{ll'}(k_m;x)\;+\;\beta_{ll'}E^{TM}_{ll'}(k_m;x)\Big),$$

where

$$\begin{aligned}\alpha_{ll'}&=-\sqrt{-1}\omega\varepsilon_m\mu_m\int_{\partial D}\overline{\widetilde{E}^{TM}_{ll'}}(k_m;y)\cdot\varphi(y)+k_m^2\int_{\partial D}\overline{\widetilde{E}^{TE}_{ll'}}(k_m;y)\cdot\psi(y),\\ \beta_{ll'}&=-\sqrt{-1}\omega\varepsilon_m\mu_m\int_{\partial D}\overline{\widetilde{E}^{TE}_{ll'}}(k_m;y)\cdot\varphi(y)-\omega^2\varepsilon_m^2\int_{\partial D}\overline{\widetilde{E}^{TM}_{ll'}}(k_m;y)\cdot\psi(y).\end{aligned}$$

Let $(\varphi^{TE}_{pp'}, \psi^{TE}_{pp'})$ be the solution to (6.7) when

$$E^i = \widetilde{E}^{TE}_{pp'}(k_m; y) \quad \text{and } H^i = \widetilde{H}^{TE}_{pp'}(k_m; y),$$

and $(\varphi^{TM}_{pp'}, \psi^{TM}_{pp'})$ when

$$E^i = \widetilde{E}^{TM}_{pp'}(k_m; y) \quad \text{and } H^i = \widetilde{H}^{TM}_{pp'}(k_m; y).$$

DEFINITION 6.1 (Scattering Coefficients). The scattering coefficients

$$\left(W^{TE,TE}_{ll',pp'}, W^{TE,TM}_{ll',pp'}, W^{TM,TE}_{ll',pp'}, W^{TM,TM}_{ll',pp'}\right)$$

associated with the permittivity and the permeability distributions ε, μ and the frequency ω (or k_c, k_m, D) are defined to be

$$W^{TE,TE}_{ll',pp'} = -\sqrt{-1}\omega\varepsilon_m\mu_m \int_{\partial D} \overline{\widetilde{E}^{TM}_{ll'}}(k_m; y) \cdot \varphi^{TE}_{pp'}(y)\, d\sigma(y) + k_m^2 \int_{\partial D} \overline{\widetilde{E}^{TE}_{ll'}}(k_m; y) \cdot \psi^{TE}_{pp'}(y)\, d\sigma(y),$$
$$W^{TE,TM}_{ll',pp'} = -\sqrt{-1}\omega\varepsilon_m\mu_m \int_{\partial D} \overline{\widetilde{E}^{TM}_{ll'}}(k_m; y) \cdot \varphi^{TM}_{pp'}(y)\, d\sigma(y) + k_m^2 \int_{\partial D} \overline{\widetilde{E}^{TE}_{ll'}}(k_m; y) \cdot \psi^{TM}_{pp'}(y)\, d\sigma(y),$$
$$W^{TM,TE}_{ll',pp'} = -\sqrt{-1}\omega\varepsilon_m\mu_m \int_{\partial D} \overline{\widetilde{E}^{TE}_{ll'}}(k_m; y) \cdot \varphi^{TE}_{pp'}(y)\, d\sigma(y) - \omega^2\varepsilon_m^2 \int_{\partial D} \overline{\widetilde{E}^{TM}_{ll'}}(k_m; y) \cdot \psi^{TE}_{pp'}(y)\, d\sigma(y),$$
$$W^{TM,TM}_{ll',pp'} = -\sqrt{-1}\omega\varepsilon_m\mu_m \int_{\partial D} \overline{\widetilde{E}^{TE}_{ll'}}(k_m; y) \cdot \varphi^{TM}_{pp'}(y)\, d\sigma(y) - \omega^2\varepsilon_m^2 \int_{\partial D} \overline{\widetilde{E}^{TM}_{ll'}}(k_m; y) \cdot {}^{TM}_{pp'}(y)\, d\sigma(y).$$

As can be seen, the scattering coefficients appear naturally in the expansion of the scattering amplitude. One first obtains the following estimates for the decay of the scattering coefficients.

LEMMA 6.2. *There exists a constant C depending on $(\varepsilon, \mu, \omega)$ such that*

$$\left|W^{TE,TE}_{ll',pp'}[\varepsilon, \mu, \omega]\right| \leq \frac{C^{l+p}}{l^l p^p} \tag{6.21}$$

for all $l, l', p, p' \in \mathbb{N}$. The same estimates hold for $W^{TE,TM}_{ll',pp'}$, $W^{TM,TE}_{ll',pp'}$, and $W^{TM,TM}_{ll',pp'}$.

PROOF. Let (φ, ψ) be the solution to (6.7) with $E^i(y) = \widetilde{E}^{TE}_{pp'}(k_m; y)$ and $H^i = -\frac{\sqrt{-1}}{\omega\mu_m}\nabla \times E^i$. Recall that the spherical Bessel function j_p behaves as

$$j_p(t) = \frac{t^p}{1 \cdot 3 \cdots (2p+1)}\left(1 + O\left(\frac{1}{p}\right)\right) \quad \text{as } p \to \infty,$$

uniformly on compact subsets of $\mathbb{R}$. Using Stirling's formula

$$p! = \sqrt{2\pi p}(p/e)^p(1 + o(1)),$$

one has

$$j_p(t) = O\left(\frac{C^p t^p}{p^p}\right) \quad \text{as } p \to \infty, \tag{6.22}$$

uniformly on compact subsets of $\mathbb{R}$ with a constant C independent of p. Thus one has

$$\|E^i\|_{TH(\mathrm{div}, \partial D)} + \|H^i\|_{TH(\mathrm{div}, \partial D)} \leq \frac{C'^p}{p^p}$$

for some constant C'. It then follows from (6.8) that

$$\|\varphi\|_{L^2(\partial D)} + \|\psi\|_{L^2(\partial D)} \leq \frac{C^p}{p^p}$$

for another constant C. So one gets (6.21) from the definition of the scattering coefficients. $\square$

Now suppose that the incoming wave is of the form

$$E^i(x) = \sum_{p=1}^{\infty} \sum_{p'=-p}^{p} \left(a_{pp'} \widetilde{E}_{pp'}^{TE}(k_m; x) + b_{pp'} \widetilde{E}_{pp'}^{TM}(k_m; x) \right) \tag{6.23}$$

for some constants $a_{pp'}$ and $b_{pp'}$. Then the solution (φ, ψ) to (6.7) is given by

$$\varphi = \sum_{p=1}^{\infty} \sum_{p'=-p}^{p} \left(a_{pp'} \varphi_{pp'}^{TE} + b_{pp'} \varphi_{pp'}^{TM} \right),$$

$$\psi = \sum_{p=1}^{\infty} \sum_{p'=-p}^{p} \left(a_{pp'} \psi_{pp'}^{TE} + b_{pp'} \psi_{pp'}^{TM} \right).$$

By (6.20) and Definition 6.1, the solution E to (6.3) can be represented as

$$(E - E^i)(x) = \sum_{l=1}^{\infty} \frac{\sqrt{-1} k_m}{l(l+1)} \sum_{l'=-l}^{l} \left(\alpha_{ll'} E_{ll'}^{TE}(k_m; x) \ + \ \beta_{ll'} E_{ll'}^{TM}(k_m; x) \right), \quad |x| \to \infty, \tag{6.24}$$

where

$$\begin{cases} \alpha_{ll'} = \displaystyle\sum_{p=1}^{\infty} \sum_{p'=-p}^{p} \left(a_{pp'} W_{ll',pp'}^{TE,TE} + b_{pp'} W_{ll',pp'}^{TE,TM} \right), \\ \beta_{ll'} = \displaystyle\sum_{p=1}^{\infty} \sum_{p'=-p}^{p} \left(a_{pp'} W_{ll',pp'}^{TM,TE} + b_{pp'} W_{ll',pp'}^{TM,TM} \right). \end{cases} \tag{6.25}$$

6.3. Multi-layer structure and its scattering coefficients

Code:	6.1 Scattering Coefficients for Maxwell's Equations	DemoSCoeffMaxwell.m

Here we consider a multi-layered structure and explain how to compute its scattering coefficients. A numerical example is also presented. The multi-layered structure is defined as follows: For positive numbers $r_1, \ldots, r_{L+1}$ with $2 = r_1 > r_2 > \cdots r_{L+1} = 1$, let

$$A_j := \{x : r_{j+1} \leq |x| < r_j\}, \quad j = 1, \ldots, L,$$

$$A_0 := \mathbb{R}^3 \setminus \overline{B_2(\mathbf{0})}, \quad A_{L+1} (= D) := \{x : |x| < 1\},$$

where $B_2(\mathbf{0})$ denotes the central ball of radius 2 and

$$\Gamma_j = \{|x| = r_j\}, \quad j = 1, \ldots, L+1.$$

Let (μ_j, ϵ_j) be the pair of permeability and permittivity parameters of A_j for $j = 1, \ldots, L+1$. Set $\mu_0 = 1$ and $\epsilon_0 = 1$. Then define the permeability and permittivity distributions of the layered structure to be

$$\mu = \sum_{j=0}^{L+1} \mu_j \chi(A_j) \quad \text{and} \quad \epsilon = \sum_{j=0}^{L+1} \epsilon_j \chi(A_j). \tag{6.26}$$

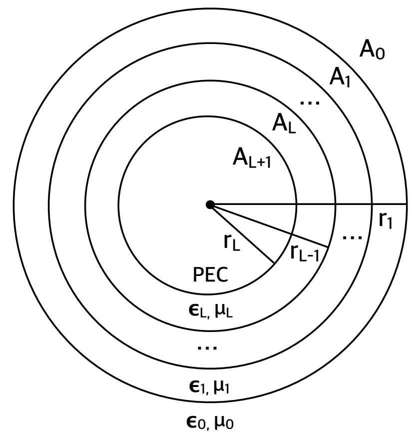

FIGURE 6.1. a multi-layered structure

The scattering coefficients $\left(W^{TE,TE}_{(n,m)(p,q)}, W^{TE,TM}_{(n,m)(p,q)}, W^{TM,TE}_{(n,m)(p,q)}, W^{TM,TM}_{(n,m)(p,q)}\right)$ are defined as before, namely, if E^i given as in (6.23), the scattered field $E - E^i$ can be expanded as (6.24) and (6.25). The transmission condition on each interface $\mathbf{\Gamma}_j$ is given by

$$[\hat{x} \times E] = [\hat{x} \times H] = 0. \tag{6.27}$$

Assume that the core A_{L+1} is perfectly conducting (PEC), that is,

$$E \times \nu = 0 \quad \text{on } \Gamma_{L+1} = \partial A_{L+1}. \tag{6.28}$$

Thanks to the symmetry of the layered (radial) structure, the scattering coefficients are much simpler than the general case. In fact, if the incident field is given by $E^i = \widetilde{E}^{TE}_{n,m}$, then the solution E to (6.1) takes the form

$$E(x) = \tilde{a}_j \widetilde{E}^{TE}_{n,m}(x) + a_j E^{TE}_{n,m}(x), \quad x \in A_j, \quad j = 0, \dots, L, \tag{6.29}$$

with $\tilde{a}_0 = 1$. From (6.16) and (6.17), the interface condition (6.27) amounts to

$$\begin{aligned} &\begin{bmatrix} j_n(k_j r_j) & h_n^{(1)}(k_j r_j) \\ \dfrac{1}{\mu_j}\mathcal{J}_n(k_j r_j) & \dfrac{1}{\mu_j}\mathcal{H}_n(k_j r_j) \end{bmatrix} \begin{bmatrix} \tilde{a}_j \\ a_j \end{bmatrix} \\ &= \begin{bmatrix} j_n(k_{j-1} r_j) & h_n^{(1)}(k_{j-1} r_j) \\ \dfrac{1}{\mu_{j-1}}\mathcal{J}_n(k_{j-1} r_j) & \dfrac{1}{\mu_{j-1}}\mathcal{H}_n(k_{j-1} r_j) \end{bmatrix} \begin{bmatrix} \tilde{a}_{j-1} \\ a_{j-1} \end{bmatrix}, \quad j = 1, \dots, L, \end{aligned} \tag{6.30}$$

where $\mathcal{H}_n(t) = h_n^{(1)}(t) + t\left(h_n^{(1)}\right)'(t)$ and $\mathcal{J}_n(t) = j_n(t) + tj_n'(t)$, and the PEC boundary condition on Γ_{L+1} is

$$\begin{bmatrix} j_n(k_L) & h_n^{(1)}(k_L) \\ 0 & 0 \end{bmatrix} \begin{bmatrix} \tilde{a}_L \\ a_L \end{bmatrix} = \begin{bmatrix} 0 \\ 0 \end{bmatrix}. \tag{6.31}$$

Since the matrices appearing in (6.30) are invertible, one can see that there exist a_j and $\tilde{a}_j$, $j = 0, 1, \dots L$ satisfying (6.30) and (6.31). Similarly, one can see that if the incident field is given by $E^i = \widetilde{E}_{n,m}^{TM}(x)$, then the solution E takes the form

$$E(x) = \tilde{b}_j \widetilde{E}_{n,m}^{TM}(x) + b_j E_{n,m}^{TM}(x), \quad x \in A_j, \quad j = 0, 1, ..., L \tag{6.32}$$

for some constants b_j and $\tilde{b}_j$ ($\tilde{b}_0 = 1$). One can see now from (6.29) and (6.32) that the scattering coefficients satisfy

$$\begin{aligned} W_{(n,m)(p,q)}^{TE,TM} &= W_{(n,m)(p,q)}^{TM,TE} = 0 \quad \text{for all } (m,n) \text{ and } (p,q), \\ W_{(n,m)(p,q)}^{TE,TE} &= W_{(n,m)(p,q)}^{TM,TM} = 0 \quad \text{if } (m,n) \neq (p,q), \end{aligned}$$

and, since (6.29) and (6.32) hold independently of m, one has

$$\begin{aligned} W_{(n,0)(n,0)}^{TE,TE} &= W_{(n,m)(n,m)}^{TE,TE}, \\ W_{(n,0)(n,0)}^{TM,TM} &= W_{(n,m)(n,m)}^{TM,TM} \qquad \text{for } -n \leq m \leq n. \end{aligned}$$

Moreover, if one writes

$$W_n^{TE} := W_{(n,0)(n,0)}^{TE} \quad \text{and} \quad W_n^{TM} := W_{(n,0)(n,0)}^{TM},$$

then one has

$$W_n^{TE} = -\frac{in(n+1)}{k_0} a_0 \quad \text{and} \quad W_n^{TE} = -\frac{in(n+1)}{k_0} b_0. \tag{6.33}$$

Suppose now that $\widetilde{E}_{n,0}^{TE}$ is the incident field and the solution E is given by

$$E(x) = \tilde{a}_j \widetilde{E}_{n,0}^{TE}(x) + a_j E_{n,0}^{TE}(x), \quad x \in A_j, \quad j = 0, \dots, L,$$

with $\tilde{a}_0 = 1$, where the coefficients $\tilde{a}_j$'s and a_j's are determined by (6.30) and (6.31). From (6.30) it follows that

$$\begin{bmatrix} \tilde{a}_j \\ a_j \end{bmatrix} = \begin{bmatrix} j_n(k_j r_j) & h_n^{(1)}(k_j r_j) \\ \dfrac{1}{\mu_j}\mathcal{J}_n(k_j r_j) & \dfrac{1}{\mu_j}\mathcal{H}_n(k_j r_j) \end{bmatrix}^{-1} \begin{bmatrix} j_n(k_{j-1} r_j) & h_n^{(1)}(k_{j-1} r_j) \\ \dfrac{1}{\mu_{j-1}}\mathcal{J}_n(k_{j-1} r_j) & \dfrac{1}{\mu_{j-1}}\mathcal{H}_n(k_{j-1} r_j) \end{bmatrix} \begin{bmatrix} \tilde{a}_{j-1} \\ a_{j-1} \end{bmatrix},$$

for $j = 1, \dots, L$. Substituting these relations into (6.31) yields

$$\begin{bmatrix} 0 \\ 0 \end{bmatrix} = P_n^{TE}[\epsilon, \mu, \omega] \begin{bmatrix} \tilde{a}_0 \\ a_0 \end{bmatrix}, \tag{6.34}$$

where

$$P_n^{TE}[\epsilon,\mu,\omega] := \begin{bmatrix} p_{n,1}^{TE} & p_{n,2}^{TE} \\ 0 & 0 \end{bmatrix} = (-i\omega)^L \left(\prod_{j=1}^{L} \mu_j^{\frac{3}{2}} \epsilon_j^{\frac{1}{2}} r_j\right) \begin{bmatrix} j_n(k_L) & h_n^{(1)}(k_L) \\ 0 & 0 \end{bmatrix}$$

(6.35)

$$\times \prod_{j=1}^{L} \begin{bmatrix} \frac{1}{\mu_j}\mathcal{H}_n(k_j r_j) & -h_n^{(1)}(k_j r_j) \\ -\frac{1}{\mu_j}\mathcal{J}_n(k_j r_j) & j_n(k_j r_j) \end{bmatrix} \begin{bmatrix} j_n(k_{j-1} r_j) & h_n^{(1)}(k_{j-1} r_j) \\ \frac{1}{\mu_{j-1}}\mathcal{J}_n(k_{j-1} r_j) & \frac{1}{\mu_{j-1}}\mathcal{H}_n(k_{j-1} r_j) \end{bmatrix}.$$

Then (6.34) yields

$$W_n^{TE} = -\frac{in(n+1)}{k_0} a_0 = -\frac{in(n+1)}{k_0} \frac{p_{n,1}^{TE}}{p_{n,2}^{TE}}. \tag{6.36}$$

Similarly, for W_n^{TM}, one looks for another solution E of the form

$$E(x) = \tilde{b}_j \widetilde{E}_{n,0}^{TM}(x) + b_j E_{n,0}^{TM}(x), \quad x \in A_j, \quad j = 0, ..., L,$$

with $\tilde{b}_0 = 1$. The transmission conditions become

$$\begin{aligned} &\begin{bmatrix} \frac{1}{\epsilon_j}\mathcal{J}_n(k_j r_j) & \frac{1}{\epsilon_j}\mathcal{H}_n(k_j r_j) \\ j_n(k_j r_j) & h_n^{(1)}(k_j r_j) \end{bmatrix} \begin{bmatrix} \tilde{b}_j \\ b_j \end{bmatrix} \\ &= \begin{bmatrix} \frac{1}{\epsilon_{j-1}}\mathcal{J}_n(k_{j-1} r_j) & \frac{1}{\epsilon_{j-1}}\mathcal{H}_n(k_{j-1} r_j) \\ j_n(k_{j-1} r_j) & h_n^{(1)}(k_{j-1} r_j) \end{bmatrix} \begin{bmatrix} \tilde{b}_{j-1} \\ b_{j-1} \end{bmatrix}, \quad j = 1, \ldots, N+1, \end{aligned} \tag{6.37}$$

and the PEC boundary condition on the inner most layer is

$$\begin{bmatrix} \mathcal{J}_n(k_L) & \mathcal{H}_n(k_L) \\ 0 & 0 \end{bmatrix} \begin{bmatrix} \tilde{b}_L \\ b_L \end{bmatrix} = \begin{bmatrix} 0 \\ 0 \end{bmatrix}. \tag{6.38}$$

From (6.37) and (6.38), one obtains

$$\begin{bmatrix} 0 \\ 0 \end{bmatrix} = P_n^{TM}[\epsilon,\mu,\omega] \begin{bmatrix} \tilde{b}_0 \\ b_0 \end{bmatrix}, \tag{6.39}$$

where

$$P_n^{TM}[\epsilon,\mu,\omega] := \begin{bmatrix} p_{n,1}^{TM} & p_{n,2}^{TM} \\ 0 & 0 \end{bmatrix} = (i\omega)^L \left(\prod_{j=1}^{L} \mu_j^{\frac{1}{2}} \epsilon_j^{\frac{3}{2}} r_j\right) \begin{bmatrix} \mathcal{J}_n(k_L) & \mathcal{H}_n(k_L) \\ 0 & 0 \end{bmatrix}$$

(6.40)

$$\times \prod_{j=1}^{L} \begin{bmatrix} h_n^{(1)}(k_j r_j) & -\frac{1}{\epsilon_j}\mathcal{H}_n(k_j r_j) \\ -j_n(k_j r_j) & \frac{1}{\epsilon_j}\mathcal{J}_n(k_j r_j) \end{bmatrix} \begin{bmatrix} \frac{1}{\epsilon_{j-1}}\mathcal{J}_n(k_{j-1} r_j) & \frac{1}{\epsilon_{j-1}}\mathcal{H}_n(k_{j-1} r_j) \\ j_n(k_{j-1} r_j) & h_n^{(1)}(k_{j-1} r_j) \end{bmatrix}.$$

From the definition of W_n^{TM} and (6.39),

$$W_n^{TE} = -\frac{in(n+1)}{k_0} \frac{b_0}{\tilde{b}_0} = -\frac{in(n+1)}{k_0} \frac{p_{n,1}^{TM}}{p_{n,2}^{TM}}. \tag{6.41}$$

It is worth emphasizing that $p_{n,2}^{TE} \neq 0$ and $p_{n,2}^{TM} \neq 0$. In fact, if $p_{n,2}^{TE} = 0$, then (6.34) can be fulfilled with $\tilde{a}_0 = 0$ and $a_0 = 1$. This means that there exists (μ, ϵ) on $\mathbb{R}^3 \setminus \overline{D}$ such that the following problem has a solution:

$$\begin{cases} \nabla \times E = i\omega\mu H & \text{in } \mathbb{R}^3 \setminus \overline{D}, \\ \nabla \times H = -i\omega\epsilon E & \text{in } \mathbb{R}^3 \setminus \overline{D}, \\ (x \times E)\big|_+ = 0 & \text{on } \partial D, \\ E(x) = E_{n,0}^{TE}(x) & \text{for } |x| > 2. \end{cases}$$

Applying the following Green's theorem on $\Omega = \{x \mid 1 < |x| < R\}$,

$$\begin{aligned} &\int_\Omega \big(E \cdot \Delta F + \mathrm{curl} E \cdot \mathrm{curl} F + \mathrm{div} E \; \mathrm{div} F\big) dx \\ &= \int_{\partial\Omega} \big(\nu \times E \cdot \mathrm{curl} F + \nu \cdot E \; \mathrm{div} F\big) d\sigma(x) \end{aligned}$$

with $F = \overline{E_{n,0}^{TE}}(x)$ and the PEC boundary condition on $\{|x| = 1\}$, it follows that

$$\int_{|x|=R} (\nu \times E) \cdot \overline{H} d\sigma(x) = ik_0 \int_\Omega (|H|^2 - |E|^2) dx.$$

In particular, the left-hand side is real-valued. Hence,

$$\begin{aligned} \int_{|x|=R} |H \times \nu - E|^2 d\sigma(x) &= \int_{|x|=R} \big(|H \times \nu|^2 + |E|^2 - 2\Re((\nu \times E) \cdot \overline{H}\big) d\sigma(x) \\ &= \int_{|x|=R} \big(|H \times \nu|^2 + |E|^2\big) d\sigma(x). \end{aligned}$$

From the radiation condition, the left-hand side goes to zero as $R \to \infty$, which contradicts the behavior of the Hankel functions. One can show that $p_{n,2}^{TM} \neq 0$ in a similar way.

6.3.1. Numerical example. Here we demonstrate how the scattering coefficients W_n^{TE} and W_n^{TM} can be computed numerically and then present an example. For simplicity, we consider only W_n^{TE}. Recall that

$$W_n^{TE} = -\frac{in(n+1)}{k_0} a_0, \tag{6.42}$$

and the constant a_0 is determined by (6.30) and (6.31). From (6.30), we obtain

$$\begin{bmatrix} \tilde{a}_0 / a_L \\ a_0 / a_L \end{bmatrix} = (M_1^{-1} N_1)(M_2^{-1} N_2) \dots (M_L^{-1} N_L) \begin{bmatrix} \tilde{a}_L / a_L \\ 1 \end{bmatrix}, \tag{6.43}$$

where

$$M_j = \begin{bmatrix} j_n(k_j r_j) & h_n^{(1)}(k_j r_j) \\ \dfrac{1}{\mu_j} \mathcal{J}_n(k_j r_j) & \dfrac{1}{\mu_j} \mathcal{H}_n(k_j r_j) \end{bmatrix}, \quad N_j = \begin{bmatrix} j_n(k_{j-1} r_j) & h_n^{(1)}(k_{j-1} r_j) \\ \dfrac{1}{\mu_{j-1}} \mathcal{J}_n(k_{j-1} r_j) & \dfrac{1}{\mu_{j-1}} \mathcal{H}_n(k_{j-1} r_j) \end{bmatrix}.$$

From (6.31), we immediately see that

$$\frac{\tilde{a}_L}{a_L} = -\frac{h_n^{(1)}(k_L r_{L+1})}{j_n(k_L r_{L+1})}.$$

Therefore, we can compute $\tilde{a}_0 / a_L$ and a_0 / a_L. But, since $\tilde{a}_0 = 1$, we can also compute a_0 and then W_n^{TE}.

Now we present a numerical example. We set the parameters for the structure as follows: the number of layers L is $L = 3$, the radii of layers are $r_1 = 2, r_2 = 5/3, r_3 = 4/3, r_4 = 1$, and the material parameters are $(\epsilon_0, \mu_0) = (1,1), (\epsilon_0, \mu_0) = (0.5, 0.5), (\epsilon_0, \mu_0) = (2,2), (\epsilon_0, \mu_0) = (0.5, 0.5)$. The numerical result for W_n^{TE} and W_n^{TM} for $n = 1, 2, ..., 7$ is shown in Table 6.1. The decaying behavior of W_n^{TE} and W_n^{TM} is clearly shown.

n	W_n^{TE}	W_n^{TM}
1	$-0.9991 + 0.9572i$	$-0.7473 + 1.6644i$
2	$-0.7527 + 0.0960i$	$-0.7650 + 0.0992i$
3	$-0.1642 + 0.0022i$	$-0.1643 + 0.0023i$
4	$-0.0191 + 0.0000i$	$-0.0191 + 0.0000i$
5	$-0.0013 + 0.0000i$	$-0.0013 + 0.0000i$
6	$-0.0001 + 0.0000i$	$-0.0001 + 0.0000i$
7	$-0.0000 + 0.0000i$	$-0.0000 + 0.0000i$

TABLE 6.1. Scattering coefficients for a multi-layer spherical shell

CHAPTER 7

Diffraction Gratings

In this chapter we discuss periodic structures with tiny spatial features known as diffraction gratings in which light propagation is governed by diffraction. The full Maxwell's equations are used to model the energy distribution in systems involving such gratings. However, if the fields are composed of transverse time-harmonic electromagnetic waves we can reduce the Maxwell equations to two scalar Helmholtz equations. We analyze two classes of gratings:

- linear grating (one-dimensional gratings),
- crossed gratings (biperiodic or two-dimensional gratings).

We show how the diffraction grating problem can be formulated in terms of a boundary integral representation. We conclude with a demonstration of how the boundary integral representation can be used to numerically determine the electric field in the case of a linear grating.

7.0.1. Time-Harmonic Maxwell's Equations. The electromagnetic wave propagation is governed by Maxwell's equations. Throughout, we shall restrict our attention to time-harmonic electromagnetic fields with time dependence $(e^{-\sqrt{-1}\omega t})$, *i.e.*,

$$E(x,t) = E(x)e^{-\sqrt{-1}\omega t}\,, \tag{7.1}$$

$$H(x,t) = H(x)e^{-\sqrt{-1}\omega t} \tag{7.2}$$

for some operating frequency $\omega > 0$ with E and H being respectively the electric and magnetic field.

The time-harmonic Maxwell equations take the following form:

$$\nabla \times E = \sqrt{-1}\omega\mu H, \tag{7.3}$$

$$\nabla \times H = -\sqrt{-1}\omega\varepsilon E, \tag{7.4}$$

where μ is the magnetic permeability and ε is the electric permittivity. Note that from (7.3) and (7.4), it follows that

$$\nabla \cdot (\varepsilon E) = 0, \tag{7.5}$$

$$\nabla \cdot (\mu H) = 0. \tag{7.6}$$

The fields are further assumed to be nonmagnetic and $\mu = \mu_0$ (usually the magnetic permeability of vacuum). Then (7.6) becomes

$$\nabla \cdot H = 0.$$

It follows from (7.3-7.4) that the following jump conditions hold:

- the tangential components of E and H must be continuous crossing an interface,

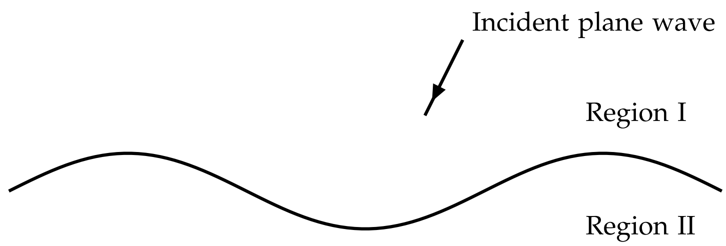

FIGURE 7.1. Grating geometry.

- the normal components of εE and H must be continuous crossing an interface.

In a homogeneous and isotropic medium, ε does not depend on x. By taking the curl of (7.3) we obtain that

$$-\Delta E + \nabla(\nabla \cdot E) = \sqrt{-1}\omega\mu_0 \nabla \times H.$$

Using (7.4), we have

$$-\Delta E + \nabla(\nabla \cdot E) = \omega^2 \varepsilon \mu_0 E$$

or the Helmholtz equation

$$\Delta E + k^2 E = 0 \tag{7.7}$$

with $k = \omega\sqrt{\varepsilon\mu_0}$.

Similarly, H satisfies

$$\Delta H + k^2 H = 0.$$

Note that in a dielectric medium k^2 is real and positive. The wavelength λ is given by $\lambda = (2\pi)/k$.

7.0.2. Grating Geometry and Fundamental Polarizations. Throughout, a grating is always assumed to be infinitely wide.

Figure 7.1 shows the grating geometry. We denote the period, height, and incident angle by Λ, h, and θ, respectively.

An alternative way to specify the periodicity is by means of ε.

For a 1-D grating (linear grating):

$$\varepsilon(x_1 + n\Lambda, x_2) = \varepsilon(x_1, x_2), \quad n \in \mathbb{Z}.$$

In the case of a crossed grating with period $\Lambda = (\Lambda_1, \Lambda_2)$ we have

$$\varepsilon(x_1 + n_1\Lambda_1,\ x_2 + n_2\Lambda_2,\ x_3) = \varepsilon(x_1, x_2, x_3),\ \forall\, n_1, n_2 \in \mathbb{Z}.$$

We assume that above the interface ε is real and positive. However, below the interface the parameter ε can be real which corresponds to a dielectric medium; complex corresponding to an absorbing or lossy medium; or perfectly conducting.

In the next three sections we shall discuss two separate cases: The perfectly conducting grating and the dielectric grating.

Suppose that a grating is illuminated under the incidence θ by a plane wave of unit amplitude propagating in Region I (Figure 7.1). The incident vector K_i lies in the (x_1, x_2) plane

$$K_i = k_1(\sin\theta, -\cos\theta, 0).$$

The electromagnetic fields are assumed to be independent of x_3. We consider the following two fundamental cases of polarization: TE (transverse electric) and TM (transverse magnetic).

In TE polarization, the electric field is parallel to the grooves or points in the x_3 direction, *i.e.*,

$$E = u(x_1, x_2)e_3$$

where u is a scalar function and (e_1, e_2, e_3) is an orthonormal basis of $\mathbb{R}^3$.

In TM polarization, the magnetic field is parallel to the grooves

$$H = u(x_1, x_2)e_3.$$

As we shall see, the resulting Maxwell equations in these two polarizations can be quite different.

7.0.3. Perfectly Conducting Gratings. In this section, the grating is assumed to be perfectly conducting. In order to treat the two fundamental polarizations simultaneously, we denote $u = E_3(x_1, x_2)$ in TE polarization; $= H_3(x_1, x_2)$ in TM polarization, where the subscript 3 stands for the third component. Assume that the grating is expressed by $x_2 = f(x_1)$. Then $u = 0$ in Region II ($x_2 < f(x_1)$). In Region I, the field u satisfies

$$\Delta u + k^2 u = 0 \text{ if } x_2 > f(x_1). \tag{7.8}$$

We next derive the boundary condition of u on $x_2 = f(x_1)$. Using the jump conditions and that E is zero in Region II, we have

$$\nu \times E = 0 \quad \text{on } x_2 = f(x_1), \tag{7.9}$$

where ν is the outward normal to Region II.

In TE polarization, $E = (0, 0, u)$, hence (7.9) implies that

$$u(x_1, f(x_1)) = 0, \tag{7.10}$$

i.e., a homogeneous Dirichlet boundary condition.

In TM polarization, $H = (0, 0, u)$. We obtain by using Maxwell's equations and the condition (7.9) that

$$\left.\frac{\partial u}{\partial \nu}\right|_{x_2 = f(x_1)} = 0, \tag{7.11}$$

which is a homogeneous Neumann boundary condition.

Define the scattered field as the difference between the total field u and the incident field $u^i = e^{\sqrt{-1}(\alpha x_1 - \beta x_2)}$

$$u^s = u - u^i. \tag{7.12}$$

Here,

$$\begin{cases} \alpha = k_1 \sin\theta, \\ \beta = k_1 \cos\theta. \end{cases} \tag{7.13}$$

Since the incident field u^i satisfies the Helmholtz equation everywhere, we can easily show that

$$\Delta u^s + k_1^2 u^s = 0 \text{ for } x_2 > f(x_1). \tag{7.14}$$

From (7.10) and (7.11), u^s satisfies either one of the following boundary conditions:

TE polarization:

$$u^s = -u^i \text{ on } x_2 = f(x_1). \tag{7.15}$$

TM polarization:

$$\frac{\partial u^s}{\partial \nu} = -\frac{\partial u^i}{\partial \nu} \text{ on } x_2 = f(x_1). \tag{7.16}$$

Next, since the problem is posed in an unbounded domain, a radiation condition is needed. We assumed that u^s is bounded when x_2 goes to infinity and consisted of outgoing plane waves. This radiation condition is also referred to as the outgoing wave condition.

The grating problem can be stated as: find a function that satisfies the Helmholtz equation (7.14), a boundary condition on $\{x_2 = f(x_1)\}$, and the outgoing wave condition.

Motivated by uniqueness, we shall seek the so–called "quasi–periodic" solutions, *i.e.*, solutions u^s such that $u^s(x_1, x_2)e^{-\sqrt{-1}\alpha x_1}$ is a periodic function of period Λ with respect to x_1 for every x_2. In fact, if the grating problem attains a unique solution then we want to show that

$$v(x_1, x_2) = u(x_1, x_2)e^{-\sqrt{-1}\alpha x_1}$$

is a periodic function of period Λ, *i.e.*,

$$v(x_1 + \Lambda, x_2) = v(x_1, x_2)$$

or equivalently

$$u^s(x_1 + \Lambda, x_2)e^{-\sqrt{-1}\alpha\Lambda} = u^s(x_1, x_2). \tag{7.17}$$

Because of uniqueness, if $w(x_1, x_2) = u^s(x_1 + \Lambda, x_2)e^{-\sqrt{-1}\alpha\Lambda}$ is also a solution of the grating problem, then it must be identical to u^s and (7.16) follows. It is obvious that w satisfies the Helmholtz equation (7.14). The boundary condition (7.15) and (7.16) are also satisfied by observing that u^i is a quasi-periodic function and using the boundary condition of u^s.

7.0.4. Grating Formula. Since $u^s(x_1, x_2)e^{-\sqrt{-1}\alpha x_1}$ is periodic in x_1, it follows by using a Fourier series expansion that

$$\begin{aligned} u^s(x_1, x_2) &= e^{\sqrt{-1}\alpha x_1} \sum_{n \in \mathbb{Z}} V_n(x_2) e^{\sqrt{-1} n \frac{2\pi}{\Lambda} x_1} \\ &= \sum_{n \in \mathbb{Z}} V_n(x_2) e^{\sqrt{-1}\alpha_n x_1} \end{aligned} \tag{7.18}$$

with

$$\alpha_n = \alpha + \frac{2\pi n}{\Lambda}, \tag{7.19}$$

or equivalently,

$$\alpha_n = k_1 \sin\theta + n\frac{2\pi}{\Lambda}. \tag{7.20}$$

Thus, in order to solve for u^s it suffices to determine $V_n(x_2)$.

Now in the region $\{x_2 > \max\{f(x_1)\}\}$, $u^s(x_1, x_2)$ satisfies the Helmholtz equation. Substituting (7.18) into the Helmholtz equation gives

$$\sum_{n\in\mathbb{Z}} \left[\frac{d^2V_n(x_2)}{dx_2^2} + (k_1^2 - \alpha_n^2)V_n(x_2)\right] e^{\sqrt{-1}n\frac{2\pi}{\Lambda}x_1} = 0.$$

Hence

$$\frac{d^2V_n(x_2)}{dx_2^2} + (k_1^2 - \alpha_n^2)V_n(x_2) = 0.$$

Define

$$\beta_n = \begin{cases} \sqrt{k_1^2 - \alpha_n^2} & k_1^2 > \alpha_n^2, \\ \sqrt{-1}\sqrt{\alpha_n^2 - k_1^2} & k_1^2 \leq \alpha_n^2. \end{cases} \tag{7.21}$$

Then, solving the simple ordinary differential equation yields

$$V_n(x_2) = A_n e^{-\beta_n x_2} + B_n e^{\sqrt{-1}\beta_n x_2}.$$

The radiation condition implies that $A_n = 0$. Actually if $|k_1| \geq |\alpha_n|$ then $e^{-\sqrt{-1}\beta_n x_2}$ represents incoming waves instead. If $|k_1| < |\alpha_n|$ then $e^{-\sqrt{-1}\beta_n x_2}$ is unbounded when x_2 goes to infinity. Therefore we arrive at the Rayleigh expansion of the form

$$\begin{aligned} u^s(x_1, x_2) \quad &= \sum_{|\alpha_n|<k_1} B_n e^{\sqrt{-1}\alpha_n x_1 + \sqrt{-1}\beta_n x_2} \quad \text{“outgoing waves”} \\ &+ \sum_{|\alpha_n|\geq k_1} B_n e^{\sqrt{-1}\alpha_n x_1 + \sqrt{-1}\beta_n x_2} \quad \text{“evanescent waves”}. \end{aligned} \tag{7.22}$$

Denote

$$U = \{n, |\alpha_n| < k_1\}.$$

Each term $(n \in U)$ of the outgoing waves in (7.22) represents a propagating plane wave, which is called the scattered wave in the n^{th} order. If $|n|$ is large $(n \notin U)$, then the corresponding term in (7.22) represents an evanescent wave $B_n e^{-\beta_n x_2} e^{\sqrt{-1}\alpha_n x_1}$ which propagates along the x_1-axis and is exponentially damped with respect to x_2. The scattered wave in the n^{th} order takes the form:

$$\psi_n(x_1, x_2) = B_n e^{\sqrt{-1}\alpha_n x_1 + \sqrt{-1}\sqrt{k_1^2 - \alpha_n^2}\ x_2} \quad \text{for } n \in U. \tag{7.23}$$

Since $|\alpha_n/k_1| < 1$, we denote

$$\frac{\alpha_n}{k_1} = \sin\theta_n, \ -\frac{\pi}{2} < \theta_n < \frac{\pi}{2}. \tag{7.24}$$

From (7.19), we have

$$\frac{\alpha_n}{k_1} = \sin\theta_n = \sin\theta + \frac{2\pi n}{k_1\Lambda} \tag{7.25}$$

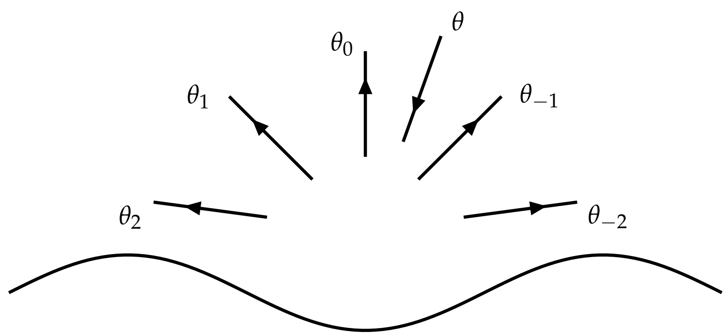

FIGURE 7.2. Geometric interpretation of the grating formula.

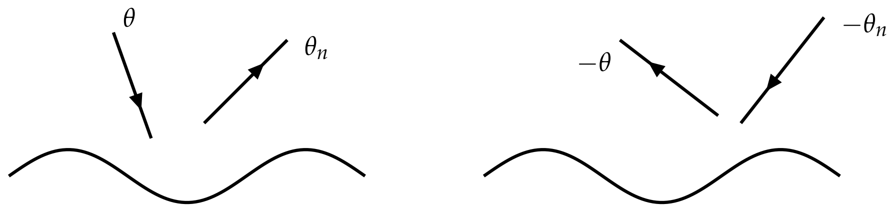

FIGURE 7.3. The reciprocity theorem.

and (7.23) becomes

$$\psi_n(x_1, x_2) = B_n e^{\sqrt{-1}k_1(x_1 \sin\theta_n + x_2 \cos\theta_n)}, \tag{7.26}$$

where θ_n is the angle of diffraction.

Thus we have derived the following grating formula:

$$\sin\theta_n = \sin\theta + n\frac{\lambda_1}{\Lambda} \text{ or } k_1 \sin\theta_n = k_1 \sin\theta + \frac{n2\pi}{\Lambda}, \tag{7.27}$$

where λ_1 is the wavelength in Medium I, recalling that

$$k_1 = \frac{2\pi}{\lambda_1}.$$

In the next theorem we state a reciprocity property.

THEOREM 7.1. *Let θ and θ_n be the angle of incidence and the angle of diffraction of the nth order. Then when the angle of incidence is $\theta' = -\theta_n$, the n^{th} scattered order propagates in the direction defined by $\theta'_n = -\theta$.*

The grating efficiency E_n is the measurement of energy in the nth propagating order. It is defined as

$$E_n = \frac{\phi_n^s}{\phi^i}, \tag{7.28}$$

where ϕ^i and ϕ_n^s are the flux of the Poynting vector associated with the incident wave and the nth scattered wave through a unit rectangle in which one side is parallel to the x_1-axis while the other is parallel to the x_3-axis. It is easy to show that

$$E_n = |B_n|^2 \frac{\cos\theta_n}{\cos\theta}. \tag{7.29}$$

We next state a simple result which is convenient in many applications. The proof is based on integration by parts.

LEMMA 7.2. *Assume that u_1 and u_2 are two functions which satisfy the Helmholtz equation*

$$\Delta u + k^2 u = 0$$

and either a homogeneous Dirichlet or a Neumann boundary condition. Then for any $x_2 > \max f(x_1)$,

$$\int_0^\Lambda (u_1 \frac{\partial u_2}{\partial x_2} - u_2 \frac{\partial u_1}{\partial x_2}) dx_1 = 0. \tag{7.30}$$

THEOREM 7.3 (The conservation of energy).

$$\sum_{n\in U} E_n = 1. \tag{7.31}$$

This is to say, the incident energy is equal to the scattered energy.

PROOF. Let u be a solution of the Helmholtz equation with either the Dirichlet or the Neumann boundary condition. Since k_1 is real, $\overline{u}$ also satisfies the equation and the boundary condition. By applying Lemma 7.2 to u and $\overline{u}$, we get

$$\frac{1}{\Lambda}\int_0^\Lambda \left(\frac{\partial \overline{u}}{\partial x_2} - \overline{u}\frac{\partial u}{\partial x_2}\right) dx_1 = 0 \text{ for } x_2 > \max f(x_1) \tag{7.32}$$

or

$$\frac{1}{\Lambda}\Im\left\{\int_0^\Lambda u\frac{\partial \overline{u}}{\partial x_2}\right\} = 0 \text{ for } x_2 > \max f(x_1). \tag{7.33}$$

Next,

$$\begin{aligned} u = e^{\sqrt{-1}\alpha x_1 - \sqrt{-1}\beta x_2} &+ \sum_{n\in U} B_n e^{\sqrt{-1}\alpha_n x_1 + \beta_n x_2} \\ &+ \sum_{n\notin U} B_n e^{\sqrt{-1}\alpha_n x_1 + \sqrt{-1}\beta_n x_2} \end{aligned} \tag{7.34}$$

and

$$\begin{aligned} \overline{u} = e^{-\sqrt{-1}\alpha x_1 + \sqrt{-1}\beta x_2} &+ \sum_{n\in U} \overline{B}_n e^{-\sqrt{-1}\alpha_n x_1 - \beta_n x_2} \\ &+ \sum_{n\notin U} \overline{B}_n e^{-\sqrt{-1}\alpha_n x_1 + \beta_n x_2}. \end{aligned} \tag{7.35}$$

Substituting (7.34) and (7.35) into (7.33), we find

$$\beta = \sum_{n\in U} \beta_n |B_n|^2,$$

or equivalently

$$\sum_{n\in U} E_n = 1.$$

□

7.0.5. Dielectric Gratings. Recall that Region II is filled with a material of real permittivity ε_2.

The solution of the grating problem satisfies:

In Region I,

$$\Delta u + k_1^2 u = 0 \qquad \text{if } x_2 > f(x_1). \tag{7.36}$$

In Region II,

$$\Delta u + k_2^2 u = 0 \qquad \text{if } x_2 < f(x_1). \tag{7.37}$$

Also, outgoing wave conditions are satisfied by $u^s = u - u^i$ (for $x_2 \to +\infty$) and by u (for $x_2 \to -\infty$).

From the jump conditions and Maxwell's equations, we have that u is continuous, $\partial u/\partial \nu$ is continuous in TE polarization, and $(1/\varepsilon)\partial u/\partial \nu$ is continuous in TM polarization.

Again, the quasi-periodicity of the field follows from the uniqueness of the solution. Then for $x_2 > \max f(x_1)$

$$u(x_1, x_2) = e^{\sqrt{-1}\alpha x_1} \sum_{n\in\mathbb{Z}} V_n(x_2) e^{\sqrt{-1}n\frac{2\pi}{\Lambda}x_1}. \tag{7.38}$$

Substituting (7.38) into (7.36) and (7.37), we obtain the Rayleigh expansion outside the groove

$$u(x_1, x_2) = e^{(\sqrt{-1}\alpha x_1 - \sqrt{-1}\beta x_2)} + \sum R_n e^{\sqrt{-1}\alpha_n x_1 + \sqrt{-1}\beta_{n1} x_2} \tag{7.39}$$

with $\alpha_n = k_1 \sin\theta + n\frac{2\pi}{\Lambda}$ and $\beta_{n1}^2 = k_1^2 - \alpha_n^2$.

If $x_2 < \min f(x_1)$

$$u(x_1, x_2) = \sum_{n\in\mathbb{Z}} T_n\, e^{\sqrt{-1}\alpha_n x_1 - \sqrt{-1}\beta_{n2} x_2}$$

with

$$\beta_{n2}^2 = k_2^2 - \alpha_n^2.$$

These two expansions contain propagating and evanescent waves depending on the value of n.

For $j = 1, 2$ denote by

$$U_j = \{n, \beta_{nj}^2 > 0\}.$$

Then if $n \in U_1$, $\alpha_n^2 < k_1^2$, we have

$$\begin{aligned} \alpha_n = k_1 \sin\theta + n\frac{2\pi}{\Lambda} = k_1 \sin\theta_{n1}, \qquad -\frac{\pi}{2} < \theta_{n1} < \frac{\pi}{2}, \\ \beta_{n1} = k_1 \cos\theta_{n1}, \end{aligned} \tag{7.40}$$

and $R_n e^{\sqrt{-1}\alpha_n x_1 + \sqrt{-1}\beta_{n1} x_2}$ represents a plane wave propagating in the θ_{n1} direction. Similarly, if $n \in U_2$,

$$\begin{aligned} \alpha_n = k_2 \sin\theta + n\frac{2\pi}{\Lambda} = k_2 \sin\theta_{n2}, \quad -\frac{\pi}{2} < \theta_{n2} < \frac{\pi}{2}, \\ \beta_{n2} = k_2 \cos\theta_{n2}, \end{aligned} \tag{7.41}$$

and $T_n e^{\sqrt{-1}\alpha_n x_1 - \sqrt{-1}\beta_{n2} x_2}$ stands for a transmitted plane wave propagating in the θ_{n2} direction.

Equations (7.40) and (7.41) are the grating formulas.

7.1. Variational Formulations

7.1.1. Model Problems: TE and TM Polarizations. Consider a time-harmonic electromagnetic plane wave incident on a slab of some optical material in $\mathbb{R}^3$, which is periodic in the x_1 direction. Throughout, the medium is assumed to be nonmagnetic and invariant in the x_3 direction. We study the diffraction problem in TM (traverse magnetic) polarization, *i.e.*, the magnetic field is transversal to the (x_1, x_2)-plane. The case when the electric field is transversal to the (x_1, x_2)-plane is called TE (transverse electric) polarization. These two polarizations are of primary importance since any other polarization may be decomposed into a simple combination of them. The differential equations derived from time harmonic Maxwell's equations are quite different for the TE and TM cases: In the TE case, $(\Delta + k^2)u = 0$, where E (the electric field vector) $= u(x_1, x_2)e_3$; In the TM case,

$$\nabla \cdot (\frac{1}{k^2}\nabla u) + u = 0,$$

where the magnetic field vector $H(x) = u(x_1, x_2)e_3$. In both cases, $k = \omega\sqrt{\varepsilon\mu_0} = \omega q$, where q is the index of refraction of the medium.

Let us first specify the problem geometry. Let S_1 and S_2 be two simple curves embedded in the strip

$$\Omega = \{(x_1, x_2) \in \mathbb{R}^2 : -b < x_2 < b\},$$

where b is some positive constant. The medium in the region Ω between S_1 and S_2 is inhomogeneous. Above the surface S_1 and below the surface S_2, the media are assumed to be homogeneous. The entire structure is taken to be periodic in the x_1-direction. Without loss of generality, we assume that S_1 and S_2 are periodic of period Λ with respect to $\mathbb{Z}$.

Let $\Omega_1 = \{x = (x_1, x_2) \in \mathbb{R}^2 : x_2 > b\}$, $\Omega_2 = \{x = (x_1, x_2) \in \mathbb{R}^2 : x_2 < -b\}$. Define the boundaries $\Gamma_1 = \{x_2 = b\}$, $\Gamma_2 = \{x_2 = -b\}$. Assume that $S_1 > S_2$ pointwise, *i.e.*, if $(x_1, x_2) \in S_1$ and $(x_1, x_2') \in S_2$, then $x_2 > x_2'$. The curves S_1 and S_2 divide Ω into three connected components. Denote the component which meets Γ_1 by Ω_1^+; the component which meets Γ_2 by Ω_2^+; and let $\Omega_0 = \Omega \setminus \left(\overline{\Omega_1^+} \cup \overline{\Omega_2^+}\right)$.

Suppose that the whole space is filled with material with a periodic dielectric coefficient function ε of period Λ,

$$\varepsilon(x) = \begin{cases} \varepsilon_1 & \text{in } \Omega_1^+ \cup \overline{\Omega}_1, \\ \varepsilon_0(x) & \text{in } \Omega_0, \\ \varepsilon_2 & \text{in } \Omega_2^+ \cup \overline{\Omega}_2, \end{cases}$$

where $\varepsilon_0(x) \in L^\infty$, ε_1 and ε_2 are constants, ε_1 is real and positive, and $\Re\,\varepsilon_2 > 0$, $\Im\,\varepsilon_2 \geq 0$. The case $\Im\,\varepsilon_2 > 0$ accounts for materials which absorb energy (see, for instance, [**?**]). For convenience, we also need the "index of refraction" $q = \sqrt{\varepsilon\mu_0}$

$$q(x) = \begin{cases} q_1 & \text{in } \Omega_1^+ \cup \overline{\Omega}_1, \\ q_0(x) & \text{in } \Omega_0, \\ q_2 & \text{in } \Omega_2^+ \cup \overline{\Omega}_2, \end{cases}$$

where ε is the dielectric constant and μ_0 is the free space magnetic permeability.

We want to solve the Helmholtz equation derived from Maxwell's system of equations

$$\nabla \cdot (\frac{1}{q^2}\nabla u) + \omega^2 u = 0 \quad \text{in } \mathbb{R}^2, \tag{7.42}$$

when an incoming plane wave

$$u^i(x_1, x_2) = e^{\sqrt{-1}\alpha x_1 - \sqrt{-1}\beta x_2}$$

is incident on S from Ω_1, where α and β are given by (7.13) with $-\pi/2 < \theta < \pi/2$ being the angle of incidence.

We are interested in "quasi-periodic" solutions u, that is, solutions $u(x_1, x_2)$ such that $u(x_1, x_2)e^{-\sqrt{-1}\alpha x_1}$ are Λ-periodic. Define $u_\alpha(x_1, x_2) = u(x_1, x_2)e^{-\sqrt{-1}\alpha x_1}$. It is easily seen that if u satisfies (7.42) then u_α satisfies

$$\nabla_\alpha \cdot (\frac{1}{q^2}\nabla_\alpha u_\alpha) + \omega^2 u_\alpha = 0 \qquad \text{in } \mathbb{R}^2, \tag{7.43}$$

where the operator ∇_α is defined by

$$\nabla_\alpha = \nabla + \sqrt{-1}(\alpha, 0).$$

We expand u_α in a Fourier series:

$$u_\alpha(x_1, x_2) = \sum_{n\in\mathbb{Z}} u_\alpha^{(n)}(x_2) e^{\sqrt{-1}\frac{2\pi n}{\Lambda}x_1}, \tag{7.44}$$

where

$$u_\alpha^{(n)}(x_2) = \frac{1}{\Lambda}\int_0^\Lambda u_\alpha(x_1, x_2) e^{-\sqrt{-1}\frac{2\pi n}{\Lambda}x_1} dx_1.$$

Introduce the sets

$$\Gamma_1' = \{x \in \mathbb{R}^2 : x_2 = b_1\}\ ,\ \ \Gamma_2' = \{x_2 = -b_1\},$$

with $0 < b_1 < b$ being such that $\Omega_0 \subseteq \{-b_1 < x_2 < b_1\}$. Let

$$D_1 = \{x \in \mathbb{R}^2 : x_2 > b_1\} \quad \text{and} \quad D_2 = \{x \in \mathbb{R}^2 : x_2 < -b_1\}.$$

Define for $j = 1, 2$ the coefficients

$$\beta_j^n(\alpha) = e^{\sqrt{-1}\gamma_j^n/2}|k_j^2 - \alpha_n^2|^{1/2} = e^{\sqrt{-1}\gamma_j^n/2}|\omega^2 q_j^2 - \alpha_n^2|^{1/2}, \quad n \in \mathbb{Z}, \tag{7.45}$$

α_n is defined by (7.19), $k_j = \omega q_j$, and

$$\gamma_j^n = \arg(k_j^2 - \alpha_n^2),\ \ 0 \le \gamma_j^n < 2\pi. \tag{7.46}$$

We assume that

$$k_j^2 \neq \alpha_n^2 \quad \text{for all } n \in \mathbb{Z}, j = 1, 2. \tag{7.47}$$

This condition excludes "resonance" cases and ensures that a fundamental solution for (7.43) exists inside D_1 and D_2. In particular, for real k_2, we have the following equivalent form of (7.45)

$$\beta_j^n(\alpha) = \begin{cases} \sqrt{k_j^2 - \alpha_n^2}, & k_j^2 > \alpha_n^2, \\ \sqrt{-1}\sqrt{\alpha_n^2 - k_j^2}, & k_j^2 < \alpha_n^2. \end{cases}$$

Notice that if $\Im k_j > 0$, then (7.47) is certainly satisfied.

From the knowledge of the fundamental solution (see, for instance, [**?**] and [**?**]), it follows that inside D_1 and D_2, u_α can be expressed as a sum of plane waves:

$$u_\alpha|_{D_j} = \sum_{n\in\mathbb{Z}} a_j^n e^{\pm\sqrt{-1}\beta_j^n(\alpha)x_2+\sqrt{-1}\frac{2\pi n}{\Lambda}x_1}, \quad j=1,2, \tag{7.48}$$

where the a_j^n are complex scalars.

We next impose a radiation condition on the scattering problem. Since β_j^n is real for at most finitely many n, there are only a finite number of propagating plane waves in the sum (7.48), the remaining waves are exponentially damped (so-called evanescent waves) or radiate (unbounded) as $|x_2| \to \infty$. We will insist that u_α is composed of bounded outgoing plane waves in D_1 and D_2, plus the incident incoming wave u^i in D_1.

From (7.44) and (7.48) we then have the condition that

$$u_\alpha^{(n)}(x_2) = \begin{cases} u_\alpha^{(n)}(b)e^{\sqrt{-1}\beta_1^n(\alpha)(x_2-b)} & \text{in } D_1 \quad \text{for } n\neq 0, \\ u_\alpha^{(0)}(b)e^{\sqrt{-1}\beta(x_2-b)} + e^{-\sqrt{-1}\beta x_2} - e^{\sqrt{-1}\beta(x_2-2b)} & \text{in } D_1 \quad \text{for } n=0, \\ u_\alpha^{(n)}(-b)e^{-\sqrt{-1}\beta_2^n(\alpha)(x_2+b)} & \text{in } D_2. \end{cases} \tag{7.49}$$

From (7.49) we can then calculate the normal derivative of $u_\alpha^n(x_2)$ on Γ_j, $j=1,2$:

$$\left.\frac{\partial u_\alpha^{(n)}}{\partial\nu}\right|_{\Gamma_j} = \begin{cases} \sqrt{-1}\beta_1^n(\alpha)u_\alpha^{(n)}(b) & \text{on } \Gamma_1 \quad \text{for } n\neq 0, \\ \sqrt{-1}\beta u_\alpha^{(0)}(b) - 2\sqrt{-1}\beta e^{-\sqrt{-1}\beta b} & \text{on } \Gamma_1 \quad \text{for } n=0, \\ \sqrt{-1}\beta_2^n(\alpha)u_\alpha^{(n)}(-b) & \text{on } \Gamma_2. \end{cases} \tag{7.50}$$

Thus from (7.48) and (7.50), it follows that

$$\left.\frac{\partial u_\alpha}{\partial\nu}\right|_{\Gamma_1} = \sum_{n\in\mathbb{Z}} \sqrt{-1}\beta_1^n(\alpha)u_\alpha^{(n)}(b)e^{\sqrt{-1}\frac{2\pi n}{\Lambda}x_1} - 2\sqrt{-1}\beta e^{-\sqrt{-1}\beta b}, \tag{7.51}$$

$$\left.\frac{\partial u_\alpha}{\partial\nu}\right|_{\Gamma_2} = \sum_{n\in\mathbb{Z}} \sqrt{-1}\beta_2^n(\alpha)u_\alpha^{(n)}(-b)e^{\sqrt{-1}\frac{2\pi n}{\Lambda}x_1}, \tag{7.52}$$

where the outward normal vector $\nu = (0,1)$ on Γ_1 and $= (0,-1)$ on Γ_2.

In particular, the above discussion yields the following simple result.

LEMMA 7.4. *Suppose that $\alpha_n^2 > k_1^2$. Then*

$$u_\alpha^{(n)}(b) = u_\alpha^{(n)}(b_1)e^{-(b-b_1)\sqrt{\alpha_n^2-k_1^2}}.$$

Similarly, if $\alpha_n^2 > |k_2|^2$, then

$$|u_\alpha^{(n)}(-b)| = |u_\alpha^{(n)}(-b_1)|e^{-(b-b_1)\sin(\gamma_2^n/2)\sqrt[4]{(\alpha_n^2-\Re(k_2^2))^2+(\Im(k_2^2))^2}}.$$

PROOF. The first identity is a simple consequence of (7.49) since k_1^2 is real. Recall that from (7.46),

$$\gamma_2^n = \arg(\Re(k_2^2) - \alpha_n^2 + \sqrt{-1}\Im(k_2^2)).$$

Using (7.49), we have

$$u_\alpha^{(n)}(-b) = u_\alpha^{(n)}(-b_1)e^{-(b-b_1)|\beta_2^n|(\sin(\gamma_2^n/2)-\sqrt{-1}\cos(\gamma_2^n/2))}$$

and hence

$$|u_\alpha^{(n)}(-b)| = |u_\alpha^{(n)}(-b_1)|e^{-(b-b_1)\sin(\gamma_2^n/2)\sqrt[4]{(\alpha_n^2-\Re(k_2^2))^2+(\Im(k_2^2))^2}},$$

which completes the proof. $\square$

REMARK 7.5. Actually, when $\alpha_n^2 \gg |k_2|^2$, the angle $\gamma_2^n/2 \leq \pi/2$ will approach $\pi/2$. Thus, there exists a fixed constant σ_0, such that

$$\delta_0 \leq \sin(\gamma_2^n/2) \leq 1 \;. \tag{7.53}$$

Since the fields u_α are Λ-periodic in x_1, we can move the problem from $\mathbb{R}^2$ to the quotient $\mathbb{R}^2/(\Lambda\mathbb{Z} \times \{0\})$. For what follows, we shall identify Ω with the cylinder $\Omega/(\Lambda\mathbb{Z} \times \{0\})$, and similarly for the boundaries $\Gamma_j \equiv \Gamma_j/\Lambda\mathbb{Z}$. Thus from now on, all functions defined on Ω and Γ_j are implicitly Λ-periodic in the x_1 variable.

For functions $f \in H^{\frac{1}{2}}(\Gamma_j)$ (the Sobolev space of Λ-periodic complex valued functions), define, in the sense of distributions, the operator T_j^α by

$$T_j^\alpha[f](x_1) = \sum_{n\in\mathbb{Z}} \sqrt{-1}\beta_j^n(\alpha) f^{(n)} e^{\sqrt{-1}\frac{2\pi n}{\Lambda}x_1}, \tag{7.54}$$

where

$$f^{(n)} = \frac{1}{\Lambda}\int_0^\Lambda f(x_1) e^{-\sqrt{-1}\frac{2\pi n}{\Lambda}x_1}\, dx_1.$$

It is necessary in our study to understand the continuity properties of the above "Dirichlet-to-Neumann" maps. Fortunately, this is trivial by observing that T_j^α is a standard pseudodifferential operator (a convolution operator) of order one from the definition of $\beta_j^n(\alpha)$. Thus the standard theory on pseudodifferential operators (see, for instance, **[?]**) applies.

LEMMA 7.6. *For $j = 1, 2$, the operator $T_j^\alpha : H^{\frac{1}{2}}(\Gamma_j) \to H^{-\frac{1}{2}}(\Gamma_j)$ is continuous.*

The scattering problem can be formulated as follows: find $u_\alpha \in H^1(\Omega)$ such that

$$\nabla_\alpha \cdot (\frac{1}{q^2}\nabla_\alpha u_\alpha) + \omega^2 u_\alpha = 0 \;\text{ in } \Omega, \tag{7.55}$$

$$T_1^\alpha[u_\alpha] - \frac{\partial u_\alpha}{\partial \nu} = 2\sqrt{-1}\beta e^{-\sqrt{-1}\beta b} \;\text{ on } \Gamma_1, \tag{7.56}$$

$$T_2^\alpha[u_\alpha] - \frac{\partial u_\alpha}{\partial \nu} = 0 \;\text{ on } \Gamma_2. \tag{7.57}$$

An equivalent form of the above system is

$$\nabla_\alpha \cdot (\frac{1}{q^2}\nabla_\alpha \widetilde{u}_\alpha) + \omega^2 \widetilde{u}_\alpha = -f \;\text{ in } \Omega, \tag{7.58}$$

$$T_1^\alpha[\widetilde{u}_\alpha] - \frac{\partial \widetilde{u}_\alpha}{\partial \nu} = 0 \;\text{ on } \Gamma_1, \tag{7.59}$$

$$T_2^\alpha[\widetilde{u}_\alpha] - \frac{\partial \widetilde{u}_\alpha}{\partial \nu} = 0 \;\text{ on } \Gamma_2, \tag{7.60}$$

where $f \in (H^1(\Omega))'$ and $\widetilde{u}_\alpha = u_\alpha - u_0$ with u_0 a fixed smooth function. In fact, u_0 may be constructed in the following way: Let u_0 be a smooth Λ-periodic function supported near the boundary Γ_1. It can be further arranged that $u_0(x_1, b) = 0$ and $-\partial_{x_2} u_0 = 2\sqrt{-1}\beta e^{-\sqrt{-1}\beta b}$ on Γ_1. Clearly, $\widetilde{u}_\alpha = u_\alpha - u_0$ solves the above equation with $f = \nabla_\alpha \cdot (\frac{1}{q^2}\nabla_\alpha u_0) + \omega^2 u_0 \in (H^1(\Omega))'$, the dual space of $H^1(\Omega)$.

For simplicity of notation, we shall denote $\widetilde{u}_\alpha$ by u_α. One can then write down an equivalent variational form: Given $f \in (H^1(\Omega))'$, find $u_\alpha \in H^1(\Omega)$ such that

$$a(u_\alpha, \phi) = (f, \phi)\ , \quad \forall \phi \in H^1(\Omega), \tag{7.61}$$

here the sesquilinear form is defined by

$$\begin{aligned} a(w_1, w_2) &= \int_\Omega \frac{1}{q^2} \nabla w_1 \cdot \nabla \overline{w_2} - \int_\Omega (\omega^2 - \frac{\alpha^2}{q^2}) w_1 \overline{w_2} - \sqrt{-1}\alpha \int_\Omega \frac{1}{q^2} (\partial_{x_1} w_1) \overline{w_2} \\ &\quad + \sqrt{-1}\alpha \int_\Omega \frac{1}{q^2} w_1 \overline{\partial_{x_1} w_2} - \int_{\Gamma_1} \frac{1}{q_1^2} T_1^\alpha [w_1] \overline{w_2} - \int_{\Gamma_2} \frac{1}{q_2^2} T_2^\alpha [w_1] \overline{w_2}, \end{aligned}$$

where $\int_{\Gamma_j}$ represents the dual pairing of $H^{-\frac{1}{2}}(\Gamma_j)$ with $H^{\frac{1}{2}}(\Gamma_j)$.

We first state the existence and uniqueness of the solution to the continuous scattering problem. The proof is from **[?, ?, ?]**.

THEOREM 7.7. *For all but a countable set of frequencies ω_j, $|\omega_j| \to +\infty$, the diffraction problem has a unique solution $u_\alpha \in H^1(\Omega)$.*

For simplicity, from now on, we shall remove the subscript and superscript and denote u_α, T_j^α by u, T_j, respectively. In the proof of Theorem 7.7, we denote $k_1^2 = k_1^2 \omega^2$ to illustrate the explicit dependence on the frequency parameter ω.

PROOF. Write $a(w_1, w_2) = B_1(w_1, w_2) + \omega^2 B_2(w_1, w_2)$ where

$$\begin{aligned} B_1(w_1, w_2) &= \int_\Omega \frac{1}{q^2} \nabla w_1 \cdot \nabla \overline{w_2} + 2 \int_\Omega \frac{\alpha^2}{q^2} w_1 \overline{w_2} - \sqrt{-1}\alpha \int_\Omega \frac{1}{q^2} (\partial_{x_1} w_1) \overline{w_2} \\ &\quad + \sqrt{-1}\alpha \int_\Omega \frac{1}{q^2} w_1 \overline{\partial_{x_1} w_2} - \int_{\Gamma_1} \frac{1}{q_1^2} T_1 [w_1] \overline{w_2} - \int_{\Gamma_2} \frac{1}{q_2^2} T_2 [w_1] \overline{w_2}, \\ B_2(w_1, w_2) &= - \int_\Omega (1 + \frac{\alpha^2}{k^2}) w_1 \overline{w_2}\ . \end{aligned}$$

It follows that

$$B_1(u,u) = \int_\Omega \frac{1}{q^2} |\nabla u|^2 + 2 \int_\Omega \frac{\alpha^2}{q^2} |u|^2 - 2\alpha \int_\Omega \frac{1}{q^2} \Im(u\ \overline{\partial_{x_1} u}) - \int_{\Gamma_1} \frac{1}{q_1^2} T_1[u]\overline{u} - \int_{\Gamma_2} \frac{1}{q_2^2} T_2[u]\overline{u}.$$

Next denote $\frac{1}{q^2} = \frac{1}{\varepsilon \mu_0}$ by $\sigma' - \sqrt{-1}\sigma''$. Clearly, $\sigma' > 0$ and $\sigma'' \geq 0$. Also, denote $\frac{1}{q_2^2}$ by $\sigma_2' - \sqrt{-1}\sigma_2''$, where $\sigma_2' > 0$ and $\sigma_2'' \geq 0$. Thus

$$\begin{aligned} \Re\{B_1(u,u)\} &= \int_\Omega \sigma' |\nabla u|^2 + 2 \int_\Omega \alpha^2 \sigma' |u|^2 - 2\alpha \int_\Omega \sigma' \Im(u\ \overline{\partial_{x_1} u}) \\ &\quad - \Re\{ \int_{\Gamma_1} \frac{1}{q_1^2} T_1[u]\overline{u} + \int_{\Gamma_2} \frac{1}{q_2^2} T_2[u]\overline{u} \} \\ &\geq \int_\Omega \frac{\sigma'}{2} |\nabla u|^2 - \Re\{ \int_{\Gamma_1} \frac{1}{q_1^2} T_1[u]\overline{u} + \int_{\Gamma_2} \frac{1}{q_2^2} T_2[u]\overline{u} \}, \end{aligned}$$

and

$$\begin{aligned}
-\Im\{B_1(u,u)\} &= \int_\Omega \sigma''|\nabla u|^2 + 2\int_\Omega \alpha^2\sigma''|u|^2 - 2\alpha\int_\Omega \sigma''\Im(u\,\overline{\partial_{x_1}u}) \\
&\quad + \Im\{\int_{\Gamma_1}\frac{1}{q_1^2}T_1[u]\overline{u} + \int_{\Gamma_2}\frac{1}{q_2^2}T_2[u]\overline{u}\} \\
&\geq \int_\Omega \frac{\sigma''}{2}|\nabla u|^2 + \Im\{\int_{\Gamma_1}\frac{1}{q_1^2}T_1[u]\overline{u} + \int_{\Gamma_2}\frac{1}{q_2^2}T_2[u]\overline{u}\}.
\end{aligned}$$

Further,

$$\begin{aligned}
-\int_{\Gamma_1}\frac{1}{q_1^2}T_1[u]\overline{u} &= -\sum\frac{1}{q_1^2}\Lambda\sqrt{-1}\beta_1^n|u^{(n)}|^2 \\
&= \sum\frac{1}{q_1^2}\Lambda(\Im\beta_1^n)\,|u^{(n)}|^2 - \sqrt{-1}\sum\frac{1}{n_1^2}\Lambda\Re\beta_1^n|u^{(n)}|^2,
\end{aligned}$$

and it is easy to see that

$$\begin{aligned}
-\int_{\Gamma_2}\frac{1}{q_2^2}T_2[u]\overline{u} &= -\sum\frac{1}{q_2^2}\sqrt{-1}\Lambda\beta_2^n|u^{(n)}(-b)|^2 \\
&= \sum_n \Lambda|\beta_2^n||u^{(n)}(-b)|^2 p_n
\end{aligned}$$

where $p_n = p_n' - \sqrt{-1}p_n''$ with

$$p_n' = -\sigma_2''\cos(\gamma_2^n/2) + \sigma_2'\sin(\gamma_2^n/2)$$

and

$$p_n'' = \sigma_2'\cos(\gamma_2^n/2) + \sigma_2''\sin(\gamma_2^n/2).$$

Recall that

$$\gamma_2^n = \arg(\Re(k_2^2) - \alpha_n^2 + \sqrt{-1}\Im(k_2^2))$$

and $0 \leq \gamma_2^n < 2\pi$. Then it follows that $p_n'' > 0$ for all n and the set $\{n : p_n' < 0\}$ is finite. It is also easy to verify that $|p_n''| > |p_n'|$ for $n \in \{n : p_n' < 0\}$. Moreover, for fixed $\omega \notin \mathcal{B}$ where $\mathcal{B}$ is defined by

$$\mathcal{B} := \{\omega : \beta_j^n(\omega) = 0,\ \ j = 1,2\},$$

we have

$$|\beta_j^n| \geq C(1+|n|^2)^{1/2},\ j = 1,2.$$

Combining the above estimates, we have

$$\begin{aligned}
|B_1(u,u)| &\geq C[\int_\Omega |\nabla u|^2 + ||u||^2_{H^{1/2}(\Gamma_1)} + \sum_{n\in\Lambda}(|p_n''| - |p_n'|)|u^{(n)}(-b)|^2 + \sum_{n\notin\Lambda}|p_n''||u^{(n)}(-b)|^2] \\
&\geq C[\int_\Omega |\nabla u|^2 + ||u||^2_{H^{1/2}(\Gamma_1)} + ||u||^2_{H^{1/2}(\Gamma_2)}] \\
&\geq C||u||^2_{H^1(\Omega)},
\end{aligned}$$

where the last inequality may be obtained by applying some standard elliptic estimates; see **[?]**. Therefore, we have shown that

$$|B_1(u,u)| \geq C\|u\|^2_{H^1(\Omega)}, \tag{7.62}$$

i.e., B_1 is a bounded coercive sesquilinear form over $H^1(\Omega)$. The Lax-Milgram lemma then gives the existence of a bounded invertible map $A_1 = A_1(\omega) : H^1(\Omega) \to$

$(H^1(\Omega))'$ such that $\langle A_1 u, v\rangle = B_1(u,v)$, where $'$ represents the dual space. Moreover, A_1^{-1} is bounded. Notice that the operator $A_2 : H^1(\Omega) \to (H^1(\Omega))'$ defined by $\langle A_2 u, v\rangle = B_2(u,v)$ is compact and independent of ω.

Holding $\omega_0 \notin \mathcal{B}$ fixed, consider the operator $A(\omega_0,\omega) = A_1(\omega_0) + \omega^2 A_2$. Since A_1 is bounded invertible and A_2 is compact, we see that $A(\omega_0,\omega)^{-1}$ exists by Fredholm theory for all $\omega \notin \mathcal{E}(\omega_0)$, where $\mathcal{E}(\omega_0)$ is some discrete set. It is clear that

$$\|A_1(\omega) - A_1(\omega_0)\| \to 0, \quad \text{as } \omega \to \omega_0.$$

Thus, since $\|A(\omega,\omega) - A(\omega_0,\omega)\| = \|A_1(\omega) - A_1(\omega_0)\|$ is small for $|\omega-\omega_0|$sufficiently small, it follows from the stability of bounded invertibility (see, for instance, Kato [**?**, Chapter 4]) that $A(\omega,\omega)^{-1}$ exists and is bounded for $|\omega-\omega_0|$ sufficiently small, $\omega \notin \mathcal{E}(\omega_0)$. Since $\omega_0 > 0$ can be an arbitrary real number, we have shown that $A(\omega,\omega)^{-1}$ exists for all but a discrete set of points. □

7.1.2. Biperiodic Structures. Consider a time-harmonic electromagnetic plane wave incident on a biperiodic structure in $\mathbb{R}^3$. The periodic structure separates two homogeneous regions. The medium inside the structure is heterogeneous. The diffraction problem is then to predict energy distributions of the reflected and transmitted waves. In this chapter, we study some mathematical aspects of the diffraction problem. We introduce a variational formulation of the diffraction problem by dielectric gratings. Our main result is concerned with the well-posedness of the model problem. It is shown that for all but possibly a discrete set of frequencies, there is a unique quasi-periodic weak solution to the diffraction problem. Our proof is based on the Hodge decomposition and a compact embedding result. An energy conservation for the weak solution is also proved. An important step of our approach is to reduce the original diffraction problem with an infinite configuration to another problem with a bounded domain. This is done by introducing a pair of transparent boundary conditions. We emphasize that the variational approach is very general. In particular, the material coefficients ε and μ are only assumed to be bounded functions. The geometry can be extremely general as well. The incident angles and grating shapes may be arbitrary. Moreover, a class of finite element methods can be formulated based on the variational approach.

7.1.3. Diffraction Problem. We first specify the geometry of the problem. Let Λ_1 and Λ_2 be two positive constants, such that the material functions ε and μ satisfy, for any $n_1, n_2 \in \mathbb{Z}$,

$$\begin{aligned} \varepsilon(x_1 + n_1\Lambda_1, x_2 + n_2\Lambda_2, x_3) &= \varepsilon(x_1,x_2,x_3), \\ \mu(x_1 + n_1\Lambda_1, x_2 + n_2\Lambda_2, x_3) &= \mu(x_1,x_2,x_3)\,. \end{aligned}$$

In addition, it is assumed that, for some fixed positive constant b and sufficiently small $\delta > 0$,

$$\begin{aligned} \varepsilon(x) &= \varepsilon_1\,,\ \ \mu(x) = \mu_1 \ \text{ for } x_3 > b-\delta, \\ \varepsilon(x) &= \varepsilon_2\,,\ \ \mu(x) = \mu_2 \ \text{ for } x_3 < -b+\delta, \end{aligned}$$

where ε_1, ε_2, μ_1, and μ_2 are positive constants. All of these assumptions are physical.

We make the following general assumptions: $\varepsilon(x)$, $\mu(x)$, and $\beta(x)$ are all real valued L^∞ functions, $\varepsilon(x) \geq \varepsilon_0$ and $\mu(x) \geq \mu_0$, where ε_0 and μ_0 are positive constants.

Let $\Omega = \{x \in \mathbb{R}^3 : -b < x_3 < b\}$, $\Omega_1 = \{x \in \mathbb{R}^3 : x_3 > b\}$, $\Omega_2 = \{x \in \mathbb{R}^3 : x_3 < -b\}$.

Consider a plane wave in Ω_1

$$E^i = se^{q\cdot x}\ ,\ H^i = pe^{\sqrt{-1}q\cdot x}\ , \tag{7.63}$$

incident on Ω. Here $q = (\alpha_1, \alpha_2, -\beta) = \omega\sqrt{\varepsilon_1\mu_1}(\cos\theta_1\cos\theta_2, \cos\theta_1\sin\theta_2, -\sin\theta_1)$ is the incident wave vector whose direction is specified by θ_1 and θ_2, with $0 < \theta_1 < \pi$ and $0 < \theta_2 \leq 2\pi$. The vectors s and p satisfy

$$s = \frac{1}{\omega\varepsilon_1}(p \times q)\ ,\ q\cdot q = \omega^2\varepsilon_1\mu_1\ ,\quad p\cdot q = 0. \tag{7.64}$$

We are interested in biperiodic solutions, *i. e.*, solutions E and H such that the fields E_α, H_α defined by, for $\alpha = (\alpha_1, \alpha_2, 0)$,

$$E_\alpha = e^{-\sqrt{-1}\alpha\cdot x}E(x_1, x_2, x_3), \tag{7.65}$$

$$H_\alpha = e^{-\sqrt{-1}\alpha\cdot x}H(x_1, x_2, x_3), \tag{7.66}$$

are periodic in the x_1-direction of period Λ_1 and in the x_2-direction of period Λ_2.

Denote

$$\nabla_\alpha = \nabla + \sqrt{-1}\alpha = \nabla + \sqrt{-1}(\alpha_1, \alpha_2, 0)\ .$$

It is easy to see from (7.3) and (7.4) that E_α and H_α satisfy

$$\nabla_\alpha \times \Big(\frac{1}{\mu}\nabla_\alpha \times E_\alpha\Big) - \omega^2\varepsilon E_\alpha = 0, \tag{7.67}$$

$$\nabla_\alpha\ \times\ E_\alpha = \sqrt{-1}\omega\mu(x)\,H_\alpha. \tag{7.68}$$

In order to solve the system of differential equations, we need boundary conditions in the x_3 direction. These conditions may be derived by the radiation condition, the periodicity of the structure, and the Green functions. To do so, we can expand E_α in a Fourier series since it is Λ periodic:

$$E_\alpha(x) = E^i_\alpha(x) + \sum_{n\in\mathbb{Z}} U^{(n)}_\alpha(x_3)e^{\sqrt{-1}(\frac{2\pi n_1}{\Lambda_1}x_1 + \frac{2\pi n_2}{\Lambda_2}x_2)}, \tag{7.69}$$

where $E^i_\alpha(x) = E^i(x)e^{-\sqrt{-1}\alpha\cdot x}$ and

$$U^{(n)}_\alpha(x_3) = \frac{1}{\Lambda_1\Lambda_2}\int_0^{\Lambda_1}\int_0^{\Lambda_2}(E_\alpha(x) - E^i_\alpha(x))e^{-\sqrt{-1}(\frac{2\pi n_1}{\Lambda_1}x_1 + \frac{2\pi n_2}{\Lambda_2}x_2)}dx_1dx_2.$$

Denote

$$\Gamma_1 = \{x \in \mathbb{R}^3 : x_3 = b\} \text{ and } \Gamma_2 = \{x_3 = -b\}.$$

Define for $j = 1, 2$ the coefficients

$$\beta^{(n)}_j(\alpha) = \begin{cases} \sqrt{\omega^2\varepsilon_j\mu_j - |\alpha_n|^2}, & \omega^2\varepsilon_j\mu_j > |\alpha_n|^2\ , \\ \sqrt{-1}\sqrt{|\alpha_n|^2 - \omega^2\varepsilon_j\mu_j}, & \omega^2\varepsilon_j\mu_j < |\alpha_n|^2, \end{cases} \tag{7.70}$$

where

$$\alpha_n = \alpha + (2\pi n_1/\Lambda_1, 2\pi n_2/\Lambda_2, 0).$$

We assume that $\omega^2\varepsilon_j \neq |\alpha_n|^2$ for all $n \in \mathbb{Z}^2$, $j = 1, 2$. This condition excludes "resonances".

For convenience, we also introduce the following notation:

$$\Lambda_j^+ = \{n \in \mathbb{Z}^2 : \ \Im(\beta_j^{(n)}) = 0\},$$
$$\Lambda_j^- = \{n \in \mathbb{Z}^2 : \ \Im(\beta_j^{(n)}) \neq 0\}.$$

Observe that inside Ω_j ($j = 1, 2$), $\varepsilon = \varepsilon_j$ and $\mu = \mu_j$, Maxwell's equations then become

$$(\Delta_\alpha + \omega^2 \varepsilon_j \mu_j) E_\alpha = 0 \ , \tag{7.71}$$

where $\Delta_\alpha = \Delta + 2\sqrt{-1}\alpha \cdot \nabla - |\alpha|^2$.

Since the medium in Ω_j ($j = 1, 2$) is homogeneous, the method of separation of variables implies that E_α can be expressed as a sum of plane waves:

$$E_\alpha|_{D_j} = E_\alpha^i(x) + \sum_{n\in\mathbb{Z}} A_j^{(n)} e^{\pm\sqrt{-1}\beta_j^{(n)} x_3 + \sqrt{-1}(\frac{2\pi n_1}{\Lambda_1} x_1 + \frac{2\pi n_2}{\Lambda_2} x_2)}, \quad j = 1, 2, \tag{7.72}$$

where the $A_j^{(n)}$ are constant (complex) vectors, where $E_\alpha^i(x) = 0$ in Ω_2.

We next impose a radiation condition on the scattering problem. Due to the (infinite) periodic structure, the usual Sommerfeld or Silver-Müller radiation condition is no longer valid. Instead, the following radiation condition based on the diffraction theory is employed: Since β_j^n is real for at most finitely many n, there are only a finite number of propagating plane waves in the sum (7.72), the remaining waves are exponentially decaying (or unbounded) as $|x_3| \to \infty$. We will insist that E_α is composed of bounded outgoing plane waves in Ω_1 and Ω_2, plus the incident (incoming) wave in Ω_1.

From (7.69) and (7.70) we deduce

$$E_\alpha^{(n)}(x_3) = \begin{cases} U_\alpha^{(n)}(b) e^{\sqrt{-1}\beta_1^{(n)}(x_3 - b)} & \text{in } \Omega_1, \\ U_\alpha^{(n)}(-b) e^{-\sqrt{-1}\beta_2^{(n)}(x_3 + b)} & \text{in } \Omega_2. \end{cases} \tag{7.73}$$

By matching the two expansions (7.69) and (7.72), we get

$$A_1^{(n)} = U_\alpha^{(n)}(b) e^{-\sqrt{-1}\beta_1^{(n)} b} \ \text{ on } \Gamma_1, \tag{7.74}$$
$$A_2^{(n)} = U_\alpha^{(n)}(-b) e^{-\sqrt{-1}\beta_2^{(n)} b} \ \text{ on } \Gamma_2. \tag{7.75}$$

Furthermore, since in the regions $\{x : \ x_3 > b - \delta\} \cup \{x : \ x_3 < -b + \delta\}$,

$$\nabla \cdot E = 0 \ , \ \ \nabla \cdot E^i = 0$$

or

$$\nabla_\alpha \cdot E_\alpha = 0 \ , \ \ \nabla_\alpha \cdot E_\alpha^i = 0,$$

we have from (7.72) that

$$\alpha_n \cdot U_\alpha^{(n)}(b) + \beta_1^{(n)} U_{\alpha,3}^{(n)}(b) = 0 \ \text{ on } \Gamma_1, \tag{7.76}$$
$$\alpha_n \cdot U_\alpha^{(n)}(-b) - \beta_2^{(n)} U_{\alpha,3}^{(n)}(-b) = 0 \ \text{ on } \Gamma_2. \tag{7.77}$$

LEMMA 7.8. *There exist boundary pseudo-differential operators B_j ($j = 1, 2$) of order one, such that*

$$\nu \times (\nabla_\alpha \times (E_\alpha - E_\alpha^i)) = B_1 P[E_\alpha - E_\alpha^i] \ \text{ on } \Gamma_1, \tag{7.78}$$
$$\nu \times (\nabla_\alpha \times E_\alpha) = B_2 P[E_\alpha] \ \text{ on } \Gamma_2, \tag{7.79}$$

where the operator B_j is defined by
(7.80)
$$B_j[f] = -\sqrt{-1}\sum_{n\in\mathbb{Z}^2}\frac{1}{\beta_j^{(n)}}\{(\beta_j^{(n)})^2(f_1^{(n)}, f_2^{(n)}, 0) + (\alpha_n\cdot f^{(n)})\alpha_n\}e^{\sqrt{-1}(\frac{2\pi n_1}{\Lambda_1}x_1+\frac{2\pi n_2}{\Lambda_2}x_2)},$$
where P is the projection onto the plane orthogonal to ν, i.e.,
$$P[f] = -\nu\times(\nu\times f),$$
and
$$f^{(n)} = \Lambda_1^{-1}\Lambda_2^{-1}\int_0^{\Lambda_1}\int_0^{\Lambda_2} f(x)e^{-\sqrt{-1}(\frac{2\pi n_1}{\Lambda_1}x_1+\frac{2\pi n_2}{\Lambda_2}x_2)}dx_1dx_2.$$
Here ν is the outward normal to Ω.

The proof may be given by using the expansion (7.72) together with (7.74–7.77), and some simple calculation.

REMARK 7.9. The Dirichlet to Neumann operator B carries the information on radiation condition in an explicit form. Here it is crucial to assume that $\beta^{(n)}$ is nonzero.

We introduce the L^2 scalar product
$$(f, g) = \int_A f\overline{g},$$
where A is the domain.

Denote by B_j^* the adjoint of B_j, that is,
$$\left(B_j[f], g\right) = \left(f, B_j^*[g]\right),$$
for any f and g in $L^2(\Gamma_j)$.

It is easily seen that the adjoint operator of B_j in the above lemma is given by
(7.81)
$$B_j^*[f] = \sqrt{-1}\sum_{n\in\mathbb{Z}^2}\frac{1}{\overline{\beta}_j^{(n)}}\{(\overline{\beta}_j^{(n)})^2(f_1^{(n)}, f_2^{(n)}, 0) + (\alpha_n\cdot f^{(n)})\alpha_n\}e^{\sqrt{-1}(\frac{2\pi n_1}{\Lambda_1}x_1+\frac{2\pi n_2}{\Lambda_2}x_2)}.$$

Define
$$\Lambda = \Lambda_1\mathbb{Z}\times\Lambda_2\mathbb{Z}\times\{0\}\subset\mathbb{R}^3.$$
Since the fields E_α are Λ-periodic, we can move the problem from $\mathbb{R}^3$ to the quotient space $\mathbb{R}^3/\Lambda$. For the remainder of the section, we shall identify Ω with the cube Ω/Λ, and similarly for the boundaries $\Gamma_j\equiv\Gamma_j/\Lambda$. Thus from now on,

all functions defined on Ω and Γ_j are implicitly Λ-periodic.

Define $\nabla_\alpha\cdot$ by $\nabla_\alpha\cdot u = (\partial_{x_1}+\sqrt{-1}\alpha_1)u_1 + (\partial_{x_2}+\sqrt{-1}\alpha_2)u_2$.

Let H^m be the mth order L^2-based Sobolev spaces of complex valued functions. We denote by $H_p^m(\Omega)$ the subset of all functions in $H^m(\Omega)$ which are the restrictions to Ω of the functions in $H^m_{\text{loc}}(\mathbb{R}^2\times(-b,b))$ that are Λ-periodic. Similarly we define $H_p^m(\Omega_j)$ and $H_p^m(\Gamma_j)$. In the future, for simplicity, we shall drop the subscript p. We shall also drop the subscript α from E_α, E_α^i, ∇_α, and $\nabla_\alpha\cdot$.

Therefore, the diffraction problem can be reformulated as follows:

$$
\left\{
\begin{array}{l}
\nabla \times (\frac{1}{\mu}\nabla \times E) - \omega^2 \varepsilon E = 0 \text{ in } \Omega, \\
\nu \times (\nabla \times E) = B_1 P[E] - f \text{ on } \Gamma_1, \\
\nu \times (\nabla \times E) = B_2 P[E] \text{ on } \Gamma_2,
\end{array}
\right.
\tag{7.82}
$$

where

$$
f = \frac{1}{\mu_1}(B_1 P[E^i]|_{\Gamma_1} - \nu \times (\nabla \times E^i)|_{\Gamma_1}).
\tag{7.83}
$$

The weak form of the above boundary value problem is to find $E \in H(\mathrm{curl}, \Omega)$, such that for any $F \in H(\mathrm{curl}, \Omega)$

$$
\begin{aligned}
&\int_\Omega \frac{1}{\mu} \nabla \times E \cdot \overline{\nabla \times F} \\
&\quad - \int_\Omega \omega^2 \varepsilon E \cdot \overline{F} + \int_{\Gamma_1} \frac{1}{\mu_1} B_1 P[E] \cdot \overline{F} + \int_{\Gamma_2} \frac{1}{\mu_2} B_2 P[E] \cdot \overline{F} = \int_{\Gamma_1} f \cdot \overline{F}.
\end{aligned}
\tag{7.84}
$$

7.1.4. The Hodge Decomposition and a Compactness Result. We present a version of the Hodge decomposition and compactness lemma. The results are crucial in the proof of our theorem on existence and uniqueness. We also state a useful trace regularity estimate. We remark that for simplicity, no attempt is made to give the most general forms of these results.

Let us begin with a simple property of the operator B_j. From now on, we define $\nabla_{\Gamma_j} \cdot$ as the surface divergence on Γ_j.

PROPOSITION 7.10. *For $j = 1, 2$ and $q \in H^1(\Omega)$*

$$
-\Re \int_{\Gamma_j} B_j P[\nabla q] \cdot \overline{\nabla q} \geq 0 \, .
$$

PROOF. Using the definitions of the operator B_j in (7.80) and $\beta_j^{(n)}$ in (7.70), we have by integration by parts on the surface

$$
\begin{aligned}
-\Re \int_{\Gamma_j} B_j P[\nabla q] \cdot \overline{\nabla q} &= \Re \int_{\Gamma_j} \nabla_\Gamma \cdot B_j P[\nabla q] \cdot \overline{q} \\
&= \Re \sum_{n \in \mathbb{Z}^2} \left\{ \sqrt{-1} \beta_j^{(n)} |\alpha_n|^2 |q^{(n)}|^2 + \frac{\sqrt{-1}}{\beta_j^{(n)}} |\alpha_n|^2 |q^{(n)}|^2 \right\} \\
&= \sum_{n \in \Lambda_j^-} \frac{(-|\beta_j^{(n)}|^2 + |\alpha_n|^2)}{|\beta_j^{(n)}|} |\alpha_n|^2 |q^{(n)}|^2 \\
&= \sum_{n \in \Lambda_j^-} \varepsilon_j \mu_j \omega^2 \frac{|\alpha_n|^2}{|\beta_j^{(n)}|} |q^{(n)}|^2 \geq 0.
\end{aligned}
$$

Recall that ∇, $\nabla \cdot$, are the shorthand notations of $\nabla + \sqrt{-1}\alpha$, $\nabla_\alpha \cdot$, respectively. $\square$

LEMMA 7.11. *For any function $f \in (H^1(\Omega))'$ which is smooth near Γ_1 and Γ_2, the boundary value problem*

$$\left\{\begin{array}{lcl} \nabla\cdot(\varepsilon\nabla p) & = & f \text{ in } \Omega, \\ \varepsilon_1 \frac{\partial p}{\partial \nu} & = & -\frac{1}{\mu_1}\nabla_\Gamma \cdot B_1 P[\nabla p] \text{ on } \Gamma_1, \\ \varepsilon_2 \frac{\partial p}{\partial \nu} & = & -\frac{1}{\mu_2}\nabla_\Gamma \cdot B_2 P[\nabla p] \text{ on } \Gamma_2, \end{array}\right. \tag{7.1}$$

has a unique solution in $H_0^1(\Omega) = \{q : \ q \in H^1(\Omega), \ \int_\Omega q = 0\}$.

PROOF. We examine the weak form of the boundary value problem (7.1). For any $q \in H_0^1(\Omega)$, multiplying both sides of (7.1) by $\overline{q}$ and integrating over Ω yield

$$\int_\Omega \nabla\cdot(\varepsilon\nabla p)\cdot\overline{q} = \int_\Omega f\cdot\overline{q}.$$

After using the boundary conditions integration by parts gives that

$$\int_\Omega \varepsilon\nabla p\cdot\overline{\nabla q} + \int_{\Gamma_1}\frac{1}{\mu_1}\nabla_\Gamma\cdot B_1 P[\nabla p]\cdot\overline{q} + \int_{\Gamma_2}\frac{1}{\mu_2}\nabla_\Gamma\cdot B_2 P[\nabla p]\cdot\overline{q} = -\int_\Omega f\cdot\overline{q}\,. \tag{7.2}$$

Denote the left hand side of (7.2) by $b(p,q)$. Keeping in mind that p and q are periodic, from integration by parts on the boundary, we obtain

$$b(p,q) = \int_\Omega \varepsilon\nabla p\cdot\overline{\nabla q} - \int_{\Gamma_1}\frac{1}{\mu_1}B_1 P[\nabla p]\cdot\overline{P[\nabla q]} - \int_{\Gamma_2}\frac{1}{\mu_2}B_2 P[\nabla p]\cdot\overline{P[\nabla q]}.$$

The variational problem takes the form: to find $p \in H_0^1(\Omega)$, such that

$$b(p,q) = -\int_\Omega f\cdot\overline{q}, \ \ \forall q \in H_0^1(\Omega).$$

It is now obvious from Proposition 7.10 that

$$\begin{aligned} \Re\, b(p,p) &= \int_\Omega \varepsilon|\nabla p|^2 - \Re\Big\{\int_{\Gamma_1}\frac{1}{\mu_1}B_1 P[\nabla p]\cdot\overline{P[\nabla p]} + \int_{\Gamma_2}\frac{1}{\mu_2}B_2 P[\nabla p]\cdot\overline{P[\nabla p]}\Big\} \\ &\geq C||\nabla p||^2_{L^2(\Omega)}. \end{aligned}$$

Therefore by a version of Poincaré's inequality ($\int_\Omega p = 0$), we obtain

$$\Re\, b(p,p) \geq C||p||^2_{H^1(\Omega)}.$$

The proof is complete by a direct application of the Lax-Milgram lemma. □

Next, we present an embedding result. Let $W(\Omega)$ be a functional space defined by

$$\Big\{u : \ \ u \in H(\text{curl},\Omega), \ \ \nabla\cdot(\varepsilon u) = 0 \text{ in } \Omega, \text{ and} \tag{7.3}$$

$$\omega^2\varepsilon_j u\cdot\nu = -\frac{1}{\mu_j}\nabla_\Gamma\cdot B_j P[u] \text{ on } \Gamma_j\,, \ \ j = 1,2\Big\}. \tag{7.4}$$

LEMMA 7.12. *The embedding from $W(\Omega)$ to $L^2(\Omega)$ is compact.*

PROOF. Let u be a function in $W(\Omega)$. Define an extension of u by

$$\tilde{u} = \left\{\begin{array}{l} u_1 \text{ in } \Omega_1, \\ u \text{ in } \Omega, \\ u_2 \text{ in } \Omega_2, \end{array}\right.$$

where u_j $(j = 1, 2)$ satisfies

$$\begin{aligned}
&\nabla \times \nabla \times u_j - \omega^2 \varepsilon_j \mu_j u_j = 0 \text{ in } \Omega_j \ , \\
&u_j \times \nu = u \times \nu \text{ on } \Gamma_j, \\
&\text{the radiation condition at the infinity.}
\end{aligned}$$

Since the medium in Ω_j is homogeneous, it may be shown that

$$\omega^2 \varepsilon_j u_j \cdot \nu = -\frac{1}{\mu_j} \nabla_\Gamma \cdot B_j P[u] \text{ on } \Gamma_j \ , \quad j = 1, 2. \tag{7.5}$$

In the following, we outline the proof of (7.5). In fact, it is easy to see that the function u_j satisfies the boundary condition

$$\nu \times \nabla \times u_j = B_j P[u_j].$$

Hence

$$\nabla_\Gamma \cdot (\nu \times \nabla \times u_j) = \nabla_\Gamma \cdot (B_j P[u_j]). \tag{7.6}$$

But

$$\nabla_\Gamma \cdot (\nu \times \nabla \times u_j) = -(\nabla \times \nabla \times u_j) \cdot \nu,$$

which together with the Maxwell equation for u_j yield that

$$-\omega^2 \varepsilon_j \mu_j u_j \cdot \nu = \nabla_\Gamma \cdot B_j P[u_j]. \tag{7.7}$$

From (7.6), (7.7), the boundary identity (7.5) follows.

Therefore from $[\tilde{u} \times \nu] = 0$, it follows that $[\tilde{u} \cdot \nu] = 0$ on Γ_j and then

$$\nabla \cdot (\varepsilon \tilde{u}) = 0 \text{ in } \overline{\Omega} \cup \Omega_1 \cup \Omega_2.$$

It follows from $[\tilde{u} \times \nu] = 0$ on Γ_j and the radiation condition that $\tilde{u} \in H(\text{curl}, D)$ for any bounded domain $D \subset \overline{\Omega} \cup \Omega_1 \cup \Omega_2$.

Now let $\{\tilde{u}_j\}$ be a sequence of functions in W that converges weakly to zero in $W(\Omega)$. Construct a cutoff function χ with the properties: χ is supported in $\tilde{\Omega} \Supset \Omega$ and $\chi = 1$ in Ω. Here $\tilde{\Omega} = \{-b' \le x_3 \le b', \ \ 0 < x_1 < \Lambda_1, \ \ 0 < x_2 < \Lambda_2\}$ with $b' > b$.

Hence

$$\{\chi \tilde{u}_j\} \subset \tilde{W} = \Big\{ v : \ v \in H(\text{curl}, \tilde{\Omega}), \ \ \nabla \cdot (\varepsilon v) = 0, \ \ \nu \times v = 0 \text{ on } x_3 = b', -b' \Big\}.$$

It follows from a well known result of Weber **[?]** that the embedding from $\tilde{W}(\tilde{\Omega})$ to $L^2(\tilde{\Omega})$ is compact. Therefore the sequence $\{\tilde{u}_j\}$ converges strongly to zero in $L^2(\Omega)$, which completes the proof. □

We now state a useful trace regularity result.

PROPOSITION 7.13. *Let D be a bounded domain. For any $\eta > 0$, there is a constant $C(\eta)$ such that the following estimate*

$$||\nu \times u||_{H^{-1/2}(\partial D)} \le \eta ||\nabla \times u||_{L^2(D)} + C(\eta) ||u||_{L^2(D)}$$

holds.

PROOF. The proof is straightforward. For the sake of completeness, we sketch it here.

For any function $\phi \in H^{1/2}(\partial D)$, consider an auxiliary problem

$$\begin{cases} \nabla \times \nabla \times w + \frac{1}{\eta^2} w &= 0 \text{ in } D, \\ -\nu \times (\nu \times w) &= \phi \text{ on } \partial D. \end{cases}$$

The result of the proposition follows immediately from estimating $|(\nu \times, \phi)|$. $\square$

7.1.5. Existence and Uniqueness of a Solution. In this section, we investigate questions on existence and uniqueness for the model problem. Our main result is as follows.

THEOREM 7.14. *For all but possibly a countable set of frequencies ω_j, $\omega_j \to +\infty$, the variational problem (7.84) admits a unique weak solution E in $H(\mathrm{curl}, \Omega)$.*

PROOF. The proof is based on the Lax-Milgram lemma. We first decompose the field E into two parts

$$E = u + \nabla p, \quad u \in H(\mathrm{curl}, \Omega), \quad p \in H^1(\Omega).$$

By choosing $E = u + \nabla p$, $F = v$ in (7.84), we arrive at

$$\begin{aligned} &\int_\Omega \frac{1}{\mu} \nabla \times u \cdot \overline{\nabla \times v} \\ &-\omega^2 \int_\Omega \varepsilon u \cdot \overline{v} + \int_{\Gamma_1} \frac{1}{\mu_1} B_1 P[u] \cdot \overline{v} + \int_{\Gamma_2} \frac{1}{\mu_2} B_2 P[u] \cdot \overline{v} \\ &-\omega^2 \int_\Omega \varepsilon \nabla p \cdot \overline{v} + \int_{\Gamma_1} \frac{1}{\mu_1} B_1 P[\nabla p] \cdot \overline{v} + \int_{\Gamma_2} \frac{1}{\mu_2} B_2 P[\nabla p] \cdot \overline{v} = \int_{\Gamma_1} f \cdot \overline{v}. \end{aligned} \tag{7.1}$$

Similarly by choosing $E = u + \nabla p$, $F = \nabla q$ in (7.84), we get

$$\begin{aligned} &-\omega^2 \int_\Omega \varepsilon u \cdot \overline{\nabla q} + \int_{\Gamma_1} \frac{1}{\mu_1} B_1 P[u] \cdot \overline{\nabla q} + \int_{\Gamma_2} \frac{1}{\mu_2} B_2 P[u] \cdot \overline{\nabla q} \\ &-\omega^2 \int_\Omega \varepsilon \nabla p \cdot \overline{\nabla q} + \int_{\Gamma_1} \frac{1}{\mu_1} B_1 P[\nabla p] \cdot \overline{\nabla q} + \int_{\Gamma_2} \frac{1}{\mu_2} B_2 P[\nabla p] \cdot \overline{\nabla q} = \int_{\Gamma_1} f \cdot \overline{\nabla q}. \end{aligned} \tag{7.2}$$

We use the following Hodge decomposition:

$$E = u + \nabla p,$$

where $p \in H^1(\Omega)$ and $u \in W(\Omega)$. The functional space W consists of all functions $U \in H(\mathrm{curl}, \Omega)$ that satisfy

$$\begin{cases} \nabla \cdot (\varepsilon u) &= 0 \text{ in } \Omega, \\ \omega^2 \varepsilon_1 u \cdot \nu &= -\frac{1}{\mu_1} \nabla_\Gamma \cdot B_1 P[u] \text{ on } \Gamma_1, \\ \omega^2 \varepsilon_2 u \cdot \nu &= -\frac{1}{\mu_2} \nabla_\Gamma \cdot B_2 P[u] \text{ on } \Gamma_2. \end{cases} \tag{7.3}$$

The fact that this decomposition is valid follows from Lemma 7.11. Actually, it is obvious to see that for any given E, Lemma 7.11 implies that there is a function p, such that $\nabla \cdot (\varepsilon \nabla p) = \nabla \cdot (\varepsilon E)$ and the suitable boundary conditions. Therefore, $u = E - \nabla p$ solves the problem (7.3).

Moreover, according to Lemma 7.12, the embedding from $W(\Omega)$ to $L^2(\Omega)$ is compact. We point out that the embedding from $H(\mathrm{curl}, \Omega)$ to $L^2(\Omega)$ is not compact.

Denote the left hand sides of (7.1), (7.2) by $a_1(u,v)$, $a_2(p,q)$, respectively.

After some simple calculation, we obtain for $u, v \in W$, $p, q \in H^1$ that

$$
\begin{aligned}
a_1(u,v) \quad = \quad & \textstyle\int_\Omega \frac{1}{\mu} \nabla \times u \cdot \overline{\nabla \times v} \\
& -\omega^2 \textstyle\int_\Omega \varepsilon u \cdot \overline{v} + \frac{1}{\mu_1} \int_{\Gamma_1} B_1 P[u] \cdot \overline{v} + \frac{1}{\mu_2} \int_{\Gamma_2} B_2 P[u] \cdot \overline{v} \\
& - \textstyle\int_{\Gamma_1} \frac{1}{\mu_1} p \ \nabla_\Gamma \cdot (\overline{(B_1^* - B_1) P[v]} \\
& - \textstyle\int_{\Gamma_2} \frac{1}{\mu_2} p \ \nabla_\Gamma \cdot (\overline{(B_2^* - B_2) P[v]})
\end{aligned}
\tag{7.4}
$$

and

$$
\begin{aligned}
a_2(p,q) \quad = \quad & -\omega^2 \textstyle\int_\Omega \varepsilon \nabla p \cdot \overline{\nabla q} \\
& + \frac{1}{\mu_1} \textstyle\int_{\Gamma_1} B_1 P[\nabla p] \cdot \overline{\nabla q} + \int_{\Gamma_2} \frac{1}{\mu_2} B_2 P[\nabla p] \cdot \overline{\nabla q}.
\end{aligned}
\tag{7.5}
$$

By taking $v = u$, $q = p$, we deduce from (7.4), (7.5) that

$$
\begin{aligned}
& a_1(u,u) - a_2(p,p) = \textstyle\int_\Omega d |\nabla \times u|^2 \\
& -\omega^2 \textstyle\int_\Omega \varepsilon |u|^2 + \frac{1}{\mu_1} \int_{\Gamma_1} B_1 P[u] \overline{u} + \frac{1}{\mu_2} \int_{\Gamma_2} B_2 P[u] \cdot \overline{u} \\
& - \textstyle\int_{\Gamma_1} \frac{1}{\mu_1} p \ \nabla_\Gamma \cdot (\overline{(B_1^* - B_1) P[v]}) - \int_{\Gamma_2} \frac{1}{\mu_2} p \ \nabla_\Gamma \cdot (\overline{(B_2^* - B_2) P[v]}) \\
& + \omega^2 \textstyle\int_\Omega \varepsilon |\nabla p|^2 \\
& - \frac{1}{\mu_1} \textstyle\int_{\Gamma_1} B_1 P[\nabla p] \cdot \overline{\nabla p} - \int_{\Gamma_2} \frac{1}{\mu_2} B_2 P[\nabla p] \cdot \overline{\nabla p} = \int_{\Gamma_1} f \cdot (\overline{u - \nabla p}).
\end{aligned}
\tag{7.6}
$$

Thus, we have

$$
\begin{aligned}
& \Re \Big\{ a_1(u,u) - a_2(p,p) \Big\} \geq d_0 ||\nabla \times u||^2_{L^2(\Omega)} + \nabla \times u \cdot \overline{u}) \\
& -\omega^2 \textstyle\int_\Omega \varepsilon |u|^2 + \Re \Big\{ \frac{1}{\mu_1} \int_{\Gamma_1} B_1 P[u] \overline{u} + \frac{1}{\mu_2} \int_{\Gamma_2} B_2 P[u] \cdot \overline{u} \Big\} \\
& -\Re \Big\{ \textstyle\int_{\Gamma_1} \frac{1}{\mu_1} p \ \nabla_\Gamma \cdot (\overline{(B_1^* - B_1) P[v]}) + \int_{\Gamma_2} \frac{1}{\mu_2} p \ \nabla_\Gamma \cdot (\overline{(B_2^* - B_2) P[v]}) \Big\} \\
& + \omega^2 \textstyle\int_\Omega \varepsilon |\nabla p|^2 - \Re \Big\{ \frac{1}{\mu_1} \int_{\Gamma_1} B_1 P[\nabla p] \cdot \overline{\nabla p} - \int_{\Gamma_2} \frac{1}{\mu_2} B_2 P(\nabla p) \cdot \overline{\nabla p} \Big\}.
\end{aligned}
\tag{7.7}
$$

We now estimate the terms on the right hand side of (7.7) one by one.

It follows from the boundary condition (7.80) that

$$
\begin{aligned}
\Re \int_{\Gamma_j} \frac{1}{\mu_j} B_j P[u] \overline{u} \quad & = \quad \frac{1}{\mu_j} \sum_{n \in \Lambda_j^-} \Big\{ |\beta_j^{(n)}| |P[u^{(n)}]|^2 - \frac{1}{|\beta_j^{(n)}|} |\alpha_n \cdot P[u^{(n)}]|^2 \Big\} \\
& \geq \quad \frac{1}{\mu_j} \sum_{n \in \Lambda_j^-} \frac{1}{|\beta_j^{(n)}|} (|\beta_j^{(n)}|^2 - |\alpha_n|^2) |P[u^{(n)}]|^2 \\
& \geq \quad -\omega^2 \varepsilon_j ||\nu \times u||^2_{H^{-1/2}(\Gamma_j)},
\end{aligned}
$$

where to get the last estimate, we have used the expression (7.70). An application of Proposition 7.13 then leads to

$$
\Re \Big\{ \int_{\Gamma_1} \frac{1}{\mu_1} B_1 P[u] \overline{u} + \int_{\Gamma_2} \frac{1}{\mu_2} B_2 P[u] \overline{u} \Big\} \geq -\eta ||\nabla \times u||^2_{L^2(\Omega)} - C(\eta) ||u||^2_{L^2(\Omega)} .
$$

We next estimate the term

$$
-\Re \Big\{ \int_{\Gamma_j} \frac{1}{\mu_j} p \ \nabla_\Gamma \cdot (\overline{(B_j^* - B_j) P[v]}) \Big\}.
$$

From (7.80) and (7.81),

$$\begin{aligned}
&\nabla_\Gamma \cdot ((B_j^* - B_j)P[v]) \\
=\ &\nabla_\Gamma \cdot \sum_{n\in\mathbb{Z}^2} \Big\{ (\sqrt{-1}\beta_j^{(n)} + \sqrt{-1}\overline{\beta}_j^{(n)})(v_1^{(n)}, v_2^{(n)}, 0) + (\frac{\sqrt{-1}}{\beta_j^{(n)})} + \frac{\sqrt{-1}}{\overline{\beta}_j^{(n)}})(\alpha_n \cdot v^{(n)})\alpha_n \Big\} e^{\sqrt{-1}(\frac{2\pi n_1}{\Lambda_1}x_1 + \frac{2\pi n_2}{\Lambda_2}x_2)} \\
=\ &-\sum_{n\in\Lambda_j^+} 2\Big\{ |\beta_j^{(n)}|\alpha_n \cdot v^{(n)} + \frac{1}{|\beta_j^{(n)}|}\alpha_n \cdot v^{(n)}|\alpha_n|^2 \Big\} e^{\sqrt{-1}(\frac{2\pi n_1}{\Lambda_1}x_1 + \frac{2\pi n_2}{\Lambda_2}x_2)}.
\end{aligned}$$

Thus

$$\begin{aligned}
&-\Re\Big\{ \int_{\Gamma_j} \frac{1}{\mu_j} p\ \nabla_\Gamma \cdot (\overline{(B_j^* - B_j)P[v]}) \Big\} \\
&= \Re \sum_{n\in\Lambda_j^+} \frac{2}{\mu_j} p^{(n)} \Big\{ |\beta_j^{(n)}|\alpha_n \cdot \overline{v}^{(n)} + \frac{1}{|\beta_j^{(n)}|}\alpha_n \cdot \overline{v}^{(n)}|\alpha_n|^2 \Big\} \\
&= \Re \sum_{n\in\Lambda_j^+} \Big\{ 2\omega^2\varepsilon_j |\beta_j^{(n)}|^{-1} p^{(n)} \alpha_n \cdot \overline{v}^{(n)} \Big\} \\
&\le C||p||_{H^{1/2}(\Gamma_j)} ||\nu \times v||_{H^{-1/2}(\Gamma_j)}.
\end{aligned}$$

Hence Proposition 7.13 and the trace theorem may be used once again to obtain that

$$-\sum_{j=1,2} \Re\Big\{ \int_{\Gamma_j} \frac{1}{\mu_j} p\ \nabla_\Gamma \cdot (\overline{(B_j^* - B_j)P[v]}) \Big\} \le \eta||p||^2_{H^1(\Omega)} + \eta||\nabla\times v||_{L^2(\Omega)} + C(\eta)||v||_{L^2(\Omega)}.$$

Finally by Proposition 7.10

$$-\Re\int_{\Gamma_j} \frac{1}{\mu_j} B_j P[\nabla p] \cdot \overline{\nabla p} = \Re \int_{\Gamma_j} \frac{1}{\mu_j} \nabla_\Gamma \cdot B_j P[\nabla p] \cdot \overline{p} \ge 0.$$

Combining the above estimates, we have shown for any $u \in W$ and $p \in H^1$ that the following Garding type estimate holds:

$$\Re\Big\{ a_1(u,u) - a_2(p,p) \Big\} \ge C_1||u||^2_{H(\mathrm{curl},\Omega)} + C_2||p||^2_{H^1(\Omega)} - C_3(||u||^2_{L^2(\Omega)} + ||p||^2_{L^2(\Omega)}).$$

Denote the left hand side of (7.84) by $a_\omega(E,F)$. Since the embedding from W to L^2 is compact and the dependence of the bilinear form $a(,)$ on ω is analytic outside a discrete set Λ (the set of resonances frequencies $\omega_j^{(n)} = \frac{1}{\varepsilon_j}|\alpha_n|^2, n \in \mathbb{Z}^2, j = 1,2$), the meromorphic Fredholm theorem holds. To prove the theorem it suffices then to find a frequency $\omega \in C \setminus \Lambda$ such that the bilinear form $a_\omega(,)$ is injective. Let us choose $\omega = \sqrt{-1}\lambda$, for some positive constant λ. If $E \in H(\mathrm{curl},\Omega)$ is such that $a_{i\lambda}(E,F) = 0$ for any $F \in H(\mathrm{curl},\Omega)$ then define the extension of E by

$$\tilde{E} = \begin{cases} E_1 \text{ in } \Omega_1, \\ E \text{ in } \Omega\ , \\ E_2 \text{ in } \Omega_2, \end{cases}$$

where E_j ($j = 1, 2$) is the unique solution in $H_{\text{loc}}(\text{curl}, \Omega_j)$ of the Maxwell equations

(7.8) $$\nabla \times \nabla \times E_j - \omega^2 \varepsilon_j \mu_j E_j = 0 \text{ in } \Omega_j \,,$$

(7.9) $$E_j \times \nu = E \times \nu \text{ on } \Gamma_j \,,$$

(7.10) the radiation condition at the infinity.

From the (transparent) boundary condition satisfied by E on Γ_j it follows that

$$[\widetilde{E} \times \nu] = [\frac{1}{\mu} \nabla \times \widetilde{E} \times \nu] = [\varepsilon \widetilde{E} \cdot \nu] = 0$$

on Γ_j. Moreover, since ω is a pure complex number, $\widetilde{E}$ is exponentially decaying as $|x_3| \to +\infty$. It follows that $\tilde{E}$ is a solution in $H(\text{curl}, \mathbb{R}^3)$ (*i.e.*, of finite energy) of the homogeneous Maxwell equations and so,

$$\int_{\mathbb{R}^3} \frac{1}{\mu} |\nabla \times \tilde{E}|^2 = 0,$$

which implies that $\tilde{E} = 0$ in $\mathbb{R}^3$. The uniqueness of a solution to the problem for this particular choice of frequency ω gives the claim. The proof is complete. □

7.1.6. Energy Conservation. In this section we study the energy distribution for our diffraction problem. In general, the energy is distributed away from the grating structure through the propagating plane waves which consist of propagating reflected modes in Ω_1 and propagating transmitted modes in Ω_2. It is measured by the coefficients of each term of the sum (7.72).

Since no energy absorption takes place, the coefficients of propagating reflected plane waves are

$$\begin{aligned} r_n &= E^{(n)}(b) e^{-\sqrt{-1}\beta_1^{(n)} b} \quad \text{for } n \neq 0, n \in \Lambda_1^+, \\ r_0 &= U^{(0)}(b) e^{-\sqrt{-1}\beta_1^{(0)} b} \quad \text{for } n = 0, \end{aligned}$$

where again $\Lambda_1^+ = \{n \in \mathbb{Z}^2 : \;\; \Im(\beta_1^{(n)}) = 0\}$. Hence, the energy of each reflected mode may be defined as

$$\frac{\beta_1^{(n)} |r_n|^2}{\beta}$$

and the total energy of all reflected modes is

$$\mathcal{E}_r = \frac{1}{\beta} \sum_{n \in \Lambda_1^+} \beta_1^{(n)} |r_n|^2.$$

Similarly, the coefficients of each propagating transmitted mode are

$$t_n = E^{(n)}(-b) e^{-\sqrt{-1}\beta_2^{(n)} b} \quad \text{for } n \in \Lambda_2^+$$

where $\Lambda_2^+ = \{n \in \mathbb{Z}^2 : \;\; \Im(\beta_2^{(n)}) = 0\}$. The energy of each transmitted mode is defined by

$$\frac{\mu_1 \beta_2^{(n)} |t_n|^2}{\mu_2 \beta}$$

and the total energy of all transmitted modes is

$$\mathcal{E}_t = \frac{\mu_1}{\mu_2 \beta} \sum_{n \in \Lambda_2^+} \beta_2^{(n)} |t_n|^2.$$

REMARK 7.15. In optics literature, the numbers $\mathcal{E}_r$ and $\mathcal{E}_t$ are called reflected and transmitted *efficiencies*, respectively. They represent the proportion of energy distributed in each propagating mode. The sum of reflected and transmitted efficiency is referred to as the grating *efficiency* [**?**].

The following result states that in the case of no energy absorption the total energy is conserved, *i.e.*, the incident energy is the same as the total energy of the propagating waves.

THEOREM 7.16. *Assume that the material coefficients $\varepsilon_0(x)$, ε_1, ε_2, $\mu(x)$, μ_1, and μ_2 are all real and positive. Then*

$$\mathcal{E}_r + \mathcal{E}_t = |s|^2 \,.$$

Thus the total energy that leaves the medium is the same as that of the incident field.

PROOF. Multiplying both sides of the equation (7.82) by $\overline{E}$ and integrating it over Ω, we obtain

$$\begin{aligned} &\int_\Omega d|\nabla \times E|^2 \\ &- \int_\Omega \omega^2 \varepsilon |E|^2 + \int_{\Gamma_1} \frac{1}{\mu_1} B_1 P[E] \cdot \overline{E} + \int_{\Gamma_2} \frac{1}{\mu_2} B_2 P[E] \cdot \overline{E} = \int_{\Gamma_1} f \cdot \overline{(}E), \end{aligned} \tag{7.1}$$

where f is defined by (7.83).

Taking the imaginary part of (7.1), we get

$$\sum_{n \in \Lambda_1^+} \frac{1}{\mu_1} \beta_1^{(n)} |E^{(n)}|^2 + \sum_{n \in \Lambda_2^+} \frac{1}{\mu_2} \beta_2^{(n)} |E^{(n)}|^2 = \frac{1}{\mu_1} \Im \left(2\sqrt{-1}\beta \int_{\Gamma_1} s \cdot \overline{E} e^{-\sqrt{-1}\beta b} \, dx \right).$$

The proof is completed by noting that

$$\begin{aligned} |r_0|^2 &= |U^{(0)} e^{-\sqrt{-1}\beta b}|^2 = |(E^{(0)} - (E^i)^{(0)}) e^{-\sqrt{-1}\beta b}|^2 \\ &= |E^{(0)}|^2 - 2\Re \left(s \cdot \overline{E^{(0)}} e^{-\sqrt{-1}\beta b}\right) + |s|^2. \end{aligned}$$

□

7.2. Boundary Integral Formulations

The boundary integral equation method was one of the first methods in grating theory. It has been used for the investigation of diffraction gratings of different kinds. In this section we present boundary integral formulations for scattering problems by dielectric periodic and biperiodic gratings.

7.2.1. Dielectric Periodic Gratings. In this section we establish an integral formulation for the diffraction problem from a one-dimensional dielectric grating. We consider (7.36) and (7.37) subject to the quasi-periodic radiation conditions on u^s derived in Subsection 7.0.5. As before, we denote the period Λ and let $\Gamma = \{x_2 = f(x_1)\}/(\Lambda\mathbb{Z} \setminus \{0\})$.

We introduce the quasi-periodic Green's function for the grating, which satisfies

$$(\Delta + k^2)G^{\alpha,k}(x,y) = \sum_{n\in\mathbb{Z}} \delta_0(x - y - (n\Lambda, 0))e^{\sqrt{-1}n\alpha\Lambda}. \tag{7.2}$$

We have

$$G^{\alpha,k}(x,y) = -\frac{\sqrt{-1}}{4} \sum_{n\in\mathbb{Z}} H_0^{(1)}(k|x - (n\Lambda, 0) - y|)e^{\sqrt{-1}n\alpha\Lambda}, \tag{7.3}$$

where $H_0^{(1)}$ is the Hankel function of the first kind of order 0.

If $k \neq |\alpha_n|, \forall\ n \in \mathbb{Z}$, where α_n is defined by (7.19), then by using Poisson's summation formula

$$\sum_{n\in\mathbb{Z}} e^{\sqrt{-1}(\frac{2\pi n}{\Lambda}+\alpha)x_1} = \sum_{n\in\mathbb{Z}} \delta_0(x_1 - n\Lambda)e^{\sqrt{-1}n\alpha\Lambda}, \tag{7.4}$$

we can equivalently represent $G^{\alpha,k}$ as

$$G^{\alpha,k}(x,y) = \sum_{n\in\mathbb{Z}} \frac{e^{\sqrt{-1}\alpha_n(x_1-y_1)+\sqrt{-1}\beta_n(x_2-y_2)}}{k^2 - \alpha_n^2}, \tag{7.5}$$

where β_n is given by

$$\beta_n = \begin{cases} \sqrt{k^2 - \alpha_n^2} & k^2 > \alpha_n^2, \\ \sqrt{-1}\sqrt{\alpha_n^2 - k^2} & k^2 < \alpha_n^2. \end{cases} \tag{7.6}$$

Let $\mathcal{S}_\Gamma^{\alpha,k}$ be the quasi-periodic single-layer potential associated with $G^{\alpha,k}$ on Γ; that is, for a given density $\varphi \in L^2(\Gamma)$,

$$\mathcal{S}_\Gamma^{\alpha,k}[\varphi](x) = \int_\Gamma G^{\alpha,k}(x,y)\varphi(y)\,d\sigma(y), \quad x \in \mathbb{R}^2.$$

Analogously to (4.14), u can be represented using the single layer potentials $\mathcal{S}_\Gamma^{\alpha,k_1}$ and $\mathcal{S}_\Gamma^{\alpha,k_2}$ as follows:

$$u(x) = \begin{cases} u^i(x) + \mathcal{S}_\Gamma^{\alpha,k_1}[\psi](x), & x \in D_1\ , \\ \mathcal{S}_\Gamma^{\alpha,k_2}[\varphi](x), & x \in D_2\ , \end{cases} \tag{7.7}$$

where the pair $(\varphi, \psi) \in L^2(\Gamma) \times L^2(\Gamma)$ satisfies

$$\begin{cases} \mathcal{S}_\Gamma^{\alpha,k_2}[\varphi] - \mathcal{S}_\Gamma^{\alpha,k_1}[\psi] = u^i \\ \left.\dfrac{\partial(\mathcal{S}_\Gamma^{\alpha,k_2}[\varphi])}{\partial\nu}\right|_- - \left.\dfrac{\partial(\mathcal{S}_\Gamma^{\alpha,k_1}[\psi])}{\partial\nu}\right|_+ = \dfrac{\partial u^i}{\partial\nu} \end{cases} \quad \text{on } \Gamma. \tag{7.8}$$

THEOREM 7.17. *For all but possibly a countable set of frequencies ω_j, $\omega_j \to +\infty$, the system of integral equations (7.8) has a unique solution $(\varphi, \psi) \in H^{-1/2}(\Gamma) \times H^{-1/2}(\Gamma)$.*

PROOF. Since the Fredholm alternative applies for (7.8), it is enough to prove uniqueness. Let $(\varphi, \psi) \in H^{-1/2}(\Gamma) \times H^{-1/2}(\Gamma)$ be a solution to (7.8) and let v be given by (7.15) with $u^i = 0$. Then, v satisfies the variational problem (7.61) and Theorem 7.7 yields that for all but a discrete set of ω, $v = 0$. □

7.2.2. Dielectric Biperiodic Gratings. We consider the diffraction problem in Subsection 7.1.3. We denote by $\Gamma = \{x_3 = f(x_1, x_2)\}/((\Lambda_1\mathbb{Z} \setminus \{0\}) \times \Lambda_2\mathbb{Z} \setminus \{0\}))$, where λ_j is the period of the grating in the direction x_j for $j = 1, 2$. Suppose that

$$\begin{aligned} \varepsilon(x) &= \varepsilon_1 , \quad \mu(x) = \mu_1 \ \text{ for } x_3 > f(x_1, x_2), \\ \varepsilon(x) &= \varepsilon_2 , \quad \mu(x) = \mu_2 \ \text{ for } x_3 < f(x_1, x_2), \end{aligned}$$

where ε_1, ε_2, μ_1, and μ_2 are positive constants.

Analogously to (6.5), the electric field E can be represented as

$$E(x) = \begin{cases} E^i(x) + \mu_m \nabla \times \vec{\mathcal{S}}_\Gamma^{\alpha,k_1}[\varphi](x) + \nabla \times \nabla \times \vec{\mathcal{S}}_\Gamma^{\alpha,k_1}[\psi](x), & x \in D_1, \\ \mu_c \nabla \times \vec{\mathcal{S}}_\Gamma^{\alpha,k_2}[\varphi](x) + \nabla \times \nabla \times \vec{\mathcal{S}}_\Gamma^{\alpha,k_2}[\psi](x), & x \in D_2, \end{cases} \tag{7.9}$$

where the pair $(\varphi, \psi) \in \left(H_T^{-\frac{1}{2}}(\mathrm{div}, \Gamma)\right)^2$ satisfies

(7.10)

$$\begin{pmatrix} \dfrac{\mu_2 + \mu_1}{2} I + \mu_2 \mathcal{M}_\Gamma^{\alpha,k_2} - \mu_1 \mathcal{M}_\Gamma^{\alpha,k_1} & \mathcal{L}_\Gamma^{\alpha,k_2} - \mathcal{L}_\Gamma^{\alpha,k_1} \\ \mathcal{L}_\Gamma^{\alpha,k_2} - \mathcal{L}_\Gamma^{\alpha,k_1} & \left(\dfrac{k_2^2}{2\mu_2} + \dfrac{k_1^2}{2\mu_1}\right) I + \dfrac{k_m^2}{\mu_2} \mathcal{M}_\Gamma^{\alpha,k_2} - \dfrac{k_1^2}{\mu_1} \mathcal{M}_\Gamma^{\alpha,k_1} \end{pmatrix} \begin{bmatrix} \varphi \\ \psi \end{bmatrix}$$
$$= \begin{bmatrix} \nu \times E^i \\ \sqrt{-1}\omega \nu \times H^i \end{bmatrix} \Bigg|_\Gamma ,$$

where $\mathcal{L}_\Gamma^{\alpha,k}$ and $\mathcal{M}_\Gamma^{\alpha,k}$ are respectively defined by (6.2) and (6.2) with Γ_k replaced with $G^{\alpha,k}$ and ∂D with Γ.

The following result can be proved similarly to Theorem 7.17.

THEOREM 7.18. *For all but possibly a countable set of frequencies ω_j, $\omega_j \to +\infty$, the system of integral equations (7.10) has a unique solution $(\varphi, \psi) \in \left(H_T^{-\frac{1}{2}}(\mathrm{div}, \Gamma)\right)^2$.*

7.3. Numerical Implementation

Code:	7.1 Periodic Dielectric Diffraction Grating	DemoDiffractionGrating.m

In this section we use the boundary integral representation of the dielectric periodic grating described in subsection 7.2.1 to numerically determine the electric field in the case of a periodic array of spherical particles located on the x_1 axis. Denote by Ω_1 and Ω_2 the region outside the particles and the region representing the particles, respectively. Let ε_j and μ_j represent the corresponding material parameters. Let $k_j = \omega\sqrt{\varepsilon_j \mu_j}$ $(j = 1, 2)$ be the wavenumber outside and inside the particles, respectively.

The discretization of the system is performed in precisely the same manner as described in subsection 4.3.1 and leads to the system of equations

$$\begin{pmatrix} S_- & -S_+ \\ \frac{1}{\mu_2} S'_- & -\frac{1}{\mu_1} S'_+ \end{pmatrix} \begin{pmatrix} \overline{\varphi} \\ \overline{\psi} \end{pmatrix} = \begin{pmatrix} u_d \\ \frac{1}{\mu_1} u_n \end{pmatrix},$$

where $S_\pm$ and $S'_\pm$ are $N \times N$ matrices given by

$$(S_-)_{ij} = G^{\alpha,k_2}(x^{(i)} - x^{(j)})|T(x^{(j)})|(t_{j+1} - t_j), \tag{7.11}$$

$$(S_+)_{ij} = G^{\alpha,k_1}(x^{(i)} - x^{(j)})|T(x^{(j)})|(t_{j+1} - t_j) \tag{7.12}$$

$$(S'_-)_{ij} = -\frac{1}{2}\delta_{ij} + \frac{\partial G^{\alpha,k_2}}{\partial \nu_x}(x^{(i)} - x^{(j)})|T(x^{(j)})|(t_{j+1} - t_j), \tag{7.13}$$

$$(S'_+)_{ij} = \frac{1}{2}\delta_{ij} + \frac{\partial G^{\alpha,k_1}}{\partial \nu_x}(x^{(i)} - x^{(j)})|T(x^{(j)})|(t_{j+1} - t_j), \tag{7.14}$$

for $i \neq j$ and $i, j = 1, 2, ..., N$, and where $G^{\alpha,k}$ is quasi-periodic Green's function from (7.3). Once we solve this system for the density functions $\overline{\varphi}$ and $\overline{\psi}$, the electric field can be calculated using

$$u(x) = \begin{cases} u_d(x) + S_+[\overline{\psi}](x), & x \in \Omega_1 , \\ S_-[\overline{\varphi}](x), & x \in \Omega_2 . \end{cases} \tag{7.15}$$

Since $G^{\alpha,k}$ is extremely slow to converge we must use the Ewald representation of the Green's function to accelerate the convergence. Recall that the Ewald representation of the quasi-periodic Green's function is given by

$$G^{\alpha,k}(x,y) = G^{\alpha,k}_{\text{spec}}(x,y) + G^{\alpha,k}_{\text{spat}}(x,y),$$

with

$$\begin{aligned} G^{\alpha,k}_{\text{spec}}(x,y) = {} & -\frac{1}{4d}\sum_{n\in\mathbb{Z}} \frac{e^{-i\alpha_n(x_1-y_1)}}{i\beta_n} \\ & \times \left[e^{i\beta_n|x_2-y_2|}\text{erfc}\left(\frac{i\beta_n}{2E} + |x_2-y_2|\mathcal{E}\right)\right. \\ & \left. + e^{-i\beta_n|x_2-y_2|}\text{erfc}\left(\frac{i\beta_n}{2E} - |x_2-y_2|\mathcal{E}\right)\right], \end{aligned}$$

$$G^{\alpha,k}_{\text{spat}}(x,y) = -\frac{1}{4\pi}\sum_{m\in\mathbb{Z}} e^{i\alpha m d}\sum_{q=0}^{\infty}\left(\frac{k}{2\mathcal{E}}\right)^{2q}\frac{1}{q!}E_{q+1}(R_m^2\mathcal{E}^2),$$

where $\alpha_n = \alpha + \frac{2\pi p}{d}$, $\beta_n = \sqrt{k^2 - \alpha_n^2}$, $\text{erfc}(z)$ is the complementary error function

$$\text{erfc}(z) = \frac{2}{\sqrt{\pi}}\int_z^\infty e^{-t^2}dt,$$

and E_q is the qth order exponential integral which is defined as

$$E_q(z) = \int_1^\infty \frac{e^{-zt}}{t^q}dt.$$

We set the array of particles to have periodicity 1, with each particle having radius 0.4. We set the incident plane wave to be $u^i(x_1, x_2) = 3e^{i(\alpha x_1 - \beta_x 2)}$ where $\alpha = k_1\sin(\theta)$, $\beta = k_1\cos(\theta)$ with $\theta = \pi/8$. As we are considering a non-magnetic material we set the permeability to be $\mu_1 = \mu_2 = 1$. For the permittivity we set $\varepsilon_1 = 1$ and $\varepsilon_2 = 5$. We set the operating frequency to be $\omega = 1$. The resulting incident, scattered, and total fields are shown in Figure 7.4.

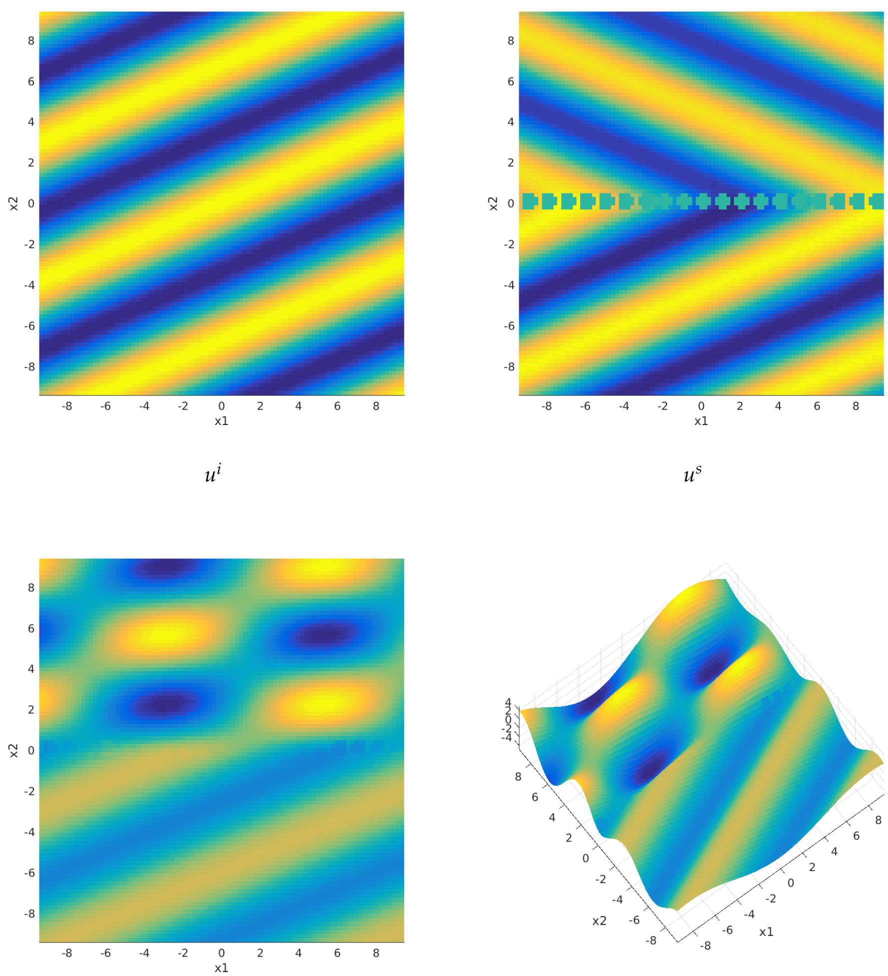

u^i u^s

u u

FIGURE 7.4. The incident electric field, scattered electric field, and total electric field for a dielectric grating consisting of a periodic array of spherical particles on the x_1 axis.

CHAPTER 8

Photonic Crystal Band Structure

Photonic crystals are structures constructed of electromagnetic materials arranged in a periodic array. They have attracted enormous interest in the last decade because of their unique optical and electromagnetic properties. Such structures have been found to exhibit interesting spectral properties with respect to classical wave propagation, including the appearance of band gaps.

In our analysis of photonic crystals we consider time-harmonic transverse electromagnetic waves with constant material parameters inside and outside of the inclusions comprising the crystal. This allows us to reduce the the Maxwell equations to two scalar Helmholtz equations. When the contrast between the material parameters inside and outside of the inclusions is high it is possible to observe gaps in the frequency spectrum for waves in photonic crystals.

As the material parameters are periodic Floquet theory is applicable. The periodic material parameters give rise to quasi-periodic fields. Applying the Floquet transform to the scattering problem in a photonic crystal allows us to decompose the problem of determining the continuous spectrum of a linear partial differential operator L acting on the entire space into determining the discrete spectra of a set of linear partial differential operators $L(\alpha)$ acting on a reference cell which can be viewed as a torus. By varying the quasi-momentum parameter α over the first Brillouin zone we can obtain the spectrum of the operator L by taking the union of the spectra of all the $L(\alpha)$ operators.

We will first discuss the relevant Floquet theory and then determine a boundary integral representation of the problem. Photonic crystal band gap calculations are prone to a problem known as 'empty resonance' so once we have properly defined this concept we will present a method incorporating a multipole expansion and lattice sums which is much less susceptible to the problem and is able to calculate the photonic crystal band structure accurately.

8.1. Floquet Transform

In this section, the Floquet transform, which in the periodic case plays the role of the Fourier transform, is established and the structure of spectra of periodic elliptic operators is discussed.

Let $f(x)$ be a function decaying sufficiently fast. We define the Floquet transform of f as follows:

$$\mathcal{U}[f](x,\alpha) = \sum_{n\in\mathbb{Z}^d} f(x-n)e^{\sqrt{-1}\alpha\cdot n}. \tag{8.1}$$

This transform is an analogue of the Fourier transform for the periodic case. The parameter α is called the quasi-momentum, and it is an analogue of the dual variable in the Fourier transform. If we shift x by a period $m \in \mathbb{Z}^d$, then we get the

Floquet condition

$$\mathcal{U}[f](x+m,\alpha) = e^{\sqrt{-1}\alpha\cdot m}\mathcal{U}[f](x,\alpha), \tag{8.2}$$

which shows that it suffices to know the function $\mathcal{U}[f](x,\alpha)$ on the unit cell $Y := [0,1)^d$ in order to recover it completely as a function of the x-variable. Moreover, $\mathcal{U}[f](x,\alpha)$ is periodic with respect to the quasi-momentum α:

$$\mathcal{U}[f](x,\alpha+2\pi m) = \mathcal{U}[f](x,\alpha), \quad m \in \mathbb{Z}^d. \tag{8.3}$$

Therefore, α can be considered as an element of the torus $\mathbb{R}^d/(2\pi\mathbb{Z}^d)$. Another way of saying this is that all information about $\mathcal{U}[f](x,\alpha)$ is contained in its values for α in the fundamental domain B of the dual lattice $2\pi\mathbb{Z}^d$. This domain is referred to as the (first) Brillouin zone.

The following result is an analogue of the Plancherel theorem when one uses the Fourier transform. Suppose that the measures $d\alpha$ and the dual torus $\mathbb{R}^d/(2\pi\mathbb{Z}^d)$ are normalized. The following theorem holds. See **[?]** for a proof.

THEOREM 8.1 (Plancherel-type theorem). *The transform*

$$\mathcal{U} : L^2(\mathbb{R}^d) \to L^2(\mathbb{R}^d/(2\pi\mathbb{Z}^d), L^2(Y))$$

is isometric. Its inverse is given by

$$\mathcal{U}^{-1}[g](x) = \int_{\mathbb{R}^d/(2\pi\mathbb{Z}^d)} g(x,\alpha)\, d\alpha,$$

where the function $g(x,\alpha) \in L^2(\mathbb{R}^d/(2\pi\mathbb{Z}^d), L^2(Y))$ is extended from Y to all $x \in \mathbb{R}^d$ according to the Floquet condition (8.2).

8.2. Structure of Spectra of Periodic Elliptic Operators

Consider a linear partial differential operator $L(x,\partial_x)$, whose coefficients are periodic with respect to $\mathbb{Z}^d, d = 2,3$. A natural question is about the type of spectrum (absolutely continuous, singular continuous, point) of L. It is not hard to prove that for a periodic elliptic operator of any order, the singular continuous spectrum is empty. For any second-order periodic operator of elliptic type, it is likely that no eigenvalues can arise. Although it has been unanimously believed by physicists for a long time, proving this statement turns out to be a difficult mathematical problem.

Due to periodicity, the operator commutes with the Floquet transform

$$\mathcal{U}[Lf](x,\alpha) = L(x,\partial_x)\mathcal{U}[f](x,\alpha).$$

For each α, the operator $L(x,\partial_x)$ now acts on functions satisfying the corresponding Floquet condition (8.2). In other words, although the differential expression of the operator stays the same, its domain changes with α. Denoting this operator by $L(\alpha)$, we see that the Floquet transform $\mathcal{U}$ expands the periodic partial differential operator L in $L^2(\mathbb{R}^d)$ into the direct integral of operators

$$\int^{\oplus}_{\mathbb{R}^d/(2\pi\mathbb{Z}^d)} L(\alpha)\, d\alpha. \tag{8.4}$$

The key point in the direct fiber decomposition (8.4) is that the operators $L(\alpha)$ act on functions defined on a torus, while the original operator acts in $\mathbb{R}^d$.

If L is a self-adjoint operator, one can prove the main spectral statement:

$$\sigma(L) = \bigcup_{\alpha \in B} \sigma(L(\alpha)), \tag{8.5}$$

where σ denotes the spectrum.

If L is elliptic, the operators $L(\alpha)$ have compact resolvents and hence discrete spectra. If L is bounded from below, the spectrum of $L(\alpha)$ accumulates only at $+\infty$. Denote by $\mu_n(\alpha)$ the nth eigenvalue of $L(\alpha)$ (counted in increasing order with their multiplicity). The function $\alpha \mapsto \mu_n(\alpha)$ is continuous in B. It is one branch of the dispersion relations and is called a band function. We conclude that the spectrum $\sigma(L)$ consists of the closed intervals (called the spectral bands)

$$\left[\min_{\alpha} \mu_n(\alpha), \max_{\alpha} \mu_n(\alpha) \right],$$

where $\min_\alpha \mu_n(\alpha) \to +\infty$ when $n \to +\infty$. In dimension $d \geq 2$, the spectral bands normally do overlap, which makes opening gaps in the spectrum of L a mathematically hard problem. But, it is still conceivable that at some locations the bands might not overlap and hence open a gap in the spectrum. It is commonly believed that the number of gaps one can open in a periodic medium in dimension $d \geq 2$ is finite.

8.3. Boundary Integral Formulation

8.3.1. Problem Formulation. The photonic crystal we consider in this chapter consists of a homogeneous background medium of constant index k which is perforated by an array of arbitrary-shaped holes periodic along each of the two orthogonal coordinate axes in $\mathbb{R}^2$. These holes are assumed to be of index 1. We assume that the structure has unit periodicity and define the unit cell $Y := [0,1]^2$.

We seek eigenfunctions u of

$$\begin{cases} \nabla \cdot (1 + (k-1)\chi(Y \setminus \overline{D}))\nabla u + \omega^2 u = 0 & \text{in } Y, \\ e^{-\sqrt{-1}\alpha\cdot x} u \text{ is periodic in the whole space,} \end{cases} \tag{8.6}$$

where $\chi(Y \setminus \overline{D})$ is the indicator function of $Y \setminus \overline{D}$. Problem (8.6) can be rewritten as

$$\begin{cases} k\Delta u + \omega^2 u = 0 & \text{in } Y \setminus \overline{D}, \\ \Delta u + \omega^2 u = 0 & \text{in } D, \\ u|_+ = u|_- & \text{on } \partial D, \\ k\dfrac{\partial u}{\partial \nu}\Big|_+ = \dfrac{\partial u}{\partial \nu}\Big|_- & \text{on } \partial D, \\ e^{-\sqrt{-1}\alpha\cdot x} u \text{ is periodic in the whole space.} \end{cases} \tag{8.7}$$

For each quasi-momentum variable α, let $\sigma_\alpha(D,k)$ be the (discrete) spectrum of (8.6). Then the spectral band of the photonic crystal is given by

$$\bigcup_{\alpha \in [0,2\pi]^2} \sigma_\alpha(D,k).$$

Note first that if D is invariant under the transformations

$$(x_1, x_2) \mapsto (-x_1, -x_2), \qquad (x_1, x_2) \mapsto (-x_1, x_2), \qquad (x_1, x_2) \mapsto (x_2, x_1), \tag{8.8}$$

then all possible eigenvalues associated with (8.7) for any $\alpha \in [0, 2\pi]^2$ must occur with α restricted to the triangular region (the reduced Brillouin zone)

$$T := \Big\{ \alpha = (\alpha_1, \alpha_2) : 0 \le \alpha_1 \le \pi, 0 \le \alpha_2 \le \alpha_1 \Big\}. \tag{8.9}$$

Consequently, to search for band gaps associated with D with the symmetries (8.8), it suffices to take $\alpha \in T$ rather than $\alpha \in [0, 2\pi]^2$.

Note also that a change of variables $x' = sx$ and a simultaneous change of the spectral parameter $\omega' = s\omega$ reduce the problem (8.7) to the similar one with the rescaled material property $(1 + (k-1)\chi(sY \setminus \overline{sD}))$. This means that in rescaling the material property of a medium, we do not need to recompute the spectrum, since its simple rescaling would suffice. Another important scaling property deals with the values of the material property. It is straightforward to compute that if we multiply the material property by a scaling factor s, the spectral problem for the new material parameter $s(1 + (k-1)\chi(sY \setminus \overline{sD}))$ can be reduced to the old one by rescaling the eigenvalues according to the formula $\omega' = \sqrt{s}\omega$. These two scaling properties mean that there is no fundamental length nor a fundamental material property value for the spectral problem (8.7).

Suppose now that ω^2 is not an eigenvalue of $-\Delta$ in $Y \setminus \overline{D}$ with the Dirichlet boundary condition on ∂D and the quasi-periodic condition on ∂Y and ω^2/k is not an eigenvalue of $-\Delta$ in D with the Dirichlet boundary condition. It can then be shown that the the solution u to (8.6) can be represented as

$$u(x) = \begin{cases} \mathcal{S}^{\alpha,\omega}[\phi](x), & x \in D, \\ H(x) + \mathcal{S}^{\alpha,\frac{\omega}{\sqrt{k}}}[\psi](x), & x \in Y \setminus \overline{D}, \end{cases} \tag{8.10}$$

for some densities ϕ and ψ in $L^2(\partial D)$, where the function H is given by

$$H(x) = -\mathcal{S}_Y^{\alpha,\frac{\omega}{\sqrt{k}}}[\frac{\partial u}{\partial \nu}|_{\partial Y}] + \mathcal{D}_Y^{\alpha,\frac{\omega}{\sqrt{k}}}[u|_{\partial Y}], \quad x \in Y.$$

Here, the quasi-periodic single- and double layer potentials are introduced in Section 3.2.1. In order to keep the notation simple, we use $\mathcal{S}^{\alpha,\omega}$ and $\mathcal{D}^{\alpha,\omega}$ instead of $\mathcal{S}_D^{\alpha,\omega}$ and $\mathcal{D}_D^{\alpha,\omega}$ for layer potentials on D.

Now due to periodicity it can be shown that $H \equiv 0$, and hence

$$u(x) = \begin{cases} \mathcal{S}^{\alpha,\omega}[\phi](x), & x \in D, \\ \mathcal{S}^{\alpha,\frac{\omega}{\sqrt{k}}}[\psi](x), & x \in Y \setminus \overline{D}. \end{cases} \tag{8.11}$$

In view of the transmission conditions in (8.7), the pair $(\phi, \psi) \in L^2(\partial D) \times L^2(\partial D)$ satisfies the following system of integral equations:

$$\begin{cases} \mathcal{S}^{\alpha,\omega}[\phi] - \mathcal{S}^{\alpha,\frac{\omega}{\sqrt{k}}}[\psi] = 0 & \text{on } \partial D, \\ \Big(-\frac{1}{2}I + (\mathcal{K}^{-\alpha,\omega})^* \Big)[\phi] - k\Big(\frac{1}{2}I + (\mathcal{K}^{-\alpha,\frac{\omega}{\sqrt{k}}})^*\Big)[\psi] = 0 & \text{on } \partial D. \end{cases} \tag{8.12}$$

The converse is also true. If $(\phi, \psi) \in L^2(\partial D) \times L^2(\partial D)$ is a nonzero solution of (8.12), then u given by (8.11) is an eigenfunction of (8.6) associated to the eigenvalue ω^2.

Suppose $\alpha \neq 0$. Let $\mathcal{A}^{\alpha,k}(\omega)$ be the operator-valued function defined by

$$\mathcal{A}^{\alpha,k}(\omega) := \begin{pmatrix} \mathcal{S}^{\alpha,\omega} & -\mathcal{S}^{\alpha,\frac{\omega}{\sqrt{k}}} \\ \frac{1}{k}\left(\frac{1}{2}I - (\mathcal{K}^{-\alpha,\omega})^*\right) & \frac{1}{2}I + (\mathcal{K}^{-\alpha,\frac{\omega}{\sqrt{k}}})^* \end{pmatrix}. \tag{8.13}$$

Then, ω^2 is an eigenvalue corresponding to u with a given quasi-momentum α if and only if ω is a characteristic value of $\mathcal{A}^{\alpha,k}$.

8.3.2. Empty resonance. The appropriate Green's function for the layer potentials used in the previous section is the quasi-biperiodic Green's function $G_\sharp^{\alpha,\omega}$ which satisfies

$$(\Delta + \omega^2)G_\sharp^{\alpha,\omega}(x,y) = \sum_{m\in\mathbb{Z}^2} \delta_0(x-y-m)e^{im\cdot\alpha}. \tag{8.14}$$

If $\omega \neq |2\pi m + \alpha|, \forall\, m \in \mathbb{Z}^2$, then $G_\sharp^{\alpha,\omega}$ has the following spectral representation:

$$G_\sharp^{\alpha,\omega}(x,y) = \sum_{n\in\mathbb{Z}^2} \frac{e^{i(2\pi m+\alpha)\cdot(x-y)}}{\omega^2 - |2\pi m + \alpha|^2}. \tag{8.15}$$

8.3.3. Empty resonance. In the context of the standard boundary integral approach to numerical computation, when the parameters ω and α are such that $\omega \sim |2\pi m + \alpha|$ for any $m \in \mathbb{Z}^2$, the quasi-periodic Green's function $G_\sharp^{\alpha,\omega}$ can have highly aberrant behaviour that makes determining characteristic values of $\mathcal{A}^{\alpha,k}(\omega)$ impossible. This phenomenon, which is known as empty resonance, is due to the resonance of the empty unit cell Y with refractive index 1 everywhere and quasi-periodic boundary conditions.

In order to deal with this issue it is necessary to use an approach that is less susceptible to the problem, or an approach that avoids it altogether. We will briefly discuss the Barnett-Greengard method for quasi-periodic fields which was developed specifically to tackle the problem of empty resonances. We will then present a numerical example in which the photonic crystal band structure is calculated using the multipole method and incoporates lattice sums, an approach which was found to be much less susceptible to the empty resonance problem.

8.4. Barnett-Greengard method

The Barnett-Greengard method avoids the problem of empty resonances by introducing a new integral representation for the problem that doesn't use the quasi-periodic Green's function. Instead, the usual free-space Green's function is used and the quasi-periodicity is enforced through auxiliary layer potentials defined on the boundary of the unit cell.

The quasi-periodicity condition in 8.6 can equivalently be written as a set of boundary conditions on the unit cell Y. Let L represent the left wall of the unit cell and B represent the bottom wall. Define $a := e^{ik_1}$ and $b := e^{ik_2}$. Then the quasi-periodicity condition can be stated as:

$$\begin{aligned} u|_{L+e_1} &= au|_L \\ \tfrac{\partial u}{\partial \nu}|_{L+e_1} &= a\tfrac{\partial u}{\partial \nu}|_L \\ u|_{B+e_2} &= bu|_B \\ \tfrac{\partial u}{\partial \nu}|_{B+e_2} &= b\tfrac{\partial u}{\partial \nu}|_B. \end{aligned}$$

Recall that the usual boundary integral formulation enables the determination of characteristic values of the operator valued function $\mathcal{A}^{\alpha,k}(\omega)$ given in 8.13 by finding the values ω such that the equation

$$\mathcal{A}^{\alpha,k}(\omega)\Psi = 0,$$

has a non-trivial solution $\Psi \in L^2(\partial D) \times L^2(\partial D)$. We note that the elements of $\mathcal{A}^{\alpha,k}(\omega)$ are quasi-periodic layer potentials. The Barnett-Greengard method uses an analogous equation

$$\mathcal{E}^{\alpha,k}(\omega)^{\alpha,k}\Psi = \kappa,$$

where

$$\mathcal{E}^{\alpha,k}(\omega) := \begin{pmatrix} A & B \\ C & Q \end{pmatrix}, \ \Psi = \begin{pmatrix} \eta \\ \xi \end{pmatrix}, \ \kappa = \begin{pmatrix} m \\ d \end{pmatrix},$$

and the operators $A, B, C,$ and Q, which will be explained shortly, involve layer potentials which utilize the free-space Green's function. η represents surface potentials for the inclusion, and ξ represents auxiliary surface potentials defined on the boundary of the unit cell. m and d are called the mismatch and the discrepancy, respectively. m represents the amount by which the matching conditions at the interface fail to be satisfied and is defined as:

$$m := \begin{pmatrix} u|_+ - u|_- \\ \frac{\partial u}{\partial \nu}|_+ - \frac{\partial u}{\partial \nu}|_- \end{pmatrix}.$$

The discrepancy d represents the amount by which the the quasi-periodicity conditions on the boundary of unit cell fail to be satisfied:

$$d := \begin{pmatrix} u|_L - a^{-1}u|_{L+e_1} \\ \frac{\partial u}{\partial \nu}|_L - a^{-1}\frac{\partial u}{\partial \nu}|_{L+e_1} \\ u|_B - b^{-1}u|_{B+e_2} \\ \frac{\partial u}{\partial \nu}|_B - b^{-1}\frac{\partial u}{\partial \nu}|_{B+e_2} \end{pmatrix}.$$

The aim is to find non-trivial surface potentials such that the mismatch and discrepancy are both zero. With that in mind, the characteristic values of the operator valued function $\mathcal{E}^{\alpha,k}(\omega)$ are the values ω such that the equation

$$\mathcal{E}^{\alpha,k}(\omega)\Psi = 0,$$

has a non-trivial solution $\Psi \in L^2(\partial D)^4$.

Before we discuss the operators used to construct $\mathcal{E}^{\alpha,k}(\omega)$ let us introduce the generalized layer potentials:

$$\tilde{\mathcal{S}}_{D_1,D_2}[\varphi](x) = \int_{\partial D_2} \sum_{m,n\in[-1,0,1]} a^m b^n G^\omega(x, y + me_1 + ne_2)\varphi(y)\, d\sigma(y), \ x \in \ D_1,$$

$$\tilde{\mathcal{D}}_{D_1,D_2}[\varphi](x) = \int_{\partial D_2} \sum_{m,n\in[-1,0,1]} a^m b^n \frac{\partial G^\omega}{\partial \nu(y)}(x, y + me_1 + ne_2)\varphi(y)\, d\sigma(y), \ x \in \ D_1,$$

$$\tilde{\mathcal{D}}^*_{D_1,D_2}[\varphi](x) = \int_{\partial D_2} \sum_{m,n\in[-1,0,1]} a^m b^n \frac{\partial G^\omega}{\partial \nu(x)}(x, y + me_1 + ne_2)\varphi(y)\, d\sigma(y), \ x \in \ D_1,$$

$$\tilde{\mathcal{T}}_{D_1,D_2}[\varphi](x) = \int_{\partial D_2} \sum_{m,n\in[-1,0,1]} a^m b^n \frac{\partial^2 G^\omega}{\partial \nu(x)\partial \nu(y)}(x, y + me_1 + ne_2)\varphi(y)\, d\sigma(y), \ x \in \ D_1.$$

These layer potentials involve summations over the nearest 3×3 neighbouring images. This direct summation over the nearest neighbours, such that their contribution will be excluded from the auxiliary quasi-periodic representation, has been found to result in much improved convergence rates in the fast multipole literature. If the curves D_1 and D_2 both represent the inclusion D we drop subscripts and use the notation $\tilde{\mathcal{S}}^{\omega}$ for the generalized single layer potential, and similarly for the other layer potentials.

Now we are in position to describe the role of the operators A, B, C, and Q. These operators are arrived at by substituting the representation formula

$$u(x) = \begin{cases} \mathcal{S}[\phi](x) + \mathcal{D}[\psi](x) & x \in D, \\ \tilde{\mathcal{S}}[\phi](x) + \tilde{\mathcal{D}}[\psi](x) + u_{QP}[\xi](x) & x \in Y \backslash \overline{D}, \end{cases}$$

into the expressions for m and d. u_{QP} is an auxiliary field that is represented by a set of layer potentials on the specific borders of the neighbouring cells that touch the borders of the unit cell, and ξ represents the auxiliary densities, associated with u_{QP} which are defined on these borders. The operator A is similar to the $\mathcal{A}^{\alpha,k}(\omega)$ operator in the usual boundary integral formulation. It describes the effect of the inclusion densities on the mismatch and is defined as:

$$A := \begin{pmatrix} I & 0 \\ 0 & I \end{pmatrix} + \begin{pmatrix} \tilde{\mathcal{D}} - \mathcal{D} & \tilde{\mathcal{S}} - \mathcal{S} \\ \tilde{\mathcal{T}} - \mathcal{T} & \tilde{\mathcal{D}}^{*} - \mathcal{D}^{*} \end{pmatrix}.$$

The operator C describes the effect of the inclusion densities on the discrepancy and is defined as:

$$C := \begin{pmatrix} \tilde{\mathcal{D}}_{L,\partial D} - a^{-1}\tilde{\mathcal{D}}_{L+e_1,\partial D} & -\tilde{\mathcal{S}}_{L,\partial D} - a^{-1}\tilde{\mathcal{S}}_{L+e_1,\partial D} \\ \tilde{\mathcal{T}}_{L,\partial D} - a^{-1}\tilde{\mathcal{T}}_{L+e_1,\partial D} & -\tilde{\mathcal{D}}^{*}_{L,\partial D} - a^{-1}\tilde{\mathcal{D}}^{*}_{L+e_1,\partial D} \\ \tilde{\mathcal{D}}_{B,\partial D} - b^{-1}\tilde{\mathcal{D}}_{B+e_2,\partial D} & -\tilde{\mathcal{S}}^{\omega}_{B,\partial D} - b^{-1}\tilde{\mathcal{S}}_{B+e_2,\partial D} \\ \tilde{\mathcal{T}}_{B,\partial D} - b^{-1}\tilde{\mathcal{T}}_{B+e_2,\partial D} & -\tilde{\mathcal{D}}^{*}_{B,\partial D} - b^{-1}\tilde{\mathcal{D}}^{*}_{B+e_2,\partial D} \end{pmatrix}.$$

Due to symmetry and translation invariance it can be shown that significant cancellation occurs when summing over the nearest neighbour terms, and therefore ther operator C can be further optimized.

The operator Q describes the effect of the auxiliary densities on the discrepancy and is defined as:

$$Q := I + \begin{pmatrix} Q_{LL} & Q_{LB} \\ Q_{BL} & Q_{BB} \end{pmatrix}$$

where

$$Q_{LL} := \begin{pmatrix} \sum\limits_{m\in[-1,1],n\in[-1,01]} ma^m b^k \mathcal{D}_{L,L+me_1+ne_2} & -\sum\limits_{m\in[-1,1],n\in[-1,01]} ma^m b^k \mathcal{S}_{L,L+me_1+ne_2} \\ \sum\limits_{m\in[-1,1],n\in[-1,01]} ma^m b^k \mathcal{T}_{L,L+me_1+ne_2} & -\sum\limits_{m\in[-1,1],n\in[-1,01]} ma^m b^k \mathcal{D}^*_{L,L+me_1+ne_2} \end{pmatrix},$$

$$Q_{LB} := \begin{pmatrix} \sum\limits_{m\in[0,1]} b^m (a\mathcal{D}_{L,B+e_1+me_2} - a^{-2}\mathcal{D}_{L,B-2e_1+me_2}) & \sum\limits_{m\in[0,1]} b^m (-a\mathcal{S}_{L,B+e_1+me_2} + a^{-2}\mathcal{S}_{L,B-2e_1+me_2}) \\ \sum\limits_{m\in[0,1]} b^m (a\mathcal{T}_{L,B+e_1+me_2} - a^{-2}\mathcal{T}_{L,B-2e_1+me_2}) & \sum\limits_{m\in[0,1]} b^m (-aD^*_{L,B+e_1+me_2} + a^{-2}D^*_{L,B-2e_1+me_2}) \end{pmatrix},$$

$$Q_{BL} := \begin{pmatrix} \sum\limits_{m\in[0,1]} a^m (b\mathcal{D}_{B,L+me_1+e_2} - b^{-2}\mathcal{D}_{B,L+me_1-2e_2}) & \sum\limits_{m\in[0,1]} a^m (-b\mathcal{S}_{B,L+me_1+e_2} + b^{-2}\mathcal{S}_{B,L+me_1-2e_2}) \\ \sum\limits_{m\in[0,1]} a^m (b\mathcal{T}_{B,L+me_1+e_2} - b^{-2}\mathcal{T}_{B,L+me_1-2e_2}) & \sum\limits_{m\in[0,1]} a^m (-b\mathcal{D}^*_{B,L+me_1+e_2} + b^{-2}\mathcal{D}^*_{B,L+me_1-2e_2}) \end{pmatrix},$$

$$Q_{BB} := \begin{pmatrix} \sum\limits_{m\in[-1,1],n\in[-1,01]} ma^m b^k \mathcal{D}_{B,B+me_1+ne_2} & -\sum\limits_{m\in[-1,1],n\in[-1,01]} ma^m b^k \mathcal{S}_{B,B+me_1+ne_2} \\ \sum\limits_{m\in[-1,1],n\in[-1,01]} ma^m b^k \mathcal{T}_{B,B+me_1+ne_2} & -\sum\limits_{m\in[-1,1],n\in[-1,01]} ma^m b^k \mathcal{D}^*_{B,B+me_1+ne_2} \end{pmatrix},$$

Again, due to symmetry and translational invariance the terms of the operator Q are subject to cancellation.

Finally, the operator B, which describes the effect of the auxiliary densities on the mismatch, is defined as:

$$B := \sum_{m\in[0,1],n\in[-1,0,1]} a^m b^n \begin{pmatrix} \mathcal{D}_{\partial D,L+me_1+ne_2} & -\mathcal{S}_{\partial D,L+me_1+ne_2} & 0 & 0 \\ \mathcal{T}_{\partial D,L+me_1+ne_2} & -\mathcal{D}^*_{\partial D,L+me_1+ne_2} & 0 & 0 \end{pmatrix} +$$
$$\sum_{m\in[-1,0,1],n\in[0,1]} a^m b^n \begin{pmatrix} 0 & 0 & \mathcal{D}_{\partial D,B+me_1+ne_2} & -\mathcal{S}_{\partial B,L+me_1+ne_2} \\ 0 & 0 & \mathcal{T}_{\partial D,B+me_1+ne_2} & -\mathcal{D}^*_{\partial D,B+me_1+ne_2} \end{pmatrix}.$$

By avoiding the use of the quasi-periodic Green's function, the Barnett-Greengard method can be used for photonic band structure calculations that are free from the issue of empty resonance.

8.5. Multipole expansion method

Code: 8.1 Photonic Crystal Band Structure	DemoBandStructure.m

When D is a circular disk of radius R, the integral equation admits an explicit represenation. In this case, the solution can be represented as a sum of cylindrical waves $J_n(kr)e^{in\theta}$ or $H_n^{(1)}(kr)e^{in\theta}$. Here we give a multipole expansion interpretation of the integral operator $\mathcal{A}^{\alpha,k}$. It results in a numerical scheme which is much more efficient than one obtained with the usual discretization.

Recall that, for each fixed k, α, we have to find a characteristic value of $\mathcal{A}^{\alpha,k}(\omega)$ defined by

$$\mathcal{A}^{\alpha,k}(\omega) := \begin{pmatrix} \mathcal{S}^{\alpha,\sqrt{k}\omega} & -\mathcal{S}^{\alpha,\omega} \\ \frac{1}{k}\frac{\partial \mathcal{S}^{\alpha,\sqrt{k}\omega}}{\partial \nu}\Big|_- & -\frac{\partial \mathcal{S}^{\alpha,\omega}}{\partial \nu}\Big|_+ \end{pmatrix}, \tag{8.16}$$

where we have replaced ω in the original operator $\mathcal{A}^{\alpha,k}$ by $\sqrt{k}\omega$. The corresponding solution is associated to TM mode and k represents the permittivity of the inclusion.

From the above expression, we see that $\mathcal{A}^{\alpha,k}$ is represented in terms of the single layer potential only. So it is enough to derive a multipole expansion version of the single layer potential.

Before computing $\mathcal{S}^{\alpha,\omega}[\varphi]$, let us first consider the single layer potential $\mathcal{S}_D^{\omega}[\varphi]$ for a single disk D. We adopt the polar coordinates (r,θ). Then, since D is a circular disk, the density function $\varphi = \varphi(\theta)$ is a 2π-periodic function. So it admits the following Fourier series expansion:

$$\varphi = \sum_{n\in\mathbb{Z}} a_n e^{\sqrt{-1}n\theta},$$

for some coefficients a_n. So we only need to compute $u := \mathcal{S}_D^{\omega}[e^{\sqrt{-1}n\theta}]$ which satisfies

$$\begin{cases} \Delta u + \omega^2 u = 0 \quad \text{in } \mathbb{R}^2 \setminus \overline{D}, \\ \Delta u + \omega^2 u = 0 \quad \text{in } D, \\ u|_+ = u|_- \quad \text{on } \partial D, \\ \dfrac{\partial u}{\partial \nu}\Big|_+ - \dfrac{\partial u}{\partial \nu}\Big|_- = e^{\sqrt{-1}n\theta} \quad \text{on } \partial D, \\ u \text{ satisfies the Sommerfeld radiation condition.} \end{cases} \tag{8.17}$$

The above equation can be easily solved by using the separation of variables technique in polar coordinates. It gives

$$\mathcal{S}_D^{\omega}[e^{\sqrt{-1}n\theta}] = \begin{cases} cJ_n(\omega R)H_n^{(1)}(\omega r)e^{\sqrt{-1}n\theta}, & |r| > R, \\ cH_n^{(1)}(\omega R)J_n(\omega r)e^{\sqrt{-1}n\theta}, & |r| \le R, \end{cases} \tag{8.18}$$

where $c = \frac{-\sqrt{-1}\pi R}{2}$.

Now we compute the quasi-periodic single layer potetntial $\mathcal{S}^{\alpha,\omega}[e^{in\theta}]$. Since

$$G_\sharp^{\alpha,\omega}(x,y) = -\frac{\sqrt{-1}}{4}\sum_{m\in\mathbb{Z}^2} H_0^{(1)}(\omega|x-y-m|)e^{\sqrt{-1}m\cdot\alpha},$$

we have

$$\begin{aligned} \mathcal{S}^{\alpha,\omega}[e^{\sqrt{-1}n\theta}] &= \mathcal{S}_D^{\omega}[e^{\sqrt{-1}n\theta}] + \sum_{m\in\mathbb{Z}^2, m\neq 0} \mathcal{S}_{D+m}^{\omega}[e^{\sqrt{-1}n\theta}]e^{im\cdot\alpha} \\ &= \mathcal{S}_D^{\omega}[e^{\sqrt{-1}n\theta}] + cJ_n(\omega R)\sum_{m\in\mathbb{Z}^2} H_n^{(1)}(\omega r_m)e^{\sqrt{-1}n\theta_m}e^{\sqrt{-1}m\cdot\alpha}. \end{aligned}$$

Here, $D+m$ means a translation of a disk D by m and (r_m, θ_m) are the polar coordinates with respect to the center of $D+m$. By applying the following addition theorem:

$$H_n^{(1)}(\omega r_m)e^{\sqrt{-1}n\theta_m} = \sum_{l\in\mathbb{Z}} (-1)^{n-l} H_{n-l}^{(1)}(\omega|m|)e^{\sqrt{-1}n\arg(m)}J_l(\omega r)e^{\sqrt{-1}l\theta},$$

we obtain

$$\mathcal{S}^{\alpha,\omega}[e^{\sqrt{-1}n\theta}] = \mathcal{S}_D^{\omega}[e^{\sqrt{-1}n\theta}] + cJ_n(\omega R)\sum_{l\in\mathbb{Z}} (-1)^{n-l} Q_{n-l} J_l(\omega r)e^{\sqrt{-1}l\theta}. \tag{8.19}$$

where Q_n is so called the lattice sum defined by

$$Q_n := \sum_{m\in\mathbb{Z}^2, m\neq 0} H_n^{(1)}(\omega|m|)e^{\sqrt{-1}n\arg(m)}e^{\sqrt{-1}m\cdot\alpha}.$$

So, from (8.18) and (8.19), we finally obtain the explicit representation of $\mathcal{S}^{\alpha,\omega}$.

For numerical computation, we should consider the truncated series

$$\sum_{n=-N}^{N} a_n \mathcal{S}^{\alpha,\omega}[e^{\sqrt{-1}n\theta}],$$

instead of $\mathcal{S}^{\alpha,\omega}[\varphi] = \sum_{n\in\mathbb{Z}} a_n \mathcal{S}^{\alpha,\omega}[e^{\sqrt{-1}n\theta}]$ for some sufficiently large $N \in \mathbb{N}$. Then, using $e^{\sqrt{-1}n\theta}$ as a basis, we have the following matrix representation of the operator $\mathcal{S}^{\alpha,\omega}$:

$$\mathcal{S}^{\alpha,\omega}[\varphi]|_{\partial D} \approx \begin{pmatrix} S_{-N,-N} & S_{-N,-(N-1)} & \cdots & S_{-N,N} \\ S_{-(N-1),-N} & S_{-(N-1),-(N-1)} & \cdots & S_{-(N-1),N} \\ \vdots & & \ddots & \vdots \\ S_{N,-N} & \cdots & \cdots & S_{NN} \end{pmatrix} \begin{pmatrix} a_{-N} \\ a_{-(N-1)} \\ \vdots \\ a_N \end{pmatrix},$$

where $S_{m,n}$ is given by

$$S_{m,n} = cJ_n(\omega R)H_n^{(1)}(\omega R)\delta_{mn} + cJ_n(\omega R)(-1)^{n-m}Q_{n-m}J_m(\omega R).$$

Similarly, we also have the following matrix representation for $\frac{\partial \mathcal{S}^{\alpha,\omega}}{\partial \nu}\big|_{\partial D}^{\pm}$:

$$\frac{\partial \mathcal{S}^{\alpha,\omega}}{\partial \nu}[\varphi]\Big|_{\partial D}^{\pm} \approx \begin{pmatrix} S'^{\pm}_{-N,-N} & S'^{\pm}_{-N,-(N-1)} & \cdots & S'^{\pm}_{-N,N} \\ S'^{\pm}_{-(N-1),-N} & S'^{\pm}_{-(N-1),-(N-1)} & \cdots & S'^{\pm}_{-(N-1),N} \\ \vdots & & \ddots & \vdots \\ S'^{\pm}_{N,-N} & \cdots & \cdots & S'^{\pm}_{NN} \end{pmatrix} \begin{pmatrix} a_{-N} \\ a_{-(N-1)} \\ \vdots \\ a_N \end{pmatrix},$$

where $S'^{\pm}_{m,n}$ is given by

$$\begin{aligned} S'^{\pm}_{m,n} = \frac{\omega}{2}\Big[\pm 1 + c\Big(J_n \cdot (H_n^{(1)})' + J_n' \cdot H_n^{(1)}\Big)(\omega R)\Big]\delta_{mn} \\ + cJ_n(\omega R)(-1)^{n-m}Q_{n-m}\omega J_m'(\omega R). \end{aligned}$$

The matrix representation of $\mathcal{A}^{\alpha,k}(\omega)$ immediately follows.

8.5.1. Computing the lattice sum efficiently. Unfortunately, the series in the definition of Q_n^α suffers from very slow convergence. Here we provide an alternative representation which converges very quickly. For $n > 0$, Q_n^α can be represented as

$$Q_n = Q_n^G + \Delta Q_n$$

where ΔQ_n is given by

$$\Delta Q_n = \sum_{m\in\mathbb{Z}} \frac{1}{\gamma_m}\left(\frac{e^{\sqrt{-1}n\theta_m}}{e^{-\sqrt{-1}\alpha(2)}e^{-\sqrt{-1}\gamma_m} - 1} + (-1)^n \frac{e^{\sqrt{-1}n\theta_m}}{e^{-\sqrt{-1}\alpha(2)}e^{-\sqrt{-1}\gamma_m} - 1}\right),$$

$$\beta_m = \alpha(1) + 2\pi m, \quad \theta_m = \sin^{-1}(\beta_m/\omega), \quad \gamma_m = \sqrt{\omega^2 - \beta_m^2},$$

and Q_n^G is given by

$$
\begin{aligned}
Q_0^G &= -1 - \frac{2\sqrt{-1}}{\pi}(-\psi(1) + \ln\frac{\omega}{4\pi}) - \frac{2\sqrt{-1}}{\widetilde{\gamma}_0} - \frac{2\sqrt{-1}(\omega^2 + 2\beta_0^2)}{(2\pi)^3}\zeta(3) \\
&\quad - 2\sqrt{-1}\sum_{m\in\mathbb{Z}} \frac{1}{\widetilde{\gamma}_m} + \frac{1}{\widetilde{\gamma}_{-m}} - \frac{1}{m\pi} - \frac{\omega^2 + 2\beta_0^2}{(2\pi m)^3},
\end{aligned}
$$

$$
\begin{aligned}
Q_{2l}^G &= -2\sqrt{-1}\frac{e^{-2\sqrt{-1}l\theta_0}}{\widetilde{\gamma}_0} - 2\sqrt{-1}\sum_{m\in\mathbb{Z}} \frac{e^{-2\sqrt{-1}l\theta_m}}{\widetilde{\gamma}_m} + \frac{e^{2\sqrt{-1}l\theta_{-m}}}{\widetilde{\gamma}_{-m}} - \frac{(-1)^l}{m\pi}\Big(\frac{\omega}{4m\pi}\Big)^{2l} \\
&\quad - 2\sqrt{-1}\frac{(-1)^l}{\pi}(\frac{\omega}{4\pi})^{2l}\zeta(2l+1) + \frac{\sqrt{-1}}{l\pi} \\
&\quad + \frac{\sqrt{-1}}{\pi}\sum_{m=1}^{l}(-1)^m 2^{2m}\frac{(l+m-1)!}{(2m)!(l-m)!}\Big(\frac{2\pi}{\omega}\Big)^{2m} B_{2m}(\frac{\alpha(1)}{2\pi}),
\end{aligned}
$$

$$
\begin{aligned}
Q_{2l-1}^G &= 2\sqrt{-1}\sum_{m\in\mathbb{Z}} \frac{e^{-\sqrt{-1}(2l-1)\theta_m}}{\widetilde{\gamma}_m} - \frac{e^{\sqrt{-1}(2l-1)\theta_{-m}}}{\widetilde{\gamma}_{-m}} + \sqrt{-1}\frac{(-1)^l\beta_0 l}{(m\pi)^2}\Big(\frac{\omega}{4m\pi}\Big)^{2l-1} \\
&\quad - 2\sqrt{-1}\frac{e^{-i(2l-1)\theta_0}}{\widetilde{\gamma}_0} + 2\frac{(-1)^l\beta_0 l}{\pi^2}\Big(\frac{\omega}{4\pi}\Big)^{2l-1}\zeta(2l+1) \\
&\quad - \frac{2}{\pi}\sum_{m=0}^{l-1}(-1)^m 2^{2m}\frac{(l+m-1)!}{(2m+1)!(l-m-1)!}\Big(\frac{2\pi}{\omega}\Big)^{2m+1} B_{2m+1}(\frac{\alpha(1)}{2\pi}),
\end{aligned}
$$

where B_m is the Bernoulli polynomial and

$$
\widetilde{\gamma}_m = \begin{cases} \sqrt{\omega^2 - \beta_m^2}, & \omega \geq \beta_m, \\ -\sqrt{-1}\sqrt{\beta_m^2 - \omega^2}, & \omega < \beta_m. \end{cases}
$$

8.5.2. Numerical example. Now we present a numerical example in which we assume D is a circular disk of radius $R = 0.42$ and $k = \infty$. The computed band structure is shown in Figure 8.1. The truncation parameter for the cylindrical waves is set to be $N = 8$. The points Γ, X and M represent $\alpha = (0,0)$, $\alpha = (\pi, 0)$ and $\alpha = (\pi,\pi)$, respectively. We plot the characteristic values ω along the boundary of the triangle ΓXM. A band gap is clearly present.

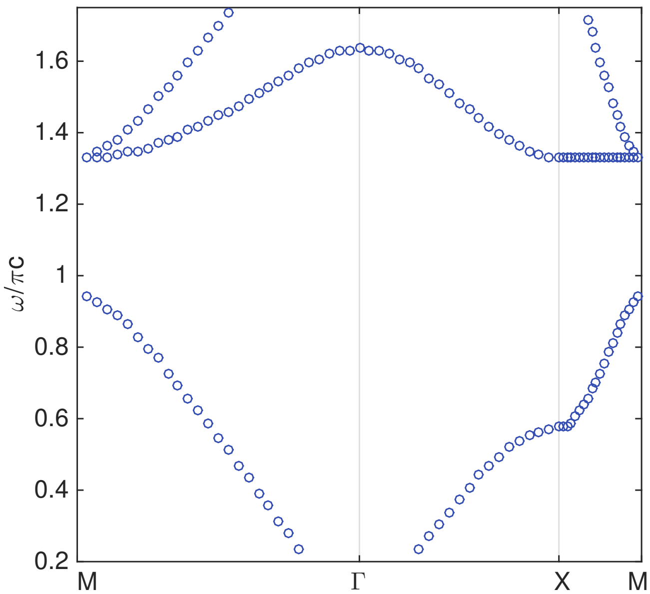

FIGURE 8.1. The band structure for a biperiodic array of circular cylinders each with radius $R = 0.42$ and $k = \infty$. The frequency is normalized to be $\omega/(\pi c)$ where c is the speed of light.

CHAPTER 9

Plasmonic Resonance

Driven by the search for new materials with interesting and unique properties, the field of nanoparticle research has grown immensely in the last decades. Plasmon resonant nanoparticles have unique capabilities of enhancing the brightness and directivity of light, confining strong electromagnetic fields, and outcoupling of light into advantageous directions. Recent advances in nanofabrication techniques have made it possible to construct complex nanostructures such as arrays using plasmonic nanoparticles as components. A thriving interest for optical studies of plasmon resonant nanoparticles is due to their recently proposed use as labels in molecular biology. New types of cancer diagnostic nanoparticles are constantly being developed. Nanoparticles are also being used in thermotherapy as nanometric heat-generators that can be activated remotely by external electromagnetic fields.

The optical response of plasmon resonant nanoparticles is dominated by the appearance of plasmon resonances over a wide range of wavelengths. For individual particles or very low concentrations in a solvent of non-interacting nanoparticles, separated from one another by distances larger than the wavelength, these resonances depend on the electromagnetic parameters of the nanoparticle, those of the surrounding material, and the particle shape and size. High scattering and absorption cross sections and strong near-fields are unique effects of plasmonic resonant nanoparticles. In order to profit from them, a rigorous understanding of the interactive effects between the particle size and shape and the contrasts in the electromagnetic parameters is required. One of the most important parameters in the context of applications is the position of the resonances in terms of wavelength or frequency. A longstanding problem is to tune this position by changing the particle size or the concentration of the nanoparticles in a solvent. It was experimentally observed, for instance, that the scaling behavior of nanoparticles is critical. The question of how the resonant properties of plasmonic nanoparticles develops with increasing size or/and concentration is therefore fundamental.

In this chapter we use the full Maxwell equations for light propagation in order to analyze plasmonic resonances for nanoparticles. We mathematically define the notion of plasmonic resonance. At the quasi-static limit, we show that plasmon resonances in nanoparticles can be treated as an eigenvalue problem for the Neumann-Poincaré integral operator and unfortunately, they are size-independent. Then we analyze the plasmon resonance shift and broadening with respect to changes in size and shape, using the layer potential techniques associated with the full Maxwell equations. We give a rigorous detailed description of the scaling behavior of plasmonic resonances to improve our understanding of light scattering by plasmonic nanoparticles beyond the quasi-static regime. On the other hand, we present an effective medium theory for resonant plasmonic systems. We treat a composite material in which plasmonic nanoparticles are embedded and isolated from each other. The particle dimension and interparticle distances are considered to be infinitely small compared with the wavelength of the interacting light. We extend the validity of the Maxwell-Garnett effective medium theory in order to describe the behavior of a system of plasmonic resonant nanoparticles. We show that by homogenizing plasmonic nanoparticles one can obtain high-contrast or negative parameter materials, depending on the used frequencies compared to the plasmonic resonant one. Finally, we discuss the plasmonic interaction between 3D metallic spheres. By clarifying the connection between Transformation Optics and the image charge method, we derive an analytic solution for two plasmonic spheres and then develop a hybrid numerical scheme for computing the field distribution.

9.1. Quasi-Static Plasmonic Resonances

9.1.1. Uniform Validity of Small-Volume Expansions. We consider the scattering problem of a time-harmonic electromagnetic wave incident on a particle D. The homogeneous medium is characterized by electric permittivity ε_m and magnetic permeability μ_m, while D is characterized by electric permittivity ε_c and magnetic permeability μ_c, both of which depend on the frequency. Define

$$k_m = \omega\sqrt{\varepsilon_m \mu_m}, \quad k_c = \omega\sqrt{\varepsilon_c \mu_c},$$

and

$$\varepsilon_D = \varepsilon_m \chi(\mathbb{R}^3 \setminus \overline{D}) + \varepsilon_c \chi(D), \quad \mu_D = \varepsilon_m \chi(\mathbb{R}^3 \setminus \overline{D}) + \varepsilon_c \chi(D).$$

For a given incident plane wave (E^i, H^i), solution to the Maxwell equations in free space (6.2), the scattering problem can be modeled by the system of equations (6.3) subject to the Silver-Müller radiation condition (6.4).

Let $D = z + \delta B$ where B contains the origin and $|B| = O(1)$. For any $x \in \partial D$, let $\widetilde{x} = \frac{x-z}{\delta} \in \partial B$ and define for each function f defined on ∂D, a corresponding function defined on B as follows

$$\eta(f)(\widetilde{x}) = f(z + \delta \widetilde{x}). \tag{9.1}$$

The following result was derived. Its proof is sketched at the end of this chapter.

THEOREM 9.1. *Let*

$$d_\sigma = \min\left\{ \mathrm{dist}\big(\lambda_\mu, \sigma((\mathcal{K}_D^0)^*) \cup -\sigma((\mathcal{K}_D^0)^*)\big), \mathrm{dist}\big(\lambda_\varepsilon, \sigma((\mathcal{K}_D^0)^*) \cup -\sigma((\mathcal{K}_D^0)^*)\big) \right\}.$$

Then, for $D = z + \delta B \Subset \mathbb{R}^3$ of class $\mathcal{C}^{1,\alpha}$ for $\alpha > 0$, the following uniform far-field expansion holds

(9.2)
$$\begin{aligned} E^s(x) \quad = \quad & -\frac{\sqrt{-1}\omega\mu_m}{\varepsilon_m} \nabla \times \mathbf{G}_{k_m}(x-z) M(\lambda_\mu, D) H^i(z) - \omega^2 \mu_m \mathbf{G}_{k_m}(x-z) M(\lambda_\varepsilon, D) E^i(z) \\ & + O(\frac{\delta^4}{d_\sigma}), \end{aligned}$$

where $\mathbf{G}_{k_m}(x-z)$ is the Dyadic Green (matrix valued) function for the full Maxwell equations defined by

$$\mathbf{G}_{k_m}(x) = \varepsilon_m \Big(\Gamma_{k_m}(x) I + \frac{1}{k_m^2} D_x^2 \Gamma_{k_m}(x) \Big), \tag{9.3}$$

and $M(\lambda_\mu, D)$ and $M(\lambda_\varepsilon, D)$ are the polarization tensors associated with D and the contrasts λ_μ and λ_ε given by (4.7) with $k = \mu_c/\mu_c$ and $k = \varepsilon_c/\varepsilon_m$, respectively.

Suppose that ε_c and μ_c are changing with respect to the angular frequency ω while ε_m and μ_m are independent of ω. Because of causality, the real and imaginary parts of ε_c and μ_c obey Kramers-Kronig relations

$$\begin{aligned} \Re F(\omega) &= -\frac{1}{\pi} \mathrm{p.v.} \int_{-\infty}^{+\infty} \frac{\Im F(\omega')}{\omega - \omega'} \, d\omega', \\ \Im F(\omega) &= \frac{1}{\pi} \mathrm{p.v.} \int_{-\infty}^{+\infty} \frac{\Re F(\omega')}{\omega - \omega'} \, d\omega', \end{aligned} \tag{9.4}$$

$F(\omega) = \varepsilon_c(\omega)$ or $\mu_c(\omega)$. The permittivity and permeability of plasmonic nanoparticles in the infrared spectral regime can be described by the Drude model given by

$$\varepsilon_c(\omega) = \varepsilon_m \big(1 - \frac{\omega_p^2}{\omega(\omega + \sqrt{-1}\tau^{-1})}\big), \quad \mu_c(\omega) = \mu_m \big(1 - F\frac{\omega^2}{\omega^2 - \omega_0^2 + \sqrt{-1}\tau^{-1}}\big), \tag{9.5}$$

where ω_p is the plasma frequency of the bulk material, τ^{-1} is the damping coefficient, F is a filling factor, and ω_0 is a localized plasmon frequency.

DEFINITION 9.2. We call ω a quasi-static plasmonic resonance if $d_\sigma(\omega) \ll 1$.

Notice that, in view of (4.7), if ω a quasi-static plasmonic resonance, then at least one of the polarization tensors $M(\lambda_\varepsilon, D)$ and $M(\lambda_\mu, D)$ blows up.

Assume that the incident fields are plane waves given by

$$\begin{aligned} E^i(x) &= p e^{\sqrt{-1}k_m d\cdot x}, \\ H^i(x) &= d \times p e^{\sqrt{-1}k_m d\cdot x}, \end{aligned}$$

where $p \in \mathbb{R}^3$ and $d \in \mathbb{R}^3$ with $|d| = 1$ are such that $p \cdot d = 0$.

From Taylor expansions on the formula of Theorem 9.1, it follows that the following far-field asymptotic expansion holds:

$$\begin{aligned} E^s(x) = &-\frac{e^{\sqrt{-1}k_m|x|}}{4\pi|x|} \Big(\omega\mu_m k_m e^{\sqrt{-1}k_m(d-\hat{x})\cdot z} \big(\hat{x} \times I\big) M(\lambda_\mu, D)(d \times p) \\ &- k_m^2 e^{\sqrt{-1}k_m(d-\hat{x})\cdot z} \big(I - \hat{x}\hat{x}^t\big) M(\lambda_\varepsilon, D) p \Big) + O(\frac{1}{|x|^2}) + O(\frac{\delta^4}{d_\sigma}) \end{aligned}$$

as $|x| \to +\infty$, where $\hat{x} = x/|x|$ and t denotes the transpose. Therefore, up to an error term of order $O(\frac{\delta^4}{d_\sigma})$, the scattering amplitude A_∞ is given by

$$A_\infty(\hat{x}) = \omega\mu_m k_m e^{\sqrt{-1}k_m(d-\hat{x})\cdot z} \big(\hat{x} \times I\big) M(\lambda_\mu, D)(d \times p) - k_m^2 e^{\sqrt{-1}k_m(d-\hat{x})\cdot z} \big(I - \hat{x}\hat{x}^t\big) M(\lambda_\varepsilon, D) p. \tag{9.6}$$

Formula (9.6) allows us to compute the extinction cross-section Q^{ext} in terms of the polarization tensors associated with the particle D and the material parameter contrasts. Moreover, an estimate for the blow up of the extinction cross-section Q^{ext} at the plasmonic resonances follows immediately from (4.7).

THEOREM 9.3. *We have*

$$Q^{ext} = \frac{4\pi}{k_m |p|^2} \Im \left[p \cdot \left[\omega \mu_m k_m (d \times I) M(\lambda_\mu, D)(d \times p) - k_m^2 (I - dd^t) M(\lambda_\varepsilon, D) p \right] \right].$$

9.2. Effective Medium Theory for Suspensions of Plasmonic Nanoparticles

In this section we derive effective properties of a system of plasmonic nanoparticles. To begin with, we consider a bounded and simply connected domain $\Omega \Subset \mathbb{R}^3$ of class $\mathcal{C}^{1,\alpha}$ for $\alpha > 0$, filled with a composite material that consists of a matrix of constant electric permittivity ε_m and a set of periodically distributed plasmonic nanoparticles with (small) period η and electric permittivity ε_c.

Let $Y = (-1/2, 1/2)^3$ be the unit cell and denote $\delta = \eta^\beta$ for $\beta > 0$. We set the (rescaled) periodic function

$$\gamma = \varepsilon_m \chi(Y \backslash \bar{D}) + \varepsilon_c \chi(D),$$

where $D = \delta B$ with $B \Subset \mathbb{R}^3$ being of class $\mathcal{C}^{1,\alpha}$ and the volume of B, $|B|$, is assumed to be equal to 1. Thus, the electric permittivity of the composite is given by the periodic function

$$\gamma_\eta(x) = \gamma(x/\eta),$$

which has period η. Now, consider the problem

$$\nabla \cdot \gamma_\eta \nabla u_\eta = 0 \quad \text{in } \Omega \tag{9.7}$$

with an appropriate boundary condition on $\partial\Omega$. Then, there exists a homogeneous, generally anisotropic, permittivity γ^*, such that the replacement, as $\eta \to 0$, of the original equation (9.7) by

$$\nabla \cdot \gamma^* \nabla u_0 = 0 \quad \text{in } \Omega$$

is a valid approximation in a certain sense. The coefficient γ^* is called an effective permittivity. It represents the overall macroscopic material property of the periodic composite made of plasmonic nanoparticles embedded in an isotropic matrix.

The (effective) matrix $\gamma^* = (\gamma^*_{pq})_{p,q=1,2,3}$ is defined by

$$\gamma^*_{pq} = \int_Y \gamma(x) \nabla u_p(x) \cdot \nabla u_q(x) dx,$$

where u_p, for $p = 1, 2, 3$, is the unique solution to the cell problem

$$\begin{cases} \nabla \cdot \gamma \nabla u_p = 0 \quad \text{in } Y, \\ u_p - x_p \quad \text{periodic (in each direction) with period 1}, \\ \int_Y u_p(x) dx = 0. \end{cases} \tag{9.8}$$

Using Green's formula, we can rewrite γ^* in the following form:

$$\gamma^*_{pq} = \varepsilon_m \int_{\partial Y} u_q(x) \frac{\partial u_p}{\partial \nu}(x) d\sigma(x). \tag{9.9}$$

The matrix γ^* depends on η as a parameter and cannot be written explicitly.

Let $\mathcal{S}^0_{D,\sharp}$ and $(\mathcal{K}^0_{D,\sharp})^*$ be respectively the single and the Neumann-Poincaré operator associated with the periodic Green's function $G_\sharp$ for $d = 3$.

We get

$$\gamma_{pq}^* = \varepsilon_m \int_{\partial Y} \big(y_q + C_q + \mathcal{S}_{D,\sharp}^0[\phi_q](y)\big) \frac{\partial\big(y_p + \mathcal{S}_{D,\sharp}^0[\phi_p](y)\big)}{\partial \nu} d\sigma(y),$$

where

$$\phi_p(y) = (\lambda_\varepsilon I - (\mathcal{K}_{D,\sharp}^0)^*)^{-1}[\nu_p](y) \quad \text{for } y \text{ in } \partial D, \tag{9.10}$$

and $p = 1, 2, 3$.

Because of the periodicity of $\mathcal{S}_{D,\sharp}^0[\phi_p]$, we get

$$\gamma_{pq}^* = \varepsilon_m \Big(\delta_{pq} + \int_{\partial Y} y_q \frac{\partial \mathcal{S}_{D,\sharp}^0[\phi_p]}{\partial \nu}(y) d\sigma(y) \Big). \tag{9.11}$$

In view of the periodicity of $\mathcal{S}_{D,\sharp}^0[\phi_p]$, the divergence theorem applied on $Y \backslash \bar{D}$ yields

$$\int_{\partial Y} y_q \frac{\partial \mathcal{S}_{D,\sharp}^0[\phi_p]}{\partial \nu}(y) = \int_{\partial D} y_q \phi_p(y) d\sigma(y).$$

Let

$$\psi_p(y) = \phi_p(\delta y) \quad \text{for } y \in \partial B.$$

Then, by (9.11), we obtain

$$\gamma^* = \varepsilon_m (I + fP), \tag{9.12}$$

where $f = |D| = \delta^3 (= \eta^{3\beta})$ is the volume fraction of D and $P = (P_{pq})_{p,q=1,2,3}$ is given by

$$P_{pq} = \int_{\partial B} y_q \psi_p(y) d\sigma(y). \tag{9.13}$$

Now we proceed with the computation of P and prove the main result of this section, which shows the validity of the Maxwell-Garnett theory uniformly with respect to the frequency under the assumptions that

$$f \ll \mathrm{dist}(\lambda_\varepsilon(\omega), \sigma((\mathcal{K}_B^0)^*))^{3/5} \quad \text{and } (I - \delta^3 R_{\lambda_\varepsilon(\omega)}^{-1} T_0)^{-1} = O(1), \tag{9.14}$$

where $R_{\lambda_\varepsilon(\omega)}^{-1}$ and T_0 are to be defined and $\mathrm{dist}(\lambda_\varepsilon(\omega), \sigma((\mathcal{K}_D^0)^*))$ is the distance between $\lambda_\varepsilon(\omega)$ and the spectrum of $(\mathcal{K}_B^0)^*$.

THEOREM 9.4. *Assume that (9.14) holds. Then we have*

$$\gamma^* = \varepsilon_m \big(I + fM(I - \frac{f}{3}M)^{-1}\big) + O\Big(\frac{f^{8/3}}{\mathrm{dist}(\lambda_\varepsilon(\omega), \sigma((\mathcal{K}_B^0)^*))^2}\Big), \tag{9.15}$$

uniformly in ω. Here, $M = M(\lambda_\varepsilon(\omega), B)$ is the polarization tensor (4.6) *associated with B and $\lambda_\varepsilon(\omega)$.*

PROOF. In view of (9.10), we can write, for $x \in \partial D$,

$$(\lambda_\varepsilon(\omega) I - (\mathcal{K}_D^0)^*)[\phi_p](x) - \int_{\partial D} \frac{\partial R(x-y)}{\partial \nu(x)} \phi_p(y) d\sigma(y) = \nu_p(x),$$

which yields, for $x \in \partial B$,

$$(\lambda_\varepsilon(\omega) I - (\mathcal{K}_B^0)^*)[\psi_p](x) - \delta^2 \int_{\partial B} \frac{\partial R(\delta(x-y))}{\partial \nu(x)} \psi_p(y) d\sigma(y) = \nu_p(x).$$

We have

$$\nabla R(\delta(x-y)) = -\frac{\delta}{3}(x-y) + O(\delta^3)$$

uniformly in $x, y \in \partial B$. Since $\int_{\partial B} \psi_p(y) d\sigma(y) = 0$, we now have

$$(R_{\lambda_\varepsilon(\omega)} - \delta^3 T_0 + \delta^5 T_1)[\psi_p](x) = \nu_p(x),$$

and so

$$(I - \delta^3 R^{-1}_{\lambda_\varepsilon(\omega)} T_0 + \delta^5 R^{-1}_{\lambda_\varepsilon(\omega)} T_1)[\psi_p](x) = R^{-1}_{\lambda_\varepsilon(\omega)}[\nu_p](x), \tag{9.16}$$

where

$$\begin{aligned} R_{\lambda_\varepsilon(\omega)}[\psi_p](x) &= (\lambda_\varepsilon(\omega) I - (\mathcal{K}_B^0)^*)[\psi_p](x), \\ T_0[\psi_p](x) &= \frac{\nu(x)}{3} \cdot \int_{\partial B} y \psi_p(y) d\sigma(y), \\ \|T_1\|_{\mathcal{L}(\mathcal{H}^*(\partial B), \mathcal{H}^*(\partial B))} &= O(1). \end{aligned}$$

Since $(\mathcal{K}_B^0)^* : \mathcal{H}^*(\partial B) \to \mathcal{H}^*(\partial B)$ is a self-adjoint, compact operator, it follows that

$$\|(\lambda_\varepsilon(\omega) I - (\mathcal{K}_B^0)^*)^{-1}\|_{\mathcal{L}(\mathcal{H}^*(\partial B), \mathcal{H}^*(\partial B))} \leq \frac{c}{\operatorname{dist}(\lambda_\varepsilon(\omega), \sigma((\mathcal{K}_B^0)^*))} \tag{9.17}$$

for a constant c.

It is clear that T_0 is a compact operator. From the fact that the imaginary part of $R_{\lambda_\varepsilon(\omega)}$ is nonzero, it follows that $I - \delta^3 R^{-1}_{\lambda_\varepsilon(\omega)} T_0$ is invertible.

Under the assumption that

$$(I - \delta^3 R^{-1}_{\lambda_\varepsilon(\omega)} T_0)^{-1} = O(1),$$
$$\delta^5 \ll \operatorname{dist}(\lambda_\varepsilon(\omega), \sigma((\mathcal{K}_B^0)^*)),$$

we get from (9.16) and (9.17)

$$\begin{aligned} \psi_p(x) &= (I - \delta^3 R^{-1}_{\lambda_\varepsilon(\omega)} T_0 + \delta^5 R^{-1}_{\lambda_\varepsilon(\omega)} T_1)^{-1} R^{-1}_{\lambda_\varepsilon(\omega)}[\nu_p](x), \\ &= (I - \delta^3 R^{-1}_{\lambda_\varepsilon(\omega)} T_0)^{-1} R^{-1}_{\lambda_\varepsilon(\omega)}[\nu_p](x) + O\Big(\frac{\delta^5}{\operatorname{dist}(\lambda_\varepsilon(\omega), \sigma((\mathcal{K}_B^0)^*))}\Big). \end{aligned}$$

Therefore, we obtain the estimate for ψ_p

$$\psi_p = O\Big(\frac{1}{\operatorname{dist}(\lambda_\varepsilon(\omega), \sigma((\mathcal{K}_B^0)^*))}\Big).$$

Now, we multiply (9.16) by y_q and integrate over ∂B. We can derive from the estimate of ψ_p that

$$P(I - \frac{f}{3}M) = M + O\Big(\frac{\delta^5}{\operatorname{dist}(\lambda_\varepsilon(\omega), \sigma((\mathcal{K}_B^0)^*))^2}\Big),$$

and therefore,

$$P = M(I + \frac{f}{3}M)^{-1} + O\Big(\frac{\delta^5}{\operatorname{dist}(\lambda_\varepsilon(\omega), \sigma((\mathcal{K}_B^0)^*)^2}\Big)$$

with P being defined by (9.13). Since $f = \delta^3$ and

$$M = O\Big(\frac{\delta^3}{\mathrm{dist}(\lambda_\varepsilon(\omega), \sigma((\mathcal{K}_B^0)^*))}\Big),$$

it follows from (9.12) that the Maxwell-Garnett formula (9.15) holds (uniformly in the frequency ω) under the assumption (9.14) on the volume fraction f. □

REMARK 9.5. As a corollary of Theorem 9.4, we see that in the case when $fM = O(1)$, which is equivalent to the scale $f = O\Big(\mathrm{dist}(\lambda_\varepsilon(\omega), \sigma((\mathcal{K}_B^0)^*))\Big)$, the matrix $fM(I - \frac{f}{3}M)^{-1}$ may have a negative-definite symmetric real part. On the other hand, if $\mathrm{dist}(\lambda_\varepsilon(\omega), \sigma((\mathcal{K}_B^0)^*)) = O(f^{1+\beta})$ for $0 < \beta < 2/3$, then the effective matrix γ^* may be very large. This provides evidence of constructing negative and high-contrast materials using plasmonic nanoparticles in appropriate regimes.

9.3. Shift in Plasmonic Resonances Due to the Particle Size

Code:	9.1 Plasmonic Resonance Shift	DemoSphereCrossSection.m DemoShellCrossSection.m

In this section we analyze the shift in the plasmonic resonance due to changes in size of the nanoparticle. We consider the original system of integral equations (6.7) for a given incident plane wave (E^i, H^i). With the same notation as in Section 6.1, the following result holds.

LEMMA 9.6. *Let η be defined by (9.1). The system of equations* (6.7) *can be rewritten as follows:*

$$\mathcal{W}_B(\delta)\begin{pmatrix} \eta(\psi) \\ \omega\eta(\phi) \end{pmatrix} = \begin{pmatrix} \dfrac{\eta(\nu \times E^i)}{\mu_m - \mu_c} \\ \dfrac{\eta(\sqrt{-1}\nu \times H^i)}{\varepsilon_m - \varepsilon_c} \end{pmatrix}\Bigg|_{\partial B}, \tag{9.18}$$

where

(9.19)

$$\mathcal{W}_B(\delta) = \begin{pmatrix} \lambda_\mu I - \mathcal{M}_B + \delta^2 \dfrac{\mu_m \mathcal{M}_{B,2}^{k_m} - \mu_c \mathcal{M}_{B,2}^{k_c}}{\mu_m - \mu_c} + O(\delta^3) & \dfrac{1}{\mu_m - \mu_c}(\delta \mathcal{L}_{B,1} + \delta^2 \mathcal{L}_{B,2}) + O(\delta^3) \\ \dfrac{1}{\varepsilon_m - \varepsilon_c}(\delta \mathcal{L}_{B,1} + \delta^2 \mathcal{L}_{B,2}) + O(\delta^3) & \lambda_\varepsilon I - \mathcal{M}_B + \delta^2 \dfrac{\varepsilon_m \mathcal{M}_{B,2}^{k_m} - \varepsilon_c \mathcal{M}_{B,2}^{k_c}}{\varepsilon_m - \varepsilon_c} + O(\delta^3) \end{pmatrix},$$

and the material parameter contrasts λ_μ and λ_ε are given by

$$\lambda_\mu = \frac{\mu_c + \mu_m}{2(\mu_m - \mu_c)}, \quad \lambda_\varepsilon = \frac{\varepsilon_c + \varepsilon_m}{2(\varepsilon_m - \varepsilon_c)}. \tag{9.20}$$

It is clear that

$$\mathcal{W}_B(0) = \mathcal{W}_{B,0} = \begin{pmatrix} \lambda_\mu I - \mathcal{M}_B & 0 \\ 0 & \lambda_\varepsilon I - \mathcal{M}_B \end{pmatrix}.$$

Moreover,

$$\mathcal{W}_B(\delta) = \mathcal{W}_{B,0} + \delta \mathcal{W}_{B,1} + \delta^2 \mathcal{W}_{B,2} + O(\delta^3),$$

in the sense that

$$\|\mathcal{W}_B(\delta) - \mathcal{W}_{B,0} - \delta \mathcal{W}_{B,1} - \delta^2 \mathcal{W}_{B,2}\| \leq C\delta^3$$

for a constant C independent of δ. Here $\|A\| = \sup_{i,j} \|A_{i,j}\|_{H_T^{-\frac{1}{2}}(\mathrm{div},\partial B)}$ for any operator-valued matrix A with entries $A_{i,j}$.

We are now interested in finding $\mathcal{W}_B^{-1}(\delta)$. The following result holds.

LEMMA 9.7. *The system of equations* (6.7) *is equivalent to*

$$
(9.21)\qquad W_B(\delta)\begin{pmatrix} \eta(\psi)^{(1)} \\ \eta(\psi)^{(2)} \\ \omega\eta(\phi)^{(1)} \\ \omega\eta(\phi)^{(2)} \end{pmatrix} = \left.\begin{pmatrix} \dfrac{\eta(\nu\times E^i)^{(1)}}{\mu_m-\mu_c} \\ \dfrac{\eta(\nu\times E^i)^{(2)}}{\mu_m-\mu_c} \\ \dfrac{\eta(\sqrt{-1}\nu\times H^i)^{(1)}}{\varepsilon_m-\varepsilon_c} \\ \dfrac{\eta(\sqrt{-1}\nu\times H^i)^{(2)}}{\varepsilon_m-\varepsilon_c} \end{pmatrix}\right|_{\partial B},
$$

where

$$
W_B(\delta) = W_{B,0} + \delta W_{B,1} + \delta^2 W_{B,2} + O(\delta^3)
$$

with

$$
\begin{aligned}
W_{B,0} &= \begin{pmatrix} \lambda_\mu I - \widetilde{\mathcal{M}}_B & O \\ O & \lambda_\varepsilon I - \widetilde{\mathcal{M}}_B \end{pmatrix}, \\
W_{B,1} &= \begin{pmatrix} O & \dfrac{1}{\mu_m-\mu_c}\widetilde{\mathcal{L}}_{B,1} \\ \dfrac{1}{\varepsilon_m-\varepsilon_c}\widetilde{\mathcal{L}}_{B,1} & O \end{pmatrix}, \\
W_{B,2} &= \begin{pmatrix} \dfrac{1}{\mu_m-\mu_c}\widetilde{\mathcal{M}}^\mu_{B,2} & \dfrac{1}{\mu_m-\mu_c}\widetilde{\mathcal{L}}_{B,2} \\ \dfrac{1}{\varepsilon_m-\varepsilon_c}\widetilde{\mathcal{L}}_{B,2} & \dfrac{1}{\varepsilon_m-\varepsilon_c}\widetilde{\mathcal{M}}^\varepsilon_{B,2} \end{pmatrix},
\end{aligned}
$$

and

$$
\begin{aligned}
\widetilde{\mathcal{M}}_B &= \begin{pmatrix} -\Delta_{\partial B}^{-1}(\mathcal{K}_B^0)^*\Delta_{\partial B} & 0 \\ \mathcal{R}_B & \mathcal{K}_B^0 \end{pmatrix}, \\
\widetilde{\mathcal{M}}^\mu_{B,2} &= \begin{pmatrix} \Delta_{\partial B}^{-1}\nabla_{\partial B}\cdot(\mu_m\mathcal{M}^{k_m}_{B,2}-\mu_c\mathcal{M}^{k_c}_{B,2})\nabla_{\partial B} & \Delta_{\partial B}^{-1}\nabla_{\partial B}\cdot(\mu_m\mathcal{M}^{k_m}_{B,2}-\mu_c\mathcal{M}^{k_c}_{B,2})\vec{\mathrm{curl}}_{\partial B} \\ -\Delta_{\partial B}^{-1}\mathrm{curl}_{\partial B}(\mu_m\mathcal{M}^{k_m}_{B,2}-\mu_c\mathcal{M}^{k_c}_{B,2})\nabla_{\partial B} & -\Delta_{\partial B}^{-1}\mathrm{curl}_{\partial B}(\mu_m\mathcal{M}^{k_m}_{B,2}-\mu_c\mathcal{M}^{k_c}_{B,2})\vec{\mathrm{curl}}_{\partial B} \end{pmatrix}, \\
\widetilde{\mathcal{M}}^\varepsilon_{B,2} &= \begin{pmatrix} \Delta_{\partial B}^{-1}\nabla_{\partial B}\cdot(\varepsilon_m\mathcal{M}^{k_m}_{B,2}-\varepsilon_c\mathcal{M}^{k_c}_{B,2})\nabla_{\partial B} & \Delta_{\partial B}^{-1}\nabla_{\partial B}\cdot(\varepsilon_m\mathcal{M}^{k_m}_{B,2}-\varepsilon_c\mathcal{M}^{k_c}_{B,2})\vec{\mathrm{curl}}_{\partial B} \\ -\Delta_{\partial B}^{-1}\mathrm{curl}_{\partial B}(\varepsilon_m\mathcal{M}^{k_m}_{B,2}-\varepsilon_c\mathcal{M}^{k_c}_{B,2})\nabla_{\partial B} & -\Delta_{\partial B}^{-1}\mathrm{curl}_{\partial B}(\varepsilon_m\mathcal{M}^{k_m}_{B,2}-\varepsilon_c\mathcal{M}^{k_c}_{B,2})\vec{\mathrm{curl}}_{\partial B} \end{pmatrix}, \\
\widetilde{\mathcal{L}}_{B,s} &= \begin{pmatrix} \Delta_{\partial B}^{-1}\nabla_{\partial B}\cdot\mathcal{L}_{B,s}\nabla_{\partial B} & \Delta_{\partial B}^{-1}\nabla_{\partial B}\cdot\mathcal{L}_{B,s}\vec{\mathrm{curl}}_{\partial B} \\ -\Delta_{\partial B}^{-1}\mathrm{curl}_{\partial B}\mathcal{L}_{B,s}\nabla_{\partial B} & -\Delta_{\partial B}^{-1}\mathrm{curl}_{\partial B}\mathcal{L}_{B,s}\vec{\mathrm{curl}}_{\partial B} \end{pmatrix}
\end{aligned}
$$

for $s = 1, 2$.

Moreover, the eigenfunctions of $W_{B,0}$ *in* $H(\partial B)^2$ *are given by*

$$
\begin{aligned}
\Psi_{1,j,i} &= \begin{pmatrix} \psi_{j,i} \\ O \end{pmatrix}, \quad j = 0,1,2,\ldots; i = 1,2,3, \\
\Psi_{2,j,i} &= \begin{pmatrix} O \\ \psi_{j,i} \end{pmatrix}, \quad j = 0,1,2,\ldots; i = 1,2,3,
\end{aligned}
$$

associated to the eigenvalues $\lambda_\mu - \lambda_{j,i}$ and $\lambda_\varepsilon - \lambda_{j,i}$, respectively, and generalized eigenfunctions of order one

$$\Psi_{1,j,3,g} = \begin{pmatrix} \psi_{j,3,g} \\ O \end{pmatrix}, \qquad \Psi_{2,j,3,g} = \begin{pmatrix} O \\ \psi_{j,3,g} \end{pmatrix},$$

associated to eigenvalues $\lambda_\mu - \lambda_{j,3}$ and $\lambda_\varepsilon - \lambda_{j,3}$, respectively, all of which form a non-orthogonal basis of $H(\partial B)^2$.

We regard the operator $W_B(\delta)$ as a perturbation of the operator $W_{B,0}$ for small δ. Using perturbation theory, we can derive the perturbed eigenvalues and their associated eigenfunctions in $H(\partial B)^2$.

We denote by $\Gamma = \big\{(k,j,i) : k = 1,2; j = 1,2,\ldots; i = 1,2,3\big\}$ the set of indices for the eigenfunctions of $W_{B,0}$ and by $\Gamma_g = \big\{(k,j,3,g) : k = 1,2; j = 1,2,\ldots\big\}$ the set of indices for the generalized eigenfunctions. We denote by γ_g the generalized eigenfunction index corresponding to eigenfunction index γ and vice-versa. We also denote by

$$\tau_\gamma = \begin{cases} \lambda_\mu - \lambda_{j,i}, & k = 1, \\ \lambda_\varepsilon - \lambda_{j,i}, & k = 2. \end{cases} \tag{9.22}$$

CONDITION 9.8. $\lambda_\mu \neq \lambda_\varepsilon$.

In the following we only consider those $\gamma \in \Gamma$ for which there is no associated generalized eigenfunction index. In other words, we only consider $\gamma = (k,i,j) \in \Gamma$ such that $\lambda_{j,i} \in \sigma_1 \cup \sigma_2$. We call this subset Γ_{sim}. Note that Condition 9.8 implies that the eigenvalues of $W_{B,0}$ indexed by $\gamma \in \Gamma_{\mathrm{sim}}$ are simple.

THEOREM 9.9. *As $\delta \to$, the perturbed eigenvalues and eigenfunctions indexed by $\gamma \in \Gamma_{\mathrm{sim}}$ have the following asymptotic expansions:*

$$\begin{aligned} \tau_\gamma(\delta) &= \tau_\gamma + \delta\tau_{\gamma,1} + \delta^2\tau_{\gamma,2} + O(\delta^3), \\ \Psi_\gamma(\delta) &= \Psi_\gamma + \delta\Psi_{\gamma,1} + O(\delta^2), \end{aligned} \tag{9.23}$$

where

$$\begin{aligned} \tau_{\gamma,1} &= \frac{\langle W_{B,1}\Psi_\gamma, \widetilde{\Psi}_\gamma\rangle_{H(\partial B)^2}}{\langle \Psi_\gamma, \widetilde{\Psi}_\gamma\rangle_{H(\partial B)^2}} = 0, \\ \tau_{\gamma,2} &= \frac{\langle W_{B,2}\Psi_\gamma, \widetilde{\Psi}_\gamma\rangle_{H(\partial B)^2} - \langle W_{B,1}\Psi_{\gamma,1}, \widetilde{\Psi}_\gamma\langle_{H(\partial B)^2}}{\langle \Psi_\gamma, \widetilde{\Psi}_\gamma\rangle_{H(\partial B)^2}}, \\ (\tau_\gamma - W_{B,0})\Psi_{\gamma,1} &= -W_{B,1}\Psi_\gamma. \end{aligned} \tag{9.24}$$

Here, $\widetilde{\Psi}_{\gamma'} \in \mathrm{Ker}(\bar{\tau}_{\gamma'} - W_{B,0}^*)$ and $W_{B,0}^*$ is the $H(\partial B)^2$ adjoint of $W_{B,0}$.

We can solve $\Psi_{\gamma,1}$. Indeed,

$$\Psi_{\gamma,1} = \sum_{\substack{\gamma'\in\Gamma \\ \gamma'\neq\gamma}} \frac{\alpha(-W_{B,1}\Psi_\gamma, \Psi_{\gamma'})\Psi_{\gamma'}}{\tau_\gamma - \tau_{\gamma'}} + \sum_{\substack{\gamma'_g\in\Gamma_g \\ \gamma'\neq\gamma}} \alpha(-W_{B,1}\Psi_\gamma, \Psi_{\gamma'_g}) \left(\frac{\Psi_{\gamma'_g}}{\tau_\gamma - \tau_{\gamma'}} + \frac{\Psi_{\gamma'}}{(\tau_\gamma - \tau_{\gamma'})^2} \right) + \alpha(-W_{B,1}\Psi_\gamma, \Psi_\gamma)\Psi_\gamma.$$

By abuse of notation,

$$\alpha(x,\Psi_\gamma) = \begin{cases} \alpha(x_1,\psi_\kappa) & \gamma=(1,j,i),\ \kappa=(j,i), \\ \alpha(x_2,\psi_\kappa) & \gamma=(2,j,i),\ \kappa=(j,i), \end{cases} \tag{9.25}$$

for

$$x = \begin{pmatrix} x_1 \\ x_2 \end{pmatrix} \in H(\partial B)^2.$$

Consider now the degenerate case $\gamma \in \Gamma\backslash\Gamma_{\text{sim}} =: \Gamma_{\text{deg}} = \{\gamma = (k,i,j) \in \Gamma$ s.t $\lambda_{j,i} \in \sigma_3\}$. It is clear that, for $\gamma \in \Gamma_{\text{deg}}$, the algebraic multiplicity of the eigenvalue τ_γ is 2 while the geometric multiplicity is 1. In this case every eigenvalue τ_γ and associated eigenfunction Ψ_γ will split into two branches, as δ goes to zero, represented by a convergent Puiseux series as

$$\begin{aligned} \tau_{\gamma,h}(\delta) &= \tau_\gamma + (-1)^h\delta^{1/2}\tau_{\gamma,1} + (-1)^{2h}\delta^{2/2}\tau_{\gamma,2} + O(\delta^{3/2}), \quad h=0,1, \\ \Psi_{\gamma,h}(\delta) &= \Psi_\gamma + (-1)^h\delta^{1/2}\Psi_{\gamma,1} + (-1)^{2h}\delta^{2/2}\Psi_{\gamma,2} + O(\delta^{3/2}), \quad h=0,1, \end{aligned} \tag{9.26}$$

where $\tau_{\gamma,j}$ and $\Psi_{\gamma,j}$ can be recovered by recurrence formulas. See Section 2.4.2 for more information.

Recall that the electric and magnetic parameters, ε_c and μ_c, depend on the frequency of the incident field, ω, following a Drude model. Therefore, the eigenvalues of the operator $W_{B,0}$ and perturbation in the eigenvalues depend on the frequency as well, that is,

$$\begin{aligned} \tau_\gamma(\delta,\omega) &= \tau_\gamma(\omega) + \delta^2\tau_{\gamma,2}(\omega) + O(\delta^3), \quad \gamma \in \Gamma_{\text{sim}}, \\ \tau_{\gamma,h}(\delta,\omega) &= \tau_\gamma + \delta^{1/2}(-1)^h\tau_{\gamma,1}(\omega) + \delta^{2/2}(-1)^{2h}\tau_{\gamma,2}(\omega) + O(\delta^{3/2}), \quad \gamma \in \Gamma_{\text{deg}}, \quad h=0,1. \end{aligned}$$

In the sequel, we will omit frequency dependence to simplify the notation. However, it is important to keep in mind that all these quantities are actually frequency dependent.

We first state the following result.

PROPOSITION 9.10. *If ω is a quasi-static plasmonic resonance, then $|\tau_\gamma| \ll 1$ and is locally minimized for some $\gamma \in \Gamma$ with τ_γ being defined by* (9.22).

Then we recall two different notions of plasmonic resonance.

DEFINITION 9.11.
- (i) We say that ω is a plasmonic resonance if $|\tau_\gamma(\delta)| \ll 1$ and is locally minimized for some $\gamma \in \Gamma_{\text{sim}}$ or $|\tau_{\gamma,h}(\delta)| \ll 1$ and is locally minimized for some $\gamma \in \Gamma_{\text{deg}}$, $h=0,1$.
- (ii) We say that ω is a first-order corrected quasi-static plasmonic resonance if $|\tau_\gamma + \delta^2\tau_{\gamma,2}| \ll 1$ and is locally minimized for some $\gamma \in \Gamma_{\text{sim}}$ or $|\tau_\gamma + \delta^{1/2}(-1)^h\tau_{\gamma,1}| \ll 1$ and is locally minimized for some $\gamma \in \Gamma_{\text{deg}}$, $h=0,1$. Here, the correction terms $\tau_{\gamma,2}$ and $\tau_{\gamma,1}$ are defined by (9.24) and (9.26).

Note that quasi-static resonance is size independent and is therefore a zero-order approximation of the plasmonic resonance in terms of the particle size while the first-order corrected quasi-static plasmonic resonance depends on the size of the nanoparticle.

We are interested in solving equation (9.21)

$$W_B(\delta)[\Psi] = f,$$

where

$$\Psi = \begin{pmatrix} \eta(\psi)^{(1)} \\ \eta(\psi)^{(2)} \\ \omega\eta(\phi)^{(1)} \\ \omega\eta(\phi)^{(2)} \end{pmatrix}, f = \left.\begin{pmatrix} \dfrac{\eta(\nu \times E^i)^{(1)}}{\mu_m - \mu_c} \\ \dfrac{\eta(\nu \times E^i)^{(2)}}{\mu_m - \mu_c} \\ \dfrac{\eta(\sqrt{-1}\nu \times H^i)^{(1)}}{\varepsilon_m - \varepsilon_c} \\ \dfrac{\eta(\sqrt{-1}\nu \times H^i)^{(2)}}{\varepsilon_m - \varepsilon_c} \end{pmatrix}\right|_{\partial B}$$

for ω close to the resonance frequencies, i.e., when $\tau_\gamma(\delta)$ is very small for some γ's $\in \Gamma_{\text{sim}}$ or $\tau_{\gamma,h}(\delta)$ is very small for some γ's $\in \Gamma_{\text{deg}}$, $h = 0, 1$. In this case, the major part of the solution would be the contributions of the excited resonance modes $\Psi_\gamma(\delta)$ and $\Psi_{\gamma,h}(\delta)$.

It is important to remark that problem (6.7) could be ill-posed if either $\Re(\varepsilon_c) \leq 0$ or $\Re(\mu_c) \leq 0$ (the imaginary part being very small), and these are precisely the cases for which we will find the resonances described above. In fact, the approach we take is to solve the problem for the cases $\Re(\varepsilon_c) > 0$ or $\Re(\mu_c) > 0$ and then, analytically continue the solution to the general case. The resonances are the values of ω for which this analytic continuation "almost" ceases to be valid.

We introduce the following definition.

DEFINITION 9.12. We call $J \subset \Gamma$ an index set of resonances if the τ_γ's are close to zero when $\gamma \in \Gamma$ and are bounded from below when $\gamma \in \Gamma^c$. More precisely, we choose a threshold number $\eta_0 > 0$ independent of ω such that

$$|\tau_\gamma| \geq \eta_0 > 0 \quad \text{for } \gamma \in J^c.$$

From now on, we shall use J as our index set of resonances. For simplicity, we assume throughout this paper that the following condition holds.

CONDITION 9.13. *We assume that* $\lambda_\mu \neq 0$, $\lambda_\varepsilon \neq 0$ *or equivalently,* $\mu_c \neq -\mu_m$, $\varepsilon_c \neq -\varepsilon_m$.

It follows that the set J is finite.

Consider the space $\mathcal{E}_J = \text{span}\{\Psi_\gamma(\delta), \Psi_{\gamma,h}(\delta);\ \gamma \in J,\ h = 0, 1\}$. Note that, under Condition 9.13, $\mathcal{E}_J$ is finite dimensional. Similarly, we define $\mathcal{E}_{J^c}$ as the spanned by $\Psi_\gamma(\delta), \Psi_{\gamma,h}(\delta);\ \gamma \in J^c$, $h = 0, 1$ and eventually other vectors to complete the base. We have $H(\partial B)^2 = \mathcal{E}_J \oplus \mathcal{E}_{J^c}$.

We define $P_J(\delta)$ and $P_{J^c}(\delta)$ as the (non-orthogonal) projection into the finite-dimensional space $\mathcal{E}_J$ and infinite-dimensional space $\mathcal{E}_{J^c}$, respectively. It is clear that, for any $f \in H(\partial B)^2$

$$f = P_J(\delta)[f] + P_{J^c}(\delta)[f].$$

Moreover, we have an explicit representation for $P_J(\delta)$

$$P_J(\delta)[f] = \sum_{\gamma \in J \cap \Gamma_{\text{sim}}} \alpha_\delta(f, \Psi_\gamma(\delta))\Psi_\gamma(\delta) + \sum_{\substack{\gamma \in J \cap \Gamma_{\text{deg}} \\ h=0,1}} \alpha_\delta(f, \Psi_{\gamma,h}(\delta))\Psi_{\gamma,h}(\delta). \tag{9.27}$$

Here,

$$\begin{aligned}
\alpha_\delta(f,\Psi_\gamma(\delta)) &= \frac{\langle f,\tilde{\Psi}_\gamma(\delta)\rangle_{H(\partial B)^2}}{\langle \Psi_\gamma(\delta),\tilde{\Psi}_\gamma(\delta)\rangle_{H(\partial B)^2}}, \quad \gamma\in J\cap\Gamma_{\text{sim}},\\
\alpha_\delta(f,\Psi_{\gamma,h}(\delta)) &= \frac{\langle f,\tilde{\Psi}_{\gamma,h}(\delta)\rangle_{H(\partial B)^2}}{\langle \Psi_{\gamma,h}(\delta),\tilde{\Psi}_{\gamma,h}(\delta)\rangle_{H(\partial B)^2}}, \quad \gamma\in J\cap\Gamma_{\text{deg}},\ h=0,1,
\end{aligned}$$

where $\widetilde{\Psi}_\gamma \in \mathrm{Ker}(\bar{\tau}_{\gamma,h}(\delta)-W_B^*(\delta))$, $\widetilde{\Psi}_{\gamma,h}\in \mathrm{Ker}(\bar{\tau}_{\gamma,h}(\delta)-W_B^*(\delta))$ and $W_B^*(\delta)$ is the $H(\partial B)^2$-adjoint of $W_B(\delta)$.

We are now ready to solve the equation $W_B(\delta)\Psi = f$. We have

(9.28)

$$\Psi = W_B^{-1}(\delta)[f] = \sum_{\gamma\in J\cap\Gamma_{\text{sim}}} \frac{\alpha_\delta(f,\Psi_\gamma(\delta))\Psi_\gamma(\delta)}{\tau_\gamma(\delta)} + \sum_{\substack{\gamma\in J\cap\Gamma_{\text{deg}}\\ h=0,1}} \frac{\alpha_\delta(f,\Psi_{\gamma,h}(\delta))\Psi_{\gamma,h}(\delta)}{\tau_{\gamma,h}(\delta)} + W_B^{-1}(\delta)P_{J^c}(\delta)[f].$$

The following lemma holds.

LEMMA 9.14. *The norm $\|W_B^{-1}(\delta)P_{J^c}(\delta)\|_{\mathcal{L}(H(\partial B)^2,H(\partial B)^2)}$ is uniformly bounded in ω and δ.*

PROOF. Consider the operator

$$W_B(\delta)|_{J^c} : P_{J^c}(\delta)H(\partial B)^2 \to P_{J^c}(\delta)H(\partial B)^2.$$

We can show that for every ω and δ, $\mathrm{dist}(\sigma(W_B(\delta)|_{J^c}),0)\geq \frac{\eta_0}{2}$, where $\sigma(W_B(\delta)|_{J^c})$ is the discrete spectrum of $W_B(\delta)|_{J^c}$. Here and throughout this section, dist denotes the distance. Then, it follows that

$$\|W_B^{-1}(\delta)P_{J^c}(\delta)[f]\| = \|W_B^{-1}(\delta)|_{J^c}P_{J^c}(\delta)[f]\| \lesssim \frac{1}{\eta_0}\exp(\frac{C_1}{\eta_0^2})\|P_{J^c}(\delta)[f]\| \lesssim \frac{1}{\eta_0}\exp(\frac{C_1}{\eta_0^2})\|f\|,$$

where the notation $A\lesssim B$ means that $A\leq CB$ for some constant C independent of A and B. □

Finally, we are ready to state our main result in this section.

THEOREM 9.15. *Let η be defined by (9.1). Under Conditions 9.8 and 9.13, the scattered field $E^s = E - E^i$ due to a single plasmonic particle has the following representation:*

$$E^s = \mu_m \nabla\times\vec{\mathcal{S}}_D^{k_m}[\psi](x) + \nabla\times\nabla\times\vec{\mathcal{S}}_D^{k_m}[\phi](x) \qquad x\in\mathbb{R}^3\backslash\bar{D},$$

where

$$\begin{aligned}
\psi &= \eta^{-1}\big(\nabla_{\partial B}\widetilde{\psi}^{(1)} + \vec{\mathrm{curl}}_{\partial B}\widetilde{\psi}^{(2)}\big),\\
\phi &= \frac{1}{\omega}\eta^{-1}\big(\nabla_{\partial B}\widetilde{\phi}^{(1)} + \vec{\mathrm{curl}}_{\partial B}\widetilde{\phi}^{(2)}\big),
\end{aligned}$$

$$\Psi = \begin{pmatrix} \widetilde{\psi}^{(1)}\\ \widetilde{\psi}^{(2)}\\ \widetilde{\phi}^{(1)}\\ \widetilde{\phi}^{(2)} \end{pmatrix} = \sum_{\gamma\in J\cap\Gamma_{\text{sim}}} \frac{\alpha(f,\Psi_\gamma)\Psi_\gamma + O(\delta)}{\tau_\gamma(\delta)} + \sum_{\gamma\in J\cap\Gamma_{\text{deg}}} \frac{\zeta_1(f)\Psi_\gamma + \zeta_2(f)\Psi_{\gamma,1} + O(\delta^{1/2})}{\tau_{\gamma,0}(\delta)\tau_{\gamma,1}(\delta)} + O(1),$$

and

$$\begin{aligned}
\zeta_1(f) &= \frac{\langle f,\tilde{\Psi}_{\gamma,1}\rangle_{H(\partial B)^2}\tau_\gamma - \langle f,\tilde{\Psi}_\gamma\rangle_{H(\partial B)^2}(\tau_{\gamma,1}+\tau_\gamma\frac{a_2}{a_1})}{a_1},\\
\zeta_2(f) &= \frac{\langle f,\tilde{\Psi}_\gamma\rangle_{H(\partial B)^2}}{a_1},\\
a_1 &= \langle \Psi_\gamma,\tilde{\Psi}_{\gamma,1}\rangle_{H(\partial B)^2} + \langle \Psi_{\gamma,1},\tilde{\Psi}_\gamma\rangle_{H(\partial B)^2},\\
a_2 &= \langle \Psi_\gamma,\tilde{\Psi}_{\gamma,2}\rangle_{H(\partial B)^2} + \langle \Psi_{\gamma,2},\tilde{\Psi}_\gamma\rangle_{H(\partial B)^2} + \langle \Psi_{\gamma,1},\tilde{\Psi}_{\gamma,1}\rangle_{H(\partial B)^2}.
\end{aligned}$$

PROOF. Recall that

$$\Psi = \sum_{\gamma\in J\cap\Gamma_{\mathrm{sim}}} \frac{\alpha_\delta(f,\Psi_\gamma(\delta))\Psi_\gamma(\delta)}{\tau_\gamma(\delta)} + \sum_{\substack{\gamma\in J\cap\Gamma_{\mathrm{deg}}\\ h=0,1}} \frac{\alpha_\delta(f,\Psi_{\gamma,h}(\delta))\Psi_{\gamma,h}(\delta)}{\tau_{\gamma,h}(\delta)} + W_B^{-1}(\delta)P_{J^c}(\delta)[f].$$

By Lemma 9.14, we have $W_B^{-1}(\delta)P_{J^c}(\delta)[f] = O(1)$.
If $\gamma\in J\cap\Gamma_{\mathrm{sim}}$, an asymptotic expansion on δ yields

$$\alpha_\delta(f,\Psi_\gamma(\delta))\Psi_\gamma(\delta) = \alpha(f,\Psi_\gamma)\Psi_\gamma + O(\delta).$$

If $\gamma\in J\cap\Gamma_{\mathrm{deg}}$ then $\langle\Psi_\gamma,\tilde{\Psi}_\gamma\rangle_{H(\partial B)^2} = 0$. Therefore, an asymptotic expansion on δ yields

$$\begin{aligned}
\alpha_\delta(f,\Psi_{\gamma,h}(\delta))\Psi_{\gamma,h}(\delta) &= \frac{(-1)^h\langle f,\tilde{\Psi}_\gamma\rangle_{H(\partial B)^2}\Psi_\gamma}{\delta^{-1/2}a_1} +\\
&\quad \frac{1}{a_1}\left((\langle f,\tilde{\Psi}_{\gamma,1}\rangle_{H(\partial B)^2} - \langle f,\tilde{\Psi}_\gamma\rangle_{H(\partial B)^2}\frac{a_2}{a_1})\Psi_\gamma + \langle f,\tilde{\Psi}_\gamma\rangle_{H(\partial B)^2}\Psi_{\gamma,1}\right)\\
&\quad +O(\delta^{1/2})
\end{aligned}$$

with

$$\begin{aligned}
a_1 &= \langle \Psi_\gamma,\tilde{\Psi}_{\gamma,1}\rangle_{H(\partial B)^2} + \langle \Psi_{\gamma,1},\tilde{\Psi}_\gamma\rangle_{H(\partial B)^2},\\
a_2 &= \langle \Psi_\gamma,\tilde{\Psi}_{\gamma,2}\rangle_{H(\partial B)^2} + \langle \Psi_{\gamma,2},\tilde{\Psi}_\gamma\rangle_{H(\partial B)^2} + \langle \Psi_{\gamma,1},\tilde{\Psi}_{\gamma,1}\rangle_{H(\partial B)^2}.
\end{aligned}$$

Since $\tau_{\gamma,h}(\delta) = \tau_\gamma + \delta^{1/2}(-1)^h\tau_{\gamma,1} + O(\delta)$, the result follows by adding the terms

$$\frac{\alpha_\delta(f,\Psi_{\gamma,0}(\delta))\Psi_{\gamma,0}(\delta)}{\tau_{\gamma,0}(\delta)} \quad\text{and}\quad \frac{\alpha_\delta(f,\Psi_{\gamma,1}(\delta))\Psi_{\gamma,1}(\delta)}{\tau_{\gamma,1}(\delta)}.$$

The proof is then complete. □

COROLLARY 9.16. *Assume the same conditions as in Theorem 9.15. Under the additional condition that*

$$\min_{\gamma\in J\cap\Gamma_{\mathrm{sim}}} |\tau_\gamma(\delta)| \gg \delta^3, \quad \min_{\gamma\in J\cap\Gamma_{\mathrm{deg}}} |\tau_\gamma(\delta)| \gg \delta, \tag{9.29}$$

we have

$$\Psi = \sum_{\gamma\in J\cap\Gamma_{\mathrm{sim}}} \frac{\alpha(f,\Psi_\gamma)\Psi_\gamma + O(\delta)}{\tau_\gamma + \delta^2\tau_{\gamma,2}} + \sum_{\gamma\in J\cap\Gamma_{\mathrm{deg}}} \frac{\zeta_1(f)\Psi_\gamma + \zeta_2(f)\Psi_{\gamma,1} + O(\delta^{1/2})}{\tau_\gamma^2 - \delta\tau_{\gamma,1}^2} + O(1).$$

COROLLARY 9.17. *Assume the same conditions as in Theorem 9.15. Under the additional condition that*

$$\min_{\gamma\in J\cap\Gamma_{\mathrm{sim}}}|\tau_\gamma(\delta)|\gg\delta^2,\quad \min_{\gamma\in J\cap\Gamma_{\mathrm{deg}}}|\tau_\gamma(\delta)|\gg\delta^{1/2}, \tag{9.30}$$

we have

$$\Psi=\sum_{\gamma\in J\cap\Gamma_{\mathrm{sim}}}\frac{\alpha(f,\Psi_\gamma)\Psi_\gamma+O(\delta)}{\tau_\gamma}+\sum_{\gamma\in J\cap\Gamma_{\mathrm{deg}}}\frac{\alpha(f,\Psi_\gamma)\Psi_\gamma}{\tau_\gamma}+\alpha(f,\Psi_{\gamma,g})\left(\frac{\Psi_{\gamma,g}}{\tau_\gamma}+\frac{\Psi_\gamma}{\tau_\gamma^2}\right)+O(1).$$

PROOF. We have

$$\begin{aligned}
\lim_{\delta\to 0}W_B^{-1}(\delta)P_{\mathrm{span}\{\Psi_{\gamma,0}(\delta),\Psi_{\gamma,1}(\delta)\}}[f] &= \lim_{\delta\to 0}\frac{\alpha_\delta(f,\Psi_{\gamma,0}(\delta))\Psi_{\gamma,0}(\delta)}{\tau_{\gamma,0}(\delta)}+\frac{\alpha_\delta(f,\Psi_{\gamma,1}(\delta))\Psi_{\gamma,1}(\delta)}{\tau_{\gamma,1}(\delta)}\\
&= W_{B,0}^{-1}(\delta)P_{\mathrm{span}\{\Psi_\gamma,\Psi_{\gamma_g}\}}[f]\\
&= \frac{\alpha(f,\Psi_\gamma)\Psi_\gamma}{\tau_\gamma}+\alpha(f,\Psi_{\gamma,g})\left(\frac{\Psi_{\gamma,g}}{\tau_\gamma}+\frac{\Psi_\gamma}{\tau_\gamma^2}\right),
\end{aligned}$$

where $\gamma\in J\cap\Gamma_{\mathrm{deg}}$, $f\in H(\partial B)^2$ and)$P_{\mathrm{span}E}$ is the projection into the linear space generated by the elements in the set E. □

REMARK 9.18. Note that for $\gamma\in J$,

$$\tau_\gamma\approx\min\Big\{\mathrm{dist}\big(\lambda_\mu,\sigma((\mathcal{K}_B^0)^*)\cup-\sigma((\mathcal{K}_B^0)^*)\big),\mathrm{dist}\big(\lambda_\varepsilon,\sigma((\mathcal{K}_B^0)^*)\cup-\sigma((\mathcal{K}_B^0)^*)\big)\Big\}.$$

It is clear, from Remark 9.18, that resonances can occur when exciting the spectrum of $(\mathcal{K}_B^0)^*$ or/and that of $-(\mathcal{K}_B^0)^*$. We substantiate in the following that only the spectrum of $(\mathcal{K}_B^0)^*$ can be excited to create the plasmonic resonances in the quasi-static regime.

Recall that

$$f=\left.\begin{pmatrix}\dfrac{\eta(\nu\times E^i)^{(1)}}{\mu_m-\mu_c}\\ \dfrac{\eta(\nu\times E^i)^{(2)}}{\mu_m-\mu_c}\\ \dfrac{\eta(\sqrt{-1}\nu\times H^i)^{(1)}}{\varepsilon_m-\varepsilon_c}\\ \dfrac{\eta(\sqrt{-1}\nu\times H^i)^{(2)}}{\varepsilon_m-\varepsilon_c}\end{pmatrix}\right|_{\partial B},$$

and therefore,

$$f_1:=\frac{\eta(\nu\times E^i)^{(1)}}{\mu_m-\mu_c}=\frac{\Delta_{\partial B}^{-1}\nabla_{\partial B}\cdot\eta(\nu\times E^i)}{\mu_m-\mu_c}.$$

Now, suppose $\gamma=(1,j,1)\in J$ (recall that J is the index set of resonances). Then $\tau_\gamma=\lambda_\mu-\lambda_{1,j}$, where $\lambda_{1,j}\in\sigma_1=\sigma(-(\mathcal{K}_B^0)^*)\backslash\sigma((\mathcal{K}_B^0)^*)$. We have

$$\alpha(f,\Psi_\gamma)=\langle\Delta_{\partial B}f_1,\varphi_{j,1}\rangle_{\mathcal{H}^*}=\alpha(f,\Psi_\gamma)=\frac{1}{\mu_m-\mu_c}\langle\nabla_{\partial B}\cdot\eta(\nu\times E^i),\varphi_{j,1}\rangle_{\mathcal{H}^*},$$

where $\varphi_{j,1}\in\mathcal{H}_0^*(\partial B)$ is a normalized eigenfunction of $(\mathcal{K}_B^0)^*(\partial B)$.

A Taylor expansion of E^i gives, for $x \in \partial D$,

$$E^i(x) = \sum_{\beta \in \mathbb{N}^3}^{\infty} \frac{(x-z)^\beta \partial^\beta E^i(z)}{|\beta|!}.$$

Thus,

$$\eta(\nu \times E^i)(\tilde{x}) = \eta(\nu)(\tilde{x}) \times E^i(z) + O(\delta),$$

and

$$\begin{aligned} \nabla_{\partial B} \cdot \eta(\nu \times E^i)(\tilde{x}) &= -\eta(\nu)(\tilde{x}) \cdot \nabla \times E^i(z) + O(\delta) \\ &= O(\delta). \end{aligned}$$

Therefore, the zeroth-order term of the expansion of $\nabla_{\partial B} \cdot \eta(\nu \times E^i)$ in δ is zero. Hence,

$$\alpha(f, \Psi_\gamma) = 0.$$

In the same way, we have

$$\begin{aligned} \alpha(f, \Psi_\gamma) &= 0, \\ \alpha(f, \Psi_{\gamma_g}) &= 0 \end{aligned}$$

for $\gamma = (2, j, 1) \in J$ and γ_g such that $\gamma \in J$.

As a result we see that the spectrum of $-(\mathcal{K}_B^0)^*$ is not excited in the zeroth-order term. However, we note that $\sigma(-(\mathcal{K}_B^0)^*)$ can be excited in higher-order terms.

Finally, we sketch a proof of Theorem 9.1. From (6.5), we have

$$E^s(x) = \mu_m \nabla \times \vec{\mathcal{S}}_D^{k_m}[\psi](x) + \nabla \times \nabla \times \vec{\mathcal{S}}_D^{k_m}[\phi](x), \quad x \in \mathbb{R}^3 \setminus \overline{D},$$

where ψ and ϕ are determined by (9.18). Since $\mathcal{W}_B(\delta) = \mathcal{W}_{B,0} + O(\delta)$, formula (9.2) follows.

9.3.1. Numerical examples. Here we present numerical examples to demonstrate the shift of the plasmonic resonance. The first example involves a spherical nanoparticle of radius R with permittivity ϵ_c. For the permittivity ϵ_c, we use Drude's model as follows: $\epsilon_c(\omega) = 1 - \omega_p^2/(\omega(\omega + i\gamma))$ where $\omega_p = 5.8(eV)$ and $\gamma = 0.2$. We compute the extinction cross section Q^{ext} as a function of the operating wavelength $\lambda = 2\pi c/\omega$. Due to spherical symmetry, it can be shown that Q^{ext} has the following simple representation

$$Q^{ext} = \frac{2}{(k_m R)^2} \sum_{n=1}^{\infty} (2n+1) \Re\{ \frac{\sqrt{-1} k_m}{n(n+1)} (W_n^{TE} + W_n^{TM}) \},$$

where W_n^{TE} and W_n^{TM} are the scattering cofficients of a spherical structure. We have already seen how to compute W_n^{TE} and W_n^{TM}. We repeatedly plot Q^{ext} while changing the radius R from 5 nm to 30 nm in Figure 9.1. The shift of the plasmonic resonance is clearly shown.

We also present a numerical example of a spherical shell with outer radius R and inner radius $R/2$. We assume that the outer sphere has permittivity ϵ_c and that the inner sphere has the same permittivity as background. In Figure 9.1, we plot Q^{ext} for the shell for various values of radius R. Again, the shift of plasmon resonance is clearly shown.

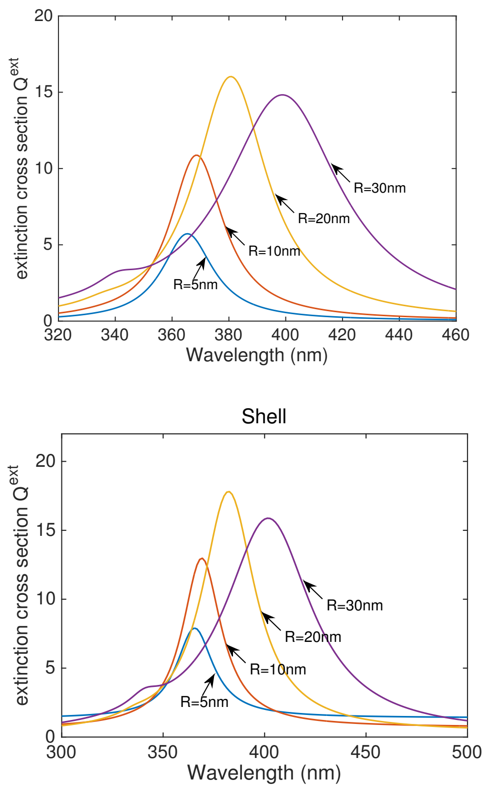

FIGURE 9.1. Extinction cross section Q^{ext} for a spherical nanoparticle and a shell of radius R. We change the radius R from 5 nm to 30 nm. The inner radius of the shell is set to be $R/2$. The shift of plasmon resonance is clearly shown.

9.4. Plasmonic resonance for a system of 3D spheres

Code:	9.2 Plasmonic Resonance for Nearly Touching Spheres	DemoApproxVsExact.m DemoHybridThreeSpheres.m

Confining light at the nanoscale is challenging due to the diffraction limit. Strongly localized surface plasmon modes in singular metallic structures, such as sharp tips and two nearly touching surfaces, offer a promising route to overcome this difficulty. Recently, Transformation Optics (TO) has been applied to analyze various structural singularities and then provides novel physical insights for a broadband nanofocusing of light.

Among 3D singular structures, the system of nearly touching spheres is of fundamental importance. In the narrow gap regions, a large field enhancement occurs. The significant spectral shift of resonance mode also occurs due to the plasmon hybridization. A cluster of plasmonic spheres such as a heptamer and a octamer can support collective resonance modes such as Fano resonances. For theoretical investigations of these phenomena, the numerical computation plays

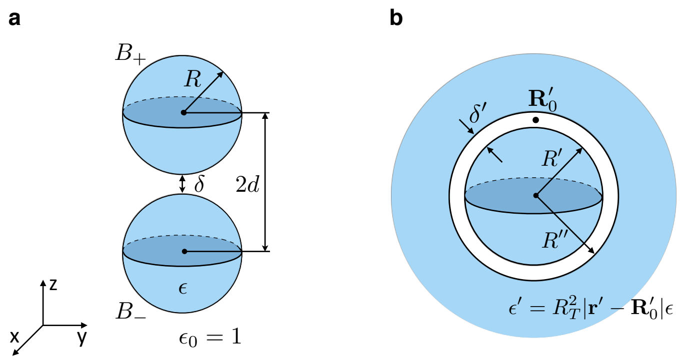

FIGURE 9.2. **Two spheres and the TO inversion mapping.**
a) Two identical spheres, each of radius R and permittivity ϵ, are separated by a distance δ. The distance between their centers is $2d$. The background permittivity is $\epsilon_0 = 1$.
b) The TO inverion mapping transforms the lower sphere B_- (or the upper sphere B_+) into a sphere of radius R' (or a hollow sphere of radius R'') centered at the origin, respectively.

a important role. Unfortunately, in the nearly touching case, it is quite challenging to compute the field distribution in the gap accurately. In fact, the required computational cost dramatically increases as the spheres get closer. The multipole expansion method requires a large number of spherical harmonics and the finite element method (or boundary element method) requires very fine mesh in the gap. Moreover, the linear systems to be solved are ill-conditioned. So conventional numerical methods are time consuming or inaccurate for this extreme case.

Here we present a hybrid numerical scheme that overcomes difficulty. The key idea of our hybrid scheme is to clarify the connection between Transformation Optics and the image charge method.

9.4.1. Two metallic spheres. We consider the two metallic spheres which are shown in Fig. 9.2. The permittivity ϵ of each individual sphere is modeled as $\epsilon = 1 - \omega_p^2/(\omega(\omega + i\gamma))$ where ω is the operating frequency, ω_p is the plasma frequency and γ is the damping parameter. We fit Palik's data for silver by adding a few Lorentz terms. We shall assume that the plasmonic spheres are small compared to optical wavelengths so that the quasi-static approximation can be adopted.

9.4.2. Transformation Optics. Let us briefly review the TO approach by Pendry et al. To transform two spheres into a concentric shell, Pendry et al. introduced the inversion transformation Φ defined as

$$\mathbf{r}' = \Phi(\mathbf{r}) = R_T^2(\mathbf{r} - \mathbf{R}_0)/|\mathbf{r} - \mathbf{R}_0|^2 + \mathbf{R}_0' \tag{9.31}$$

where $\mathbf{R}_0, \mathbf{R}_0'$ and R_T are given parameters. This inversion mapping induces the inhomogeneous permittivity $\epsilon'(\mathbf{r}') = R_T^2|\mathbf{r}' - \mathbf{R}_0'|\epsilon$ in the transformed space. Then,

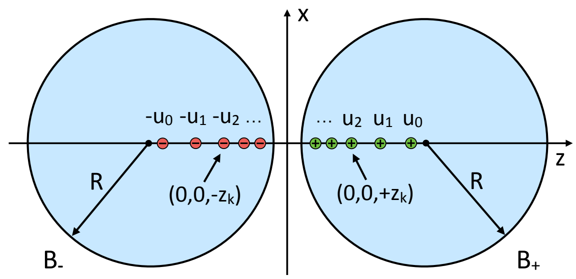

FIGURE 9.3. **Image charges for two spheres.** Red and green circles represent image charges placed along the z-axis.

by taking advantage of the symmetry of the shell, the electric potential can be represented in terms of the following basis functions:

$$\mathcal{M}_{n,\pm}^{m}(\mathbf{r}) = |\mathbf{r}' - \mathbf{R}_0'|(r')^{\pm(n+\frac{1}{2})-\frac{1}{2}} Y_n^m(\theta', \phi') \tag{9.32}$$

where, $\{Y_n^m\}$ are the spherical harmonics. We will call $\mathcal{M}_{n,\pm}^m$ a TO basis.

Let us assume that two plasmonic spheres $B_+ \cup B_-$ are placed in a uniform incident field $(0, 0, E_0\mathrm{Re}\{e^{i\omega t}\})$. Then the (quasi-static) electrical potential V outside the two spheres can be represented in the following form:

$$V(\mathbf{r}) = -E_0 z + \sum_{n=0}^{\infty} A_n \left(\mathcal{M}_{n,+}^0(\mathbf{r}) - \mathcal{M}_{n,-}^0(\mathbf{r})\right) \tag{9.33}$$

Here, the coefficients A_n can be determined by solving some tridiagonal system. Unfortunately, it cannot be solved analytically.

9.4.3. Method of image charges. Now we discuss the method of images. Since the imaging rule for a pair of cylinders is simple, an exact image series solution and its properties can be easily derived. However, for two dielectric spheres, an exact solution cannot be obtained due to the appearance of a continuous line image source. Poladian observed that the continuous source can be well approximated by a point charge and then derived an approximate but analytic image series solution. Let us briefly review Poladian's solution for two dielectric spheres. Let $\tau = (\epsilon - 1)/(\epsilon + 1)$, $s = \cosh^{-1}(d/R)$ and $\alpha = R \sinh s$. Suppose that two point charges of strength ± 1 are located at $(0, 0, \pm z_0) \in B_\pm$, respectively. By Poladian's imaging rule, they produce an infinite series of image charges of strength $\pm u_k$ at $(0, 0, \pm z_k)$ for $k = 0, 1, 2, ...$, where z_k and u_k are given by

$$z_k = \alpha \coth(ks + s + t_0), \quad u_k = \tau^k \frac{\sinh(s + t_0)}{\sinh(ks + s + t_0)}. \tag{9.34}$$

Here, the parameter t_0 is such that $z_0 = \alpha \coth(s + t_0)$. See Fig. 9.3. The potential $U(\mathbf{r})$ generated by all the above image charges is given by

$$U(\mathbf{r}) = \sum_{k=0}^{\infty} u_k (G(\mathbf{r} - \mathbf{z}_k) - G(\mathbf{r} + \mathbf{z}_k)) \tag{9.35}$$

where $\mathbf{z}_k = (0, 0, z_k)$ and $G(\mathbf{r}) = 1/(4\pi|\mathbf{r}|)$.

Let us consider the potential V outside the two spheres when a uniform incident field $(0, 0, E_0\mathrm{Re}\{e^{i\omega t}\})$ is applied. Let p_0 be the induced polarizability when a single sphere is subjected to the uniform incident field, that is, $p_0 = E_0 R^3 2\tau/(3-\tau)$. Using the potential $U(\mathbf{r})$, we can derive an approximate solution for $V(\mathbf{r})$. For $|\tau| \approx 1$, we have

$$V(\mathbf{r}) \approx -E_0 z + 4\pi p_0 \frac{\partial(U(\mathbf{r}))}{\partial z_0}\Big|_{z_0=d} + QU(\mathbf{r})|_{z_0=d}, \tag{9.36}$$

where Q is a constant chosen so that the right-hand side in equation (9.36) has no net flux on the surface of each sphere. The accuracy of the approximate formula, equation (9.36), improves as $|\epsilon|$ increases and it becomes exact when $|\epsilon| = \infty$. Moreover, its accuracy is pretty good even if the value of $|\epsilon|$ is moderate.

We now explain the difficulty involved in applying the the image series solution, equation (9.36), to the case of plasmonic spheres. In view of the expressions for u_k, equation (9.34), we can see that equation (9.36) is not convergent when $|\tau| > e^s$. For plasmonic materials such as gold and silver, the real part of the permittivity ϵ is negative over the optical frequencies and this means that the corresponding parameter $|\tau|$ can attain any value in the interval (e^s, ∞). Moreover, it turns out that all the plasmonic resonant values for τ are contained in the set $\{\tau \in \mathbb{C} : |\tau| > e^s\}$. So, equation (9.36) cannot describe the plasmonic interaction between the spheres due to the non-convergence.

9.4.4. Analytical solution for two plasmonic spheres. Here we present an analytic approximate solution for two plasmonic spheres in a uniform incident field $(0, 0, E_0\mathrm{Re}\{e^{i\omega t}\})$. More importantly, we shall see that our analytical approximation completely captures the singular behavior of the exact solution. This feature is essential in developing our hybrid numerical scheme.

The solution which is valid for two plasmonic spheres can be derived by establishing the explicit connection between TO and the method of image charges. We can convert the image series into a TO-type solution by using the explicit connection formula. The result is shown in the following theorem.

THEOREM 9.19. *If $|\tau| \approx 1$, the following approximation for the electric potential $V(\mathbf{r})$ holds: for $\mathbf{r} \in \mathbb{R}^3 \setminus (B_+ \cup B_-)$,*

$$V(\mathbf{r}) \approx -E_0 z + \sum_{n=0}^{\infty} \widetilde{A}_n \left(\mathcal{M}^0_{n,+}(\mathbf{r}) - \mathcal{M}^0_{n,-}(\mathbf{r})\right) \tag{9.37}$$

where the coefficient $\widetilde{A}_n$ is given by

$$\begin{aligned} \widetilde{A}_n &= E_0 \frac{2\tau\alpha}{3-\tau} \cdot \frac{2n+1-\gamma_0}{e^{(2n+1)s}-\tau} \\ \gamma_0 &= \sum_{n=0}^{\infty} \frac{2n+1}{e^{(2n+1)s}-\tau} \Big/ \sum_{n=0}^{\infty} \frac{1}{e^{(2n+1)s}-\tau}. \end{aligned} \tag{9.38}$$

As expected, the above approximate expression is valid even if $|\tau| > e^s$. Therefore, it can furnish useful information about the plasmonic interaction between the two spheres. As a first demonstration, let us investigate the (approximate) resonance condition, that is, the condition for τ at which the coefficients $\widetilde{A}_n$ diverge. One might conclude that the resonance condition is given by $\tau = e^{(2n+1)s}$. However, one can see that $\widetilde{A}_n$ has a removable singularity at each $\tau = e^{(2n+1)s}$. In fact,

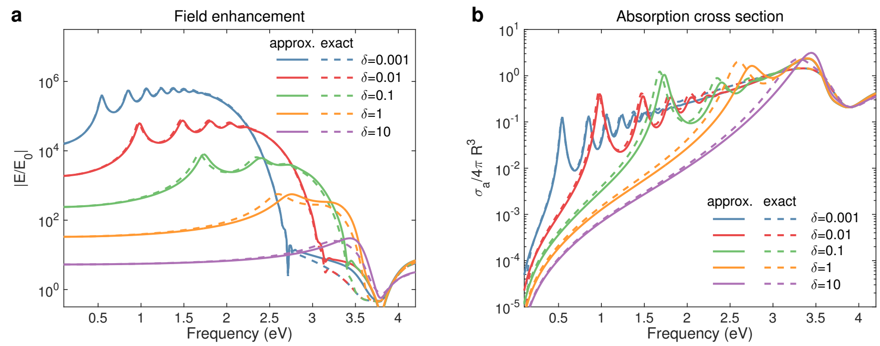

FIGURE 9.4. **Exact solution vs Analytic approximation. a,** Field enhancement plot as a function of frequency ω for various separation distances δ. The solid lines represent the approximate analytical solution and the dashed lines represent the exact solution. Two identical silver spheres of radius 30 nm are considered. **b,** Same as **a** but for the absorption cross section.

the (approximate) resonance condition turns out to be

$$\sum_{n=0}^{\infty} \frac{1}{e^{(2n+1)s} - \tau} = 0. \tag{9.39}$$

In other words, the plasmonic resonance happens when τ is one of the zeros of equation (9.39). It turns out that the zeros $\{\tau_n\}_{n=0}^{\infty}$ lie on the positive real axis and satisfy, for $n = 0, 1, 2, ...,$

$$e^{(2n+1)s} < \tau_n < e^{(2n+3)s}. \tag{9.40}$$

The above estimate helps us understand the asymptotic behavior of the resonance when two spheres get closer. As the separation distance δ goes to zero, the parameter s also goes to zero (in fact, $s = O(\delta^{1/2})$). Then, in view of equation (9.40), τ_n will converge to 1 and the corresponding permittivity ϵ_n goes to infinity. This means that a red-shift of the (bright) resonance modes occurs. Since the approximate analytical formula for V becomes more accurate as $|\epsilon|$ increases, we can expect that accuracy improves as the separation distance goes to zero. It also indicates that our formula captures the singular nature of the field distribution completely. Furthermore, the difference between τ_n and τ_{n+1} decreases, which means that the spectrum becomes almost continuous.

We now derive approximate formulas for the field at the gap and for the absorption cross section. From Theorem 9.19, we obtain the following:

$$\begin{aligned} E(0,0,0) \approx E_0 - E_0 \frac{8\tau}{3-\tau} \bigg[& \sum_{n=0}^{\infty} \frac{(2n+1)^2}{e^{(2n+1)s} - \tau} (-1)^n \\ & - \gamma_0 \sum_{n=0}^{\infty} \frac{2n+1}{e^{(2n+1)s} - \tau} (-1)^n \bigg]. \end{aligned} \tag{9.41}$$

In the quasi-static approximation, the absorption cross section σ_a is defined by $\sigma_a = \omega \mathrm{Im}\{p\}$, where p is the polarizability of the system of two spheres. From

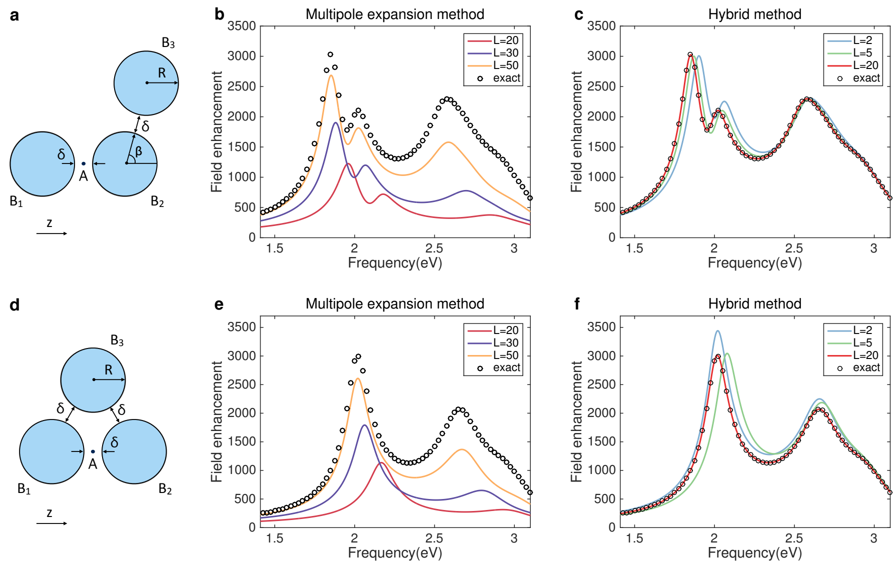

FIGURE 9.5. **Multipole expansion method vs Hybrid scheme.**
a) d) Two examples of three spheres configuration.
b) c) The field enhancement at point A as a function of frequency for the configuration **a** using the multipole expansion method and the hybrid method, respectively. The parameters are given as $R = 30$ nm, $\delta = 0.25$ nm and $\beta = 80°$. The uniform incident field $(0, 0, \mathrm{Re}\{e^{i\omega t}\})$ is applied.
e) f) Same as **b) c)** but for the configuration **d)**.

Theorem 9.19, σ_a is approximated as follows:

$$\begin{aligned}\sigma_a \approx \omega E_0 \frac{8\tau\alpha^3}{3-\tau}\Bigg[&\sum_{n=0}^{\infty}\frac{(2n+1)^2}{e^{(2n+1)s}-\tau} \\ &-\left(\sum_{n=0}^{\infty}\frac{2n+1}{e^{(2n+1)s}-\tau}\right)^2 \Bigg/ \sum_{n=0}^{\infty}\frac{1}{e^{(2n+1)s}-\tau}\Bigg].\end{aligned} \tag{9.42}$$

We compare the above approximate formulas with the exact ones. Fig. 9.4 represents respectively the field enhancement and the absorption cross section σ_a as functions of the frequency ω for various distances ranging from 0.001 nm to 10 nm. The strong accuracy of our approximate formulas over broad ranges of frequencies and gap distances is clearly shown. As mentioned previously, the accuracy improves as the spheres get closer. It is also worth highlighting the red-shift of the plasmonic resonance modes as the separation distance δ goes to zero.

9.4.5. Hybrid numerical scheme for a many-spheres system. Now we consider a system involving an arbitrary number of plasmonic spheres. If all the spheres are well separated, then the multipole expansion method is efficient and accurate for computing the field distribution. However, when the spheres are close to each other, the problem becomes very challenging since the charge densities on each sphere are nearly singular. To overcome this difficulty, Cheng and Greengard developed a hybrid numerical scheme combining the multipole expansion and the method of images.

Let us briefly explain the main idea of Cheng and Greengard's method. In the standard multipole expansion method, the potential is represented as a sum of general multipole sources $\mathcal{Y}_{lm}(\mathbf{r}) = Y_l^m(\theta,\phi)/r^{l+1}$ located at the center of each of the spheres. Suppose that a pair of spheres is close to touching. For convenience, let us identify the pair as $B_+ \cup B_-$. A multipole source $\mathcal{Y}_{lm}$ located at the center of B_+ generates an infinite sequence of image multipole sources by Poladian's imaging rule. Let us denote the resulting image multipole potential by U_{lm}^+. We also define U_{lm}^- in a similar way. Roughly speaking, Cheng and Greengard modified the multipole expansion method by replacing a multipole source $\mathcal{Y}_{lm}$ with its corresponding image multipole series $U_{lm}^{\pm}$.

Since the image series $U_{lm}^{\pm}$ captures the close-to-touching interactions analytically, their scheme is very efficient and highly accurate even if the distance between the spheres is extremely small. However, the image mulipole series $U_{lm}^{\pm}$ are not convergent for $|\tau| > e^s$. Hence it cannot be applied to cluster of plasmonic spheres. Therefore, in order to extend Cheng and Greengard's method to the plasmonic case, it is essential to establish an explicit connection between the image multipole series $U_{lm}^{\pm}$ and TO. We develop a hybrid numerical scheme valid for plasmonics spheres by replacing the image multipole series with its TO version.

Next, we present numerical examples to illustrate the hybrid method. We consider two examples of the three-spheres configuration shown in Figs. **??**a and **??**d. We provide a comparison between multipole expansion method and the hybrid method by plotting the field enhancement at the gap center A. For the numerical implementation, only a finite number of the multipoles $\mathcal{Y}_{lm}$ or hybrid multipoles $U_{lm}^{\pm}$ should be used. Let L be the truncation number for the order l. In Figures 9.5 **b)** and 9.5 **e)**, the field enhancement is computed using the standard multipole expansion method. The computations give inaccurate results even if we include a large number of multipole sources with $L = 50$. On the contrary, the hybrid method gives pretty accurate results even for small values of L such as $L = 2$ and 5 (Figures 9.5 **c)** and 9.5 **f)**). Furthermore, 99% accuracy can be achieved using only $L = 20$. For each hybrid multipole $U_{lm}^{\pm}$, the TO harmonics are included up to order $n = 300$ to ensure convergence and we note that the multipole can be evaluated very efficiently.

To achieve 99.9% accuracy at the first resonant peak, it is necessary to set $L = 150$ in the multipole expansion method which means a $68,400 \times 68,400$ linear system needs to be solved. However, the same accuracy can be achieved with only $L = 23$ in the hybrid method. The corresponding linear system has size $1,725 \times 1,725$ and it can be solved $2,000$ times faster than the multipole expansion method.

CHAPTER 10

Plasmonic Metasurfaces

A metasurface is a composite material layer, designed and optimized in order to control and transform electromagnetic fields. The layer thickness is negligible with respect to the wavelength in the surrounding space. The composite structure forming the metasurface is assumed to behave as a material in the electromagnetic sense, meaning that it can be homogenized on the wavelength scale, and the metasurface can be adequately characterized by its effective, surface-averaged properties.

In this chapter, we consider the scattering by a thin layer of periodic plasmonic nanoparticles mounted on a perfectly conducting sheet. We design the thin layer to have anomalous reflection properties and therefore it can be viewed as a metasurface. As the thickness of the layer, which is of the same order as the diameter of the individual nanoparticles, is negligible compared to the wavelength, it can be approximated by an impedance boundary condition. Our main result is to show that at some resonant frequencies the impedance blows up, allowing for a significant reduction of the scattering from the plate. Using the spectral properties of the periodic Neumann-Poincaré operator defined in (10.6), we investigate the dependency of the impedance with respect to changes in the nanoparticle geometry and configuration. We fully characterize the resonant frequencies in terms of the periodicity, the shape and the material parameters of the nanoparticles. As the period of the array is much smaller than the wavelength, the resonant frequencies of the array of nanoparticles differ significantly from those of single nanoparticles. As shown in this chapter, they are associated with eigenvalues of a periodic Neumann-Poincaré type operator. In contrast with quasi-static plasmonic resonances of single nanoparticles, they depend on the particle size. For simplicity, only one-dimensional arrays embedded in $\mathbb{R}^2$ are considered in this chapter. The extension to the two-dimensional case is straightforward and the dependence of the plasmonic resonances on the parameters of the lattice is easy to derive.

We present numerical results to illustrate our main results in this chapter, which open a door to a mathematical and numerical framework for realizing full control of waves using metasurfaces. Our approach applies to any example of periodic distributions of resonators having (subwavelength) resonances in the quasi-static regime. It provides a framework for explaining the observed extraordinary or meta-properties of such structures and for optimizing these properties. For simplicity, we only consider the scalar wave equation and use a two-dimensional setup.

10.1. Setting of the Problem

Code:	10.1 Plasmonic Metasurfaces	DemoPlasmonicMetasurface.m

We use the Helmholtz equation to model the propagation of light. As mentioned before, this approximation can be viewed as a special case of Maxwell's equations, when the incident wave u^i is transverse magnetic or transverse electric polarized.

Consider a particle occupying a bounded domain $D \Subset \mathbb{R}^2$ of class $\mathcal{C}^{1,\eta}$ for some $\eta > 0$ and with size of order $\delta \ll 1$. The particle is characterized by electric permittivity ε_c and magnetic permeability μ_c, both of which may depend on the frequency of the incident wave. Assume that $\Im m\, \varepsilon_c > 0, \Re e\, \mu_c < 0, \Im m\, \mu_c > 0$ and define

$$k_m = \omega\sqrt{\varepsilon_m \mu_m}, \quad k_c = \omega\sqrt{\varepsilon_c \mu_c},$$

where ε_m and μ_m are the permittivity and permeability of free space, respectively, and ω is the frequency. Throughout this chapter, we assume that ε_m and μ_m are real and positive and k_m is of order 1.

We consider the configuration shown in Figure 10.1, where a particle D is repeated periodically in the x_1-axis with period δ, and is of a distance of order δ from the boundary $x_2 = 0$ of the half-space $\mathbb{R}^2_+ := \{(x_1, x_2) \in \mathbb{R}^2,\ x_2 > 0\}$. We denote by $\mathcal{D}$ this collection of periodically arranged particles and $\Omega := \mathbb{R}^2_+ \setminus \overline{\mathcal{D}}$.

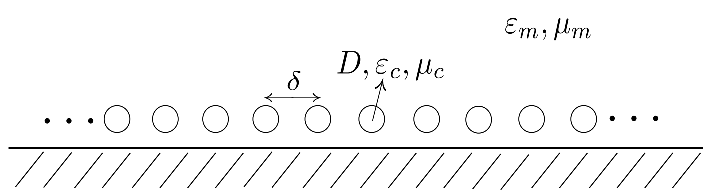

FIGURE 10.1. Thin layer of nanoparticles in the half-space.

Let $u^i(x) = e^{\sqrt{-1}k_m d\cdot x}$ be the incident wave. Here, d is the unit incidence direction. The scattering problem is modeled as follows:

$$(10.1) \qquad \begin{cases} \nabla \cdot \dfrac{1}{\mu_{\mathcal{D}}} \nabla u + \omega^2 \varepsilon_{\mathcal{D}} u = 0 \quad \text{in } \mathbb{R}^2_+ \setminus \partial\mathcal{D}, \\ u_+ - u_- = 0 \quad \text{on } \partial\mathcal{D}, \\ \dfrac{1}{\mu_m} \dfrac{\partial u}{\partial \nu}\bigg|_+ - \dfrac{1}{\mu_c} \dfrac{\partial u}{\partial \nu}\bigg|_- = 0 \quad \text{on } \partial\mathcal{D}, \\ u - u^i \ \text{ satisfies an outgoing radiation condition at infinity,} \\ u = 0 \quad \text{on } \partial\mathbb{R}^2_+ = \{(x_1, 0),\ x_1 \in \mathbb{R}\}, \end{cases}$$

where

$$\varepsilon_{\mathcal{D}} = \varepsilon_m \chi(\Omega) + \varepsilon_c \chi(\mathcal{D}), \quad \mu_{\mathcal{D}} = \varepsilon_m \chi(\Omega) + \varepsilon_c \chi(\mathcal{D}),$$

and $\partial/\partial\nu$ denotes the outward normal derivative on $\partial\mathcal{D}$.

Under the assumption that the wavelength of the incident wave is much larger than the size of the nanoparticle, a certain homogenization occurs, and we can construct $z \in \mathbb{C}$ such that the solution to

$$
\begin{cases}
\Delta u_{\text{app}} + k_m^2 u_{\text{app}} = 0 \quad \text{in } \mathbb{R}^2_+, \\
u_{\text{app}} + \delta z \frac{\partial u_{\text{app}}}{\partial x_2} = 0 \quad \text{on } \partial\mathbb{R}^2_+, \\
u_{\text{app}} - u^i \ \text{ satisfies outgoing radiation condition at infinity,}
\end{cases}
\tag{10.2}
$$

gives the leading order approximation for u. We refer to $u_{\text{app}} + \delta z \partial u_{\text{app}} / \partial x_2 = 0$ as the equivalent impedance boundary condition for problem (10.1).

10.2. Boundary-Layer Corrector and Effective Impedance

In order to compute z, we introduce the following asymptotic expansion:

$$
u = u^{(0)} + u^{(0)}_{BL} + \delta(u^{(1)} + u^{(1)}_{BL}) + \ldots ,
\tag{10.3}
$$

where the leading-order term $u^{(0)}$ is solution to

$$
\begin{cases}
\Delta u^{(0)} + k_m^2 u^{(0)} = 0 \quad \text{in } \mathbb{R}^2_+, \\
u^{(0)} = 0 \quad \text{on } \partial\mathbb{R}^2_+, \\
u^{(0)} - u^i \ \text{ satisfies an outgoing radiation condition at infinity.}
\end{cases}
$$

The boundary-layer correctors $u^{(0)}_{BL}$ and $u^{(1)}_{BL}$ have to be exponentially decaying in the x_2-direction. Note that $u^{(0)}_{BL}$ is introduced in order to correct (up to the first order in δ) the transmission condition on the boundary of the nanoparticles, which is not satisfied by the leading-order term $u^{(0)}$ in the asymptotic expansion of u, while $u^{(1)}_{BL}$ is a higher-order correction term and does not contribute to the first-order equivalent boundary condition in (10.2).

We next construct the corrector $u^{(0)}_{BL}$. We first introduce a function α and a complex constant α_∞ such that they satisfy the rescaled problem

$$
\begin{cases}
\Delta \alpha = 0 \quad \text{in } \left(\mathbb{R}^2_+ \backslash \overline{\mathcal{B}}\right) \cup \mathcal{B}, \\
\alpha|_+ - \alpha|_- = 0 \quad \text{on } \partial\mathcal{B}, \\
\dfrac{1}{\mu_m} \dfrac{\partial \alpha}{\partial \nu}\Big|_+ - \dfrac{1}{\mu_c} \dfrac{\partial \alpha}{\partial \nu}\Big|_- = \Big(\dfrac{1}{\mu_c} - \dfrac{1}{\mu_m}\Big)\nu_2 \quad \text{on } \partial\mathcal{B}, \\
\alpha = 0 \quad \text{on } \partial\mathbb{R}^2_+, \\
\alpha - \alpha_\infty \text{ is exponentially decaying as } x_2 \to +\infty.
\end{cases}
\tag{10.4}
$$

Here, $\nu = (\nu_1, \nu_2)$ and $B = D/\delta$ is repeated periodically in the x_1-axis with period 1 and $\mathcal{B}$ is the collection of these periodically arranged particles.

Then $u^{(0)}_{BL}$ is defined by

$$
u^{(0)}_{BL}(x) := \delta \frac{\partial u^{(0)}}{\partial x_2}(x_1, 0) \left(\alpha(\frac{x}{\delta}) - \alpha_\infty\right).
$$

The corrector $u^{(1)}$ can be found to be the solution to

$$\begin{cases} \Delta u^{(1)} + k_m^2 u^{(1)} = 0 \quad \text{in } \mathbb{R}^2_+, \\ u^{(1)} = \alpha_\infty \frac{\partial u^{(0)}}{\partial x_2} \quad \text{on } \partial\mathbb{R}^2_+, \\ u^{(1)} \ \text{satisfies an outgoing radiation condition at infinity.} \end{cases}$$

By writing

$$u_{\text{app}} = u^{(0)} + u_{BL}^{(0)} + \delta u^{(1)}, \tag{10.5}$$

we arrive at (10.2) with $z = -\alpha_\infty$, up to a second-order term in δ. We summarize the above results in the following theorem.

THEOREM 10.1. *The solution u_{app} to (10.2) with $z = -\alpha_\infty$ approximates pointwisely (for $x_2 > 0$) the exact solution u to (10.1) as $\delta \to 0$, up to a second-order term in δ.*

In order to compute α_∞, we derive an integral representation for the solution α to (10.4). We make use of the periodic Green function $G_\sharp$ defined by (3.1). Let

$$G_\sharp^+(x,y) = G_\sharp\big((x_1 - y_1, x_2 - y_2)\big) - G_\sharp\big((x_1 - y_1, -x_2 - y_2)\big),$$

which is the periodic Green's function in the upper half-space with Dirichlet boundary conditions, and define

$$\begin{aligned} \mathcal{S}_{B\sharp}^+ : H^{-\frac{1}{2}}(\partial B) \quad &\longrightarrow \quad H^1_{\text{loc}}(\mathbb{R}^2), H^{\frac{1}{2}}(\partial B) \\ \varphi \quad &\longmapsto \quad \mathcal{S}_{B,\sharp}^+[\varphi](x) = \int_{\partial B} G_\sharp^+(x,y)\varphi(y)d\sigma(y) \end{aligned}$$

for $x \in \mathbb{R}^2_+, x \in \partial B$ and

$$\begin{aligned} &(\mathcal{K}_{B\sharp}^*)^+ : H^{-\frac{1}{2}}(\partial B) \longrightarrow H^{-\frac{1}{2}}(\partial B) \\ &\varphi \longmapsto (\mathcal{K}_{B,\sharp}^*)^+[\varphi](x) = \int_{\partial B} \frac{\partial G_\sharp^+(x,y)}{\partial \nu(x)} \varphi(y)d\sigma(y) \end{aligned} \tag{10.6}$$

for $x \in \partial B$.

It is clear that the results of Lemma 3.2 hold true for $\mathcal{S}_{B\sharp}^+$ and $(\mathcal{K}_{B\sharp}^*)^+$. Moreover, for any $\varphi \in H^{-\frac{1}{2}}(\partial B)$, we have

$$\mathcal{S}_{B,\sharp}^+[\varphi](x) = 0 \quad \text{for } x \in \partial\mathbb{R}^2_+.$$

Now, we can readily see that α can be represented as $\alpha = \mathcal{S}_{B,\sharp}^+[\varphi]$, where $\varphi \in H^{-\frac{1}{2}}(\partial B)$ satisfies

$$\frac{1}{\mu_m}\frac{\partial \mathcal{S}_{B,\sharp}^+[\varphi]}{\partial \nu}\bigg|_+ - \frac{1}{\mu_c}\frac{\partial \mathcal{S}_{B,\sharp}^+[\varphi]}{\partial \nu}\bigg|_- = \Big(\frac{1}{\mu_c} - \frac{1}{\mu_m}\Big)\nu_2 \quad \text{on } \partial B.$$

Using the jump formula from Lemma 3.2, we arrive at

$$\big(\lambda_\mu I - (\mathcal{K}_{B\sharp}^*)^+\big)[\varphi] = \nu_2,$$

where

$$\lambda_\mu = \frac{\mu_c + \mu_m}{2(\mu_c - \mu_m)}.$$

Therefore, using item (v) in Lemma 3.2 on the characterization of the spectrum of $\mathcal{K}_{B\sharp}^*$ and the fact that the spectra of $(\mathcal{K}_{B\sharp}^*)^+$ and $\mathcal{K}_{B\sharp}^*$ are the same, we obtain that

$$\alpha = \mathcal{S}_{B,\sharp}^+\big(\lambda_\mu I - (\mathcal{K}_{B\sharp}^*)^+\big)^{-1}[\nu_2].$$

LEMMA 10.2. *Let $x = (x_1, x_2)$. Then, for $x_2 \to +\infty$, the following asymptotic expansion holds:*

$$\alpha = \alpha_\infty + O(e^{-x_2}),$$

with

$$\alpha_\infty = -\int_{\partial B} y_2\big(\lambda_\mu I - (\mathcal{K}_{B\sharp}^*)^+\big)^{-1}[\nu_2](y)d\sigma(y).$$

PROOF. The result follows from an asymptotic analysis of $G_\sharp^+(x,y)$. Indeed, suppose that $x_2 \to +\infty$, we have

$$\begin{aligned}
&G_\sharp^+(x,y) = \tfrac{1}{4\pi}\ln\big(\sinh^2(\pi(x_2-y_2)) + \sin^2(\pi(x_1-y_1))\big)\\
&-\frac{1}{4\pi}\ln\big(\sinh^2(\pi(x_2+y_2)) + \sin^2(\pi(x_1-y_1))\big)\\
&= \frac{1}{4\pi}\ln\big(\sinh^2(\pi(x_2-y_2))\big)\\
&-\frac{1}{4\pi}\ln\big(\sinh^2(\pi(x_2+y_2))\big)\\
&+O\Big(\ln\Big(1+\frac{1}{\sinh^2(x_2)}\Big)\Big)\\
&= \frac{1}{2\pi}\Big(\ln\Big(\frac{e^{\pi(x_2-y_2)} - e^{-\pi(x_2+y_2)}}{2}\Big)\\
&-\ln\Big(\frac{e^{\pi(x_2+y_2)} - e^{-\pi(x_2-y_2)}}{2}\Big)\Big) + O\Big(\ln\Big(1+e^{-x_2^2}\Big)\Big)\\
&= -y_2 + O(e^{-x_2}),
\end{aligned}$$

which yields the desired result. $\square$

Finally, it is important to note that α_∞ depends on the geometry and size of the particle B.

As $(\mathcal{K}_{B\sharp}^*)^+ : \mathcal{H}_0^* \to \mathcal{H}_0^*$ is a compact self-adjoint operator, where $\mathcal{H}_0^*$ is defined as in Lemma 3.2, we can write

$$\begin{aligned}
\alpha_\infty &= -\int_{\partial B} y_2\big(\lambda_\mu I - (\mathcal{K}_{B\sharp}^*)^+\big)^{-1}[\nu_2](y)d\sigma(y),\\
&= -\int_{\partial B} y_2 \sum_{j=1}^{\infty} \frac{\langle \varphi_j, \nu_2\rangle_{\mathcal{H}_0^*}\varphi_j(y)}{\lambda_\mu - \lambda_j} d\sigma(y),\\
&= \sum_{j=1}^{\infty} \frac{\langle \varphi_j, \nu_2\rangle_{\mathcal{H}_0^*}\langle \varphi_j, y_2\rangle_{-\frac{1}{2},\frac{1}{2}}}{\lambda_\mu - \lambda_j},
\end{aligned}$$

where $\lambda_1, \lambda_2, \ldots$ are the eigenvalues of $(\mathcal{K}_{B\sharp}^*)^+$ and $\varphi_1, \varphi_2, \ldots$ is a corresponding orthornormal basis of eigenvectors.

On the other hand, by integrating by parts we get

$$\langle \varphi_j, y_2 \rangle_{-\frac{1}{2},\frac{1}{2}} = \frac{1}{\frac{1}{2} - \lambda_j} \langle \varphi_j, \nu_2 \rangle_{\mathcal{H}_0^*}.$$

This, together with the fact that $\Im m\, \lambda_\mu < 0$ (by the Drude model (9.5)), yields the following lemma.

LEMMA 10.3. *We have* $\Im m\, \alpha_\infty > 0$.

Finally, we give a formula for the shape derivative of α_∞. This formula can be used to optimize $|\alpha_\infty|$, for a given frequency ω, in terms of the shape B of the nanoparticle. Let B_η be an η-perturbation of B; *i.e.*, let $h \in \mathcal{C}^1(\partial B)$ and ∂B_η be given by

$$\partial B_\eta = \Big\{ x + \eta h(x) \nu(x), x \in \partial B \Big\}.$$

It can be shown that

$$\begin{aligned} \alpha_\infty(B_\eta) &= \alpha_\infty(B) + \eta(\frac{\mu_m}{\mu_c} - 1) \\ &\quad \times \int_{\partial B} h \Big[\frac{\partial v}{\partial \nu}\big|_- \frac{\partial w}{\partial \nu}\big|_- + \frac{\mu_c}{\mu_m} \frac{\partial v}{\partial T}\big|_- \frac{\partial w}{\partial T}\big|_- \Big] \, d\sigma, \end{aligned}$$

where $\partial/\partial T$ is the tangential derivative on ∂B, v and w periodic with respect to x_1 of period 1 and satisfy

$$\begin{cases} \Delta v = 0 \quad \text{in } \Big(\mathbb{R}^2_+ \backslash \overline{\mathcal{B}}\Big) \cup \mathcal{B}, \\ v|_+ - v|_- = 0 \quad \text{on } \partial\mathcal{B}, \\ \dfrac{\partial v}{\partial \nu}\Big|_+ - \dfrac{\mu_m}{\mu_c} \dfrac{\partial v}{\partial \nu}\Big|_- = 0 \quad \text{on } \partial\mathcal{B}, \\ v - x_2 \to 0 \quad \text{as } x_2 \to +\infty, \end{cases}$$

and

$$\begin{cases} \Delta w = 0 \quad \text{in } \Big(\mathbb{R}^2_+ \backslash \overline{\mathcal{B}}\Big) \cup \mathcal{B}, \\ \dfrac{\mu_m}{\mu_c} w|_+ - w|_- = 0 \quad \text{on } \partial\mathcal{B}, \\ \dfrac{\partial w}{\partial \nu}\Big|_+ - \dfrac{\partial w}{\partial \nu}\Big|_- = 0 \quad \text{on } \partial\mathcal{B}, \\ w - x_2 \to 0 \quad \text{as } x_2 \to +\infty, \end{cases}$$

respectively. Therefore, the following proposition holds.

PROPOSITION 10.4. *The shape derivative* $d_S \alpha_\infty(B)$ *of* α_∞ *is given by*

$$d_S \alpha_\infty(B) = (\frac{\mu_m}{\mu_c} - 1) \Big[\frac{\partial v}{\partial \nu}\big|_- \frac{\partial w}{\partial \nu}\big|_- + \frac{\mu_c}{\mu_m} \frac{\partial v}{\partial T}\big|_- \frac{\partial w}{\partial T}\big|_- \Big].$$

If we aim to maximize the functional $J := \frac{1}{2}|\alpha_\infty|^2$ over B, then it can be easily seen that J is Fréchet differentiable and its Fréchet derivative is given by

$$\Re e\, d_S \alpha_\infty(B) \overline{\alpha_\infty(B)}.$$

In order to include cases where topology changes and multiple components are allowed, a level-set version of the optimization procedure described below can be developed.

10.3. Numerical illustration

We now demonstrate the dependence of the equivalent boundary condition parameter α_∞ on the incident wavelength for various nanoparticle configurations. We use the Drude model for the permeability of background material, which is water, and the nanoparticles which are gold. The Drude model for the permeability μ is given by

$$\mu(\omega) = 1 - \frac{\omega_p^2}{\omega^2 + i\tau\omega}.$$

In particular, to model gold nanoparticles we choose the plasma frequency ω_p to be

$$\omega_p = 9.03 \times 2\pi \times \frac{1.6 \times 10^{-19}}{6.6 \times 10^{-34}},$$

and the damping coefficient τ to be

$$\tau = 0.053 \times 2\pi \times \frac{1.6 \times 10^{-19}}{6.6 \times 10^{-34}}.$$

The discretization of the boundary of the nanoparticle, along with the computation of the Neumann-Poincaré operator $(\mathcal{K}^*_{B\sharp})^+$, where B is a disk, is performed in the same fashion as in Section 1.7 We then calculate

$$\alpha_\infty = -\int_{\partial B} y_2 \big(\lambda_\mu I - (\mathcal{K}^*_{B\sharp})^+\big)^{-1}[\nu_2](y) d\sigma(y),$$

and plot its modulus $|\alpha_\infty|$ for a range of wavelengths in the interval $[150 \times 10^{-9}, 350 \times 10^{-9}]$.

In Figure 10.2 we place the row of nanoparticles a distance of 0.5 from the surface $\partial\mathbb{R}^2_+$ and vary the radii from 0.1 to 0.4. In Figure 10.3 we set the nanoparticle radius to be 0.2 and observe the change in $|\alpha_\infty|$ when we first position the nanoparticles a distance of 0.25 from the surface, and then a distance of 0.75.

In Figures 10.4 and 10.5 we demonstrate that in the case of a single row of nanoparticles we have a distinct resonance peak, whereas in in the case of three well-separated nanoparticles (all in the unit cell) we have delocalized resonances.

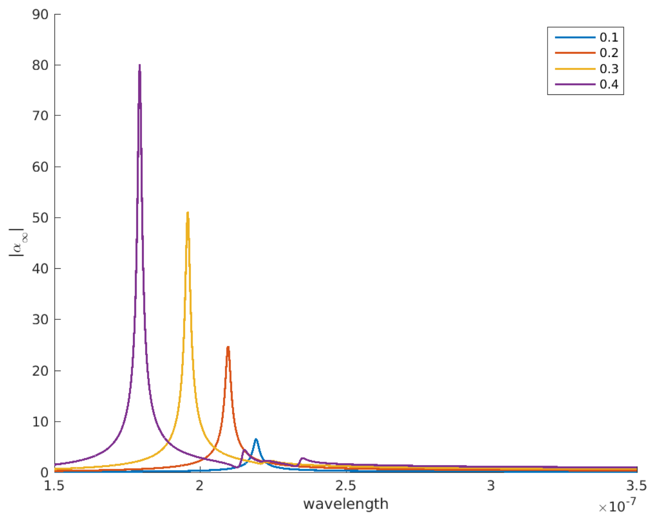

FIGURE 10.2. $|\alpha_\infty|$ as a function of wavelength for a set of radii varying from 0.1 to 0.4.

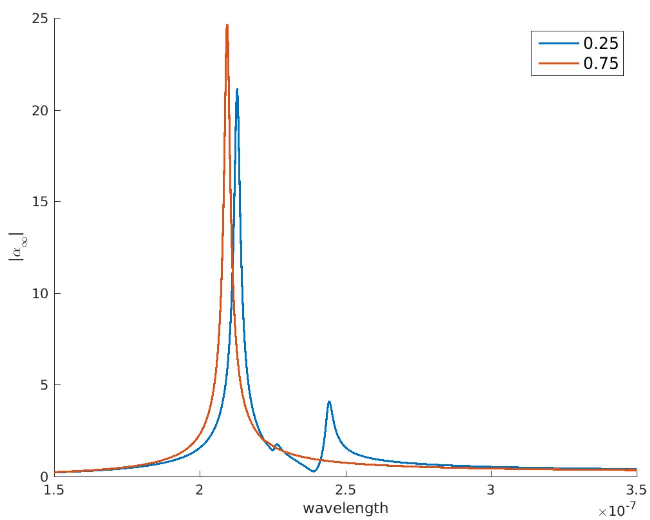

FIGURE 10.3. $|\alpha_\infty|$ as a function of wavelength for a set of radii for a disk of radius 0.2 as for distances of 0.25 and 0.75 from the boundary at $x_2 = 0$.

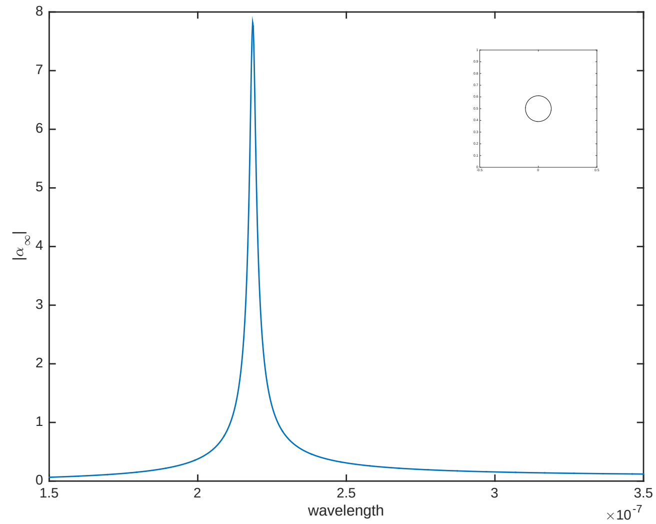

FIGURE 10.4. We observe a strong localized resonant peak in the case of a single row of nanoparticles.

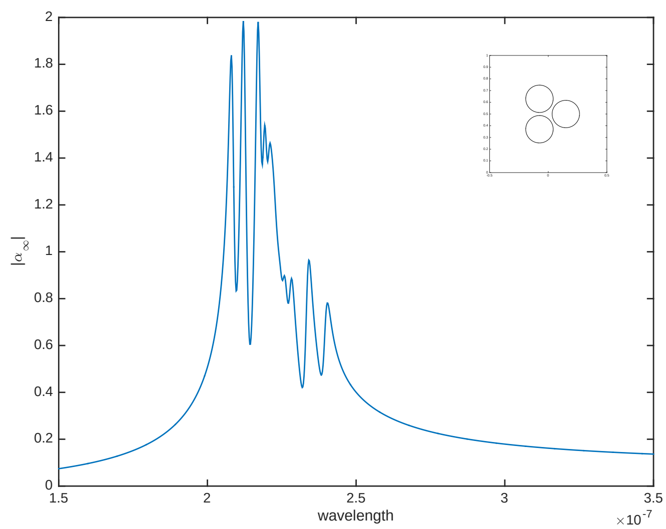

FIGURE 10.5. When we have three nanoparticles in each cell of the array we observe delocalized resonance.

CHAPTER 11

Near-Cloaking

11.1. Introduction

Cloaking is to make a target invisible with respect to probing by electromagnetic or elastic waves. An extensive work has been produced on cloaking in the context of electromagnetic and elastic waves. Many schemes for cloaking are currently under active investigation. These include interior cloaking, where the cloaking region is inside the cloaking device, and exterior cloaking in which the cloaking region is outside the cloaking device.

In this chapter, we focus on interior cloaking and describe effective near-cloaking structures for electromagnetic and elastic scattering problems. The focus of the next chapter will be placed on exterior cloaking.

In interior cloaking, the difficulty is to construct material parameter distributions of a cloaking structure such that any target placed inside the structure is undetectable to waves. One approach is to use transformation optics (also called the scheme of changing variables). It takes advantage of the fact that the equations governing electromagnetic and acoustic wave propagation have transformation laws under change of variables. This allows one to design structures that bend waves around a hidden region, returning them to their original path on the far side. The change of variables based cloaking method uses a singular transformation to boost the material properties so that it makes a cloaking region look like a point to outside measurements. However, this transformation induces the singularity of material constants in the transversal direction (also in the tangential direction in two dimensions), which causes difficulty both in the theory and applications. To overcome this weakness, so called 'near-cloaking' is naturally considered, which is a regularization or an approximation of singular cloaking. Instead of the singular transformation, one can use a regular one to push forward the material parameters, in which a small ball is blown up to the cloaking region. Enhanced cloaking can be achieved by using a cancellation technique. The approach is to first design a multi-coated structure around a small perfect insulator to significantly reduce its effect on boundary or scattering cross-section measurements. The multi-coating cancels the generalized polarization tensors or the scattering coefficients of the cloaking device. One then obtains a near-cloaking structure by pushing forward the multi-coated structure around a small object via the standard blow-up transformation technique.

The purpose of this chapter is to review the cancellation technique. We first design a structure coated around a particle to have vanishing scattering coefficients of lower orders and show that the order of perturbation due to a small particle can be reduced significantly. We then obtain near-cloaking structure by pushing forward the multi-coated structure around a small object via the usual blow-up transformation. We prove that the structures with vanishing scattering coefficients enhance near-cloaking. We emphasize that such a structure achieves near-cloaking for a band of frequencies. We also show that near-cloaking becomes increasingly difficult as the cloaked object becomes bigger or the operating frequency becomes higher. The difficulty scales inversely proportionally to the object diameter or the frequency.

11.2. Near-Cloaking for the Full Maxwell Equations

In this section, the scattering coefficients vanishing approach to consider near-cloaking for the full Maxwell equations. These S-vanishing structures are, prior to using the transformation optics, layered-structures are designed so that their first two scattering coefficients W_n^{TE} and W_n^{TM} defined in section 6.3 vanish. We therefore construct multilayered structures whose scattering coefficients vanish, which are called *S-vanishing structures*.

11.2.1. Far field pattern. Using (6.24), (6.25), and the behavior of the spherical Bessel functions, the far-field pattern of the scattered wave $(E - E^i)$ can be estimated. We define the scattering amplitude $A_\infty[\varepsilon, \mu, \omega]$ by

$$E(x) - E^i(x) = \frac{e^{\sqrt{-1}k_m|x|}}{k_m|x|} A_\infty[\varepsilon, \mu, \omega](\hat{x}) + o(|x|^{-1}) \quad \text{as } |x| \to \infty. \tag{11.1}$$

Since the spherical Bessel function $h_l^{(1)}$ behaves like

$$\begin{cases} h_l^{(1)}(t) \sim \dfrac{1}{t} e^{\sqrt{-1}t} e^{-\sqrt{-1}\frac{l+1}{2}\pi} & \text{as } t \to \infty, \\ (h_l^{(1)})'(t) \sim \dfrac{1}{t} e^{\sqrt{-1}t} e^{-\sqrt{-1}\frac{l}{2}\pi} & \text{as } t \to \infty, \end{cases}$$

one can easily see by using (6.16) that

$$\begin{cases} E_{ll'}^{TE}(k_m; x) \sim \dfrac{e^{\sqrt{-1}k_m|x|}}{k_m|x|} e^{-\sqrt{-1}\frac{l+1}{2}\pi} \left(-\sqrt{l(l+1)} \right) V_{ll'}(\hat{x}) & \text{as } |x| \to \infty, \\ E_{ll'}^{TM}(k_m; x) \sim \dfrac{e^{\sqrt{-1}k_m|x|}}{k_m|x|} \sqrt{\dfrac{\mu_m}{\varepsilon_m}} e^{-\sqrt{-1}\frac{l+1}{2}\pi} \left(-\sqrt{l(l+1)} \right) U_{ll'}(\hat{x}) & \text{as } |x| \to \infty. \end{cases}$$

Therefore, the following result holds.

PROPOSITION 11.1. *If E^i is given by (6.23), then the corresponding scattering amplitude can be expanded as*

$$A_\infty[\varepsilon, \mu, \omega](\hat{x}) = \sum_{l=1}^{\infty} \frac{-(\sqrt{-1})^{-l} k_m}{\sqrt{l(l+1)}} \sum_{l'=-l}^{l} \left(\alpha_{ll'} V_{ll'}(\hat{x}) + \beta_{ll'} \sqrt{\frac{\mu_m}{\varepsilon_m}} U_{ll'}(\hat{x}) \right), \tag{11.2}$$

where $\alpha_{ll'}$ and $\beta_{ll'}$ are defined by (6.25).

Consider the case where the incident wave E^i is given by a plane wave $e^{\sqrt{-1}k_m d\cdot x}c$ with $d \in S$ and $d \cdot c = 0$. It follows from (6.19) that

$$e^{\sqrt{-1}k\cdot x}c = \sum_{p=1}^{\infty} \frac{4\pi(\sqrt{-1})^p}{\sqrt{p(p+1)}} \sum_{p'=-p}^{p} \left[-\sqrt{-1} \big(V_{pp'}(d) \cdot c \big) \widetilde{E}_{pp'}^{TE}(k_m; x) - \sqrt{\frac{\varepsilon_m}{\mu_m}} \big(U_{pp'}(d) \cdot c \big) \widetilde{E}_{pp'}^{TM}(k_m; x) \right],$$

and therefore,

$$a_{pp'} = -\frac{4\pi(\sqrt{-1})^{p+1}}{\sqrt{p(p+1)}}(V_{pp'}(d)\cdot c) \quad \text{and} \quad b_{pp'} = -\frac{4\pi(\sqrt{-1})^{p}}{\sqrt{p(p+1)}}\sqrt{\frac{\varepsilon_m}{\mu_m}}(U_{pp'}(d)\cdot c).$$

Hence, the scattering amplitude, denoted by $A_\infty[\varepsilon,\mu,\omega](c,d;\hat{x})$, is given by (11.2) with

(11.3)

$$\begin{cases} \alpha_{ll'} = \displaystyle\sum_{p=1}^{\infty}\sum_{p'=-p}^{p}\frac{4\pi(\sqrt{-1})^{p}}{\sqrt{p(p+1)}}\left[-\sqrt{-1}(V_{pp'}(d)\cdot c)W_{ll',pp'}^{TE,TE} - \sqrt{\frac{\varepsilon_m}{\mu_m}}(U_{pp'}(d)\cdot c)W_{ll',pp'}^{TE,TM}\right], \\ \beta_{ll'} = \displaystyle\sum_{p=1}^{\infty}\sum_{p'=-p}^{p}\frac{4\pi(\sqrt{-1})^{p}}{\sqrt{p(p+1)}}\left[-\sqrt{-1}(V_{pp'}(d)\cdot c)W_{ll',pp'}^{TM,TE} - \sqrt{\frac{\varepsilon_m}{\mu_m}}(U_{pp'}(d)\cdot c)W_{ll',pp'}^{TM,TM}\right], \end{cases}$$

which shows that the scattering coefficients appear in the expansion of the scattering amplitude.

11.2.2. low frequency behavior of the scattering coefficients. The low frequency behavior of the scattering coefficients is now investigated. Let $\Gamma(x) := -1/(4\pi|x|)$ denote the fundamental solution corresponding to the case $k=0$, and $\mathcal{M}_D$ the associated boundary integral operator:

$$\mathcal{M}_D[\varphi](x) := \text{p.v.}\int_{\partial D}\nu(x)\times\Big(\nabla_x\times\big(\Gamma(x-y)\varphi(y)\big)\Big)d\sigma(y), \quad \varphi\in TH(\text{div},\partial D).$$

Analogously to (6.7), one can prove that there is a unique solution $(\varphi^{(0)},\psi^{(0)})\in TH(\text{div},\partial D)\times TH(\text{div},\partial D)$ to the following equations:

(11.4)

$$\begin{bmatrix} (\mu_1-\mu_0)\left(\dfrac{\mu_1+\mu_0}{2(\mu_1-\mu_0)}I+\mathcal{M}_D\right) & 0 \\ 0 & (\epsilon_1-\epsilon_0)\left(\dfrac{\epsilon_1+\epsilon_0}{2(\epsilon_1-\epsilon_0)}I+\mathcal{M}_D\right) \end{bmatrix}\begin{bmatrix}\varphi^{(0)} \\ \omega\psi^{(0)}\end{bmatrix} = \begin{bmatrix}E^i\times\nu \\ iH^i\times\nu\end{bmatrix}\Bigg|_{\partial D}.$$

In fact, since ∂D is $\mathcal{C}^{1,\alpha}$, $\mathcal{M}_D$ is compact and one may apply the Fredholm alternative to prove unique solvability of above equation. Moreover, one has

(11.5)

$$\|\varphi^{(0)}\|_{TH(\text{div},\partial D)}+\omega\|\psi^{(0)}\|_{TH(\text{div},\partial D)} \le C(\|E^i\times\nu\|_{TH(\text{div},\partial D)}+\|H^i\times\nu\|_{TH(\text{div},\partial D)}),$$

with a constant $C=C(\epsilon,\mu)$.

Let ρ be a small positive number and consider the boundary integral equation (6.7) with k, k_0, and ω replaced by ρk, ρk_0, and $\rho\omega$, respectively. Then, one has

$$\mathcal{M}_D^{\rho k}-\mathcal{M}_D = O(\rho^2), \quad \mathcal{M}_D^{\rho k_0}-\mathcal{M}_D = O(\rho^2),$$

and

$$\mathcal{L}_D^{\rho k}-\mathcal{L}_D^{\rho k_0} = O(\rho^2).$$

Since

$$\left(\frac{k^2}{2\mu_1}+\frac{k_0^2}{2\mu_0}\right)I+\frac{k^2}{\mu_1}\mathcal{M}_D^{k}-\frac{k_0^2}{\mu_0}\mathcal{M}_D^{k_0} = \rho^2\omega^2\left[\frac{\epsilon_1+\epsilon_0}{2}I+(\epsilon_1-\epsilon_0)\mathcal{M}_D+O(\rho^2)\right],$$

if one expresses the solution (φ,ψ) to (6.7) as $({}',{}^{-}) := ({}'^{\rho},\rho\omega{}^{-\rho})$, then it satisfies

$$\Big(A+O(\rho)\Big)\begin{bmatrix}\varphi^{\rho} \\ \rho\omega\psi^{\rho}\end{bmatrix} = \begin{bmatrix}E^i\times\nu \\ iH^i\times\nu\end{bmatrix}\Bigg|_{\partial D},$$

where A is the 2-by-2 matrix appeared in the left-hand side of (11.4). From the invertibility of A, it follows that there are constants ρ_0 and $C = C(\epsilon, \mu, \omega)$ independent of ρ as long as $\rho \leq \rho_0$ such that

(11.6)

$$\|\varphi^\rho\|_{TH(\mathrm{div},\partial D)} + \rho\omega\|\psi^\rho\|_{TH(\mathrm{div},\partial D)} \leq C\big(\|E^i \times \nu\|_{TH(\mathrm{div},\partial D)} + \|H^i \times \nu\|_{TH(\mathrm{div},\partial D)}\big).$$

LEMMA 11.2. *There exists ρ_0 such that, for all $\rho \leq \rho_0$,*

$$\left| W^{TE,TE}_{(n,m)(p,q)}[\epsilon, \mu, \rho\omega] \right| \leq \frac{C^{n+p}}{n^n p^p} \rho^{n+p+1}, \tag{11.7}$$

for all $n, m, p, q \in \mathbb{N}$, where the constant C depends on (ϵ, μ, ω) but is independent of ρ. The same estimate holds for $W^{TE,TM}_{(n,m)(p,q)}$, $W^{TM,TE}_{(n,m)(p,q)}$, and $W^{TM,TM}_{(n,m)(p,q)}$.

PROOF. Let (φ, ψ) be the solution to (6.7) with $E^i(y) = \widetilde{E}^{TE}_{p,q}(\rho k_0; y)$ and $H^i = -\frac{i}{\rho\omega\mu_0} \nabla \times E^i$. Then, from (6.22), it follows that

$$\big\|E^{i,\rho}\big\|_{TH(\mathrm{div},\partial D)} + \big\|H^{i,\rho}\big\|_{TH(\mathrm{div},\partial D)} \leq \frac{C^p}{p^p} \rho^p,$$

where C is independent of ρ, and hence

$$\big\|\varphi^\rho\big\|_{L^2(\partial D)} + \rho\big\|\psi^\rho\big\|_{L^2(\partial D)} \leq \frac{C^p}{p^p} \rho^p,$$

for $\rho \leq \rho_0$ for some ρ_0. So one gets (11.7) from the definition of the scattering coefficients in Definition 6.1. □

11.2.3. S-vanishing Structures. We will use a multi-layer structure defined in section **??** to construct the near cloaking structure at low frequencies. In section 6.3, using the symmetry of the layered radial structure, the scattering coefficients are reduced to W^{TE}_n and W^{TM}_n, given by (6.36) and (6.41).

To construct the S-vanishing structure at a fixed frequency ω, one looks for (μ, ϵ) such that

$$W^{TE}_n[\epsilon, \mu, \omega] = 0,\ W^{TM}_n[\epsilon, \mu, \omega] = 0, \quad n = 1, \ldots, N,$$

for some N. More ambitiously one may look for a structure (μ, ϵ) for a fixed ω such that

$$W^{TE}_n[\mu, \epsilon, \rho\omega] = 0, \quad W^{TM}_n[\mu, \epsilon, \rho\omega] = 0$$

for all $1 \leq n \leq N$ and $\rho \leq \rho_0$ for some ρ_0. Such a structure may not exist. So instead one looks for a structure such that

$$W^{TE}_n[\mu, \epsilon, \rho\omega] = o(\rho^{2N+1}), \quad W^{TM}_n[\mu, \epsilon, \rho\omega] = o(\rho^{2N+1}), \tag{11.8}$$

for all $1 \leq n \leq N$ and $\rho \leq \rho_0$ for some ρ_0. Such a structure is called an *S-vanishing structure of order N at low frequencies*. In the following subsection, the scattering coefficients are expanded at low frequencies and conditions for the magnetic permeability and the electric permittivity to be an S-vanishing structure are derived.

Suppose that (μ, ϵ) is an S-vanishing structure of order N at low frequencies. Let the incident wave E^i be given by a plane wave $e^{\sqrt{-1}\rho\mathbf{k}\cdot x}\mathbf{c}$ with $|\mathbf{k}| = k_0 (= \omega\sqrt{\varepsilon_0\mu_0})$ and $\mathbf{k} \cdot \mathbf{c} = 0$. From (11.3), the corresponding scattering amplitude,

$\mathbf{A}_\infty[\mu,\epsilon,\rho\omega](\mathbf{c},\hat{\mathbf{k}}:=\mathbf{k}/|\mathbf{k}|;\hat{\mathbf{x}}:=\mathbf{x}/|\mathbf{x}|)$, is given by (11.2) with the following $\alpha_{n,m}$ and $\beta_{n,m}$:

$$\begin{cases} \alpha_{n,m} = \dfrac{4\pi(\sqrt{-1})^n}{\sqrt{n(n+1)}}(\mathbf{V}_{n,m}(\hat{\mathbf{k}})\cdot\mathbf{c})W_n^{TE}[\mu,\epsilon,\rho\omega], \\ \beta_{n,m} = -\dfrac{4\pi(\sqrt{-1})^n}{\sqrt{n(n+1)}}\dfrac{1}{\sqrt{-1}\omega\mu_0}(\mathbf{U}_{n,m}(\hat{\mathbf{k}})\cdot\mathbf{c})W_n^{TM}[\mu,\epsilon,\rho\omega]. \end{cases}$$

Applying (11.7) and (11.8),

$$\mathbf{A}_\infty[\mu,\epsilon,\rho\omega](\mathbf{c},\hat{\mathbf{k}};\hat{x}) = o(\rho^{2N+1}) \tag{11.9}$$

uniformly in $(\hat{\mathbf{k}},\hat{x})$ if $\rho \le \rho_0$. Thus using such a structure, the visibility of scattering amplitude is greatly reduced.

11.2.4. Asymptotic Expansion of the Scattering Coefficients. The spherical Bessel functions of the first and second kinds have the series expansions

$$j_n(t) = \sum_{l=0}^{\infty}\frac{(-1)^l t^{n+2l}}{2^l l! 1\cdot 3\cdots(2n+2l+1)}$$

and

$$y_n(t) = -\frac{(2n)!}{2^n n!}\sum_{l=0}^{\infty}\frac{(-1)^l t^{2l-n-1}}{2^l l!(-2n+1)(-2n+3)\cdots(-2n+2l-1)}.$$

So, using the notation of double factorials, which is defined by

$$n!! := \begin{cases} n\cdot(n-2)\ldots 3\cdot 1 & \text{if } n>0 \text{ is odd,} \\ n\cdot(n-2)\ldots 4\cdot 2 & \text{if } n>0 \text{ is even,} \\ 1 & \text{if } n=-1,0, \end{cases}$$

one has

$$j_n(t) = \frac{t^n}{(2n+1)!!}\big(1+o(t)\big) \quad \text{for } t \ll 1 \tag{11.10}$$

and

$$y_n(t) = -\big((2n-1)!!\big)t^{-n+1}\big(1+o(t)\big) \quad \text{for } t \ll 1. \tag{11.11}$$

One now computes $P_n^{TE}[\epsilon,\mu,t]$ for small t. For $n \ge 1$,

$$\begin{aligned} P_n^{TE}[\epsilon,\mu,t] &= (-\sqrt{-1}t)^L\left(\prod_{j=1}^{L}\mu_j^{\frac{3}{2}}\epsilon_j^{\frac{1}{2}}r_j\right)\begin{bmatrix}\dfrac{z_L^n}{(2n+1)!!}t^n+o(t^n) & \dfrac{-\sqrt{-1}Q(n)}{z_L^{n+1}}t^{-n-1} \\ 0 & 0\end{bmatrix} \\ &\times\prod_{j=1}^{L}\left(\begin{bmatrix}\dfrac{\sqrt{-1}Q(n)n}{\mu_j(z_jr_j)^{n+1}}t^{-n-1}+o(t^{-n-1}) & \dfrac{\sqrt{-1}Q(n)}{(z_jr_j)^{n+1}}t^{-n-1}+o(t^{-n-1}) \\ \dfrac{-(n+1)(z_jr_j)^n}{\mu_j(2n+1)!!}t^n+o(t^n) & \dfrac{(z_jr_j)^n}{(2n+1)!!}t^n+o(t^n)\end{bmatrix}\right. \\ &\qquad\left.\begin{bmatrix}\dfrac{(z_{j-1}r_j)^n}{(2n+1)!!}t^n+o(t^n) & \dfrac{-\sqrt{-1}Q(n)}{(z_{j-1}r_j)^{n+1}}t^{-n-1}+o(t^{-n-1}) \\ \dfrac{(n+1)(z_{j-1}r_j)^n}{\mu_{j-1}(2n+1)!!}t^n+o(t^n) & \dfrac{\sqrt{-1}Q(n)n}{\mu_{j-1}(z_{j-1}r_j)^{n+1}}t^{-n-1}+o(t^{-n-1})\end{bmatrix}\right), \end{aligned}$$

where $z_j = \sqrt{\epsilon_j \mu_j}$ and $Q(n) = (2n-1)!!$. One then has

$$P_n^{TE}[\epsilon,\mu,t] = \begin{bmatrix} \frac{z_L^n}{(2n+1)!!} t^n + o(t^n) & \frac{-\sqrt{-1}Q(n)}{z_L^{n+1}} t^{-n-1} + o(t^{-n-1}) \\ 0 & 0 \end{bmatrix} \times$$

$$\prod_{j=1}^{L} \begin{bmatrix} \frac{Q(n) z_{j-1}^n}{(2n+1)!! z_j^n} (n + \frac{(n+1)\mu_j}{\mu_{j-1}})(1+o(1)) & (-\sqrt{-1}) \frac{(Q(n))^2 n}{z_j^n z_{j-1}^{n+1} r_j^{2n+1}} (1 - \frac{\mu_j}{\mu_{j-1}}) t^{-2n-1}(1+o(1)) \\ \sqrt{-1} \frac{z_{j-1}^n z_j^{n+1} r_j^{2n+1}(n+1)}{((2n+1)!!)^2} (1 - \frac{\mu_j}{\mu_{j-1}}) t^{2n+1}(1+o(1)) & \frac{Q(n) z_j^{n+1}}{(2n+1)!! z_{j-1}^{n+1}} (n+1+\frac{n\mu_j}{\mu_{j-1}})(1+o(1)) \end{bmatrix}.$$

Similarly, for the transverse magnetic case, one has

$$P_n^{TM}[\epsilon,\mu,t] = \begin{bmatrix} \frac{(n+1) z_L^n}{(2n+1)!!} t^n + o(t^n) & \frac{-\sqrt{-1} n Q(n)}{z_L^{n+1}} t^{-n-1} + o(t^{-n-1}) \\ 0 & 0 \end{bmatrix} \times$$

$$\prod_{j=1}^{L} \begin{bmatrix} \frac{Q(n) z_{j-1}^n}{(2n+1)!! z_j^n} \left((n + \frac{\epsilon_j}{\epsilon_{j-1}}(n+1) \right)(1+o(1)) & (-\sqrt{-1}) \frac{(Q(n))^2 n}{z_j^n z_{j-1}^{n+1} r_j^{2n+1}} \left(1 - \frac{\epsilon_j}{\epsilon_{j-1}}\right) t^{-2n-1}(1+o(1)) \\ \sqrt{-1} \frac{z_{j-1}^n z_j^{n+1} r_j^{2n+1}(n+1)}{((2n+1)!!)^2} \left(1 - \frac{\epsilon_j}{\epsilon_{j-1}}\right) t^{2n+1}(1+o(1)) & \frac{Q(n) z_j^{n+1}}{(2n+1)!! z_{j-1}^{n+1}} \left(n+1+\frac{\epsilon_j}{\epsilon_{j-1}} n\right)(1+o(1)) \end{bmatrix}.$$

Using the behavior of spherical Bessel functions for small arguments, one can see that $p_{n,1}^{TE}$ and $p_{n,2}^{TE}$ admit the following expansions:

$$p_{n,1}^{TE}[\mu,\epsilon,t] = t^n \left(\sum_{l=0}^{N-n} f_{n,l}^{TE}(\mu,\epsilon) t^{2l} + o(t^{2N-2n}) \right) \tag{11.12}$$

and

$$p_{n,2}^{TE}[\mu,\epsilon,t] = t^{-n-1} \left(\sum_{l=0}^{N-n} g_{n,l}^{TE}(\mu,\epsilon) t^{2l} + o(t^{2N-2n}) \right). \tag{11.13}$$

Similarly, $p_{n,1}^{TM}$ and $p_{n,2}^{TM}$ have the following expansions:

$$p_{n,1}^{TM}[\mu,\epsilon,t] = t^n \left(\sum_{l=0}^{N-n} f_{n,l}^{TM}(\mu,\epsilon) t^{2l} + o(t^{2N-2n}) \right) \tag{11.14}$$

and

$$p_{n,2}^{TM}[\mu,\epsilon,t] = t^{-n-1} \left(\sum_{l=0}^{N-n} g_{n,l}^{TM}(\mu,\epsilon) t^{2l} + o(t^{2N-2n}) \right) \tag{11.15}$$

for $t = \rho\omega$ and some functions $f_{n,l}^{TE}, g_{n,l}^{TE}, f_{n,l}^{TM}$, and $g_{n,l}^{TM}$ independent of t.

LEMMA 11.3. *For any pair of (μ,ϵ), one has*

$$g_{n,0}^{TE}(\mu,\epsilon) \neq 0 \tag{11.16}$$

and

$$g_{n,0}^{TM}(\mu,\epsilon) \neq 0. \tag{11.17}$$

PROOF. Assume that there exists a pair of (μ, ϵ) such that $g_{n,0}^{TE}(\mu, \epsilon) = 0$. Since $p_{n,2}^{TE}[\mu, \epsilon, \rho\omega] = o(\rho^{-n-1})$, the solution given by (6.29) with $a_0 = 1$ and $\tilde{a}_0 = 0$ satisfies

$$\begin{cases} \nabla \times \left(\dfrac{1}{\mu}\nabla \times \mathbf{E}\right) - \rho^2\omega^2\epsilon\mathbf{E} = 0 & \text{in } \mathbb{R}^3 \setminus \overline{D}, \\ \nabla \cdot \mathbf{E} = 0 & \text{in } \mathbb{R}^3 \setminus \overline{D}, \\ (\nu \times \mathbf{E})\big|_+ = o(\rho^{-(n+1)}) & \text{on } \partial D, \\ \mathbf{E}(x) = h_n^{(1)}(\rho k_0 |x|)\mathbf{V}_{n,0}(\hat{x}) & \text{for } |x| > 2. \end{cases}$$

Let $\mathbf{V}(x) = \lim_{\rho \to 0} \rho^{n+1}\mathbf{E}(x)$. Using (11.11) one knows that the limit $\mathbf{V}$ satisfies

$$\begin{cases} \nabla \times \left(\dfrac{1}{\mu}\nabla \times \mathbf{V}\right) = 0 & \text{in } \mathbb{R}^3 \setminus \overline{D}, \\ \nabla \cdot \mathbf{V} = 0 & \text{in } \mathbb{R}^3 \setminus \overline{D}, \\ (\nu \times \mathbf{V})\big|_+ = 0 & \text{on } \partial D, \\ \mathbf{V}(x) = -\big((2n-1)!!\big)\mathbf{V}_{n,0}(\hat{x}) & \text{for } |x| > 2. \end{cases}$$

Since $\mathbf{V}_{n,0}(\hat{x}) = O(|x|^{-1})$, one gets $\mathbf{V}(x) = 0$ by Green's formula, which is a contradiction. Thus $g_{n,0}^{TE}(\mu, \epsilon) \neq 0$. In a similar way, (11.17) can be proved. $\square$

From Lemma 11.3, one obtains the following result.

PROPOSITION 11.4. *One has*

$$W_n^{TE}[\mu, \epsilon, t] = t^{2n+1} \sum_{l=0}^{N-n} W_{n,l}^{TE}[\mu, \epsilon] t^{2l} + o(t^{2N+1})$$

and

$$W_n^{TM}[\mu, \epsilon, t] = t^{2n+1} \sum_{l=0}^{N-n} W_{n,l}^{TM}[\mu, \epsilon] t^{2l} + o(t^{2N+1}),$$

where $t = \rho\omega$ and the coefficients $W_{n,l}^{TE}[\mu, \epsilon]$ and $W_{n,l}^{TM}[\mu, \epsilon]$ are independent of t.

Hence, if one has (μ, ϵ) such that

$$W_{n,l}^{TE}[\mu, \epsilon] = W_{n,l}^{TM}[\mu, \epsilon] = 0, \quad \text{for all } 1 \leq n \leq N,\ 0 \leq l \leq (N-n), \tag{11.18}$$

(μ, ϵ) satisfies (11.8); in other words, it is an *S-vanishing structure of order N at low frequencies*. It is quite challenging to construct (μ, ϵ) analytically satisfying (11.18). The next subsection presents some numerical examples of such structures.

11.2.5. Numerical Implementation.

Code:	11.1 Near Cloaking for Maxwell's Equations	DemoNearCloaking.m

In this section we demonstrate some numerical examples of S-vanishing structures of order N at low frequencies based on (11.18). As in the previous sections, we do this using a gradient descent method for a suitable energy functional. We symbolically compute the scattering coefficients. In the place of spherical Bessel functions and spherical Hankel functions, we use their low-frequency expansions and symbolically compute W_n^{TE} and W_n^{TM} to obtain $W_{n,l}^{TE}$ and $W_{n,l}^{TM}$.

The following example is a S-vanishing structure of order $N = 2$ made of 6 multilayers. The radii of the concentric disks are $r_j = 2 - \frac{j-1}{6}$ for $j = 1, \ldots, 7$.

From Proposition 11.4, the nonzero leading terms of $W_n^{TE}[\mu,\epsilon,t]$ and $W_n^{TM}[\mu,\epsilon,t]$ up to t^5 are

- $[t^3,t^5]$ terms in $W_1^{TE}[\mu,\epsilon,t]$, *i.e.*, $W_{1,0}^{TE}, W_{1,1}^{TE}$,
- $[t^3,t^5]$ terms in $W_1^{TM}[\mu,\epsilon,t]$, *i.e.*, $W_{1,0}^{TM}, W_{1,1}^{TM}$,
- $[t^5]$ term in $W_2^{TE}[\mu,\epsilon,t]$, *i.e.*, $W_{2,0}^{TE}$,
- $[t^5]$ term in $W_2^{TM}[\mu,\epsilon,t]$, *i.e.*, $W_{2,0}^{TM}$.

Consider the mapping

$$(\boldsymbol{\mu},\epsilon) \longrightarrow (W_{1,0}^{TE}, W_{1,1}^{TE}, W_{1,0}^{TM}, W_{1,1}^{TM}, W_{2,0}^{TE}, W_{2,0}^{TM}), \tag{11.19}$$

where, $\mu = (\mu_1,\ldots,\mu_6)$ and $\epsilon = (\epsilon_1,\ldots,\epsilon_6)$. One looks for (μ,ϵ) in which the right-hand side of (11.19) is as small as possible. Since (11.19) is a nonlinear equation, we solve it iteratively. Initially, we set $\mu = \mu^{(0)}$ and $\epsilon = \epsilon^{(0)}$. We then iteratively modify $(\mu^{(i)},\epsilon^{(i)})$

$$[\boldsymbol{\mu}^{(i+1)}\ \epsilon^{(i+1)}]^T = [\boldsymbol{\mu}^{(i)}\ \epsilon^{(i)}]^T - A_i^{\dagger}\mathbf{b}^{(i)}, \tag{11.20}$$

where $A_i^{\dagger}$ is the pseudoinverse of

$$A_i := \frac{\partial(W_{1,0}^{TE}, W_{1,1}^{TE},\ldots,W_{2,0}^{TM})}{\partial(\mu,\epsilon)}\Big|_{(\mu,\epsilon)=(\mu^{(i)},\epsilon^{(i)})},$$

and

$$\mathbf{b}^{(i)} = \begin{bmatrix} W_{1,0}^{TE} \\ W_{1,1}^{TE} \\ \vdots \\ W_{2,0}^{TM} \end{bmatrix}\Bigg|_{(\mu,\epsilon)=(\mu^{(i)},\epsilon^{(i)})}.$$

Example 1. Figure 11.1 and Figure 11.2 show computational results for a 6-layer S-vanishing structure of order $N=2$. We sets $r = (2,\frac{11}{6},\ldots,\frac{7}{6})$, $\mu^{(0)} = (3,6,3,6,3,6)$ and $\epsilon^{(0)} = (3,6,3,6,3,6)$ and modify them following (11.20) with the constraints that μ and ϵ belongs to the interval between 0.1 and 10. The obtained material parameters are $\mu = (0.1000, 1.1113, 0.2977, 2.0436, 0.1000, 1.8260)$ and $\epsilon = (0.4356, 1.1461, 0.2899, 1.8199, 0.1000, 3.1233)$, respectively. In contrast to the no-layer structure with PEC condition at $|x|=1$, the obtained multilayer structure has nearly zero coefficients for $W_n^{TE}[\mu,\epsilon,t]$ and $W_n^{TM}[\mu,\epsilon,t]$ up to t^5.

11.3. Enhancement of near cloaking

In this section we constructs a cloaking structure based on the following lemma.

LEMMA 11.5. *Let F be an orientation-preserving diffeomorphism of $\mathbb{R}^3$ onto $\mathbb{R}^3$ such that $F(x)$ is identity for $|x|$ large enough. If (E,H) is a solution to*

$$\begin{cases} \nabla\times E = i\omega\mu H & \text{in } \mathbb{R}^3, \\ \nabla\times H = -i\omega\epsilon E & \text{in } \mathbb{R}^3, \\ (E-E^i, H-H^i) \text{ is radiating}, \end{cases} \tag{11.21}$$

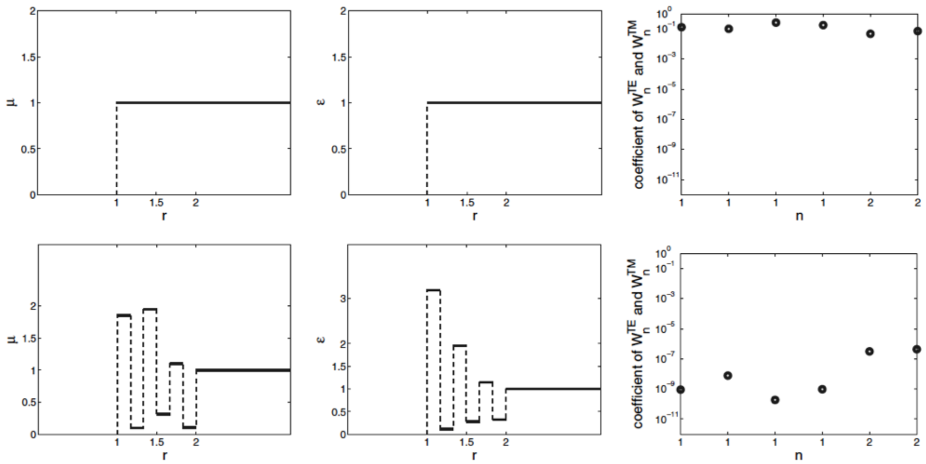

FIGURE 11.1. This figure shows the graph of the material parameters and the corresponding coefficients in $W_n^{TE}[\mu, \epsilon, t]$ and $W_n^{TM}[\mu, \epsilon, t]$ up to t^5. The first row is for the no-layer case, and the second row is for a 6-layer S-vanishing structure of order $N = 2$, which is explained in Example 1. In the third column, the y-axis shows $(W_{1,0}^{TE}, W_{1,1}^{TE}, W_{1,0}^{TM}, W_{1,1}^{TM}, W_{2,0}^{TE}, W_{2,0}^{TM})$ from left to right.

then $(\widetilde{E}, \widetilde{H})$ *defined by* $(\widetilde{E}(y), \widetilde{H}(y)) = \big((DF)^{-T}E(F^{-1}(y)), (DF)^{-T}H(F^{-1}(y))\big)$ *satisfies*

$$\begin{cases} \nabla \times \widetilde{E} = i\omega(F_*\mu)\widetilde{H} & \text{in } \mathbb{R}^3, \\ \nabla \times \widetilde{H} = -i\omega(F_*\epsilon)\widetilde{E} & \text{in } \mathbb{R}^3, \\ (\widetilde{E} - \widetilde{E}^i, \widetilde{H} - \widetilde{H}^i) \text{ is radiating,} \end{cases}$$

where $(\widetilde{E}^i(y), \widetilde{H}^i(y)) = \big((DF)^{-T}E^i(F^{-1}(y)), (DF)^{-T}H^i(F^{-1}(y))\big)$,

$$(F_*\mu)(y) = \frac{DF(x)\mu(x)DF^T(x)}{\det(DF(x))}, \quad \text{and} \quad (F_*\epsilon)(y) = \frac{DF(x)\epsilon(x)DF^T(x)}{\det(DF(x))},$$

with $x = F^{-1}(y)$ *and* DF *is the Jacobian matrix of* F.

Hence,

$$A[\mu, \epsilon, \omega] = A[F_*\mu, F_*\epsilon, \omega].$$

To compute the scattering amplitude which corresponds to the material parameters before the transformation, we consider the following scaling function, for small parameter ρ,

$$\Psi_{\frac{1}{\rho}}(x) = \frac{1}{\rho}x, \quad x \in \mathbb{R}^3.$$

Then we have the following relation between the scattering amplitudes, which correspond to two sets of differently scaled material parameters and frequency:

$$A_\infty\left[\mu \circ \Psi_{\frac{1}{\rho}}, \epsilon \circ \Psi_{\frac{1}{\rho}}, \omega\right] = A_\infty[\mu, \epsilon, \rho\omega]. \tag{11.22}$$

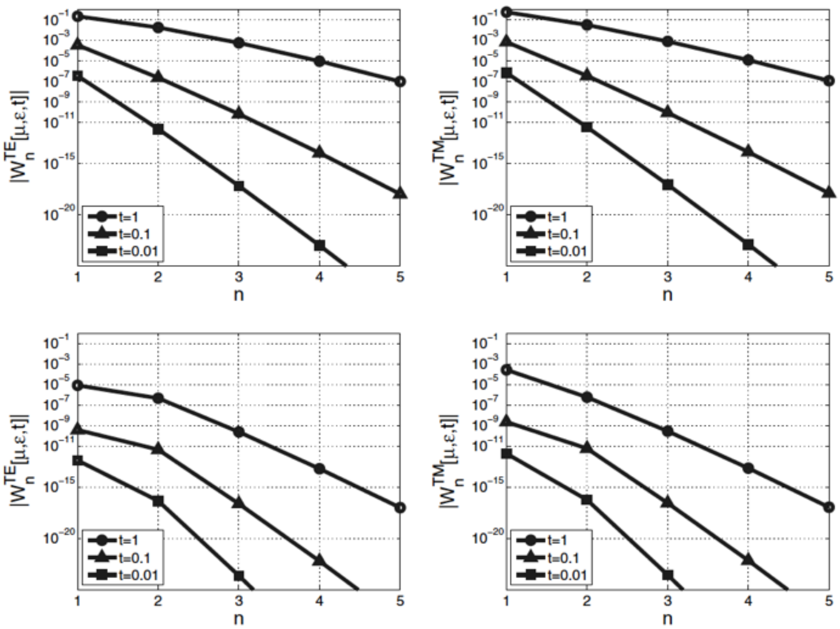

FIGURE 11.2. This figure shows the graph of $W_n^{TE}[\mu,\epsilon,t]$ and $W_n^{TM}[\mu,\epsilon,t]$ for various values of t. The first row is for the no-layer case, and the second row is for a 6-layer S-vanishing structure of order $N = 2$ which is explained in Example 1. The values of W_n^{TE} and W_n^{TM} are much smaller in the S-vanishing structure than in the no-layer structure.

To see this, consider (E, H) which satisfies

$$\begin{cases} (\nabla \times E)(x) = i\omega\big(\mu \circ \Psi_{\frac{1}{\rho}}\big)(x)H(x) & \text{for } x \in \mathbb{R}^3 \setminus \overline{B_\rho}, \\ (\nabla \times H)(x) = -i\omega\big(\epsilon \circ \Psi_{\frac{1}{\rho}}\big)(x)E(x) & \text{for } x \in \mathbb{R}^3 \setminus \overline{B_\rho}, \\ \hat{x} \times E(x) = 0 & \text{on } \partial B_\rho, \\ (E - E^i, H - H^i) \text{ is radiating,} \end{cases}$$

with the incident wave $E^i(x) = e^{i\mathbf{k}\cdot x}\hat{\mathbf{c}}$ and $H^i = \frac{1}{i\omega\mu_0}\nabla \times E^i$ with $\mathbf{k} \cdot \hat{\mathbf{c}} = 0$ and $|\mathbf{k}| = k_0$. Here B_ρ is the ball of radius ρ centered at the origin. Set $y = \frac{1}{\rho}x$ and define

$$\big(\widetilde{E}(y), \widetilde{H}(y)\big) := \Big(\big(E \circ \Psi_{\frac{1}{\rho}}^{-1}\big)(y), \big(H \circ \Psi_{\frac{1}{\rho}}^{-1}\big)(y)\Big) = \Big(\big(E \circ \Psi_\rho\big)(y), \big(H \circ \Psi_\rho\big)(y)\Big)$$

and

$$\big(\widetilde{E}^i(y), \widetilde{H}^i(y)\big) := \Big(\big(E^i \circ \Psi_\rho\big)(y), \big(H^i \circ \Psi_\rho\big)(y)\Big).$$

Then, one has

$$\begin{cases} \left(\nabla_y \times \widetilde{E}\right)(y) = i\rho\omega\mu(y)\widetilde{H}(y) & \text{for } y \in \mathbb{R}^3 \setminus \overline{B_1} \\ \left(\nabla_y \times \widetilde{H}\right)(y) = -i\rho\omega\epsilon(y)\widetilde{E}(y) & \text{for } y \in \mathbb{R}^3 \setminus \overline{B_1}, \\ \hat{y} \times \widetilde{E}(y) = 0 & \text{on } \partial B_1, \\ (\widetilde{E} - \widetilde{E}^i, \widetilde{H} - \widetilde{H}^i) \text{ is radiating} \end{cases}$$

Recall that the scattered wave can be represented using the scattering amplitude as follows:

$$(E - E^i)(x) \sim \frac{e^{ik_0|x|}}{k_0|x|} A_\infty \left[\mu \circ \Psi_{\frac{1}{\rho}}, \epsilon \circ \Psi_{\frac{1}{\rho}}, \omega\right](\mathbf{c}, \hat{\mathbf{k}}; \hat{x}) \quad \text{as } |x| \to \infty,$$

and

$$(\widetilde{E} - \widetilde{E}^i)(y) \sim \frac{e^{ik_0\rho|y|}}{k_0\rho|y|} A_\infty[\mu, \epsilon, \omega](\mathbf{c}, \hat{\mathbf{k}}; \hat{x}) \quad \text{as } |y| \to \infty.$$

Since the left-hand sides of the previous equations are coincident, we have (11.22).

Suppose that (μ, ϵ) is an S-vanishing structure of order N at low frequencies as in Section 11.2. From (11.9) and (11.22). Then we have

$$A_\infty \left[\mu \circ \Psi_{\frac{1}{\rho}}, \epsilon \circ \Psi_{\frac{1}{\rho}}, \omega\right](\mathbf{c}, \hat{\mathbf{k}}; \hat{x}) = o(\rho^{2N+1}) \tag{11.23}$$

. We define the diffeomorphism F_ρ as

$$F_\rho(x) := \begin{cases} x & \text{for } |x| \geq 2, \\ \left(\dfrac{3-4\rho}{2(1-\rho)} + \dfrac{1}{4(1-\rho)}|x|\right)\dfrac{x}{|x|} & \text{for } 2\rho \leq |x| \leq 2, \\ \left(\dfrac{1}{2} + \dfrac{1}{2\rho}|x|\right)\dfrac{x}{|x|} & \text{for } \rho \leq |x| \leq 2\rho, \\ \dfrac{x}{\rho} & \text{for } |x| \leq \rho. \end{cases}$$

Then using (11.23) and Lemma 11.5 we obtain the main result of this chapter.

THEOREM 11.6. *If (μ, ϵ) is a S-vanishing structure of order N at low frequencies, then there exists ρ_0 such that*

$$A_\infty \left[(F_\rho)_*(\mu \circ \Psi_{\frac{1}{\rho}}), (F_\rho)_*(\epsilon \circ \Psi_{\frac{1}{\rho}}), \omega\right](\mathbf{c}, \hat{\mathbf{k}}; \hat{x}) = o(\rho^{2N+1}),$$

for all $\rho \leq \rho_0$, uniformly in $(\hat{\mathbf{k}}, \hat{x})$.

Note that the cloaking structure $\left((F_\rho)_*(\mu \circ \Psi_{\frac{1}{\rho}}), (F_\rho)_*(\epsilon \circ \Psi_{\frac{1}{\rho}})\right)$ in Theorem 11.6 satisfies the PEC boundary condition on $|x| = 1$.

CHAPTER 12

Anomalous Resonance Cloaking and Shielding

12.1. Introduction

We consider the dielectric problem with a source term αf, proportional to f, which models the quasi-static (zero-frequency) transverse magnetic regime. The cloaking of the source is achieved in a region external to a plasmonic structure. The plasmonic structure consists of a shell having relative permittivity $-1+\sqrt{-1}\delta$ with δ modeling losses.

The cloaking issue is directly linked to the existence of anomalous localized resonance (ALR), which is tied to the fact that an elliptic system of equations can exhibit localization effects near the boundary of ellipticity. The plasmonic structure exhibits ALR if, as the loss parameter δ goes to zero, the magnitude of the quasi-static in-plane electric field diverges throughout a specific region (with sharp boundary not defined by any discontinuities in the relative permittivity), called the anomalous resonance region, but converges to a smooth field outside that region.

To state the problem, let Ω be a bounded domain in $\mathbb{R}^2$ and let D be a domain whose closure is contained in Ω. Throughout this chapter, we assume that Ω and D are smooth. For a given loss parameter $\delta > 0$, the permittivity distribution in $\mathbb{R}^2$ is given by

$$\varepsilon_\delta = \begin{cases} 1 & \text{in } \mathbb{R}^2 \setminus \overline{\Omega}\,, \\ -1+\sqrt{-1}\delta & \text{in } \Omega \setminus \overline{D}\,, \\ 1 & \text{in } D\,. \end{cases} \tag{12.1}$$

We may consider the configuration as a core with permittivity 1 coated by the shell $\Omega \setminus \overline{D}$ with permittivity $-1+\sqrt{-1}\delta$. For a given function f compactly supported in $\mathbb{R}^2$ satisfying

$$\int_{\mathbb{R}^2} f\,dx = 0 \tag{12.2}$$

(which physically is required by conservation of charge), we consider the following dielectric problem:

$$\nabla \cdot \varepsilon_\delta \nabla V_\delta = \alpha f \quad \text{in } \mathbb{R}^2\,, \tag{12.3}$$

with the decay condition $V_\delta(x) \to 0$ as $|x| \to \infty$.

A fundamental problem is to identify those sources f such that when $\alpha = 1$ then first

$$E_\delta := \int_{\Omega\setminus\overline{D}} \delta |\nabla V_\delta|^2 dx \to \infty \quad \text{as } \delta \to 0\,. \tag{12.4}$$

and second V_δ remains bounded outside some radius a:

(12.5)
$$|V_\delta(x)| < C, \quad \text{when } |x| > a$$

for some constants C and a independent of δ (which requires that the ball B_a contains the entire region of anomalous localized resonance). The quantity E_δ is proportional to the electromagnetic power dissipated into heat by the time harmonic electrical field averaged over time. Hence (12.4) implies an infinite amount of energy dissipated per unit time in the limit $\delta \to 0$ which is unphysical. If instead we choose $\alpha = 1/\sqrt{E_\delta}$ then the source αf will produce the same power independent of δ and the new associated solution V_δ (which is the previous solution V_δ multiplied by α) will approach zero outside the radius a: cloaking due to anomalous localized resonance (CALR) occurs. The conditions (12.4) and (12.5) are sufficient to ensure CALR: a necessary and sufficient condition is that (with $\alpha = 1$) $V_\delta/\sqrt{E_\delta}$ goes to zero outside some radius as $\delta \to 0$. We also consider a weaker blow-up of the energy dissipation, namely,

(12.6)
$$\limsup_{\delta \to 0} E_\delta = \infty .$$

We say that weak CALR takes place if (12.6) holds (in addition to (12.5)). Then the (renormalized) source $f/\sqrt{E_\delta}$ will be essentially invisible for an infinite sequence of small values of δ tending to zero (but would be visible for values of δ interspersed between this sequence if CALR does not additionaly hold).

The aim of this chapter is to review a general method based on the potential theory to study cloaking due to anomalous resonance. Using layer potential techniques, we reduce the problem to a singularly perturbed system of integral equations. The system is non-self-adjoint. A symmetrization technique can be applied in the general case. In the case of an annulus (D is the disk of radius r_i and Ω is the concentric disk of radius r_e), it is known [**?**] that there exists a critical radius (the cloaking radius)

(12.7)
$$r_\star = \sqrt{r_e^3 r_i^{-1}} .$$

such that any finite collection of dipole sources located at fixed positions within the annulus $B_{r_\star} \setminus \overline{B}_e$ is cloaked. We show that if f is an integrable function supported in $E \subset B_{r_\star} \setminus \overline{B}_e$ satisfying (12.2) and the Newtonian potential of f does not extend as a harmonic function in $B_{r_\star}$, then weak CALR takes place. Moreover, we show that if the Fourier coefficients of the Newtonian potential of f satisfy a mild gap condition, then CALR takes place. Conversely we show that if the source function f is supported outside $B_{r_\star}$ then (12.4) does not happen and no cloaking occurs.

We also show that a cylindrical superlens can also act as a new kind of electrostatic shielding device if the core is eccentric to the shell. While such a conventional device shields a region enclosed by the device, a superlens with an eccentric core can shield a non-coated region which is located outside the device. Moreover, the size of the shielded region can be arbitrarily large while that of the device is fixed. We call this phenomenon *shielding at a distance*. The key element to study in the eccentric case is the Möbius transformation via which a concentric annulus is transformed into an eccentric one. We also provide various numerical examples to show the cloaking effect and shielding effect due to anomalous resonance.

12.2. Layer Potential Formulation

As in Chapter 2, for ∂D or $\partial\Omega$, we denote, respectively, the single and double layer potentials of a function $\phi \in L^2$ as $\mathcal{S}_D^0[\phi]$ and $\mathcal{D}_\Omega^0[\phi]$. We also introduce the associated Neumann-Poincaré operators $\mathcal{K}_D^0$ and $\mathcal{K}_\Omega^0$.

Let F be the Newtonian potential of f, *i.e.*,

$$F(x) = \int_{\mathbb{R}^2} \Gamma(x,y) f(y) dy, \quad x \in \mathbb{R}^2. \tag{12.8}$$

Then F satisfies $\Delta F = f$ in $\mathbb{R}^2$, and the solution V_δ to (12.3) may be represented as

$$V_\delta(x) = F(x) + \mathcal{S}_D^0[\phi_i](x) + \mathcal{S}_\Omega^0[\phi_e](x) \tag{12.9}$$

for some functions $\phi_i \in L_0^2(\partial D)$ and $\phi_e \in L_0^2(\partial\Omega)$ (L_0^2 is the collection of all square integrable functions with the integral zero). The transmission conditions along the interfaces $\partial\Omega$ and ∂D satisfied by V_δ read

$$\begin{aligned} (-1+\sqrt{-1}\delta)\frac{\partial V_\delta}{\partial \nu}\Big|_+ &= \frac{\partial V_\delta}{\partial \nu}\Big|_- \quad \text{on } \partial D, \\ \frac{\partial V_\delta}{\partial \nu}\Big|_+ &= (-1+\sqrt{-1}\delta)\frac{\partial V_\delta}{\partial \nu}\Big|_- \quad \text{on } \partial \Omega. \end{aligned}$$

Hence the pair of potentials (ϕ_i, ϕ_e) is the solution to the following system of integral equations:

$$\begin{cases} (-1+\sqrt{-1}\delta)\dfrac{\partial \mathcal{S}_D^0[\phi_i]}{\partial \nu_i}\Big|_+ - \dfrac{\partial \mathcal{S}_D^0[\phi_i]}{\partial \nu_i}\Big|_- + (-2+\sqrt{-1}\delta)\dfrac{\partial \mathcal{S}_\Omega^0[\phi_e]}{\partial \nu_i} = (2-\sqrt{-1}\delta)\dfrac{\partial F}{\partial \nu_i} \quad \text{on } \partial D, \\ (2-\sqrt{-1}\delta)\dfrac{\partial \mathcal{S}_D^0[\phi_i]}{\partial \nu_e} + \dfrac{\partial \mathcal{S}_\Omega^0[\phi_e]}{\partial \nu_e}\Big|_+ - (-1+\sqrt{-1}\delta)\dfrac{\partial \mathcal{S}_\Omega^0[\phi_e]}{\partial \nu_e}\Big|_- = (-2+\sqrt{-1}\delta)\dfrac{\partial F}{\partial \nu_e} \quad \text{on } \partial \Omega. \end{cases}$$

Note that we have used the notation ν_i and ν_e to indicate the outward normal on ∂D and $\partial\Omega$, respectively. Using the jump formula for the normal derivative of the single layer potentials, the above equations can be rewritten as

$$\begin{bmatrix} -z_\delta I + (\mathcal{K}_D^0)^* & \dfrac{\partial}{\partial \nu_i}\mathcal{S}_\Omega^0 \\ \dfrac{\partial}{\partial \nu_e}\mathcal{S}_D^0 & z_\delta I + (\mathcal{K}_\Omega^0)^* \end{bmatrix} \begin{bmatrix} \phi_i \\ \phi_e \end{bmatrix} = - \begin{bmatrix} \dfrac{\partial F}{\partial \nu_i} \\ \dfrac{\partial F}{\partial \nu_e} \end{bmatrix} \tag{12.10}$$

on $L_0^2(\partial D) \times L_0^2(\partial\Omega)$, where we set

$$z_\delta = \frac{\sqrt{-1}\delta}{2(2-\sqrt{-1}\delta)}. \tag{12.11}$$

Note that the operator in (12.10) can be viewed as a compact perturbation of the operator

$$R_\delta := \begin{bmatrix} -z_\delta I + (\mathcal{K}_D^0)^* & 0 \\ 0 & z_\delta I + (\mathcal{K}_\Omega^0)^* \end{bmatrix}. \tag{12.12}$$

Recall that the eigenvalues of $(\mathcal{K}_D^0)^*$ and $(\mathcal{K}_\Omega^0)^*$ lie in the interval $]-\frac{1}{2}, \frac{1}{2}]$. Observe that $z_\delta \to 0$ as $\delta \to 0$ and that there are sequences of eigenvalues of $(\mathcal{K}_D^0)^*$ and $(\mathcal{K}_\Omega^0)^*$ approaching 0 since $(\mathcal{K}_D^0)^*$ and $(\mathcal{K}_\Omega^0)^*$ are compact. So 0 is the essential singularity of the operator valued meromorphic function

$$\lambda \in \mathbb{C} \mapsto (\lambda I + (\mathcal{K}_\Omega^0)^*)^{-1}.$$

This causes a serious difficulty in dealing with (12.10). We emphasize that $(\mathcal{K}_\Omega^0)^*$ is not self-adjoint in general. In fact, $(\mathcal{K}_\Omega^0)^*$ is self-adjoint only when $\partial\Omega$ is a circle or a sphere.

Let $\mathcal{H} = L^2(\partial D) \times L^2(\partial\Omega)$. We write (12.10) in a slightly different form. We first apply the operator

$$\begin{bmatrix} -I & 0 \\ 0 & I \end{bmatrix} : \mathcal{H} \to \mathcal{H}$$

to (12.10). Then the equation becomes

$$\begin{bmatrix} z_\delta I - (\mathcal{K}_D^0)^* & -\dfrac{\partial}{\partial \nu_i}\mathcal{S}_\Omega^0 \\ \dfrac{\partial}{\partial \nu_e}\mathcal{S}_D^0 & z_\delta I + (\mathcal{K}_\Omega^0)^* \end{bmatrix} \begin{bmatrix} \phi_i \\ \phi_e \end{bmatrix} = \begin{bmatrix} \dfrac{\partial F}{\partial \nu_i} \\ -\dfrac{\partial F}{\partial \nu_e} \end{bmatrix}. \tag{12.13}$$

Let the Neumann-Poincaré-type operator $\mathbb{K}^* : \mathcal{H} \to \mathcal{H}$ be defined by

$$\mathbb{K}^* := \begin{bmatrix} -(\mathcal{K}_D^0)^* & -\dfrac{\partial}{\partial \nu_i}\mathcal{S}_\Omega^0 \\ \dfrac{\partial}{\partial \nu_e}\mathcal{S}_D^0 & (\mathcal{K}_\Omega^0)^* \end{bmatrix}, \tag{12.14}$$

and let

$$\Phi := \begin{bmatrix} \phi_i \\ \phi_e \end{bmatrix}, \quad g := \begin{bmatrix} \dfrac{\partial F}{\partial \nu_i} \\ -\dfrac{\partial F}{\partial \nu_e} \end{bmatrix}. \tag{12.15}$$

Then, (12.13) can be rewritten in the form

$$(z_\delta \mathbb{I} + \mathbb{K}^*)\Phi = g, \tag{12.16}$$

where $\mathbb{I}$ is given by

$$\mathbb{I} = \begin{bmatrix} I & 0 \\ 0 & I \end{bmatrix}.$$

12.3. Explicit computations for an annulus

Let B be the disk of radius r_0 is centered at the origin, then one can easily see that for each integer $n \neq 0$

$$\mathcal{S}_B^0[e^{\sqrt{-1}n\theta}](x) = \begin{cases} -\dfrac{r_0}{2|n|}\left(\dfrac{r}{r_0}\right)^{|n|} e^{\sqrt{-1}n\theta} & \text{if } |x| = r < r_0, \\ -\dfrac{r_0}{2|n|}\left(\dfrac{r_0}{r}\right)^{|n|} e^{\sqrt{-1}n\theta} & \text{if } |x| = r > r_0, \end{cases} \tag{12.17}$$

and hence

$$\frac{\partial}{\partial r}\mathcal{S}_B^0[e^{\sqrt{-1}n\theta}](x) = \begin{cases} -\dfrac{1}{2}\left(\dfrac{r}{r_0}\right)^{|n|-1} e^{\sqrt{-1}n\theta} & \text{if } |x| = r < r_0, \\ \dfrac{1}{2}\left(\dfrac{r_0}{r}\right)^{|n|+1} e^{\sqrt{-1}n\theta} & \text{if } |x| = r > r_0. \end{cases} \tag{12.18}$$

We also get, for any integer n,

$$\mathcal{D}_B^0[e^{\sqrt{-1}n\theta}](x) = \begin{cases} \dfrac{1}{2}\left(\dfrac{r}{r_0}\right)^{|n|} e^{\sqrt{-1}n\theta} & \text{if } |x| = r < r_0, \\ -\dfrac{1}{2}\left(\dfrac{r_0}{r}\right)^{|n|} e^{\sqrt{-1}n\theta} & \text{if } |x| = r > r_0. \end{cases}$$

It follows from (**??**) that

$$(\mathcal{K}_B^0)^*[e^{\sqrt{-1}n\theta}] = 0 \quad \forall n \neq 0. \tag{12.19}$$

As $\mathcal{K}_\Omega^0[1] = 1/2$, it follows that, when B is a disk, $\mathcal{K}_B^0$ is a rank one operator whose only non-zero eigenvalue is $1/2$. On the other hand, from $\mathcal{K}_B^0[1] = 1/2$ it also follows that

$$\mathcal{S}_B^0[1](x) = \begin{cases} \ln r_0 & \text{if } |x| = r < r_0, \\ \ln |x| & \text{if } |x| = r > r_0, \end{cases} \tag{12.20}$$

and hence

$$\frac{\partial}{\partial r}\mathcal{S}_B^0[1](x) = \begin{cases} 0 & \text{if } |x| = r < r_0, \\ \dfrac{1}{r} & \text{if } |x| = r > r_0. \end{cases} \tag{12.21}$$

Let Ω_i and Ω_e be two concentric disks in $\mathbb{R}^2$ with radii $r_i < r_e$. Define $(\mathcal{K}^0_{\Omega_e \setminus \overline{\Omega}_i})^*$ by

$$(\mathcal{K}^0_{\Omega_e \setminus \overline{\Omega}_i})^* = \begin{pmatrix} -(\mathcal{K}^0_{\Omega_i})^* & -\frac{\partial}{\partial \nu^i}\mathcal{S}^0_{\Omega_e} \\ \frac{\partial}{\partial \nu^e}\mathcal{S}^0_{\Omega_i} & (\mathcal{K}^0_{\Omega_e})^* \end{pmatrix}, \tag{12.22}$$

where ν^i and ν^e are the outward normal vectors to $\partial\Omega_i$ and Ω_e, respectively. Let the operator $\mathbb{S}_{\Omega_e \setminus \overline{\Omega}_i}$ be given by

$$\mathbb{S}_{\Omega_e \setminus \overline{\Omega}_i} = \begin{pmatrix} \mathcal{S}^0_{\Omega_e} & \mathcal{S}^0_{\Omega_i}\big|_{\partial\Omega_e} \\ \mathcal{S}^0_{\Omega_e}\big|_{\partial\Omega_i} & \mathcal{S}^0_{\Omega_i} \end{pmatrix}.$$

Then, following the arguments given in Subsection **??**, we can prove that $(\mathcal{K}^0_{\Omega_e \setminus \overline{\Omega}_i})^*$ is compact and self-adjoint for the inner product

$$\langle \varphi, \psi \rangle_{\mathcal{H}^*} := -\langle \mathbb{S}_{\Omega_e \setminus \overline{\Omega}_i}[\psi], \varphi \rangle_{1/2,-1/2} \quad \text{for } \varphi, \psi \in H^{-1/2}(\partial\Omega_e) \times H^{-1/2}(\partial\Omega_i). \tag{12.23}$$

The following lemma from [**?**] gives the eigenvalues and eigenvectors of the Neumann-Poincaré operator $(\mathcal{K}^0_{\Omega_e \setminus \overline{\Omega}_i})^*$ associated with the circular shell $\Omega_e \setminus \overline{\Omega_i}$ on $\mathcal{H}^*$.

LEMMA 12.1. *The eigenvalues of $(\mathcal{K}^0_{\Omega_e \setminus \overline{\Omega}_i})^*$ on $\mathcal{H}^*$ are*

$$-\frac{1}{2}, \frac{1}{2}, -\frac{1}{2}\left(\frac{r_i}{r_e}\right)^n, \frac{1}{2}\left(\frac{r_i}{r_e}\right)^n, \quad n = 1, 2, \ldots,$$

and corresponding eigenvectors are

$$\begin{bmatrix} 1 \\ -\frac{1}{r_e} \end{bmatrix}, \begin{bmatrix} 0 \\ 1 \end{bmatrix}, \begin{bmatrix} e^{\pm\sqrt{-1}n\theta} \\ \frac{r_i}{r_e} e^{\pm\sqrt{-1}n\theta} \end{bmatrix}, \begin{bmatrix} e^{\pm\sqrt{-1}n\theta} \\ -\frac{r_i}{r_e} e^{\pm\sqrt{-1}n\theta} \end{bmatrix}, \quad n = 1, 2, \ldots.$$

PROOF. We first prove that $\pm 1/2$ are eigenvalues of $(\mathcal{K}^0_{\Omega_e\setminus\overline{\Omega}_i})^*$ on $\mathcal{H}^*$. From (12.21) we have

$$(\mathcal{K}^0_{\Omega_e\setminus\overline{\Omega}_i})^* \begin{bmatrix} a \\ b \end{bmatrix} = \begin{pmatrix} -\frac{1}{2} & 0 \\ \frac{1}{r_e} & \frac{1}{2} \end{pmatrix} \begin{bmatrix} a \\ b \end{bmatrix},$$

where a and b are constants. So $\pm 1/2$ are eigenvalues of $(\mathcal{K}^0_{\Omega_e\setminus\overline{\Omega}_i})^*$ on $\mathcal{H}^*$.

Now we consider $(\mathcal{K}^0_{\Omega_e\setminus\overline{\Omega}_i})^*$ on $\mathcal{H}^*_0$ defined by

$$\mathcal{H}^*_0 := \{\varphi \in \mathcal{H}^* :< 1, \varphi >_{1/2,-1/2} = 0\}.$$

Because of (12.19) it follows that

$$(\mathcal{K}^0_{\Omega_e\setminus\overline{\Omega}_i})^* = \begin{pmatrix} 0 & -\dfrac{\partial}{\partial \nu^i}\mathcal{S}^0_{\Omega_e} \\ \dfrac{\partial}{\partial \nu^e}\mathcal{S}^0_{\Omega_i} & 0 \end{pmatrix}$$

on $\mathcal{H}^*_0$ and hence we have from (12.18) that

$$(\mathcal{K}^0_{\Omega_e\setminus\overline{\Omega}_i})^* \begin{bmatrix} e^{\sqrt{-1}n\theta} \\ 0 \end{bmatrix} = \frac{1}{2}(\frac{r_i}{r_e})^{|n|+1} \begin{bmatrix} 0 \\ e^{\sqrt{-1}n\theta} \end{bmatrix} \tag{12.24}$$

and

$$(\mathcal{K}^0_{\Omega_e\setminus\overline{\Omega}_i})^* \begin{bmatrix} 0 \\ e^{\sqrt{-1}n\theta} \end{bmatrix} = \frac{1}{2}(\frac{r_i}{r_e})^{|n|-1} \begin{bmatrix} e^{\sqrt{-1}n\theta} \\ 0 \end{bmatrix} \tag{12.25}$$

for all $n \neq 0$, which completes the proof of the lemma. □

REMARK 12.2. From Lemma 12.1, it follows that the eigenvalues of $(\mathcal{K}^0_{\Omega_e\setminus\overline{\Omega}_i})^*$ on $\mathcal{H}^*_0$ are $\pm(1/2)(r_i/r_e)^j$ and $(\mathcal{K}^0_{\Omega_e\setminus\overline{\Omega}_i})^*$ as an operator on $\mathcal{H}^*$ has the trivial kernel, *i.e.*,

$$\mathrm{Ker}\,(\mathcal{K}^0_{\Omega_e\setminus\overline{\Omega}_i})^* = \{0\}. \tag{12.26}$$

12.4. Anomalous Resonance in an Annulus

In this section we consider the anomalous resonance when the domains Ω and D are concentric disks. We calculate the explicit form of the limiting solution. Throughout this section, we set $\Omega = B_e = \{|x| < r_e\}$ and $D = B_i = \{|x| < r_i\}$, where $r_e > r_i$.

According to (12.24) and (12.25), if Φ is given by

$$\Phi = \sum_{n\neq 0} \begin{bmatrix} \varphi_i^n \\ \varphi_e^n \end{bmatrix} e^{\sqrt{-1}n\theta},$$

then

$$\mathbb{K}^*\Phi = \sum_{n\neq 0} \begin{bmatrix} \dfrac{\rho^{|n|-1}}{2}\varphi_e^n \\ \dfrac{\rho^{|n|+1}}{2}\varphi_i^n \end{bmatrix} e^{\sqrt{-1}n\theta}.$$

Thus, if g is given by

$$g = \sum_{n\neq 0} \begin{bmatrix} g_i^n \\ g_e^n \end{bmatrix} e^{\sqrt{-1}n\theta},$$

the integral equations (12.16) are equivalent to

$$
\begin{cases} z_\delta \phi_i^n + \dfrac{\rho^{|n|-1}}{2} \phi_e^n = g_i^n \,, \\ z_\delta \phi_e^n + \dfrac{\rho^{|n|+1}}{2} \phi_i^n = g_e^n \,, \end{cases} \tag{12.27}
$$

for every $|n| \geq 1$. It is readily seen that the solution $\Phi = (\phi_i, \phi_e)$ to (12.27) is given by

$$
\begin{aligned}
\phi_i &= 2 \sum_{n \neq 0} \frac{2 z_\delta g_i^n - \rho^{|n|-1} g_e^n}{4 z_\delta^2 - \rho^{2|n|}} e^{\sqrt{-1} n\theta} \,, \\
\phi_e &= 2 \sum_{n \neq 0} \frac{2 z_\delta g_e^n - \rho^{|n|+1} g_i^n}{4 z_\delta^2 - \rho^{2|n|}} e^{\sqrt{-1} n\theta} \,.
\end{aligned}
$$

If the source is located outside the structure, *i.e.*, f is supported in $\mathbb{R}^2 \setminus \overline{B}_e$, then the Newtonian potential of f, F, is harmonic in B_e and

$$
F(x) = c - \sum_{n \neq 0} \frac{g_e^n}{|n| r_e^{|n|-1}} r^{|n|} e^{\sqrt{-1} n\theta} \,, \tag{12.28}
$$

for $|x| \leq r_e$, where g is defined by (12.15). Thus we have

$$
g_i^n = -g_e^n \rho^{|n|-1} \,. \tag{12.29}
$$

Here, g_e^n is the Fourier coefficient of $-\frac{\partial F}{\partial \nu_e}$ on Γ_e, or in other words,

$$
-\frac{\partial F}{\partial \nu_e} = \sum_{n \neq 0} g_e^n e^{\sqrt{-1} n\theta} \,. \tag{12.30}
$$

We then get

$$
\begin{cases} \phi_i = -2 \displaystyle\sum_{n \neq 0} \frac{(2 z_\delta + 1) \rho^{|n|-1} g_e^n}{4 z_\delta^2 - \rho^{2|n|}} e^{\sqrt{-1} n\theta} \,, \\ \phi_e = 2 \displaystyle\sum_{n \neq 0} \frac{(2 z_\delta + \rho^{2|n|}) g_e^n}{4 z_\delta^2 - \rho^{2|n|}} e^{\sqrt{-1} n\theta} \,. \end{cases} \tag{12.31}
$$

Therefore, from (12.17) we find that

$$
\mathcal{S}_D^0[\phi_i](x) + \mathcal{S}_\Omega^0[\phi_e](x) = \sum_{n \neq 0} \frac{2(r_i^{2|n|} - r_e^{2|n|}) z_\delta}{|n| r_e^{|n|-1} (4 z_\delta^2 - \rho^{2|n|})} \frac{g_e^n}{r^{|n|}} e^{\sqrt{-1} n\theta}, \quad r_e < r = |x| \,, \tag{12.32}
$$

and

$$
\mathcal{S}_D^0[\phi_i](x) = -\sum_{n \neq 0} \frac{r_i^{2|n|} (2 z_\delta + 1)}{|n| r_e^{|n|-1} (\rho^{2|n|} - 4 z_\delta^2)} \frac{g_e^n}{r^{|n|}} e^{\sqrt{-1} n\theta}, \quad r_i < r = |x| < r_e \,, \tag{12.33}
$$

$$
\mathcal{S}_\Omega^0[\phi_e](x) = \sum_{n \neq 0} \frac{(2 z_\delta + \rho^{2|n|})}{|n| r_e^{|n|-1} (\rho^{2|n|} - 4 z_\delta^2)} g_e^n r^{|n|} e^{\sqrt{-1} n\theta}, \quad r_i < r = |x| < r_e \,. \tag{12.34}
$$

We next obtain the following lemma which provides essential estimates for the investigation of this section.

LEMMA 12.3. *There exists δ_0 such that*

$$E_\delta := \int_{B_e\setminus\overline{B_i}} \delta|\nabla V_\delta|^2 \approx \sum_{n\neq 0} \frac{\delta|g_e^n|^2}{|n|(\frac{\delta^2}{4}+\rho^{2|n|})} \tag{12.35}$$

uniformly in $\delta \le \delta_0$.

PROOF. Using (12.28), (12.33), and (12.34), one can see that

$$V_\delta(x) = c + r_e \sum_{n\neq 0} \left[\frac{r_i^{2|n|}}{r^{|n|}}(2z_\delta+1) - (4z_\delta^2+2z_\delta)r^{|n|} \right] \frac{g_e^n e^{\sqrt{-1}n\theta}}{|n| r_e^{|n|}(4z_\delta^2-\rho^{2|n|})}.$$

Then straightforward computations yield that

$$E_\delta \approx r_e^2 \sum_{n\neq 0} \delta(1-\rho^{2|n|}) \left| \frac{2z_\delta+1}{4z_\delta^2+\rho^{2|n|}} \right|^2 (4|z_\delta|^2-\rho^{2|n|}) \frac{|g_e^n|^2}{|n|}.$$

If δ is sufficiently small, then one can also easily show that

$$|4z_\delta^2-\rho^{2|n|}| \approx \frac{\delta^2}{4}+\rho^{2|n|}.$$

Therefore we get (12.35) and the proof is complete. □

We next investigate the behavior of the series in the right hand side of (12.35). Let

$$N_\delta = \frac{\ln(\delta/2)}{\ln\rho}. \tag{12.36}$$

If $|n| \le N_\delta$, then $(\delta/2) \le \rho^{|n|}$, and hence

$$\sum_{n\neq 0} \frac{\delta|g_e^n|^2}{|n|(\frac{\delta^2}{4}+\rho^{2|n|})} \ge \sum_{0\neq|n|\le N_\delta} \frac{\delta|g_e^n|^2}{|n|(\frac{\delta^2}{4}+\rho^{2|n|})} \ge \frac{1}{2}\sum_{0\neq|n|\le N_\delta} \frac{\delta|g_e^n|^2}{|n|\rho^{2|n|}}. \tag{12.37}$$

Suppose that

$$\limsup_{|n|\to\infty} \frac{|g_e^n|^2}{|n|\rho^{|n|}} = \infty. \tag{12.38}$$

Then there is a subsequence $\{n_k\}$ with $|n_1| < |n_2| < \cdots$ such that

$$\lim_{k\to\infty} \frac{|g_e^{n_k}|^2}{|n_k|\rho^{|n_k|}} = \infty. \tag{12.39}$$

If we take $\delta = 2\rho^{|n_k|}$, then $N_\delta = |n_k|$ and

$$\sum_{0\neq|n|\le N_\delta} \frac{\delta|g_e^n|^2}{|n|\rho^{2|n|}} = \rho^{|n_k|} \sum_{0\neq|n|\le|n_k|} \frac{|g_e^n|^2}{|n|\rho^{2|n|}} \ge \frac{|g_e^{|n_k|}|^2}{|n_k|\rho^{|n_k|}}. \tag{12.40}$$

Thus we obtain from (12.35) that

$$\lim_{k\to\infty} E_{\rho^{|n_k|}} = \infty. \tag{12.41}$$

We emphasize that (12.38) is not enough to guarantee (12.4). We now impose an additional condition for CALR to occur. We assume that $\{g_e^n\}$ satisfies the following gap property:

GP : There exists a sequence $\{n_k\}$ with $|n_1| < |n_2| < \cdots$ such that

$$\lim_{k\to\infty} \rho^{|n_{k+1}|-|n_k|} \frac{|g_e^{n_k}|^2}{|n_k|\rho^{|n_k|}} = \infty .$$

If GP holds, then we immediately see that (12.38) holds, but the converse is not true. If (12.38) holds, *i.e.*, there is a subsequence $\{n_k\}$ with $|n_1| < |n_2| < \cdots$ satisfying (12.39) and the gap $|n_{k+1}| - |n_k|$ is bounded, then GP holds. In particular, if

$$\lim_{n\to\infty} \frac{|g_e^n|^2}{|n|\rho^{|n|}} = \infty , \tag{12.42}$$

then GP holds.

Assume that $\{g_e^n\}$ satisfies GP and $\{n_k\}$ is such a sequence. Let $\delta = 2\rho^\alpha$ for some α and let $k(\alpha)$ be the number such that

$$|n_{k(\alpha)}| \le \alpha < |n_{k(\alpha)+1}|.$$

Then, we have

(12.43)
$$\sum_{0\ne|n|\le N_\delta} \frac{\delta|g_e^n|^2}{|n|\rho^{2|n|}} = \rho^\alpha \sum_{0\ne|n|\le\alpha} \frac{|g_e^n|^2}{|n|\rho^{2|n|}} \ge \rho^{|n_{k(\alpha)+1}|-|n_{k(\alpha)}|} \frac{|g_e^{n_{k(\alpha)}}|^2}{|n_{k(\alpha)}|\rho^{|n_{k(\alpha)}|}} \to \infty ,$$

as $\alpha \to \infty$.

We obtain the following lemma.

LEMMA 12.4. *If (12.38) holds, then*

$$\limsup_{\delta\to 0} E_\delta = \infty . \tag{12.44}$$

If $\{g_e^n\}$ satisfies the condition GP, then

$$\lim_{\delta\to 0} E_\delta = \infty . \tag{12.45}$$

Suppose that the source function is supported inside the radius $r_\star = \sqrt{r_e^3 r_i^{-1}}$. Then its Newtonian potential cannot be extended harmonically in $|x| < r_\star$ in general. So, if F is given by

$$F = c - \sum_{n\ne 0} a_n r^{|n|} e^{\sqrt{-1}n\theta}, \quad r < r_e , \tag{12.46}$$

then the radius of convergence is less than $r_\star$. Thus we have

$$\limsup_{|n|\to\infty} |n||a_n|^2 r_\star^{2|n|} = \infty , \tag{12.47}$$

i.e., (12.38) holds. The GP condition is equivalent to that there exists $\{n_k\}$ with $|n_1| < |n_2| < \cdots$ such that

$$\lim_{k\to\infty} \rho^{|n_{k+1}|-|n_k|} |n_k||a_{n_k}|^2 r_\star^{2|n_k|} = +\infty . \tag{12.48}$$

The following is the main theorem of this section.

THEOREM 12.5. *Let f be a source function supported in $\mathbb{R}^2 \setminus \overline{B}_e$ and F be the Newtonian potential of f.*

(i) *If F does not extend as a harmonic function in $B_{r_\star}$, then weak CALR occurs, i.e.,*

$$\limsup_{\delta\to 0} E_\delta = \infty \tag{12.49}$$

and (12.5) holds with $a = r_e^2/r_i$.

(ii) *If the Fourier coefficients of F satisfy (12.48), then CALR occurs, i.e.,*

$$\lim_{\delta\to 0} E_\delta = \infty \tag{12.50}$$

and (12.5) holds with $a = r_e^2/r_i$.

(iii) *If F extends as a harmonic function in a neighborhood of $\overline{B_{r_\star}}$, then CALR does not occur, i.e.,*

$$E_\delta < C \tag{12.51}$$

for some C independent of δ.

PROOF. If F does not extend as a harmonic function in $B_{r_\star}$, then (12.38) holds. Thus we have (12.49). If (12.48) holds, then (12.50) holds by Lemma 12.4. Moreover, by (12.32), we see that

$$\begin{aligned}|V_\delta| &\le |F| + \sum_{n\neq 0}\left|\frac{2(r_i^{2|n|}-r_e^{2|n|})z_\delta}{|n|r_e^{|n|-1}(4z_\delta^2-\rho^{2|n|})}\frac{g_e^n}{r^{|n|}}\right| \le |F| + C\sum_{n\neq 0}\frac{\delta r_e^{|n|}}{(\frac{\delta^2}{4}+\rho^{2|n|})|n|r^{|n|}}\\ &\le |F| + C\sum_{n\neq 0}\frac{r_e^{2|n|}}{|n|r_i^{|n|}r^{|n|}} < C, \quad \text{if} \quad r=|x|>\frac{r_e^2}{r_i}\end{aligned}$$

for some constants C which may differ at each occurrence.

If F extends as a harmonic function in a neighborhood of $\overline{B_{r_\star}}$, then the power series of F, which is given by (12.28), converges for $r < r_\star + 2\epsilon$ for some $\epsilon > 0$. Therefore there exists a constant C such that

$$\frac{|g_e^n|}{|n|r_e^{|n|-1}} \le C\frac{1}{(r_\star+\epsilon)^{|n|}}$$

for all n. It then follows that

$$|g_e^n| \le C(r_e^2\rho^{-1}+r_e\epsilon)^{-|n|/2}r_e^{|n|} \le (\rho^{-1}+\epsilon)^{-|n|/2} \tag{12.52}$$

for all n. This tells us that

$$\sum_{n\neq 0}\frac{\delta|g_e^n|^2}{|n|(\delta^2+\rho^{2|n|})} \le \sum_{n\neq 0}\frac{|g_e^n|^2}{2|n|\rho^{|n|}} \le \sum_{n\neq 0}\frac{1}{2|n|(1+\epsilon\rho)^{|n|}}.$$

This completes the proof. □

If f is a dipole in $B_{r_\star}\setminus\overline{B}_e$, i.e., $f(x) = a\cdot\nabla\delta_y(x)$ for a vector a and $y \in B_{r_\star}\setminus\overline{B}_e$ where δ_y is the Dirac delta function at y. Then $F(x) = a\cdot\nabla\Gamma(x,y)$. From the following expansion of the fundamental solution of the Laplacian:

$$\frac{(-1)^{|\alpha|}}{\alpha!}\partial^\alpha\Gamma(x,0) = \frac{-1}{2\pi|\alpha|}\left[a_\alpha^{|\alpha|}\frac{\cos|\alpha|\theta}{r^{|\alpha|}} + b_\alpha^{|\alpha|}\frac{\sin|\alpha|\theta}{r^{|\alpha|}}\right], \tag{12.53}$$

we have

$$\Gamma(x,y) = \sum_{n=1}^\infty\frac{-1}{2\pi n}\left[\frac{\cos n\theta_y}{r_y^n}r^n\cos n\theta + \frac{\sin n\theta_y}{r_y^n}r^n\sin n\theta\right] + C. \tag{12.54}$$

Then we see that the Fourier coefficients of F has the growth rate r_y^{-n} and satisfies (12.48), and hence CALR takes place. Similarly CALR takes place for a sum of dipole sources at different fixed positions in $B_{r_\star} \setminus \overline{B}_e$.

If f is a quadrapole, *i.e.*,

$$f(x) = A : \nabla\nabla\delta_y(x) = \sum_{i,j=1}^{2} a_{ij} \frac{\partial^2}{\partial x_i \partial x_j} \delta_y(x)$$

for a 2×2 matrix $A = (a_{ij})$ and $y \in B_{r_\star} \setminus \overline{B}_e$. Then

$$F(x) = \sum_{i,j=1}^{2} a_{ij} \frac{\partial^2 \Gamma(x,y)}{\partial x_i \partial x_j} .$$

Thus CALR takes place. This is in agreement with the numerical result in [**?**].

If f is supported in $\mathbb{R}^2 \setminus \overline{B}_{r_\star}$, then F is harmonic in a neighborhood of $\overline{B}_{r_\star}$, and hence CALR does not occur by Theorem 12.5. In fact, we can say more about the behavior of the solution V_δ as $\delta \to 0$ which is related to the observation in [**?, ?**] that in the limit $\delta \to 0$ the annulus itself becomes invisible to sources that are sufficiently far away.

THEOREM 12.6. *If f is supported in $\mathbb{R}^2 \setminus \overline{B}_{r_\star}$, then (12.51) holds (with $\alpha = 1$ in (12.3)). Moreover, we have*

$$\sup_{|x| \geq r_\star} |V_\delta(x) - F(x)| \to 0 \quad \textit{as} \quad \delta \to 0 . \tag{12.55}$$

PROOF. Since $\operatorname{supp} f \subset \mathbb{R}^2 \setminus \overline{B}_{r_\star}$, the power series of F, which is given by (12.28), converges for $r < r_\star + 2\epsilon$ for some $\epsilon > 0$.

According to (12.32), if $r_e < r = |x|$, then we have

$$V_\delta(x) - F(x) = \sum_{n \neq 0} \frac{2(r_e^{2|n|} - r_i^{2|n|}) z_\delta}{|n| r_e^{|n|-1} (\rho^{2|n|} - 4z_\delta^2)} \frac{g_e^n}{r^{|n|}} e^{\sqrt{-1} n \theta} .$$

If $|x| = r_\star$, then the identity

$$\frac{(r_e^{2|n|} - r_i^{2|n|}) z_\delta}{|n| r_e^{|n|-1} (\rho^{2|n|} - 4z_\delta^2)} \frac{g_e^n}{r_\star^{|n|}} = \frac{(1 - \rho^{2|n|}) z_\delta}{(\rho^{|n|} - 4z_\delta^2 \rho^{-|n|})} \frac{g_e^n r_\star^{|n|}}{|n| r_e^{|n|-1}}$$

holds and

$$\begin{aligned} \left| \frac{(1 - \rho^{2|n|}) z_\delta}{(\rho^{|n|} - 4z_\delta^2 \rho^{-|n|})} \right| &\leq \left| \frac{1}{(z_\delta^{-1} \rho^{|n|} - z_\delta \rho^{-|n|})} \right| \\ &\leq \left| \frac{1}{\Im m(z_\delta^{-1} \rho^{|n|} - z_\delta \rho^{-|n|})} \right| = \left(\frac{\delta}{4 + \delta^2} \rho^{-|n|} + \frac{1}{\delta} \rho^{|n|} \right)^{-1} . \end{aligned}$$

It then follows from (12.52) that

$$|V_\delta(x) - F(x)| \leq 2 \sum_{n \neq 0} \left(\frac{\delta}{4 + \delta^2} \rho^{-|n|} + \frac{1}{\delta} \rho^{|n|} \right)^{-1} \frac{r_e}{|n|} \left(\frac{\rho^{-1}}{\rho^{-1} + \epsilon} \right)^{|n|/2} ,$$

and hence

$$|V_\delta(x) - F(x)| \to 0 \quad \text{as } \delta \to 0 .$$

Since $V_\delta - F$ is harmonic in $|x| > r_e$ and tends to 0 as $|x| \to \infty$, we obtain (12.55) by the maximum principle. This completes the proof. □

Theorem 12.6 shows that any source supported outside $B_{r_\star}$ cannot make the blow-up of the power dissipation happen and is not cloaked. In fact, it is known that we can recover the source f from its Newtonian potential F outside $B_{r_\star}$ since f is supported outside $\overline{B}_{r_\star}$. Therefore we infer from (12.55) that f may be recovered approximately by observing V_δ outside $B_{r_\star}$.

12.5. Shielding at a distance

In this section, we show that a cylindrical superlens can also act as a new kind of electrostatic shielding device if the core is eccentric to the shell. The historical root of electrostatic shielding reaches back to 1896 when Michael Faraday discovered that a region coated with a conducting material is not affected by external electric fields. While such a conventional method shields a region enclosed by the device, a superlens with an eccentric core can shield a non-coated region which is located outside the device. Moreover, the size of the shielded region can be arbitrarily large while that of the device is fixed. We call this phenomenon *shielding at a distance*. The aim of this section is to investigate the conditions required for shielding at a distance and geometric features such as the location and size of the shielded region. The key element to study in the eccentric case is the Möbius transformation via which a concentric annulus is transformed into an eccentric one. The electrostatic properties of the eccentric superlens can be derived in a straightforward way from those of the concentric case since the Möbius transformation is a conformal mapping.

12.5.1. ALR of the concentric annulus. For convenience, we briefly review the anomalous resonance caused by the concentric superlens whose geometry is described in Figure 12.1(a).

We first fix some notations. We let Ω_i and Ω_e denote circular disks centered at the origin with the radii ρ_i and ρ_e, respectively, satisfying $0 < \rho_i < \rho_e < 1$. Identifying $\mathbb{R}^2$ as $\mathbb{C}$, they can be represented as

$$\Omega_i = \{z \in \mathbb{C} : |z| < \rho_i\} \quad \text{and} \quad \Omega_e = \{z \in \mathbb{C} : |z| < \rho_e\}.$$

The core Ω_i and the background $\mathbb{R}^2 \setminus \overline{\Omega_e}$ are assumed to be occupied by the isotropic material of permittivity 1 and the shell $\Omega_e \setminus \overline{\Omega_i}$ by the plasmonic material of permittivity $-1 + i\delta$ with a given loss parameter $\delta > 0$, *i.e.*, the permittivity distribution ϵ_δ is given by

$$\epsilon_\delta = \begin{cases} 1 & \text{in the core,} \\ -1 + i\delta & \text{in the shell,} \\ 1 & \text{in the background.} \end{cases} \tag{12.56}$$

We also assume the annulus structure to be small compared to the operating wavelength so that it can adopt the quasi-static approximation. Then the (quasi-static) electric potential V_δ satisfies

$$\nabla \cdot \epsilon_\delta \nabla V_\delta = f \quad \text{in } \mathbb{C}, \tag{12.57}$$

where f represents an electrical source. We assume that f is a point multipole source of order n located at a location $z_0 \in \mathbb{R}^2 \setminus \overline{\Omega_e}$. Then the potential F generated

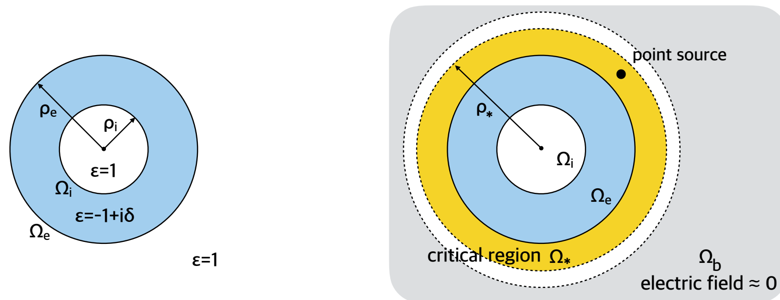

FIGURE 12.1. Cloaking due to the anomalous localized resonance: (a) shows the structure of the superlens with concentric core; (b) illustrates the cloaking effect.

by the source f can be represented as

$$F(z) = \sum_{k=1}^{n} \mathrm{Re}\{c_k(z - z_0)^{-k}\}, \quad z \in \mathbb{C},$$

with complex coefficients c_k's. When $n = 1$, the source f (or the potential F) means a point dipole source.

Then the anomalous localized resonance can be summarized as follows.

(i) the dissipation energy W_δ diverges as the loss parameter δ goes to zero if and only if a point source f is located inside the region $\Omega_* := \{|z| < \rho_*\}$, where $\rho_* := \sqrt{\rho_e^3/\rho_i}$ and W_δ is given by

$$W_\delta := \mathrm{Im} \int_{\mathbb{R}^2} \epsilon_\delta |\nabla V_\delta|^2 \, dx = \delta \int_{\Omega_e \setminus \overline{\Omega_i}} |\nabla V_\delta|^2. \tag{12.58}$$

Let us call Ω_* (or ρ_*) *the critical region* (or *the critical radius*), respectively.

(ii) the electric field $-\nabla V_\delta$ stays bounded outside some circular region regardless of δ. More precisely, we have

$$|\nabla V_\delta(z)| \leq C, \quad z \in \Omega_b := \{|z| > \rho_e^2/\rho_i\}, \tag{12.59}$$

for some constant C independent of δ. Here, the subscript 'b' in Ω_b indicates the boundedness of the electric field. Let us call Ω_b *the calm region*.

12.5.2. Möbius transformation. In this section, we will show that the concentric annulus can be transformed into an eccentric one by applying the Möbius transformation Φ defined as

$$\zeta = \Phi(z) := a\frac{z+1}{z-1} \tag{12.60}$$

with a given positive number a. We shall also discuss how the critical region is transformed depending on the ciritical paramter ρ_*.

The function Φ is a conformal mapping from $\mathbb{C} \setminus \{1\}$ to $\mathbb{C} \setminus \{a\}$. It maps the point $z = 1$ to infinity, infinity to $\zeta = a$, and $z = 0$ to $\zeta = -a$. It maps a circle centered at the origin, say $S_\rho := \{z \in \mathbb{C} : |z| = \rho\}$, to the circle given by

$$\Phi(S_\rho) = \{z \in \mathbb{C} : |z - c| = r\}, \quad \text{where } c = a\frac{\rho^2+1}{\rho^2-1} \text{ and } r = \frac{2a}{|\rho - \rho^{-1}|}. \tag{12.61}$$

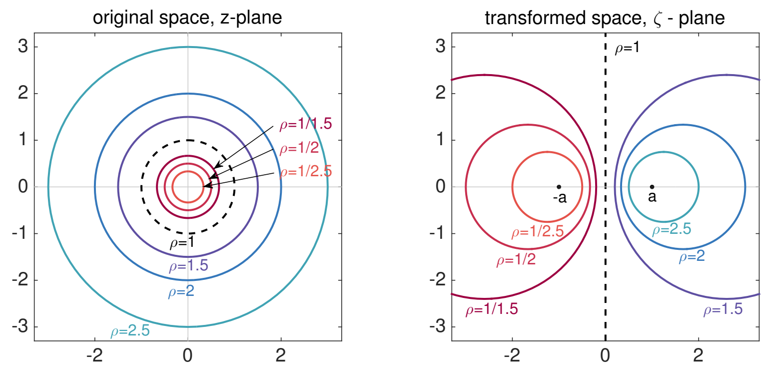

FIGURE 12.2. The Möbius transformation Φ defined in (12.60) maps 0, ∞, 1 to $-a$, $+a$, ∞, respectively. The left figure shows radial coordinate curves $\{|z| = \rho\}$, $\rho > 0$, and the right figure their images transformed by Φ with $a = 1$. Concentric circles satisfying $\rho \neq 1$ are transformed into eccentric ones.

So the concentric circles S_ρ's with $\rho \neq 1$ are transformed to eccentric ones in ζ-plane; see Figure 12.2.

Let us discuss how the concentric superlens described in section 12.5.1 is geometrically transformed by the mapping Φ. Note that for $0 < \rho < 1$, the transformed circle $\Phi(S_\rho)$ always lies in the left half-plane of $\mathbb{C}$. Since we assume that $0 < \rho_i < \rho_e < 1$, the concentric annulus in z-plane is changed to an eccentric one contained in the left half ζ-plane. We let $\widetilde{\Omega}_i$ (or $\widetilde{\Omega}_e$) denote the transformed disk of Ω_i (or Ω_e), respectively.

Now we consider the critical region $\Omega_* = \{|z| < \rho_*\}$ and the calm region Ω_b. Let us denote the transformed critical region (or calm region) by $\widetilde{\Omega}_*$ (or $\widetilde{\Omega}_b$), respectively. The shape of $\widetilde{\Omega}_*$ can be very different depending on the value of ρ_*. Suppose $0 < \rho_* < 1$ for a moment. Then the region $\widetilde{\Omega}_*$ is a circular disk contained in the left half ζ-plane. Next, assume that $\rho_* > 1$. In this case, $\widetilde{\Omega}_*$ becomes the region outside a disk which is disjoint from the eccentric annulus. Contrary to the case when $\rho_* < 1$, the region $\widetilde{\Omega}_*$ is now unbounded. Similarly, the shape of $\widetilde{\Omega}_b$ depends on the paramter $\rho_b := \rho_e^2/\rho_i$. If $0 < \rho_b < 1$, $\widetilde{\Omega}_b$ is a region outside a circle. But, if $\rho_b > 1$, $\widetilde{\Omega}_b$ becomes a bounded circular region which does not intersect with the eccentric superlens. This unbounded (or bounded) feature of the shape of $\widetilde{\Omega}_*$ (or $\widetilde{\Omega}_b$) will be essentially used to design a new shielding device.

12.5.3. Potential in the transformed space. Here, we will transform the potential V_δ via the Möbius map Φ and then show that the resulting potential describes the physics of the eccentric superlens. Let us define the transformed potential $\widetilde{V}_\delta$ by $\widetilde{V}_\delta(\zeta) := V_\delta \circ \Phi^{-1}(\zeta)$. Since the Möbius transformation Φ is a conformal mapping, it preserves the harmonicity of the potential and interface conditions. It can be easily shown that the transformed potential V_δ satisfies

$$\nabla \cdot \widetilde{\epsilon}_\delta \nabla \widetilde{V}_\delta = \widetilde{f} \quad \text{in } \mathbb{C}, \tag{12.62}$$

where $\widetilde{f}(\zeta) = \frac{1}{|\Phi'|^2}(f \circ \Phi^{-1})(\zeta)$ and the permittivity $\widetilde{\epsilon}_\delta$ is given by

$$\widetilde{\epsilon}_\delta(\zeta) = \begin{cases} 1 & \text{in } \widetilde{\Omega}_i, \\ -1 + i\delta & \text{in } \widetilde{\Omega}_e \setminus \overline{\widetilde{\Omega}_i}, \\ 1 & \text{in the background.} \end{cases} \tag{12.63}$$

Therefore, the transformed potential $\widetilde{V}_\delta$ represents the quasistatic electrical potential of the eccentric superlens (12.63) induced by the source $\tilde{f}(\zeta)$.

Now we consider some physical properties in the transformed space. The dissipation energy $\widetilde{W}_\delta$ in the transformed space turns out to be the same as the original one W_δ as follows:

$$\widetilde{W}_\delta = \delta \int_{\partial(\widetilde{\Omega}_e \setminus \widetilde{\Omega}_i)} \widetilde{V}_\delta \frac{\partial \widetilde{V}_\delta}{\partial \widetilde{n}} \, d\widetilde{l} = \delta \int_{\partial(\Omega_e \setminus \Omega_i)} V_\delta \frac{1}{|\Phi'|} \frac{\partial V_\delta}{\partial n} |\Phi'| \, dl = W_\delta. \tag{12.64}$$

In the derviation we have used the Green's identity and the harmonicity of the potentials V_δ and $\widetilde{V}_\delta$.

The point source f is transformed into another point source at a different location. To see this, we recall that the source f is located at $z = z_0$ in the original space. It generates the potential $F(z) = \sum_{k=1}^n \operatorname{Re}\{c_k (z - z_0)^{-k}\}$. By the map Φ, the potential F becomes $\widetilde{F} := F \circ \Phi^{-1}$ which is of the following form:

$$\widetilde{F}(\zeta) = \sum_{k=1}^{n} \operatorname{Re}\left\{ d_n (\zeta - \zeta_0)^{-k} \right\}, \tag{12.65}$$

where d_k's are complex constants and $\zeta_0 := \Phi(z_0)$. So the transformed source $\widetilde{f}$ is a point multipole source of order n located at $\zeta = \zeta_0$. It is also worth remarking that, if the point source f is located at $z_0 = 1$ in the originial space, then $\widetilde{f}$ becomes a multipole source at infinity in the transformed space. In fact, its corresponding potential $\widetilde{F}$ is of the following form:

$$\widetilde{F}(\zeta) = \sum_{k=1}^{n} \operatorname{Re}\left\{ e_k \zeta^k \right\}$$

for some complex constants e_k. For example, if $n = 1$, then the source $\widetilde{f}$ (or potential $\widetilde{F}$) represents a uniform incident field.

12.5.4. Shielding at a distance due to anomalous resonance. In this section, we analyze the anomalous resonance in the eccentric annulus and explain how a new kind of shielding effect can arise. In view of the previous section, the mathematical description of anomalous resonance in the eccentric case can be directly obtained from that in the concentric case as follows:

(i) the dissipation energy $\widetilde{W}_\delta$ diverges as the loss parameter δ goes to zero if and only if a point source $\widetilde{f}$ is located inside the region $\widetilde{\Omega}_*$.

(ii) the electric field $-\nabla \widetilde{V}_\delta$ stays bounded in the calm region $\widetilde{\Omega}_b$ regardless of δ, *i.e.*,

$$|\nabla \widetilde{V}_\delta(\zeta)| \le C, \quad \zeta \in \widetilde{\Omega}_b, \tag{12.66}$$

for some constant C independent of δ.

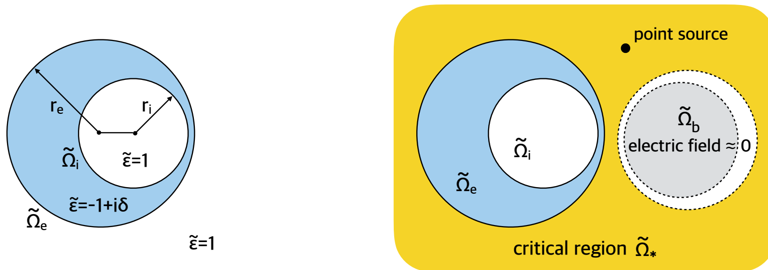

FIGURE 12.3. Shielding at a distance due to the anomalous localized resonance: (left) shows the structure of the superlens with the eccentric core; (right) illustrates shielding at a distance.

Now we discuss a new shielding effect. Suppose the parameters ρ_i and ρ_e satisfy $\rho_* = \sqrt{\rho_e^3/\rho_i} > 1$. Then, as explained in section 12.5.2, the calm region $\widetilde{\Omega}_b$ becomes a bounded circular region which does not intersect with the eccentric structure. If a point source is located within the critical region $\widetilde{\Omega}_*$, then the anomalous resonance occurs and the normalized electric field $-\nabla V_\delta/\sqrt{E_\delta}$ is nearly zero inside the calm region $\widetilde{\Omega}_b$. So the bounded circular region $\widetilde{\Omega}_b$ is not affected by any surrounding point source located in $\widetilde{\Omega}_*$. In other words, the shielding effect does occur in $\widetilde{\Omega}_b$, but there is a significant difference in this shielding effect compared to the standard one. There is no additional material enclosing the region $\widetilde{\Omega}_b$; the eccentric structure is located disjointly. So we call this effect 'shielding at a distance' and $\widetilde{\Omega}_b$ 'the shielding region'. The condition for its occurrence can be summarized as follows: shielding at a distance happens in $\widetilde{\Omega}_b$ if and only if the critical parameter ρ_* and the source location ζ_0 satisfy

$$\rho_* > 1 \text{ and } \zeta_0 \in \widetilde{\Omega}_*. \tag{12.67}$$

The shielding effect occurs for not only a point source but also an external field like a uniform incident field $\widetilde{F}(\zeta) = -\mathrm{Re}\{E_0\zeta\}$ for a complex constant E_0. As mentioned previously, an external field of the form $\mathrm{Re}\{\sum_{k=1}^n e_k\zeta^k\}$ can be considered as a point source at $\zeta = \infty$. Since the critical region $\widetilde{\Omega}_*$ contains the point at inifinity when $\rho_* > 1$, the anomalous resonance will happen and then the circular bounded region $\widetilde{\Omega}_b$ will be shielded. It is worth remarking that, unlike in the the eccentric case, the anomalous resonance cannot result from any external field with source at infinity for the concentric case.

12.5.5. Numerical illustration.

Code:	12.1 Anomalous Resonance - Cloaking and Shielding	DemoCloakALR.m DemoCloakNonALR.m DemoShieldDipoleALR.m DemoShieldDipoleNonALR.m DemoShieldUniformALR.m DemoShieldUniformNonALR.m

In this section we demonstrate shielding at a distance by showing several examples of the field distribution generated by an eccentric annulus and a point source. To compute the field distribution, we use an analytic solution derived by applying a separation of variables method in polar coordinates to the concentric case and then using the Möbius transformation Φ.

For all the examples below, we fix $\rho_e = 0.7$ for the concentric shell and $a = 1$ for the Möbius transformation. We also fix the loss parameter as $\delta = 10^{-12}$.

Example 1 (Cloaking of a dipole source) We first present an eccentric annulus which acts as a cloaking device (Figure 12.4). Since we want to make a 'cloaking' device, we need ρ_b to satisfy the condition $\rho_b < 1$. Setting $\rho_i = 0.55$ for this example, we have $\rho_b = \rho_e^2/\rho_i = 0.89 < 1$ ($\rho_* = (\rho_e^3/\rho_i)^{1/2} = 0.79$). Then by applying the Möbius transformation Φ, the concentric annulus is transformed to the following eccentric structure from (12.61): the outer region $\widetilde{\Omega}_e = \Phi(\Omega_e)$ is the circular disk of radius 2.75 centered at $(-2.92, 0)$ and the core $\widetilde{\Omega}_i = \Phi(\Omega_i)$ is of radius 1.58 centered at $(-1.87, 0)$. The boundaries of the physical regions $\partial\widetilde{\Omega}_i$ and $\partial\widetilde{\Omega}_e$ are plotted as solid white curves in Figure 12.4. On the other hand, the critical region's boundary $\partial\widetilde{\Omega}_*$, which is not a material interface, and is the circle of radius 4.08 centered at $(-4.55, 0)$, is plotted as a dashed white circle. We refrain from ploting the calm region's boundary $\partial\widetilde{\Omega}_b$ in the figure for the sake of the simplicity; it is relatively close to $\partial\widetilde{\Omega}_*$. Note that the calm region $\widetilde{\Omega}_b$ is an unbounded region whose boundary is slightly outside of $\partial\widetilde{\Omega}_*$.

In Figure 12.4(a), we assume that a dipole source $\widetilde{F}(\zeta) = \Re\{\overline{b}(\zeta - \zeta_0)^{-1}\}$ is located at $\zeta_0 = (-3.4, 8.5)$ with the dipole moment $b = (3, -3)$. The point source is plotted as a small solid disk (in white). It is clearly seen that the field distribution is smooth over the entire region except at the dipole source. That is, the anomalous resonance does not occur. We can detect the dipole source by measuring the perturbation of the electric field.

In Figure 12.4(b), we change the location of the source to $\zeta_0 = (-3.4, 3.5)$ so that the source's location belongs to the critical region $\widetilde{\Omega}_*$. Then the anomalous resonance does occur, as shown in the figure. As a result, the potential ouside the white dashed circle becomes nearly constant. In other words, the dipole source is almost cloaked.

Example 2 (Shielding at a distance for a dipole source) Next we show that changing the size of the core allows for shielding at a distance to happen for a dipole source (Figure 12.5).

In Figure 12.5(a), we set $\rho_i = 0.55$ as in Example 1. We also assume that a dipole source $\widetilde{F}(\zeta) = \Re\{\overline{b}(\zeta - \zeta_0)^{-1}\}$ is located at $\zeta_0 = (5, 5)$ with the dipole moment $b = (3, 3)$. Since the source is located outside the critical region, the anomalous resonance does not happen.

Now let us change the size of the core. To make the shielding at distance occur, the critical radius ρ_* satisfies the condition $\rho_* > 1$. We set $\rho_i = 0.2$ so that $\rho_* = \sqrt{\rho_e^3/\rho_i} = 1.31 > 1$. Then, the core $\widetilde{\Omega}_i = \Phi(\Omega_i)$ becomes the circular disk of radius 0.42 centered at $(-1.08, 0)$. The critical region $\widetilde{\Omega}_*$ becomes the region outside the circle of radius 3.53 centered at $(4.06, 0)$. The resulting eccentric annulus and the critical region are illustrated in Figure 12.5(b). Note that the source is contained in the new critical region $\widetilde{\Omega}_*$ and $\rho_* > 1$. In other words, the condition (12.67)

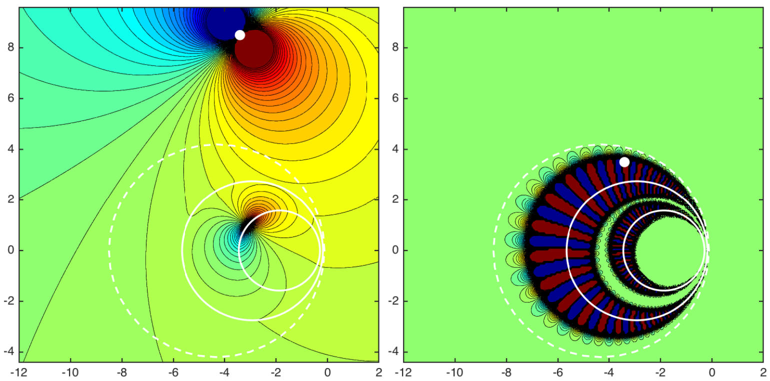

FIGURE 12.4. Cloaking for a dipole source. We set $\rho_i = 0.55$, $\rho_e = 0.7$ and $a = 1$. The dipole source is located at $\zeta_0 = (-3.4, 8.5)$ in the left figure and at $\zeta_0 = (-3.4, 3.5)$ in the right figure. **(left)** A dipole source (small solid disk in white) is located outside the critical region $\widetilde{\Omega}_*$ (white dashed circle). The field outside $\widetilde{\Omega}_*$ is significantly perturbed by the source. **(right)** A dipole source is located inside the critical region $\widetilde{\Omega}_*$. The anomalous resonance happens near the superlens but the field outside $\widetilde{\Omega}_*$ becomes nearly zero. The source becomes almost cloaked. The plot range is from -10 (blue) to 10 (red).

for shielding at a distance is satisfied. Indeed, inside the white dashed circle, the potential becomes nearly constant while there is an anomalous resonance outside. Thus, sheiding at a distance occurs.

Example 3 (Shielding at a distance for a uniform field) Finally, we consider shielding at a distance for a uniform field (Figure 12.6). We keep the parameters a, ρ_i and ρ_e as in the previous example but change the dipole source to a uniform field $\widetilde{F}(\zeta) = -\Re\{E_0\zeta\}$ with $E_0 = 1$. As mentioned previously, an external field can be considered as a point source located at infinity.

In the left figure, the critical region does not contain infinity. So the anomalous resonance does not happen. The uniform field can be easily detected. In the right figure, we changed the core as in the previous example. Now the critical region (the region outside the white dashed circle) does contain infinity. So the anomalous resonance does happen. Again, the potential becomes nearly constant in the region inside the dashed circle. This means there is shielding at a distance for a uniform field.

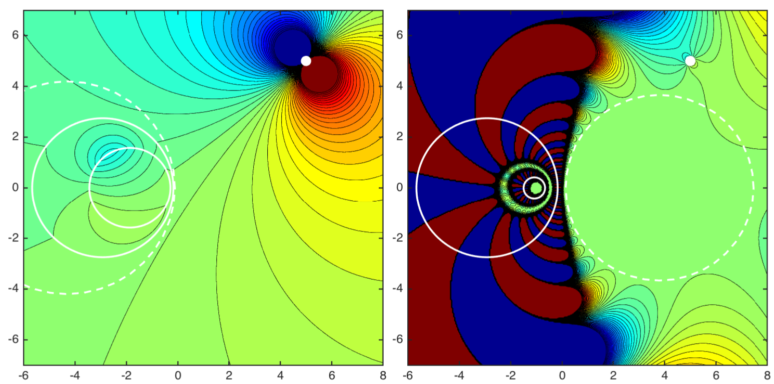

FIGURE 12.5. Shielding at a distance for a dipole source. We set $\rho_e = 0.7$, $a = 1$ and $\zeta_0 = (5, 5)$. We also set $\rho_i = 0.55$ in the left figure and $\rho_i = 0.2$ in the right figure. **(left)** The critical region $\widetilde{\Omega}_*$ (white dashed line) contains the eccentric superlens (white solid lines). The field outside the white dashed circle is significantly perturbed by the source. **(right)** The critical region is now the region outside the white dashed circle which no longer contains the superlens. The field inside the white dashed circle is nearly zero and so shielding occurs. The plot range is from -10 (blue) to 10 (red).

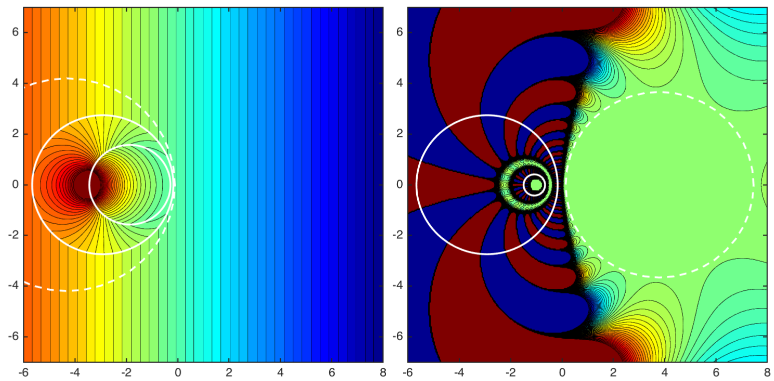

FIGURE 12.6. Shielding at a distance for a uniform field. We set $\rho_e = 0.7$ and $a = 1$. We also set $\rho_i = 0.55$ in the left figure and $\rho_i = 0.2$ in the right figure. **(left)** The critical region $\widetilde{\Omega}_*$ (white dashed line) contains the eccentric superlens (white solid lines). The uniform incident field is nearly unperturbed outside the white dashed circle. **(right)** The critical region $\widetilde{\Omega}_*$ is the region outside the white dashed circle which does not contain the superlens any longer. The field inside the white dashed circle is nearly zero and so shielding occurs. The plot range is from -15 (blue) to 15 (red).

Bibliography

[1] Atkinson, Kendall, and Weimin Han. "Numerical Solution of Fredholm Integral Equations of the Second Kind." Cambridge University Press, 2009.

[2] Kress, Rainer, V. Maz'ya, and V. Kozlov. Linear integral equations. Vol. 17. Berlin: Springer-Verlag, 1989.

[3] Klöckner, Andreas, et al. "Quadrature by expansion: A new method for the evaluation of layer potentials." Journal of Computational Physics 252, 332-349, 2013.